

# RO ADIOLOGY AND NCOLOGY



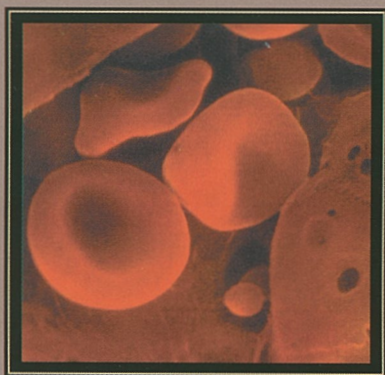
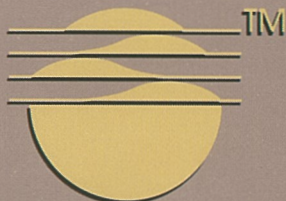
1998  
Vol. 32 No. 1  
Ljubljana

ISSN 1318-2099  
UDC 616-006  
CODEN: RONCEM





# EPO/MA<sup>TM</sup>

EPOETIN OMEGA



REKOMBINANTNI  
HUMANI  
ERITROPOETIN  
IZ CELIC  
BHK; r-HuEPO

ZA DOBRO  
VSEH,  
KI GA  
POTREBUJEJO

 **lek** v sodelovanju z  *E. Ciano*

*Podrobnejše informacije dobite pri proizvajalcu*

*Radiology and Oncology* is a journal devoted to publication of original contributions in diagnostic and interventional radiology, computerized tomography, ultrasound, magnetic resonance, nuclear medicine, radiotherapy, clinical and experimental oncology, radiobiology, radiophysics and radiation protection.

Editor-in-Chief

**Gregor Serša**

*Ljubljana, Slovenia*

Executive Editor

**Viljem Kovač**

*Ljubljana, Slovenia*

Editor-in-Chief Emeritus

**Tomaž Benulič**

*Ljubljana, Slovenia*

Editorial board

**Marija Auersperg**

*Ljubljana, Slovenia*

**Nada Bešenski**

*Zagreb, Croatia*

**Karl H. Bohuslavizki**

*Hamburg, Germany*

**Haris Boko**

*Zagreb, Croatia*

**Nataša V. Budihna**

*Ljubljana, Slovenia*

**Marjan Budihna**

*Ljubljana, Slovenia*

**Malte Clausen**

*Hamburg, Germany*

**Christoph Clemm**

*München, Germany*

**Mario Corsi**

*Udine, Italy*

**Christian Dittrich**

*Vienna, Austria*

**Ivan Drinković**

*Zagreb, Croatia*

**Gillian Duchesne**

*Melbourne, Australia*

**Béla Fornet**

*Budapest, Hungary*

**Tullio Giraldi**

*Trieste, Italy*

**Andrija Hebrang**

*Zagreb, Croatia*

**László Horváth**

*Pécs, Hungary*

**Berta Jereb**

*Ljubljana, Slovenia*

**Vladimir Jevtič**

*Ljubljana, Slovenia*

**H. Dieter Kogelnik**

*Salzburg, Austria*

**Jurij Lindtner**

*Ljubljana, Slovenia*

**Ivan Lovasić**

*Rijeka, Croatia*

**Marijan Lovrenčić**

*Zagreb, Croatia*

**Luka Milas**

*Houston, USA*

**Metka Milčinski**

*Ljubljana, Slovenia*

**Maja Osmak**

*Zagreb, Croatia*

**Branko Palčič**

*Vancouver, Canada*

**Jurica Papa**

*Zagreb, Croatia*

**Dušan Pavčnik**

*Portland, USA*

**Stojan Plesničar**

*Ljubljana, Slovenia*

**Ervin B. Podgoršak**

*Montreal, Canada*

**Jan C. Roos**

*Amsterdam, Netherlands*

**Slavko Šimunić**

*Zagreb, Croatia*

**Lojze Šmid**

*Ljubljana, Slovenia*

**Borut Štabuc**

*Ljubljana, Slovenia*

**Andrea Veronesi**

*Gorizia, Italy*

**Živa Zupančič**

*Ljubljana, Slovenia*

*Publishers*

**Slovenian Medical Association – Slovenian Association of Radiology, Nuclear Medicine Society,  
Slovenian Society for Radiotherapy and Oncology, and Slovenian Cancer Society  
Croatian Medical Association – Croatian Society of Radiology**

*Affiliated with*

**Societas Radiologorum Hungarorum  
Friuli-Venezia Giulia regional groups of S.I.R.M.  
(Italian Society of Medical Radiology)**

*Correspondence address*

**Radiology and Oncology**

**Institute of Oncology**

**Vrazov trg 4**

**SI-1000 Ljubljana**

**Slovenia**

**Tel: +386 61 132 00 68**

**Tel/Fax: +386 61 133 74 10**

*Reader for English*

**Olga Shrestha**

*Design*

**Monika Fink-Serša**

*Key words*

**Eva Klemenčič**

*Secretaries*

**Milica Harisch**

**Betka Savski**

*Printed by*

**Imprint d.o.o., Ljubljana, Slovenia**

*Published quarterly in 1000 copies*

**Bank account number 50101 678 48454**

**Foreign currency account number**

**50100-620-133-27620-5130/6**

**NLB – Ljubljanska banka d.d. – Ljubljana**

**Subscription fee for institutions 100 \$, individuals 50 \$**

**Single issue for institutions 30 \$, individuals 20 \$**

*The publication of this journal is subsidized by the Ministry of Science and Technology of the Republic of Slovenia.*

*According to the opinion of the Government of the Republic of Slovenia, Public Relation and Media Office, the journal Radiology and Oncology is a publication of informative value, and as such subject to taxation by 5% sales tax.*

*Indexed and abstracted by:*

**BIOMEDICINA SLOVENICA**

**CHEMICAL ABSTRACTS**

**EXCERPTA MEDICA**

*This journal is printed on acid-free paper*

*Radiology and Oncology is now available on the internet at: <http://www.onko-i.si/radiolog/rno.htm>*



## FOREWORD

The international conference LIFE SCIENCES '97 & 2<sup>nd</sup> SLOVENIAN-CROATIAN MEETING ON MOLECULAR ONCOLOGY TODAY was held at Gozd Martuljek, Slovenia, October 16-19, 1997. This conference, one in a series of traditional Life Sciences conferences was, devoted to the topic of *Biophysics and Biology of Tumors*.

The conference gathered 180 scientists from Slovenia and abroad working on basic as well as clinical aspects of cancer. There were three key-note lectures, 55 oral presentations and 65 poster presentations. The main topics touched upon the issues of molecular oncology, electrochemotherapy, biological diagnostic and prognostic factors, immune system and biological response modifiers, experimental oncology, membranes, MR imaging and EPR spectroscopy, and new technologies.

This special issue of Radiology and Oncology is bringing selected scientific reports presented at LIFE SCIENCES '97 & 2<sup>nd</sup> SLOVENIAN-CROATIAN MEETING ON MOLECULAR ONCOLOGY TODAY to the scientific community as peer-reviewed papers. The issue is organized according to the topics of the submitted papers into several sections. It starts with molecular oncology, followed by the papers on experimental oncology, MR imaging and EPR spectroscopy, membranes and radiophysics.

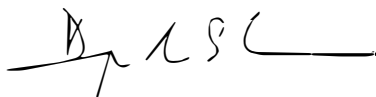
The organization of the conference and this special issue of Radiology and Oncology were made possible by financial assistance of Ministry of Science and Technology of the Republic of Slovenia and other sponsors. We would like to thank the key-note lecturers, invited speakers, participants, all chairmen and co-chairmen, and those who reviewed the manuscripts.

We hope that this compilation of papers presented at the conference will contribute to continuation and intensification of research in preclinical oncology, as well as its application in clinical practice.

Gregor Serša



Damijan Miklavčič



LIFE SCIENCES '97  
&  
2<sup>nd</sup> SLOVENIAN-CROATIAN MEETING  
ON MOLECULAR ONCOLOGY TODAY

Gozd Martuljek, Slovenia, October 16-19, 1997

**Organised by:** Slovenian Biophysical Society & Institute of Oncology, Ljubljana

**In co-operation with:** Physiological Society of Slovenia, Slovenian Genetic Society, Slovenian Immunological Society, Slovenian Medical Association, Oncology Section, Slovenian Pharmacological Society, Slovenian Society for Medical and Biological Engineering, Society of Stereology and Quantitative Image Analysis, Faculty of Electrical Engineering, University of Ljubljana, Institute Rudjer Bošković, Zagreb

**Organising committee:** Gregor Serša, president; Damijan Miklavčič, secretary; Janez Škrk, Maja Čemažar, Tomaž Jarm, Jani Pušenjak, Srdjan Novaković

**Scientific committee:** T. Bajd (SLO), D.J. Chaplin (UK), M. Čarman-Kržan (SLO), F. Demšar (SLO), N.J.F. Dodd (UK), P. Dovč (SLO), I. Eržen (SLO), D. Gabel (D), D. Glavač (SLO), R. Golouh (SLO), R. Heller (USA), M. Kirschfink (D), R. Komel (SLO), V. Kotnik (SLO), T. Lah (SLO), J. Lindtner (SLO), L.M. Mir (F), E. Neumann (D), M. Osmak (CRO), Z. Rudolf (SLO), M. Schara (SLO), F. Sevšek (SLO), G. Stanta (I), S. Svetina (SLO), M. Šentjurs (SLO), B. Štabuc (SLO), A. Štalc (SLO), M. Štefančič (SLO), M. Us-Kraševac (SLO), T. Valentinčič (SLO), L. Vodovnik (SLO), R. Zorec (SLO), N. Zovko (CRO)

**Sponsored by:** Ministry of Science and Technology of the Republic of Slovenia, Slovenian Academy of Sciences and Arts, Institute for Rehabilitation of the Republic of Slovenia, Muscular Dystrophy Association of Slovenia, The Bioelectrochemical Society, Electrinstitute Milan Vidmar, Dr. J. Cholewa Foundation, Adriamed d.o.o. – Hoffmann La Roche Diagnostics Systems, Becton Dickinson – Kemomed d.o.o., BIA d.o.o., Birografika BORI d.o.o., Bristol-Myers Squibb d.o.o., DZS d.d., Karanta d.o.o., Kemofarmacija d.d., Krka d.d., Labormed d.o.o., Lek d.d., Ljubljanske mlekarne d.d., Mikro + Polo d.o.o., PETROL d.d., SALUS d.d., STOP Slovenian Travel Agency d.d.

# CONTENTS

## MOLECULAR ONCOLOGY

---

<b>Digression on membrane electroporation and electroporative delivery of drugs and genes</b> <i>Neumann E, Kakorin S</i>	<b>7</b>
<b>Molecular alterations induced in drug-resistant cells</b> <i>Osmak M</i>	<b>19</b>
<b>Genetic polymorphisms of xenobiotic metabolizing enzymes in human colorectal cancer</b> <i>Dolžan V, Ravnik-Glavač M, Breskvar K</i>	<b>35</b>
<b>In vitro generation of cytotoxic T lymphocytes against mutated ras peptides</b> <i>Juretić A, Šamiija M, Krajina Z, Eljuga D, Turić M, Heberer M, Spagnoli GC</i>	<b>41</b>
<b>Differential expression of Bcl-2 protein in non-irradiated or UVC-irradiated murine myleoid (ML) cells</b> <i>Popović-Hadžija M, Poljak-Blaži M</i>	<b>47</b>

## EXPERIMENTAL ONCOLOGY

---

<b>Direct delivery of chemotherapeutic agents for the treatment of hepatomas and sarcomas in rat models</b> <i>Pendas S, Jaroszeski MJ, Gilbert R, Hyacinthe M, Dang V, Hickey J, Pottinger C, Illingworth P, Heller R</i>	<b>53</b>
<b>Longitudinal study of malignancy associated changes in progressive cervical dysplasia</b> <i>Fležar M, Lavrenčak J, Žganec M, Uš-Krašovec M</i>	<b>65</b>
<b>Image cytometry analysis of normal buccal mucosa smears: influence of smoking and sex related differences</b> <i>Lavrenčak J, Fležar M, Žganec M, Uš-Krašovec M</i>	<b>71</b>



<b>The number of mitoses in simple and complex type carcinomas of the mammary gland in dogs</b> <i>Juntos P</i>	77
<b>Influence of UV-B radiation on Norway spruce seedlings (<i>Picea abies</i> (L.) Karst.)</b> <i>Bavcon J, Gogala N, Gaberščik A</i>	83
<hr/> <b>MR IMAGING AND EPR SPECTROSCOPY</b> <hr/>	
<b>Monitoring drug release and polymer erosion from therapeutically used biodegradable drug carriers by EPR and MRI in vitro and in vivo</b> <i>Mäder K</i>	89
<b>Bone marrow toxicity and antitumor action of adriamycin in relation to the antioxidant effects of melatonin</b> <i>Rapozzi V, Perissin L, Zorzet S, Comelli M, Mavelli I, Šentjerc M, Pregelj A, Schara M, Giral di T</i>	95
<b>Diffusion-weighted magnetic resonance imaging in the early detection of tumor response to therapy</b> <i>Dodd NJF, Zhao S, Moore JV</i>	103
<hr/> <b>MEMBRANES</b> <hr/>	
<b>Plasma membrane fluidity alterations in cancerous tissue</b> <i>Šentjerc M, Sok M, Serša G</i>	109
<b>On mechanisms of cell plasma membrane vesiculation</b> <i>Kralj-Iglič V, Batista U, Hägerstrand H, Iglič A, Majhenc J, Sok M</i>	119
<hr/> <b>RADIOPHYSICS</b> <hr/>	
<b>Tertiary collimator system for stereotactic radiosurgery with linear accelerator</b> <i>Casar B</i>	125
<hr/> <b>SLOVENIAN ABSTRACTS</b> <hr/>	
<hr/> <b>NOTICES</b> <hr/>	

## review

# Digression on membrane electroporation and electroporative delivery of drugs and genes

Eberhard Neumann and Sergej Kakorin

*Physical and Biophysical Chemistry, Faculty of Chemistry, University of Bielefeld, Germany*

---

## Introduction

A new kind of cell surgery has recently been developed by a combination of drugs and genes with electric voltage pulses. The novel surgery operates on the level of the cell membrane and uses membrane electroporation as a scalpel to greatly facilitate the penetration of drugs, especially chemotherapeutics and genes through electroporated membrane patches of a cell.

The phenomenon of membrane electroporation (ME) is methodologically an electric technique which renders lipid membranes porous and permeable, transiently and reversibly, by external high voltage pulses. It is of practical importance that the *primary* structural changes induced by ME, condition the electroporated membrane for a variety of *secondary* processes such as, for instance, the permeation of otherwise impermeable substances.

The *structural* concept of ME was derived from *functional* changes; explicitly from the

*Key words: membrane electroporation; gene transfer; drug delivery; lipid vesicle*

electrically induced permeability changes, indirectly judged from the partial release of intracellular components<sup>1</sup> or from the uptake of macromolecules such as DNA.<sup>2,3</sup> The electrically facilitated uptake of foreign genes is called the direct electroporative gene transfer or electrotransformation of cells. Similarly, electrofusion of single cells to large syncytia<sup>4</sup> and electroinsertion of foreign membrane proteins<sup>5</sup> into electroporated membranes are based on electrically induced structural changes of ME.

For the time being the method of ME is widely used to manipulate all kinds of cells, organelles and even intact tissue. ME is applied to enhance iontophoretic drug transport through skin, see, e.g., Pliquett et al.<sup>6</sup>, or to introduce chemotherapeutics into cancer tissue, an approach pioneered by L. Mir.<sup>7</sup>

It is fair to say that, despite the attractive features of the various ME phenomena, the details of the molecular mechanism of ME itself are not yet known. On the same line, the mechanisms of various secondary processes coupled to ME have not been clarified yet. Therefore, reliable directives can not be given for specific analytical and cell-manipulative applications. However, model studies on cells and lipid vesicles have provided some insight into guidelines for the planning

---

Correspondence to: Prof Eberhard Neumann, Physical and Biophysical Chemistry, Faculty of Chemistry, University of Bielefeld, P. O. Box 100 131, D-33501 Bielefeld, Germany, Fax: +49 521 106 29 81; E-mail: eberhard.neuman@post.uni-bielefeld.de

of trials and for the optimization of existing procedures.

In this review a few fundamental aspects are selected which are important to consider when ME is to be applied to cells and tissue. We shall discuss some details of electric field induced structural changes leading to chemically specific pore states in the membrane (Figure 1). The rigorous thermodynamic and kinetic analysis of electroporation data shows that the structural changes increase *continuously* by time and electric field strength. Massive permeability changes, for instance reflected in large conductivity changes, or release and uptake of larger molecules are, however, associated with threshold field strengths (Figure 2) and delay times. Furthermore, the transport of drug-like dyes and DNA through electroporated membranes is characterized by transient interaction of the permeants with larger, but occluded, pores during the permeation process.

### Why model systems?

Clearly, a goal-directed application of ME to cells and tissue requires knowledge of the molecular mechanisms. Due to the enormous complexity of cellular membranes, however, many fundamental problems of ME have to be studied at first on a simpler level of model membranes, such as lipid bilayer membranes or unilamellar lipid vesicles. When the primary processes are physico-chemically understood, the specific electroporative properties of real cell membranes and living tissue can also be quantitatively rationalized.

#### Membrane curvature

The importance of membrane curvature for ME in the context of protein adsorption and partial surface insertion has been studied with vesicles of different size, i.e., for different curvatures. Electrooptical studies using

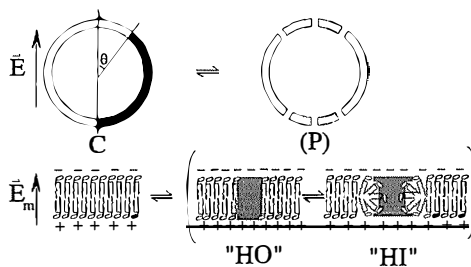


**Figure 1.** Chemical state transitions for the lipid rearrangements in the pore edges of the lipid vesicle membrane. Water entrance in the membrane is induced by an electric field causing the ionic interfacial polarization analogous to condenser plates (+, -), where  $\theta$  is the polar angle.  $E$  is the externally applied field and  $E_m$  the induced membrane field. C denotes the closed bilayer state and (P) the porous state of hydrophobic (HO) and hydrophilic (HI) pores.

optical membrane probes like lipid-coupled 1,6 diphenyl-1,3,5-hexatriene ( $\beta$ -DPH-lipid) showed that an increased curvature (smaller vesicle radius) facilitates the electric pore formation. This observation was quantified<sup>8</sup> in terms of the energy content resulting from the different packing density of the lipid molecules in the two membrane leaflets of curved membranes; see, e.g., Seifert and Lipowsky<sup>9</sup> and references cited therein.

#### Electrolyte concentration

The importance of the electrolyte contents on both sides of membranes with charged lipids has become apparent when salt-filled vesicles were investigated. Different electrolyte concentrations cause different charge screening. The effect of this difference is theoretically described in terms of an increase in the membrane spontaneous curvature. Large concentration gradients across charged membranes of small vesicles permit electroporative efflux of electrolyte ions at surprisingly low transmembrane potential differences, for instance  $|\Delta\phi| = 37.5$  mV at a vesicle radius of  $a = 50$  nm and pulse durations of  $t_E = 100$  ms<sup>10</sup> compared with  $|\Delta\phi| \approx 500$  mV for planar (i.e., not curved) membranes.<sup>11</sup>



## The pore concept – more than just semantics

No doubt, the various electroporative transport phenomena of release and uptake of substances clearly reflect transient permeability changes ultimately caused by external voltage pulses.<sup>12,13</sup> Membrane permeability changes and other electroporative secondary phenomena, however, result from field-induced structural changes in the membrane phase, leading to transient, yet long-lived permeation sites, pathways, channels or pores.<sup>3,14,15</sup>

### Hydrophilic pores

Interestingly, field-induced penetration of small ions, of drug-like dyes and even the highly charged polyelectrolyte DNA, is also observed in the after-field time period, i.e. in the absence of the electrodiffusive driving force. Therefore, the electrically induced permeation sites must be polarized and specifi-

cally ordered, local structures which are potentially open for diffusion of permeantes. These local structures of lipids are long-lived (milliseconds to seconds) compared to the field pulse durations (typically 10  $\mu$ s to 10 ms). Thus, the local permeation structures may be safely called transient pores or electropores in model membranes as well as in the lipid part of cell membranes. The special structural order of a long-lived pore may be modeled by the so-called inverted or hydrophilic (HI) pore (Figure 1).<sup>16</sup> On the same line, the massive ion transport through planar membranes, as observed in the dramatic conductivity increase when a voltage ( $\geq 100 - 500$  mV) is applied, can hardly be rationalized without field-induced open passages or pores; see, e.g., the review by Weaver and Chizmadzhev.<sup>15</sup>

### Attempts of pore visualization

Nevertheless, visible evidence for small electropores, such as electromicrographs, is not available. But the permeation of a permeant through an electroporated membrane patch has also not been visualized up to now. The large pore-like crater structures or volcanoes of 50 nm to 0.1  $\mu$ m diameter, observed in electroporated red blood cells, most probably result from specific membrane-cytoskeleton interactions.<sup>12</sup> Voltage-sensitive fluorescence microscopy at the membrane level has shown that the transmembrane potential in the pole caps of sea urchin eggs is largely decreased, indicating that there the ionic conductivity of the membrane is increased, providing evidence for electropores.<sup>13</sup>

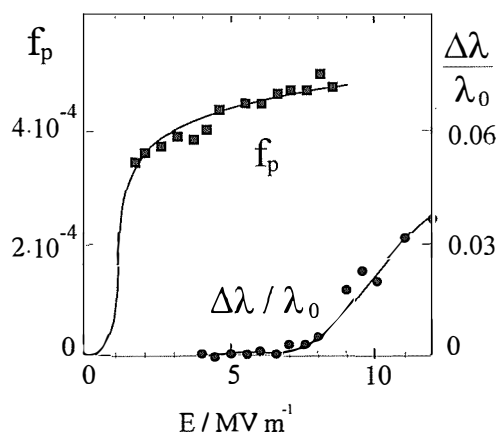


**Figure 2.** The fraction of the electroporated membrane area  $f_p$  smoothly increases with the field strength  $E$ , whereas the massive conductivity increase ( $\Delta\lambda / \lambda_0$ ) of the suspension of the salt filled vesicles of radius  $a = 160 \pm 30$  nm indicates an apparent threshold value. The ratio  $f_p = S_p / S_p^0$  was calculated from the electrooptic relaxations, yielding characteristic rate parameters of the electroporation – resealing cycle in its coupling to ion transport. Data from Neumann and Kakorin<sup>16</sup>;  $\lambda_0 = 7.5 \mu\text{Scm}^{-1}$ ,  $T = 293$  K (20° C).

### Born energy and transport

Membrane electroporabilization for small ions and larger ionic molecules can not be simply described by a permeation across the densely packed lipids of an electrically modified membrane.<sup>14</sup> Theoretically, a small ion

such as  $\text{Na}^+(\text{aq})$  of 0.4 nm diameter and of charge  $e = 1.6 \times 10^{-19}$  C, passing through a lipid membrane of 5 nm thickness encounters the Born energy barrier of  $\Delta W_{\text{Born}} \approx 65$  kT, where  $kT \approx 4.14 \times 10^{-21}$  J. Hence, the required transmembrane voltage to overcome this barrier amounts to 1.7 V. An even larger voltage of 7 V would be needed for divalent ions such as  $\text{Ca}^{2+}$  or  $\text{Mg}^{2+}$ . Nevertheless, the transmembrane potential required to electroporate the cell membrane usually does not exceed 0.5 V.<sup>15</sup> The reduction of the energy barrier can be readily achieved by a transient aqueous pore, which is the structural basis of the theory of electroporation. Certainly, the stationary open electropores can only be small (about 1 nm diameter) in order to prevent discharging of the membrane interface by ion conduction.<sup>15,16</sup> Because of the small size, these electropores can not be observed directly by electron microscopy. In any case, there appears to be no alternative to aqueous pores to rationalize the transport of ions and molecules through the electroporated membrane.<sup>14</sup>

### Electrochemical thermodynamics of pore formation

Undoubtedly, the field-induced structural change leading to an aqueous pore in the lipid phase of the membrane is a chemical process promoted in the electric force field. The actual membrane field  $E_m$  is enormously amplified by interfacial polarization caused by the external field  $E$ <sup>16</sup>, see below. In  $E$ , the redistribution of charges in the electrolyte solution adjacent to the membrane results in a charge distribution which is equivalent to condenser plates, the membrane being the dielectrics. However, unlike conventional solid state dielectrics, the lipid membrane is a highly dynamic phase of *mobile* lipid molecules in contact with *mobile* water molecules; the lipid membrane is hydrophobically kept

together by the aqueous environment. Such a charged condenser with both mobile interior and mobile environment favors the entrance of water molecules to produce localized cross-membrane pores (P) with higher dielectric constant  $\epsilon_W \approx 80$  compared with  $\epsilon_L \approx 2$  of the replaced lipids (state C). In this sense, the lipid membrane in electrolyte solutions is an open system with respect to  $\text{H}_2\text{O}$  molecules, and surplus ions, charging the condenser in the presence of an external field<sup>16</sup>.

### The electrochemical model for the electroporation-resealing cycle

Chemically, the field-induced cycle of pore formation and resealing, after the electric field is switched off at the end of a pulse, can be viewed as a state transition from the intact closed lipid state (C) to the porous state (P) according to the reaction scheme:



The state transition involves a cooperative cluster ( $L_n$ ) of  $n$  lipids  $L$  forming an electropore.<sup>16,17</sup> The extent of membrane electroporation  $y$  is defined by the concentration ratio

$$y = \frac{[\text{P}]}{[\text{P}] + [\text{C}]} = \frac{K}{1 + K} \quad (2)$$

where  $K = [\text{P}]/[\text{C}] = k_1/k_{-1}$  is the equilibrium distribution constant,  $k_1$  the rate coefficient for the step  $\text{C} \rightarrow \text{P}$  and  $k_{-1}$  the rate coefficient for the resealing step ( $\text{C} \leftarrow \text{P}$ ). In an external electric field, the distribution in Eq. (1) is shifted in the direction of increasing  $[\text{P}]$  or, expressed differently, from  $y[0] \ll 1$  at  $E = 0$  to  $y(E)$  at  $E$ . Note that, for the frequently encountered observation of very small pore densities (see Figure 2), i.e.,  $K \ll 1$ , Eq. (2) yields  $y = f_p \approx K$ . Hence the thermodynamic, field-dependent quantity  $K$  is directly obtained from the experimental degree of poration.

Kinetically, the reaction rate equation for the time course of the electroporation-resealing cycle reads:

$$\frac{d[P]}{dt} = -\frac{d[C]}{dt} = k_1[C] - k_{-1}[P] \quad (3)$$

Mass conservation dictates that the total concentration is  $[C_0] = [P] + [C]$ . Substitution into Eq. (3) and integration yield the time course of pore formation:

$$[P(t)] = [C_0] \cdot \frac{K}{1+K} \left(1 - e^{-t/\tau}\right) \quad (4)$$

where  $[P_\infty] = [C_0] K / (1+K)$  is the amplitude of the relaxation process and

$$\tau = (k_1 + k_{-1})^{-1} = [k_{-1} (1 + K)]^{-1} \quad (5)$$

is the relaxation time or mean poration time. It is readily seen that from the experimentally accessible quantities  $\tau$  and  $K$ , both rate coefficients,  $k_1$  and  $k_{-1}$ , can be determined.

The symbol  $P$  may include several different pore states. If, for instance, we have to describe the pore formation by the sequence  $C = HO = HI$ , then  $(P)$  represents the equilibrium  $HO = HI$  between hydrophobic (HO) and hydrophilic (HI) pore states, see Figure 1, and a normal mode analysis is required.<sup>17</sup>

### Energetics of membrane electroporation

The molar work energy difference  $\Delta G_m = G_m(P) - G_m(C)$  between the two states  $C$  and  $P$  in the presence of an electric field must be expressed in terms of the standard value  $\Delta_r \hat{G}^0$  of the transformed Gibbs reaction energy ( $\hat{G}$ ) in order to relate the energetics to  $K$ .

Straightforward thermodynamics<sup>18</sup> yields

$$\Delta_r \hat{G}^0 = -RT \ln K \quad (6)$$

where  $R = N_A k_B$  is the gas constant,  $k_B$  the

Boltzmann constant and  $N_A$  the Avogadro constant.

The difference term  $\Delta_r \hat{G}^0$ , or equivalently  $\ln K$ , is generally the sum of chemical and physical contributions<sup>16</sup>:

$$\Delta_r \hat{G}^0 = \Delta_r \hat{G}^0 - \int \Delta_r M dE_m + \int \Delta_r \gamma dL + \int \Delta_r \Gamma dS + \int \Delta_r \beta dH \quad (7)$$

Note that  $\Delta_r = d/d\xi$ , where  $\xi$  is the molar advancement of a state transition. Here  $\Delta_r \hat{G}^0$  is the chemical contribution,  $\int \Delta_r M dE_m$  the molar electric polarization term,  $\int \Delta_r \gamma dL$  the molar pore edge energy,  $\int \Delta_r \Gamma dS$  the molar pore surface energy term,  $\int \Delta_r \beta dH$  the molar curvature energy term. The single terms are separately considered as follows:

### Chemical contribution

The pure concentration changes of the lipid and water molecules involved in the formation of an aqueous pore with edges are covered by the conventional standard value  $\Delta_r G^0 = \sum_j \sum_\alpha \nu_j^\alpha \mu_j^{0,\alpha}$  of the Gibbs reaction energy, where  $\nu_j^\alpha$  and  $\mu_j^{0,\alpha}$  are the stoichiometric coefficient and the standard chemical potential of the participating molecule  $J$ , respectively, constituting the phase  $\alpha$ , i.e. either state  $C$  or state  $P$ . Here,  $\Delta_r G^0 = (\mu_w^0 + \mu_L^0)_p - (\mu_w^0 + \mu_L^0)_c$ .

### Electric polarization term

The electric reaction moment  $\Delta_r M = M_m(P) - M_m(C)$  in the electric polarization term  $\int \Delta_r M dE_m$  refers to the difference in the molar dipole moments  $M_m$  of state  $C$  and  $P$ , respectively.

The field-induced reaction moment in the electrochemical model is given by<sup>17</sup>:

$$\Delta_r M = N_A \cdot V_p \cdot \Delta_r P \quad (8)$$

where  $V_p = \pi r_p^2 \cdot d$  is the (induced) pore volume of the assumed cylindrical pore of



radius  $r_p$  and  $d \approx 5$  nm is the dielectric membrane thickness.

Analogous with the physical analysis by Abidor et al.,<sup>19</sup> the reaction polarization is defined as:

$$\Delta_r P = \varepsilon_0(\varepsilon_W - \varepsilon_L) E_m, \quad (9)$$

where  $\varepsilon_0$  is the dielectric vacuum permittivity. The difference  $\varepsilon_W - \varepsilon_L$  in the dielectric constants of water  $\varepsilon_W$  (20°C) = 80.4 and of lipids  $\varepsilon_L = 2.1$  refers to the replacement of lipids by water. Since  $\varepsilon_W \gg \varepsilon_L$ , the formation of aqueous pores is strongly favored in the presence of a cross-membrane potential difference  $\Delta\varphi_m$  induced by the interfacial Maxwell-Wagner polarization. We use here the approximation  $E_m = -\Delta\varphi_m/d$  for the membrane field valid for the small pores of low conductance.<sup>15</sup>

The stationary value of the induced potential difference  $\Delta\varphi_m$  in the spherical membrane of a vesicle of radius  $a$  is dependent on the positional angle  $\theta$  between the membrane site considered and the direction of the external field vector  $E$  (Figure 1):

$$\Delta\varphi_m = -\frac{3}{2}a \cdot E \cdot f(\lambda_m) \cos\theta \quad (10)$$

The conductivity factor ( $\lambda_m$ ) can be generally expressed in terms of  $a$  and  $d$  and the conductivities  $\lambda_m$ ,  $\lambda_i$ ,  $\lambda_o$  of the membrane, the cell (vesicle) interior and the external solution, respectively.<sup>20</sup> Commonly,  $d \ll a$  and  $\lambda_m \ll \lambda_o$ ,  $\lambda_i$  such that  $f(\lambda_m) = [1 + \lambda_m(2 + \lambda_i/\lambda_o) / (2 \lambda_i d/a)]^{-1}$ . For  $\lambda_m \approx 0$ ,  $f(\lambda_m) = 1$ . It is readily seen from Eq. (10) that the field amplification is quantified as  $E_m = -\Delta\varphi_m/d = (3/2)(a/d) \cdot E \cdot f(\lambda_m) \cos\theta$ , where the ratio  $a/d$  is the geometric amplification factor of interfacial membrane polarization.

The final expression of the electrical energy term (at  $\theta$ ) is obtained by sequential insertions and integration of Eq. (8). Explicitly<sup>16,17</sup>,

$$\begin{aligned} \int_0^{E_m} \Delta_r M dE_m &= \\ &= \frac{9\pi\varepsilon_0 \cdot a^2 \cdot (\varepsilon_W - \varepsilon_L) \cdot r_p^2 \cdot N_A}{8 \cdot d} f^2(\lambda_m) \cdot \cos^2\theta \cdot E^2 \end{aligned} \quad (11)$$

where we see that the polarization energy depends on the square of the field strength.

If the relation between  $K$  and  $E$  can be formulated as  $K = K_0 \cdot \exp[\int \Delta_r M dE_m/RT]$ , where  $K_0$  refers to  $E = 0$ , Eq. (11) can be used to obtain the mean pore radius  $r_p$  from the field dependence of  $K$  or of  $y$  (the degree of poration).

We recall that the actual data always reflect  $\theta$  angle averages (Figure 1).<sup>17</sup> Since  $[P]$  defines a surface area  $S_p = N_p \cdot \pi r_p^2$  of  $N_p$  pores with maximally  $S_p^0 = N_p \cdot \pi \cdot r_p^2$ , the fraction of porated area is given by

$$f_p = \frac{[P]}{[P_{\max}]} = \frac{S_p}{S_p^0} = \frac{1}{2} \int_0^\pi \frac{K(\theta)}{1 + K(\theta)} \sin\theta d\theta \quad (12)$$

where  $f_p$  is the  $\theta$ -average of  $y = K(\theta) / (1 + K(\theta))$ , with  $[P_{\max}] = [C_0]$ . It is found that  $f_p$  is usually very small<sup>21</sup>, e.g.,  $f_p \leq 0.003$ , i.e. 0.3%. This value certainly corresponds to a small pore density, required for a low value of  $\lambda_m$ .

### Curvature energy term

The explicit expression for the curvature energy term of vesicles of radius  $a$  is given by:<sup>16</sup>

$$\begin{aligned} \int \Delta_r \beta dH &= N_A \int (\beta_p - \beta_C) dH \approx \\ &\approx - \frac{64 \cdot N_A \cdot \pi^2 \alpha \cdot \kappa \cdot r_p^2 \cdot \zeta}{d} \left( \frac{1}{a} + \frac{H_0^{\text{el}}}{2\pi\alpha} \right) \end{aligned} \quad (13)$$

Note that the aqueous pore part has no curvature, hence the curvature term is  $\beta_p - \beta_C = -\beta_C$ .  $H$  is the curvature inclusively the spontaneous curvature  $H_0$ . If  $H_0 = 0$ , then in the case of spherical vesicles we have  $H = 1/a$ .  $H_0^{\text{el}}$  is the electrical part of the spontaneous curvature<sup>16</sup>,  $\kappa$  is the elastic module,  $\alpha$  is a material constant,  $\zeta$  is a geometric fac-

tor characterizing the pore conicity.<sup>9</sup> It is noted that the molar curvature term  $\int \Delta_r \beta dH$  can be as large as  $10 RT$ .<sup>8</sup> Therefore, for small vesicles or small organelles and cells, the curvature term is very important for the energetics of ME.

Eq. (13) shows that the larger the curvature and the larger the  $H_0^{\text{el}}$  term, the larger is the energetically favorable release of Gibbs energy during pore formation. Strongly curved membranes appear to be electroporated easier than planar membrane parts.

#### *Pore edge energy and surface tension*

In Eq. (7),  $\gamma$  is the line tension or pore edge energy density and  $L$  is the edge length,  $\Gamma$  is the surface energy density and  $S$  is the pore surface in the surface plane of the membrane. Explicitly, for cylindrical pores we obtain the pore edge energy term:

$$\int_0^L \Delta_r \gamma dL = N_A \int_0^L (\gamma_P - \gamma_C) dL = 2\pi N_A \cdot \gamma \cdot r_p \quad (14)$$

where  $\gamma_P = \gamma$  since  $\gamma_C = 0$  (no edge) and  $L = 2\pi r_p$  is the circumference line.

The surface pressure term

$$\int \Delta_r \Gamma dS = N_A \int_0^S (\Gamma_P - \Gamma_C) dS \quad (15)$$

is usually negligibly small because the difference in  $\Gamma$  between the states P and C is in the order of  $\leq 1 \text{ mNm}^{-1}$ ; see, e.g., Steiner and Adam<sup>22</sup>.

We recall that the conventional chemical term covering concentration changes of lipids and water in the pore edge and pore volume is given by  $\Delta_r G^0 = -RT \ln K_0$ . Applying this relation and Eqs. (11) – (14) to Eq. (6), we obtain the explicit expression:

$$K = K_0 \cdot \exp \left[ -\frac{N_A}{RT} \left\{ 2\pi r_p \cdot \gamma - \beta \cdot \left( \frac{1}{a} + \frac{H_0^{\text{el}}}{2\pi\alpha} \right) + \frac{\int \Delta_r M dE_m}{RT} \right\} \right] \quad (16)$$

Experimentally,  $K$  can be determined from

the fraction  $y$  of the porated surface as a function of the field strength. It remarked that  $K$  is exponentially dependent on the square of  $E$ , see Eq. (11). Therefore, the dependence of  $K$  or  $y$  on  $E$  is much stronger than linear such that the plot of  $y$  or  $f_p$  versus  $E$  (see Figure 2) shows an initial part of almost no change in  $y$ . This “lag phase” is very frequently qualified to indicate a threshold of the field strength. The thermodynamic analysis shows that ME is highly non-linear, yet continuous in  $E$ . Thus the structural aspect inherent in our membrane electroporation model is not associated with a threshold of the field strength. However, the pore density necessary to permit a secondary phenomenon such as massive ion conduction, release and uptake of substances, may very well be operationally described in terms of a threshold field strength (Figure 2).

The chemical thermodynamical concept has turned out to be applicable to the analysis of ME of vesicles, cells and organelles. For instance, it has been found that the stationary value of the mean pore radius within the pulse duration of  $10 \mu\text{s}$  is rather small:  $\bar{r}_p = 0.35 \pm 0.05 \text{ nm}$ , just permitting free passage of small ions.<sup>17</sup> At higher field intensities and longer pulse durations the pore radius may increase up to  $\bar{r}_p \leq 1.2 \text{ nm}$ , leading to the influx of large drug-like dye molecules into the cell interior,<sup>23</sup> see below.

#### **Electroporative cell deformations**

Using lipid vesicles filled with electrolyte as a model for cells and organelles, it has been shown that ME is causing appreciable increases in the rate and extent of electromechanical shape deformations<sup>10,21</sup>. The overall shape deformation under the field-induced Maxwell stress is associated with several kinetically distinct phases. In the case of vesicles, the initial very rapid phase in the  $\mu\text{s}$  time range is the electroporative elonga-

tion from the spherical shape to an ellipsoid in the direction of the field vector  $E$ . In this phase, called phase 0 (Figure 3), there is no measurable release of salt ions, hence the internal volume of the vesicle remains constant. Elongation is therefore only possible if, in the absence of membrane undulations in small vesicles, the membrane surface can increase by ME. The formation of aqueous pores means entrance of water and increase in the membrane surface.

In the second, slower phase (ms time range), called phase I (Figure 3), there is efflux of salt ions under Maxwell stress through the electropores created in phase 0, leading to a decrease in the vesicle volume under practically constant membrane surface (including the surfaces of the aqueous pores). The kinetic analysis of the volume decrease yields the membrane bending rigidity  $\kappa = 3.0 \pm 0.3 \times 10^{-20} \text{ J}$ .<sup>21</sup> At the field strength  $E = 1.0 \text{ MV m}^{-1}$  and in the range of pulse duration  $5 \leq t_E/\text{ms} \leq 60$ , the number of water-permeable electropores is found to be  $N_p = 35 \pm 5$  per vesicle of radius  $a = 50 \text{ nm}$ , with mean pore radius  $\bar{r}_p = 0.9 \pm 0.1 \text{ nm}$ .

The kinetic analysis developed for vesicles is readily applied to cell membranes. The results aim at physical-chemical guidelines to optimize the membrane electroporation techniques for the direct transfer of drugs and genes into tissue cells.

Interestingly, there is appreciable efflux of salt ions in the after-field period lasting several seconds. This very important observation suggests that there are not only long-lived open pores but also that the structural basis of the longevity cannot be simple hydrophobic (HO) pores (Figure 1). More complicated higher order structures must have been created by ME, which face higher activation barriers for annealing in the absence of the electric field. A candidate for the higher order structure is the so called hydrophilic (HI) pore. In this sense, ME can hardly be called a breakdown phenomenon.

Rather, the reorganization of the lipids in the pore wall leads to a local cluster structure defining an aqueous pore which has a larger electric dipole moment, and thus a higher orientational order than the equivalent space of lipids.

### Electroporative transport of drugs and genes

Contrary to the electroporative transport of small salt ions, the transport kinetics of larger macromolecules such as drug-like dyes and DNA, reflects transient interactions with larger pores. The pore size seems to indicate the size of the macromolecule or parts of it which are transiently located within the membrane during the transport process. For instance, the mean pore radius  $\bar{r}_p = 1.2 \pm 0.1 \text{ nm}$ , derived from the analysis of the transport of the drug-like dye Serva blue G (SBG), appears to be rather large, although it is in line with previous estimates of possible pore sizes.<sup>15</sup> An open pore of this size should lead to a significant increase in the transmembrane conductivity, reducing locally the transmembrane voltage,<sup>16</sup> eventually causing leakage of cell components and finally cell death. It should be noted that the detection of the dye-permeable pore state is only possible when the dye molecules are (interactively) passing through the pore (Figure 4). There-

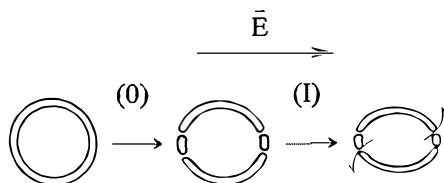


**Figure 3.** Sequence of events in the electromechanical deformation of a membrane system of unilamellar lipid vesicles or biological cells. Phase 0: Fast ( $\mu\text{s}$ ) membrane electroporation rapidly coupled to electroporative deformation at constant volume and slight (0.01 – 0.3%) increase in membrane surface area. Phase I: Slow (ms – min) electromechanical deformation at constant membrane surface area and decreasing volume due to efflux of the internal solution through the electropores.

fore, the pore is temporarily occluded by the dye molecule, reducing the conductivity for small ions compared with a dye-free pore of the same radius. Similar arguments apply for the leak pores associated with the transport of DNA.<sup>24,25</sup>

#### Dye uptake by mouse B cells

As an example for the transport of dye-like drugs, the color change of electroporated intact FcγR<sup>+</sup> mouse B cells (line IIA1.6) after direct electroporative transfer of the dye SBG ( $M_r$  854) into the cell interior is shown to be prevailing due to diffusion of the dye *after* the electric field pulse. Hence, the dye transport is described by the First Fick's law where, as a novelty, time-integrated flow coefficients were introduced.<sup>23</sup> The chemical-kinetic analysis suggests three different pore states (P) in the reaction cascade ( $C \rightleftharpoons P_1 \rightleftharpoons P_2 \rightleftharpoons P_3$ ) to model the sigmoid kinetics of pore formation as well as the biphasic pore resealing. The rate coefficient for pore formation  $k_p$  is dependent on the external electric field strength  $E$  and pulse duration  $t_E$ . At  $E = 2.1$  kV cm<sup>-1</sup> and  $t_E = 200$  μs,  $k_p = 2.4 \pm 0.2 \times 10^3$  s<sup>-1</sup> at  $T = 293$  K; the respective (field-dependent) flow coefficient and permeability coefficient are  $k_f^0 = 1.0 \pm 0.1 \times 10^{-2}$  s<sup>-1</sup> and  $P^0 = 2$  cm s<sup>-1</sup>, respectively.

The maximum value of the fractional surface area of the dye-conductive pores is  $0.035 \pm 0.003$  % and the maximum pore number is  $N_p = 1.5 \pm 0.1 \times 10^5$  per average cell. The diffusion coefficient for SBG,  $D = 10^{-6}$  cm<sup>2</sup> s<sup>-1</sup>, is slightly smaller than that of free dye diffusion indicating transient interaction of the dye with the pore lipids during translocation. The mean radii of the three pore states are  $\bar{r}(P_1) = 0.7 \pm 0.1$  nm,  $\bar{r}(P_2) = 1.0 \pm 0.1$  nm,  $\bar{r}(P_3) = 1.2 \pm 0.1$  nm, respectively. The resealing rate coefficients are  $k_{-2} = 4.0 \pm 0.5 \times 10^{-2}$  s<sup>-1</sup> and  $k_{-3} = 4.5 \pm 0.5 \times 10^{-3}$  s<sup>-1</sup>, independent of  $E$ . At zero field, the overall equilibrium constant of the pore states (P) relative to closed membrane states (C) is  $K_p^0 = [P]/[C] = 0.02 \pm 0.002$ , indicating  $2.0 \pm 0.2$  % water associated with the lipid membrane.<sup>23</sup>

Finally, the results of SBG cell coloring and the new analytical framework may also serve as a guideline for the optimization of the electroporative delivery of drugs which are similar in structure to SBG, for instance, bleomycin successfully used in the new discipline of electrochemotherapy.<sup>7</sup>

#### Kinetics of DNA uptake by yeast cells

In a detailed kinetic study it was found that the direct transfer of plasmid DNA (YEϕ 351, 5.6 kbp, supercoiled,  $M_r \approx 35 \cdot 10^6$ ) by

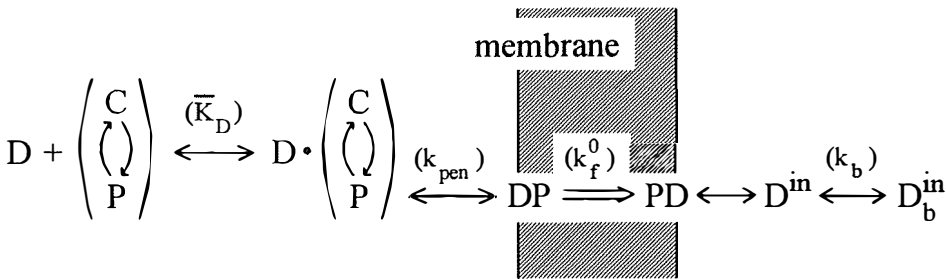


**Figure 4.** Scheme for the coupling of the binding of a macromolecule (D), either a dye-like drug or DNA (described by the equilibrium constant  $K_D$  of overall binding), electrodiffusive penetration (rate coefficient  $k_{pen}$ ) into the outer surface of the membrane and translocation across the membrane, in terms of the Nernst-Planck transport coefficient ( $k_f^0$ ); and the binding of the internalized DNA or dye molecule ( $D^{in}$ ) to a cell component  $b$  to yield the interaction complex  $D \bullet b$  as the starting point for the actual genetic cell transformation or cell coloring, respectively.

membrane electroporation of yeast cells (*Saccharomyces cerevisiae*, strain AH 215) is basically due to (electro)diffusive processes.<sup>26</sup> The rate-limiting step for the cell transformation, however, is a bimolecular DNA binding interaction in the cell interior. Both the adsorption of DNA, directly measured with <sup>32</sup>P-dC DNA, and the number of transformants are collinearly enhanced with increasing total concentrations [D<sub>t</sub>] and [Ca<sub>t</sub>] of DNA and of Ca<sup>2+</sup>, respectively. At [Ca<sub>t</sub>] = 1 mM, the half-saturation or equilibrium binding constant is  $\bar{K}_D = 15 \pm 1$  nM at 293 K (20 °C). The optimal transformation frequency is  $TF_{opt} = 4.1 \pm 0.4 \times 10^{-5}$  if a single exponential pulse of initial field strength  $E_0 = 4$  kV cm<sup>-1</sup> and decay time constant  $\tau_E = 45$  ms is applied at [D<sub>t</sub>] = 2.7 nM and 10<sup>8</sup> cells in 0.1 ml. The dependence of TF on [Ca<sub>t</sub>] yields the equilibrium constants  $K_{Ca}^0 = 1.8 \pm 0.2$  mM (in the absence of DNA) and  $K_{Ca}' = 0.8 \pm 0.1$  mM (at 2.7 nM DNA) well comparable with  $K_{Ca}^0 = 2.3 \pm 0.2$  mM and  $K_{Ca}' = 1.0 \pm 0.1$  mM derived from electrophoresis data.<sup>26</sup>

In yeast cells, too, the appearance of a DNA molecule in its whole length in the cell interior is clearly an after-field event. At  $E_0 = 4.0$  kV cm<sup>-1</sup> and  $T = 293$  K, the flow coefficient of DNA through the porous membrane patches is  $k_f^0 = 7.0 \pm 0.1 \times 10^3$  s<sup>-1</sup> and the electrodiffusion (D) of DNA is about 10 times more effective than simple diffusion (D<sub>0</sub>): the diffusion coefficient ratio is  $D / D_0 \approx 10.3$ . The mean radius of these pores is  $r_p = 0.39 \pm 0.05$  nm and the mean number of pores per cell (diameter 5.5 μm) is  $N_p = 2.2 \pm 0.2 \times 10^4$ . The maximum membrane area which is involved in the electrodiffusive penetration of adsorbed DNA into the outer surface of the electroporated cell membrane patches is only  $0.023 \pm 0.002$  % of the total cell surface. The surface penetration is followed either by further electrodiffusive, or by passive (after field) diffusive, translocation of the inserted DNA into the cell interior.

For practical purposes of optimum trans-

formation efficiency, 1 mM Ca<sup>2+</sup> is necessary for sufficient DNA binding and the relatively long pulse duration of 20 – 40 ms is required to achieve efficient electrodiffusive transport across the cell wall and into the outer surface of electroporated cell membrane patches.

### Acknowledgments

We thank the Deutsche Forschungsgemeinschaft for grant Ne 227/9-2 to E. Neumann.

### References

1. Neumann E, Rosenheck K. Permeability changes induced by electric impulses in vesicular membranes. *J Membrane Biol* 1972; **10**: 279-90.
2. Wong TK, Neumann E. Electric field mediated gene transfer. *Biophys Biochem Res Commun* 1982; **107**: 584-7.
3. Neumann E, Schaefer-Ridder M, Wang Y, Hofschneider PH: Gene transfer into mouse lyoma cells by electroporation in high electric fields. *EMBO J* 1982; **1**: 841-5.
4. Neumann E, Gerisch G, Opatz K. Cell fusion induced by electric impulses applied to dictyostelium. *Naturwissenschaften* 1980; **67**: 414-5.
5. Mouneimne Y, Tosi PF, Gazitt Y, Nicolau C. Electro-insertion of xenoglycophorin into the red blood cell membrane. *Biochem Biophys Res Commun* 1989; **159**: 34-40.
6. Pliquett U, Zewert TE, Chen T, Langer R, Weaver JC. Imaging of fluorescent molecule and small ion-transport through human stratum-corneum during high-voltage pulsing-localized transport regions are involved. *Biophys Chem* 1996; **58**: 185-204.
7. Mir LM, Orlowski S, Belehradek JJr, Teissie J, Rols MP, Serša G, Miklavčič D, Gilbert R, Heller R. Bio-medical applications of electric pulses with special emphasis on antitumor electrochemotherapy. *Bioelectrochem Bioenerg* 1995; **38**: 203-7.
8. Tönsing K, Kakorin S, Neumann E, Liemann S, Huber R. Annexin V and vesicle membrane electroporation. *Eur Biophys J* 1997; **26**: 307-18.
9. Seifert U, Lipowsky R. Morphology of Vesicles. In Lipowsky R, Sackmann E, ed. *Structure and Dynamics of Membranes 1A*. Amsterdam: Elsevier; 1995: 403-63.



10. Kakorin S, Redeker E, Neumann E. Electroporative deformation of salt filled lipid vesicles. *Eur Biophys J* 1998; **27**: 43-53.
11. Winterhalter M, Klotz K-H, Benz R, Arnold WM. On the dynamics of the electric field induced breakdown in lipid membranes. *IEEE Trans Ind Appl* 1996; **32**: 125-8.
12. Chang C. Structure and dynamics of electric field-induced membrane pores as revealed by rapid-freezing electron microscopy. in Chang C, Chassy M, Saunders J, Sowers A. ed. *Guide to electroporation and electrofusion*. San Diego: Academic Press, 1992: 9-28.
13. Hibino M, Itoh H, Kinoshita K. Time courses of cell electroporation as revealed by submicrosecond imaging of transmembrane potential. *Biophys J* 1993; **64**: 1789-800.
14. Weaver JC. Molecular-basis for cell-membrane electroporation. *Annals of the New York Academy of Sciences* 1994; **720**: 141-52.
15. Weaver J, Chizmadzhev Yu. Theory of electroporation: A review. *Bioelectrochem Bioenerg* 1996; **41**: 135-60.
16. Neumann E, Kakorin S. Electrooptics of membrane electroporation and vesicle shape deformation. *Curr Opin Colloid Interface Sci* 1996; **1**: 790-9.
17. Kakorin S, Stoylov SP, Neumann E. Electro-optics of membrane electroporation in diphenylhexatriene-doped lipid bilayer vesicles. *Biophys Chem* 1996; **58**: 109-16.
18. Neumann E. Chemical electric field effects in biological macromolecules. *Prog Biophys molec Biol* 1986; **47**: 197-231.
19. Abidor IG, Arakelyan VB, Chernomordik LV, Chizmadzhev YA, Pastuchenko VP, Tarasevich MR. Electric breakdown of bilayer lipid membrane. I. The main experimental facts and their theoretical discussion. *Bioelectrochem Bioenerg* 1979; **6**: 37-52.
20. Neumann E. The Relaxation Hysteresis of Membrane Electroporation. In: Neumann E, Sowers AE, Jordan C, eds. *Electroporation and Electrofusion in Cell Biology*. New York: Plenum Press, 1989: 61-82.
21. Kakorin S, Neumann E. Kinetics of electroporation deformation of lipid vesicles and biological cells in an electric field. *Ber Bunsenges Phys Chem* 1998; **102**: 1-6.
22. Steiner U, Adam G. Interfacial properties of hydrophilic surfaces of phospholipid films as determined by method of contact angles. *Cell Biophysics* 1984; **6**: 279-99.
23. Neumann E, Toensing K, Kakorin S, Budde P, Frey J. Mechanism of electroporative dye uptake by mouse B cells. *Biophys J* 1998; **74**: 98-108.
24. Spassova M, Tsoneva I, Petrov AG, Petkova JJ, Neumann E. Dip patch clamp currents suggest electrodiffusive transport of the polyelectrolyte DNA through lipid bilayers. *Biophys Chem* 1994; **52**: 267-74.
25. Hristova NI, Tsoneva I, Neumann E. Sphingosine-mediated electroporative DNA transfer through lipid bilayers. *FEBS Lett* 1997; **415**: 81-6.
26. Neumann E, Kakorin S, Tsoneva I, Nikolova B, Tomov T. Calcium-mediated DNA adsorption to yeast cells and kinetics of cell transformation. *Biophys J* 1996; **71**: 868-77.



## Molecular alterations induced in drug-resistant cells

Maja Osmak

*Instiut Rudjer Bošković, Zagreb, Croatia*

---

*The major obstacle to the ultimate success in cancer therapy is the ability of tumor cells to develop resistance to anticancer drugs. Several molecular mechanisms have been suggested to be involved in drug-resistance: a) decrease in the intracellular drug accumulation (increased activity of membrane transporters such as P-glycoprotein or multidrug-resistance-associated protein), b) changes in intracellular detoxification system (increased concentrations of glutathione or metallothioneins, or increased activity of related enzymes), c) alteration in nuclear enzymes (enhanced DNA repair and/or better tolerance of DNA damage, decreased activity of topoisomerases), d) altered expression of oncogenes (inducing increased level of protective molecules in cells or the inhibition of apoptosis). Drug resistance is a multifactorial phenomenon. The complexity of molecular alterations in drug-resistant cells is and will stay the main problem for the successful treatment of cancer.*

*Key words: drug resistance, tumor cells; cancer chemotherapy*

---

### Introduction

Chemotherapy is one of the proven strategies against malignant tumors, especially if the lesions are spread systematically. In many patients, first regimens are successful in reducing tumor size and are sometimes even able to eliminate all clinically detectable tumor masses. But most often, the successful treatments are relatively short lasting. In a vast majority, a certain number of tumor cells will survive and thus become a source of recurrent disease.

Chemotherapy of cancer may fail for vari-

ous reasons. Among these, drug resistance is the most important one. This phenomenon was first observed by Sidney Farber (who introduced chemotherapy into cancer treatment) in 1948.<sup>1</sup> Almost fifty years later the molecular mechanisms involved in this process have been unravelled.

Resistance may be primary (intrinsic): the tumor cells do not respond from the start. Drug-resistance may be secondary (acquired): under the selection pressure of cytotoxic drugs tumor cells are able to develop certain mechanisms which render them resistant to these drugs. The tumor initially responds to therapy, but tumor growth resumes and the patient relapses.

Knowledge regarding the genetic nature and biochemical nature of drug resistance

---

Correspondence to: Maja Osmak Ph.D., Rudjer Bošković Institute, Bijenička cesta 54, 10000 Zagreb, Croatia. Tel: +385 1 456 11 45; Fax: +385 1 456 11 77; E-mail: osmak@olimp.irb.hr

has been derived largely from cellular systems. By step-wise increase in the drug dose, highly resistant cell lines can be obtained. The mechanisms of drug resistance can be defined by comparing the biochemical and biological characteristics of parental and resistant cells.

A search for the cause or causes of drug resistance mechanisms has been occupying the attention of cancer researchers for more than four decades. Today it is known that several molecular mechanisms can be involved in drug-resistance. The most important one will be presented in this review.

**Reduced intracellular accumulation:  
transport proteins**

A broad spectrum resistance to cytotoxic drugs, termed multidrug resistance (MDR),

involves simultaneous resistance to a wide array of natural, semisynthetic and synthetic compounds. The most common of them are shown in Table 1. They do not have similar structure or the same cytotoxic intracellular target, but are amphipathic and are preferentially soluble in lipid.

Multidrug resistance is caused by overexpression of a 170 kDa plasma membrane - associated glycoprotein (P-glycoprotein, Pgp; Table 1). It is an energy dependent efflux pump that decreases intracellular drug accumulation.<sup>2-4</sup> Pgps are coded by *MDR* gene family. The number of members varies between species. Human possess two *MDR* genes, *MDR1* and *MDR2*. Of these, only *MDR1* can confer a drug resistance phenotype.<sup>5</sup> Multidrug resistant cells, particularly those which display high levels of resistance, often possess an increased copy number of the *MDR1* gene.<sup>2,4</sup>

It was noted that Pgp bore a remarkable

**Table 1.** Characteristics of transport proteins: P-glycoprotein and MRP protein

Name	P-glycoprotein (Pgp)	MRP (multidrug resistance-associated protein)
Encoded by	<i>MDR1</i> gene	<i>MRP</i> gene
Mol. weight	170 kDa	190 kDa
Length	4.5 kb mRNA	6.5 kb mRNA
Number of amino acid	1268	1531
Discovered in	1970 year	1992 year
Resistance to	Anthracyclines, Vinca alkaloids, Podophyllotoxins, Colchicine, paclitaxel	Anthracyclines, Vinca alkaloids Arsenic and antimony-centered oxyanions
Normal tissues distribution (high levels)	Adrenal gland, kidney, liver, large intestine, pancreas, bile duct, lung, breast, prostate, gravid uterus	Testes, skeletal muscle, heart, kidney, lung
Tumor tissues distribution	Colonic, renal, hepatoma, adrenocortical, phaeochromocytoma	Leukemias ( acute myeloid, chronic lymphocytic, acute myeloid, B-chronic lymphocytic),lung (NSCLC), anaplastic thyroid, neuroblastoma
Functions	Transport of xenobiotics Transport of hormones	Transport of leukotriene Transport of GSH-conjugates Transport of heavy metal oxyanions "MOAT" (multispecific organic anion transporter)

According to references <sup>2-4</sup> and <sup>9</sup>

structural similarity to bacterial transport proteins, particularly those transporting haemolysin.<sup>6</sup> Presumably, in evolutionary terms, it represents a highly conserved component of the cell. P-glycoprotein is detectable at a high concentration in certain normal tissues (Table 1). The disposition of the Pgp on the luminal surface of kidney brush border, on the mucosal surface of the large intestine, and on the bile canalicular surface of hepatocytes, indicates a normal role in transport and/or protection against exogenous toxins. High levels of Pgp were found in different tumors as well, specially in those arising from the normal tissue with a high Pgp level.<sup>2-4</sup>

Pgp overexpression has been associated with multidrug resistance in many drug-selected cell lines.<sup>7</sup> The final evidence that *MDR* gene is involved in multidrug resistance came from transfection studies: *MDR1* gene inserted into retroviral expression vector confers a complete multidrug resistance phenotype.<sup>5</sup>

Recently, another member of the ATP-binding cassette transporter superfamily was isolated from non-Pgp small cell lung carcinoma cells, multidrug resistance-associated protein (MRP).<sup>8</sup> It also lowers intracellular drug accumulation, conferring a pattern of drug resistance similar to that of the resistance-conferring Pgps.<sup>9</sup> However, there may be some differences. For example, MRP confers only low resistance to paclitaxel and colchicine, which are reported among the best "substrates" for Pgp. Another notable difference is the ability of MRP to confer low resistance to arsenic and antimony-centered oxyanions. The characteristics of this protein are given in Table 1.

MRP has been identified in non-Pgp multidrug resistant cell lines from a variety of tumor types.<sup>9</sup> Transfection of an MRP expression vector into HeLa cells demonstrated conclusively that the protein conferred resistance to drugs.<sup>10</sup>

Some recent observations suggest that elevated MRP expression may occur prior to *MDR*.<sup>11,12</sup>

### Decreased drug uptake

Decreased intracellular drug accumulation may occur due to decreased drug uptake, for drugs that enter the cells by the help of a cellular transport system. Loss or inactivation of this transport system may cause drug resistance, as it was observed for melphalan,<sup>13</sup> methotrexate<sup>14</sup> or cisplatin.<sup>15</sup>

### Glutathione

Glutathione (GSH) is a simple tripeptide that contributes to more than 90% of intracellular non-protein sulphydryl compounds.<sup>16,17</sup> It is present in virtually all eucariotic cells. It is also synthesized by tumors, some of which exhibit high cellular levels of glutathione and high capacity for the synthesis of glutathione.

Glutathione plays an important role in cellular metabolism and in the protection of cells against free radicals induced oxidant injury (Table 2). It has been implicated in cell resistance to a number of cytotoxic drugs, particularly to alkylating agents and cisplatin.<sup>18-22</sup> There are a number of potential mechanisms by which GSH may affect cellular response to cytostatics. These include conjugation of electrophilic compounds, frequently catalyzed by the glutathione S-transferases (GST). In addition, GSH can detoxify oxygen-induced free radicals and organoperoxides using GSH-peroxidases.<sup>23</sup>

GSH may participate in the resistant phenotype in two ways. In cytoplasm it may bind electrophilic compounds, thus making them less dangerous. In nucleus, GSH may support the repair of the damage induced in DNA: by maintaining functional repair

**Table 2.** Functions of glutathione in metabolism and immune response

Functions	Antioxidant
	Conjugation with different compounds (exogenous, the products of metabolism)
	Amino acid transport
	Support of primary antibody response
	Regulation of T-lymphocyte proliferation
	Co-enzyme for multiple enzymatic reactions
	Thiol-disulfide exchange in protein synthesis and degradation
	DNA precursor synthesis
	Enzyme activation
	Regulation of microtubule formation
	Negative control of NF-κB activation
Deficiency	Increased sensitivity to irradiation and different toxic compounds
	Oxidant stress
	Cataract formation
	Impaired function of both T and B lymphocyte function and immune function in general

According to references <sup>16</sup> and <sup>17</sup>

enzymes or by maintaining deoxyribonucleotide triphosphate pool size.<sup>24</sup>

An argument for the potential role of GSH in resistance is based on the observation that the toxicity of many cytotoxic agents can be increased by lowering cellular GSH (as by adding specific inhibitor of GSH synthesis-buthionine sulfoximine).<sup>25,26</sup>

**Glutathione S-transferases**

Glutathione S-transferases (GST) are an important part of the Phase II detoxification system that metabolizes many lipophilic drugs and other foreign compounds, including anticancer drugs.<sup>27-29</sup> The overall result of this system is the conversion of lipophilic chemicals to more polar derivatives, thus facilitating their inactivation and elimination. GST are abundant and together may constitute up to about 5 % of soluble cellular protein. Their

importance supports the finding that they perform specific detoxification, structural and transport function in many phyla: from bacteria to humans.

GST catalyze direct coupling of GSH to electrophilic drugs, thus making a less toxic and more readily excreted metabolic compound.

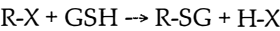


**Figure 1.** Conjugation reaction catalyzed by GSTs

Further, they may exhibit ligand binding function, by non-covalent binding of non-substrate hydrophobic ligands (such as heme, bilirubin, some steroids, and some lipophilic cytostatics).<sup>27-29</sup>

The diverse biological functions of GSH/GST system are mediated by multiple GST enzymes. The genome of most species encode several different isoenzymes of GSTs. In eucaryotic cells, there are five classes of GST. Four are found in cytosol, while the fifth class, the microsomal GST, is found primarily in the hepatic endoplasmic reticulum.

The microsomal GST are functional trimers with molecular weights of 17 kDa. Cytosol GST are both mono- and heterodimeric complexes formed of GST subunits that range in size from 23 to 28 kDa. The classification of the cytosolic GST into alpha, pi and mu, and recently identified theta classes was originally based on physical and catalytic properties. Among them, GST pi was found at elevated levels in many tumor tissues relative to matched normal tissues.<sup>30,31</sup>

Several anticancer drugs have been definitively identified as GST substrates (Table 3). Therefore, it is not surprising that elevated levels of GST were found in cells resistant to some of these drugs like cisplatin, doxorubicin, melphalan etc.<sup>27-29</sup>

The final confirmation of GST involvement in drug resistance came from the transfection experiments.<sup>32</sup> The tranfection with

**Table 3.** Anticancer drugs: substrates for glutathione S-transferases

Direct evidence for involvement in drug resistance	Indirect evidence for involvement in drug resistance
Chlorambucil	Bleomycin
Melphalan	Hepsulfam
Nitrogen mustard	Mitomycin C
Phosphoramidate mustard	Adriamycin
Acrolein	Cisplatin
BCNU	Carboplatin
Hydroxyalkenals	
Ethacrinic acid	
Steroids	

According to reference <sup>27</sup>

GST imparts a small but significant (and clinically relevant) increase in resistance to cisplatin (GST mu), doxorubicin (GST pi) or chlorambucil and melphalan (GST alpha).

### Glutathione peroxidase

Glutathione peroxidase catalyzes the reduction of potentially toxic peroxides to alcohols by oxidizing GSH to its disulfide form (GSSG). GSSG is returned to GSH with the concomitant oxidation of coenzyme NADPH to NADP<sup>+</sup>. GST enzyme can catalyze a selenium-independent GSH peroxidase activity leading to the detoxification of lipid and nucleic acid hydroperoxides. This redox cycle may play an essential role in protecting cells from damage of lipid peroxidation generated during normal metabolism or by redox recycling of many drugs.

Doxorubicin is one of the agents known to generate free radicals and peroxides. GST as well as the selenium -dependent enzyme GSH peroxidase can deactivate these metabolites through peroxidative mechanisms, resulting in decreased cytotoxicity. In tumor cells resistant to doxorubicin, increased levels of selen -dependent GSH peroxidase were found.<sup>33,34</sup>

### Metallothionein

Metallothioneins (MT) were first discovered as a family of inducible proteins involved in Zn<sup>2+</sup> and Cu<sup>2+</sup> homeostasis and in the detoxification of heavy metals.<sup>35,36</sup> They are evolutionary conserved low molecular weight intracellular proteins with unusually high level of cysteine content, that constitute the major fraction of the intracellular protein thiols.

Today is known that metallothioneins are a part of generalized cell response to environmental stress: the abundant nucleophilic thiol-rich groups in MT can react with many electrophilic toxins, participate in controlling the intracellular redox potential, and act as scavengers of oxygen radicals generated during the metabolism of xenobiotics. They can be induced by environmental stimuli such as epinephrine, glucocorticoids, thermal injury, cytokines, cyclic nucleotides, phorbol esters, UV light, etc., suggesting a protective function and a role in cell growth and proliferation.<sup>35,36</sup>

Metallothioneins are attractive candidates as modulators of cellular sensitivity to anticancer drugs. Elevated levels of MT have been observed in some malignant cells with acquired resistance to antineoplastic drugs, such as cisplatin.<sup>37-40</sup> Increases in intracellular MT by gene-transfer-produced resistance



to cisplatin, melphalan and chlorambucil, and less to doxorubicin and bleomycin<sup>38</sup> or N-methyl-N-nitro-N-nitrosoguanidine (MN-NG) and methyl nitrosourea (MNU).<sup>41</sup> In most MT overexpressing cell lines, however, induction of MT did not cause a parallel increase in resistance. Therefore, the resistance associated with MT overexpression was not due to direct binding of the drug to MT. The study of Kaina and co-workers suggest that MT may participate as a cofactor or regulatory element in the repair or tolerance of toxic alkylating drugs.<sup>41</sup>

Nevertheless, increases in MT do not always result in a phenotype that is less sensitive to the toxic effects of antineoplastic drugs.<sup>42</sup> Thus, the protective role of MT has been questioned. Recently, transgenic mice lacking functional MT have been produced by homologous recombination of disrupted MTI and II genes. The embryonic cells of these mice exhibit enhanced sensitivity to cisplatin, melphalan, bleomycin, cytarabine or MNNG, confirming the protective function of metallothioneins against cytotoxic drugs.<sup>43</sup>

### Gene amplification

One of the important mechanisms of drug resistance is gene amplification. The first observation of this phenomenon was noted by Biedler and Spengler. They found chromosome elongation in cultured hamster cells resistant to methotrexate (MTX) and called this extra DNA "homogeneously staining regions" (HSR).<sup>44</sup> Schimke and co-workers then showed that the extra DNA contains extra copies of the gene for the enzyme dihydrofolate reductase (DHFR), explaining the increased enzyme levels in the resistant cell.<sup>45,46</sup> The amplified DNA may either be present in chromosomes as HSRs or free, as minute chromatin particles usually present in metaphase spreads as pair minutes, called double minutes (DM).

After the initial demonstration that cells can overcome the MTX inhibition of DHFR by overproducing the enzyme by means of gene amplification, numerous other examples of this mechanism have been reported: for MDR,<sup>2,4</sup> for metallothioneins<sup>35,36</sup> etc.

### DNA repair

The resistance to some cytotoxic drugs can be caused by enhanced ability of cells to repair the DNA induced damage or to tolerate their presence. One of the most studied phenomena in this respect is resistance to cisplatin.

It has been well established that cisplatin binds to DNA and that these adducts contribute to cellular toxicity. In a number of cisplatin resistant cell lines, an enhanced repair of DNA lesions has been demonstrated.<sup>21,22</sup> Thus, Eastman and Schulte provided direct evidence for increased repair showing that the predominant lesions, cis-GG adducts, were more rapidly removed from resistant than sensitive cells.<sup>47</sup> These resistant L1210 cells can also reactivate a cisplatin-damage plasmid more readily than sensitive parental cells.<sup>48</sup> However, a correlation of repair activity with drug-resistance has not always been demonstrated: L1210 cells with 100-fold resistance to cisplatin, removed cis-GG intra-strand adducts only slightly better than 20-fold resistant cells.<sup>47</sup>

Repair of platinum damage in very specific regions of the genome is a possible characteristic of enhanced repair in resistant cells. If only active genes are more efficiently repaired in resistant cells, then it is not likely that a significant change in overall platination levels or repair rates will occur. Enhanced gene-specific repair could explain some of the controversial results found in such investigations. While preferential repair of the interstrand cross-link in active versus

inactive regions was not found in Chinese hamster ovary cells,<sup>49</sup> it was demonstrated in resistant human ovarian 2008 cells.<sup>50</sup>

It was observed that some cisplatin-resistant cell may have higher DNA platination than parental cells,<sup>51</sup> or may tolerate several fold more platinum on their DNA at equitoxic concentrations as sensitive cells.<sup>52,53</sup> Considering these facts, the concept of enhanced tolerance to DNA damage was suggested as a potential mechanism of resistance. However, the basis of this phenomenon is not well understood.

Several groups have described DNA-binding proteins that retard the mobility of cisplatin-damaged DNA fragments in non-denaturing polyacrylamide gels. It has been hypothesized that these proteins are either involved in DNA repair by shielding adducts from repair, or are involved in transcription.<sup>54</sup> A number of cisplatin-resistant cells have been investigated for changes in these DNA damage-recognition proteins.<sup>22</sup> However, no obvious correlation between the expression of DNA damage-recognition proteins and resistance to cisplatin was found.

Some of the recent papers suggest that resistance to DNA damage can be acquired via the loss of DNA mismatched repair activity. The DNA mismatch repair system acts after DNA replication and corrects non-Watson-Crick base pair and other replication errors. Human cells lacking mismatch repair activity have high spontaneous mutation rates. Also, they may be resistant to certain cytostatics, such as etoposide,<sup>55</sup> cisplatin<sup>56</sup> or N-methyl-N-nitro-N-nitrosoguanidine.<sup>57</sup>

### DNA topoisomerase

Besides MDR, some resistant cell lines exhibit atypical multidrug resistance (at-MDR). At-MDR is distinguished from the MDR in the following ways: a) lack of cross-resistance to the *Vinca* alkaloids,<sup>58</sup> b) absence of a drug

accumulation defect,<sup>58</sup> c) relative insensitivity to modulation of resistance by verapamil or chloroquine typical inhibitors of P-glycoprotein,<sup>59</sup> and d) lack of overexpression of the MDR1 gene or its product, Pgp.<sup>59</sup>

At-MDR involves altered activity of topoisomerases II. Topoisomerases II are enzymes that catalyze changes in the secondary and tertiary structures of DNA. They are necessary for replication, recombination and transcription, as well as in mitotic chromosome condensation and segregation. Topoisomerases II act via introduction of a transient double-stranded break in one segment of a DNA molecule through which a second DNA duplex is passed before religation of the break.<sup>60</sup>

The levels of these enzymes are markedly higher in exponentially growing than in quiescent cell lines. Two distinct forms of topoisomerase II exist in human cells, termed  $\alpha$  (170 kDa form) and  $\beta$  (180 kDa form).<sup>61</sup> They differ not only in molecular weight but also in their patterns of expression and their apparent sensitivity to anticancer drugs.<sup>62</sup> In cell lines the expression of the  $\alpha$  isoform has been shown to be strictly proliferation dependent, whereas the  $\beta$  isoform is presented in both dividing and non-dividing cells.

There are some inhibitors of topoisomerase II (doxorubicin, epirubicin, mitoxantrone, etoposide, teniposide) that trap the "cleavable complex" resulting in increased DNA scissions and inhibition of rejoining.<sup>60,63,64</sup> These protein-associated DNA lesions are directly toxic to cells. The cells with a high level of topoisomerase II are generally more sensitive to inhibitors than cells with a low level of these enzymes.

There is a number of rodent and human tumor cells lines in which resistance to topoisomerase II inhibitors are connected with decreased level of the topoisomerase II  $\alpha$  and/or  $\beta$ . The resistance mechanisms appear to be the result of a decrease in the activity of topoisomerase II.<sup>63-68</sup>

Beside topoisomerase II, drug resistance may involve the altered activity of topoisomerase I. Topoisomerase I is an enzyme abundant in actively transcribing gene regions. It has important role in DNA replication and elongation step of transcription. Contrary to topoisomerase II, topoisomerase I introduce a transient single-stranded nick in DNA and is ATP independent. Several cytostatics, such as camptothecins and actinomycin D are the poisons of topoisomerase I.<sup>60,63,64</sup> Drug induced accumulation of topoisomerase I-DNA cleavable complex is directly proportional to drug cytotoxicity and anti-tumor activity. Resistance to topoisomerase I inhibitors involves altered activity of this enzyme, that may be caused by mutation(s) in the gene coding for topoisomerase I.<sup>69</sup>

### **Oncogenes and tumor suppresser genes: signal transduction pathway and apoptosis**

In last few years interest has been focused on oncogenes and their role in drug-resistance. The direct evidence that oncogenes can be involved in drug-resistance came from transfection studies. The transfection of murine NIH3T3 cells<sup>70,71</sup> or kerytocytes<sup>72</sup> with *ras* oncogene resulted in resistance to cisplatin. *Ras* oncogene may induce resistance to doxorubicin as well.<sup>73</sup> Moreover it was found that the degree of cisplatin resistance correlated directly with the level of *c-myc* expression,<sup>74,75</sup> while the re-establishment of the normal level of *c-myc* transcription restored original sensitivity.<sup>74</sup> *C-myc* oncogene was also involved in resistance to methotrexate.<sup>76</sup> Using ribosome mediated cleavage of *c-fos* mRNA, the role of *c-fos* oncogene in resistance to cisplatin was proved.<sup>77</sup> Resistance to cisplatin was achieved by the transfection of *src* oncogene as well.<sup>78</sup>

The mechanisms by which oncogenes cause drug-resistance is not quite clear.<sup>79</sup> It has been suggested that *c-myc* oncogene

binds to DNA, and thus directly or indirectly regulates a process of DNA repair.<sup>74</sup> *Ras* oncogene might induce resistance by regulating the expression of other genes involved in the protection of cell against cytostatics. It was shown for glutathione transferase pi,<sup>80</sup> topoisomerase II,<sup>81</sup> *c-jun*,<sup>82</sup> glutathione,<sup>83</sup> MDR,<sup>84</sup> or altered membrane potential.<sup>85</sup> Scanlon hypothesized that *fos* expression is the trigger that causes the resistance response (primary DNA reparability, as indicated by DNA polymerase  $\alpha$ , DNA polymerase  $\beta$ , thymidilate synthase, DHFR and topoisomerase I expression). Consistent with this concept is the observation that transfection of sensitive cells with *c-fos* generated ethold resistance to cisplatin,<sup>77</sup> while attenuation of the elevated *c-fos* expression returned the cisplatin toxicity to that of parent population. Another oncogene, mutated *p53*, may confer resistance to many hydrophobic drugs by stimulating specifically MDR1 promoter.<sup>84</sup>

It must be mentioned, however, that not always an increased expression of *ras*, *myc* or other oncogenes caused an increased resistance to cytostatics.<sup>75,86-88</sup>

In many cases the cellular damage caused by active doses of drug is not sufficient to explain the observed toxicity. Therefore, it is possible that some determinants of inherent drug sensitivity and resistance may be independent of those which involve the formation of the drug-target complex and its immediate biochemical sequel, such as commitment to cell death. Cell death is activated by natural control processes whose function is to allow repair of low level damage to DNA while eliminating those cells in which repair is not possible. There are two modes of cell death: apoptosis and necrosis. They differ morphologically and biochemically. Necrosis is associated with cell swelling, rupture of membranes and dissolution of organized structure. That is a consequence of the loss of osmoregulation. DNA degradation occurs at

a late stage. In contrast, in apoptosis internucleosomal cleavage of genomic DNA and chromatin condensation precedes the loss of membrane integrity (Figure 2). Necrosis mostly results from a major cell insult such as that caused by serious mechanical, ischemic, or toxic damage. Apoptosis generally occurs as a response to less severe injury and is also involved in the development and remodeling of normal tissue.<sup>89,90</sup>

Apoptosis induces a wide variety of cell stresses and cytotoxic chemicals,<sup>89,90</sup> among them anticancer drugs.<sup>91-94</sup> Deregulation of normally integrated cell cycle progression appears a central signalling event in most forms of apoptosis.<sup>90</sup>

Apoptosis is a highly conserved active mechanism that requires the expression of several specific genes. Also their exact function is not quite understood, certain genes have been proposed as positive (*p53*, *c-fos*, *c-myc*, interleukin-1 converting enzyme etc.) or negative regulatory elements (*bcl-2* or glutathione redox cycle). They induce or prevent the onset of apoptosis.<sup>95-103</sup> Among them, *p53* and *bcl-2* are the most important and most studied.

*p53* protein can function as a genetic switch capable of activating  $G_1$  arrest, resulting in the repair of DNA damage.<sup>94</sup> Also, it is

required for efficient activation of apoptosis following irradiation or treatment with chemicals. Loss of *p53* function has been reported to increase resistance of tumor cells to a variety of cytotoxic drugs.<sup>95,96</sup> Recently it was shown that cells with mutated *p53* gene display perturbed  $G_1$  arrest or apoptosis. This defect appears to reduce the sensitivity to DNA-damaging agents, suggesting that inhibition of apoptosis may represent a mechanism by which tumor cells may acquire drug-resistance.<sup>95,96</sup> By transfer of normal *p53* into *p53*-defective non-small cell cancer line, an important increase in sensitivity to cisplatin was determined, which was related to the promotion of apoptosis.<sup>97</sup> However, the paper recently published by Wosikowski *et al.* suggests that alterations in *p53* gene status or protein functions are not critical for the development of multidrug resistance.<sup>98</sup>

On the other hand, *Bcl-2* protein inhibits apoptosis<sup>99,100</sup> and increases cell resistance to drugs.<sup>101</sup> Recently, *bcl-2* related gene products have been reported. One of them, *Bax*, homodimerizes as well as heterodimerizes with *Bcl-2* protein. The *Bcl-2*:*Bax* ratio may determine survival or death after an apoptotic stimulus.<sup>102</sup>

Therefore, oncogenes and tumor suppressor genes may be involved in drug resistance in two ways: by increasing the level of protective molecules in cells or by inhibiting apoptosis.

### Other factors

In doxorubicin treated cells an altered pattern of intracellular drug distribution was observed. The initial accumulation of drug in perinuclear location was followed by the development of a punctate pattern of the drug scattered throughout the cytoplasm. This pattern was suggestive of a process of drug sequestration, possibly followed by vesicle transport. In resistant cells, alteration in

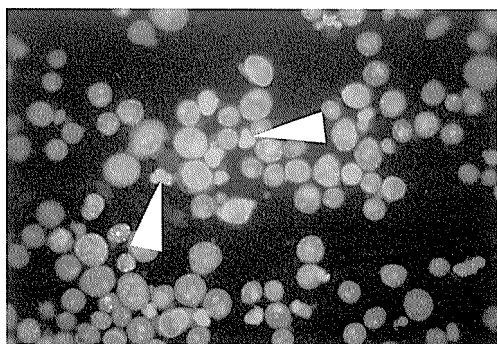


**Figure 2.** HeLa cells obtained 48 hours after a 1-hour treatment with 150  $\mu$ M cisplatin. Apoptotic cells showed typical chromatin condensation, fragmented nuclei and cellular shrinkage (arrowhead), while intact nuclei exhibit "mottled" fluorescence. From reference <sup>91</sup>.

the intracellular drug distribution was accompanied by a decrease in nuclear *versus* cytoplasm drug ratio.<sup>104,105</sup>

There is more and more evidence, that drug resistance is a multifactorial phenomenon (only for very low doses of the drug a single mechanism can be involved in drug-resistance. Thus, for instance, in cells resistant to cisplatin altered drug accumulation, increased levels of glutathione and related enzymes, metallothioneins, increased repair and altered expression of oncogenes could be observed.<sup>21,22,39,40</sup> In methotrexate resistant cells, decreased uptake of this drug, decreased polyglutamation, decreased affinity to DHFR and increased levels of target enzyme are the most common cause of drug resistance to MTX.<sup>106</sup> It should be mentioned, however, that all of these mechanisms need not be induced in drug resistant cells. So, in cisplatin resistant human laryngeal carcinoma cells only decreased platinum accumulation was connected with resistance to cisplatin, while no alteration in oncogene expression, no involvement of glutathione, glutathione transferase or metallothioneins was determined.<sup>40,87</sup>

Due to induction of several protective molecular mechanisms, resistant cells obtained after treatment with a single drug, can become resistant to various unrelated drugs (Table 4). The schedule of drug-resistance development can also influence the resistance pattern. Even with the same treatment schedule, clones with different cross-resistance patterns occur.<sup>109</sup>

It is generally accepted that the resistance to drugs can be induced by treatment with chemicals. However, in last several years it became obvious that also ionizing irradiation can induce drug resistance in irradiated cells<sup>110-114</sup> by the same mechanisms that are involved in resistance development induced by cytostatics.<sup>112,114-120</sup> This fact, if supported *in vivo*, and specially in clinic, is of the utmost importance for the patients. Namely, if irradiation precedes chemotherapy, it can reduce the success of combined therapy.

In conclusion, drug resistance is a complex, multifactorial phenomenon, which may involve decreased intracellular drug accumulation, increased detoxification, increased DNA repair, decreased activity of topoisomerases, gene amplification, altered onco-

**Table 4.** Drug sensitivity pattern of resistant cell lines

Cell line	Drug used for resistance development	Treatment schedule	Resistant to	Sensitive to
Laryngeal carcinoma <sup>1</sup>	vincristine	acute continuous	DOX, MTX DOX, MTX, 5-FU	CDDP CDDP
Cervical carcinoma <sup>2</sup>	cisplatin	acute continuous	VCR, DOX, ETO, MTX, 5-FU VCR, MTX	
Laryngeal carcinoma <sup>3</sup>	cisplatin	acute continuous	VCR, MMC VCR, MMC, 5-FU	ETO, DOX
Breast adeno-carcinoma <sup>4</sup>		doxorubicin	continuous	VCR, VBL, CDDP, CBDCA, (MMC, 5-FU)*

<sup>1</sup> reference 107, <sup>2</sup> reference 39, <sup>3</sup> reference 108, <sup>4</sup> reference 88.

\* Significant resistance only at higher doses.

Acute = 1 hour treatment; continuous = 24 hours treatment

VCR= vincristine, VBL= vinblastine, DOX = doxorubicin, ETO = etoposide, MTX = methotrexate, 5-FU = 5-fluorouracil, CDDP= cisplatin, CBDCA= carboplatin, MMC= mitomycin C.

gene and tumor suppressor gene expression, as well as inhibition of apoptosis. Resistance pattern of anticancer drugs is determined by the a) genotype of the cells, b) genotoxic agent involved in resistance development, and c) treatment schedule. The complexity of drug-resistance mechanisms, as well as sometimes conflicting experimental data suggest the need to continue such investigation and clarify the cascade of events involved in this process.

## References

- Farber S, Diamond LK, Mercer RD, Sylvester RF, Wolff JA. Temporary remission in acute leukemia in children produced by folic acid antagonist, 4-aminopteroyl - glutamic acid (aminopterin). *N Engl J Med* 1948; **238**: 787-93
- Endicott JA, Ling V. The biochemistry of P-glycoprotein mediated multidrug resistance. *Ann Rev Biochem* 1989; **58**: 137-71.
- Kayne SB. Multidrug resistance. *Oncology Today* 1990; **2**: 4-7.
- Gottesman MM, Pastan I. Biochemistry of multidrug resistance mediated by the multidrug transporter. *Ann Rev Biochem* 1993; **62**: 385-429.
- Ueda K, Cardarelli C, Gottesman MM, Pastan I. Expression of a full length cDNA for the human "MDR1" gene confers resistance to colchicine, doxorubicin and vinblastine. *Proc Natl Acad USA* 1987; **84**: 3004-8.
- Gerlach JH, Endicott JA, Jurakna PE, Henderson G, Sarangi F, Deuchars KL, Ling V. Homology between P-glycoprotein and a bacterial haemolysin transport protein suggests a model for multidrug resistance. *Nature* 1986; **324**: 485-9.
- Nielsen D, Skovgaard T. P-glycoprotein as multidrug transporter: a critical review of current multidrug resistant cell lines. *Biochem Biophys Acta* 1992; **1139**: 169-83.
- Cole SPC, Bhardwaj G, Gerlach JH, Mackie JE, Grant CE, Almquist KC, Stewart AJ, Kurz EU, Duncan AMV, Deeley RG. Overexpression of a transporter gene in a multidrug-resistant human lung cancer cell line. *Science* (Washington DC) 1992; **258**: 1650-4.
- Loe DW, Deeley RG, Cole SPC. Biology of the multidrug resistance-associated protein, MRP. *Eur J Cancer* 1996; **32A**: 945-57.
- Grant CE, Valdimarsson G, Hipfner DR, Almquist KC, Cole SPC, Deeley RG. Overexpression of multidrug resistance-associated protein (MRP) increases resistance to natural product drugs. *Cancer Res* 1994; **54**: 357-61.
- Slapak CA, Mizunuma N, Kufe DW. Expression of the multidrug resistance-associated protein and P-glycoprotein in doxorubicin-selected human myeloid leukemia cells. *Blood* 1994; **84**: 3113-21.
- Brock I, Hipfner DR, Nielsen BS, Jensen PB, Deeley RG, Cole SPC, Sehested M. Sequential coexpression of the multidrug resistance genes *MRP* and *mdr1* and their products in VP-16 (Etoposide)-selected H69 small cell lung cancer cells. *Cancer Res* 1995; **55**: 459-62.
- Goldenberg GJ, Vanstone CL, Israels LG, Ilse D, Bihler I. Evidence of a transport carrier of nitrogen mustard-sensitive and -resistant L5178Y lymphoblasts. *Cancer Res* 1970; **30**: 2258-91.
- Sirotnak FM, Maccio DM, Kelleher LE, Goutas LJ. Relative frequency and kinetic properties of transport-defective phenotypes among methotrexate-resistant L-1210 clonal cell lines derived in vivo. *Cancer Res* 1981; **41**: 4447-52.
- Shionoya S, Lu Y, Scanlon KJ. Properties of amino acid transport system in K 562 cells sensitive and resistant to cis-diamminedichloroplatinum(II). *Cancer Res* 1986; **46**: 3445-8.
- Meister A. Glutathione, ascorbate, and cellular protection. *Cancer Res* 1994; **54**: 1969s-75s.
- Morris PE, Gordon RB. Significance of glutathione in lung disease and implications for therapy. *Amer J Med Sci* 1994; **307**: 119-27.
- Suzakake K, Petro BJ, Vistica DT. Reduction in glutathione content of L-PAM resistant L1210 cells confers drug sensitivity. *Biochem Pharmacol* 1982; **31**: 121-4.
- Mitchell JB, Russo A. The role of glutathione in radiation and drug induced cytotoxicity. *Br J Cancer* 1987; **55**: 96-104.
- Ahmad S, Okine L, Le B, Najarian P, Vistica DT. Elevation of glutathione in phenylalanine mustard-resistant murine L1210 leukemia cells. *J Biol Chem* 1987; **262**: 15048-53.
- Scanlon KJ, Kashani-Sabet M, Tone T, Funato T. Cisplatin resistance in human cancers. *Pharmac Ther* 1991; **52**: 385-406.
- Andrew PA. Mechanisms of acquired resistance to cisplatin. In: *Anticancer Drug Resistance: Advances in Molecular and clinical Research* (Goldstein LJ and Ozols RF, eds.) Kluwer Academic Publishers, 1994, 217-48.
- Lee FYF, Siemann DW. Isolation by flow cytometry of a human ovarian tumor cell subpopulation exhibiting a high glutathione content phenotype

- and increased resistance to Adriamycin. *Int J Radiat Oncol Biol Phys* 1989; **16**: 1315-9.
24. Lai GM, Ozols RF, Young RC, Hamilton TC. Effect of glutathione on DNA repair in cisplatin-resistant human ovarian cancer cell lines. *J Nat Cancer Inst* 1989; **81**: 535-9.
  25. Hamilton TC, Winker MA, Louie KG, Batist G, Behrens BC, Tsuruo T, Grotzinger KR, Mc Koy WM, Young RC, Ozols RF. Augmentation of Adriamycin, melphalan, and cisplatin cytotoxicity in drug-resistant and drug-sensitive human ovarian carcinoma cell lines by buthionine sulfoximine mediated glutathione depletion. *Biochem Pharmacol* 1985; **34**: 2583-6.
  26. Barranco SC, Townsend CM Jr, Weintraub B, Beasley EG, McLean KK, Shaeffer J, Liu NH, Schellenberg K. Changes in glutathione content and resistance to anticancer agents in human stomach cancer cells induced by treatment with melphalan in vitro. *Cancer Res* 1990; **50**: 3614-8.
  27. Tew K. Glutathione-associated enzymes in anticancer drug resistance. *Cancer Res* 1994; **54**: 4313-20.
  28. Waxman DJ. Glutathione S-transferases: role in alkylating agent resistance and possible target for modulation chemotherapy- A review. *Cancer Res* 1990; **50**: 6449-54.
  29. Gulick AM, Fahl WE. Mammalian glutathione S-transferase: regulation of an enzyme system to achieve chemotherapeutic efficacy. *Pharmacol Ther* 1995; **66**: 237-57.
  30. Moscow JA, Fairchild CR, Madden MJ, Ransom DT, Wieand HS, O'Brien EE, Poplack DG, Cossman J, Myers CE, Cowan KH. Expression of anionic glutathione S-transferase and P-glycoprotein genes in human tissues and tumors. *Cancer Res* 1989; **49**: 1422-8.
  31. Howie AF, Forrester LM, Glancey MJ, Schlager JJ, Powis G, Beckett GJ, Hayes JD, Wolf CR. Glutathione S-transferase and glutathione peroxidase expression in normal and tumor human tissues. *Carcinogenesis* 1990; **11**: 451-8.
  32. Puchalski RB, Fahl WE. Expression of recombinant glutathione transferase p, Ya, or Yb confers resistance to alkylating agents. *Proc Natl Acad Sci USA* 1990; **87**: 2443-7.
  33. Batist G, Tople A, Sinha BK, Katki AG, Myers CE, Cowan KH. Overexpression of a novel anionic glutathione transferase in multidrug resistant breast cancer cells. *J Biol Chem* 1986; **33**: 15544-9.
  34. Kramer RA, Zakher J, Kim G. Role of glutathione redox cycle in acquired and de novo multidrug resistance. *Science* 1988; **241**: 694-7.
  35. Hamer DH. Metallothionein <sup>1,2</sup>. *Ann Rev Biochem* 1986; **55**: 913-51.
  36. Moffatt P, Denizeau F. Metallothionein in physiological and physiopathological processes. *Drug Metabol Rev* 1997; **29**: 261-307.
  37. Bakka A, Endersen L, Johnsen ABS, Edminson PD, Rugstad HE. Resistance against cis-dichlorodiammineplatinum in cultured cells with a high content of metallothionein. *Toxicol Appl Pharmacol* 1981; **61**: 215-26.
  38. Kelley SL, Basu A, Tiecher B, Hacker MP, Hamer DH, Lazo JS. Overexpression of metallothionein confers resistance to anticancer drugs. *Science* 1988; **241**: 1813-5.
  39. Osmak M, Eljuga D. The characterization of two human cervical carcinoma HeLa sublines resistant to cisplatin. *Res Exp Med* 1993; **193**: 389-96.
  40. Beketić-Orešković L, Osmak M, Jakšić M. Human larynx carcinoma cells resistant to cis-diamminedichloroplatinum(II): Mechanisms involved in resistance. *Neoplasma* 1994; **41**: 163-9.
  41. Kaina B, Lohrer H, Karin M, Herrlich P. Overexpressed human metallothionein IIA gene protects Chinese hamster ovary cells from killing by alkylating agents. *Proc Natl Acad Sci USA* 1990; **87**: 2710-4.
  42. Schilder RJ, Hall L, Monks A, Fornace AJ Jr, Ozols RF, Fojo AT, Hamilton TC. Metallothionein gene expression and resistance to cisplatin in human ovarian cancer. *Int J Cancer* 1990; **45**: 416-22.
  43. Kondo Y, Woo ES, Michalska AE, Choo KHA, Lazo JS. Metallothionein null cells have increased sensitivity to anticancer drugs. *Cancer Res* 1995; **55**: 2021-3.
  44. Biedler JL, Spengler BA. Metaphase chromosome anomaly association with drug resistance and cell specific products. *Science* 1976; **191**: 185-7.
  45. Alt FW, Kellems RE, Bertino JR, Schimke RT. Selective multiplication of dihydrofolate reductase genes in methotrexate-resistant variants of cultured murine cells. *J Biol Chem* 1978; **253**: 1357-70.
  46. Schimke RT. Gene amplification in cultured animal cells. *Cell* 1984; **37**: 705-13.
  47. Eastman A, Schulte N. Enhanced DNA repair as a mechanism of resistance to DNA cis-diamminedichloroplatinum(II). *Biochemistry* 1988; **27**: 4730-4.
  48. Sheibani N, Jennerwein MM, Eastman A. DNA repair in cells sensitive and resistant to cis-diamminedichloroplatinum(II): host cell reactivation of damaged plasmid DNA. *Biochemistry* 1989; **28**: 3120-4.
  49. Jones JC, Zhen W, Reed E, Parker RJ, Sancar A, Bohr VA. Gene-specific formation and repair of cisplatin intrastrand adducts and interstrand cross-links in Chinese hamster ovary cells. *J Biol Chem* 1991; **266**: 7101-7.
  50. Zhen W, Link CJ Jr, O'Connor PM, Reed E, Parker

- R, Howell SB, Bohr VA. Increased gene-specific repair of cisplatin interstrand cross-links in cisplatin-resistant human ovarian cancer cell lines. *Mol Cell Biol* 1992; **12**: 3689-98.
51. Strandberg MC, Bresnick E, Eastman A. The significance of DNA cross-linking to *cis*-diaminedichloroplatinum(II)-induced cytotoxicity in sensitive and resistant lines of murine leukemia L1210 cells. *Chem Biol Interact* 1982; **39**: 169-80.
52. Parker RJ, Eastman A, Bostick-Bruton F, Reed E. Acquired cisplatin resistance in human ovarian cancer cells is associated with enhanced repair of cisplatin-DNA lesions and reduced drug accumulation. *J Clin Invest* 1991; **87**: 772-7.
53. Johnson SW, Laub PB, Beesley JS, Ozols RF, Hamilton TC. Increased platinum-DNA damage tolerance is associated with cisplatin resistance and cross-resistance to various chemotherapeutic agents in unrelated human ovarian cancer cell lines. *Cancer Res* 1997; **57**: 850-6.
54. Donahue BA, Augot M, Bellon SF, Treiber DK, Toney JH, Lippard SJ. Characterization of a DNA damage-recognition protein from mammalian cells that binds to intra-strand d(GpG) and d(ApG) DNA adducts of the anticancer drug cisplatin. *Biochemistry* 1990; **29**: 5872-80.
55. De las Alas MM, Aebi S, Fink D, Howell SB, Los G. Loss of DNA mismatch repair: effects on the rate of mutation to drug resistance. *J Natl Cancer Inst* 1997; **89**: 1537-41.
56. Fink D, Zheng H, Nebel S, Norris PS, Aebi S, Lin TP, Nehme A, Christen RD, Haas M, MacLeod CL, Howell SB. In vitro and in vivo resistance to cisplatin in cells that have lost DNA mismatch repair. *Cancer Res* 1997; **57**: 1941-5.
57. Umar A, Koi M, Risinger JI, Glaab WE, Tindall KR, Kolodner RD, Boland CR, Rarrett JC, Kunkel TA. Correction of hypermutability, N-methyl-N-nitro-N-nitroso-guanidine resistance, and defective DNA mismatch repair by introducing chromosome 2 into human tumor cells with mutations in MSH2 and MSH6. *Cancer Res* 1997; **57**: 3949-55.
58. Danks MK, Yalowich JC, Beck WT. Atypical multiple drug resistance in a human leukemic cell line selected for resistance to teniposide (VM-26). *Cancer Res* 1987; **47**: 1297-301.
59. Beck WT, Cirtain MC, Danks MK, Felsted RL, Safa AR, Wolverton JS, Suttle DP, Trent JM. Pharmacological, molecular and cytogenetic analysis of "typical" multidrug-resistant human leukemic cells. *Cancer Res* 1987; **47**: 5455-60.
60. Liu LF. DNA topoisomerase poisons as antitumor drugs. *Annu Rev Biochem* 1989; **58**: 351-75.
61. Drake FH, Hofmann GA, Bartus HF, Mattern MR, Crooke ST, Mirabelli CK. Biochemical and pharmacological properties of p170 and p180 forms of topoisomerase II. *Biochem* 1989; **28**: 8154-60.
62. Woessner RD, Mattern MR, Mirabelli CK, Johnson RK, Drake FH. Proliferation- and cycle-dependent differences in expression of the 170 kDa and 180 kDa forms of topoisomerase II in NIH 3T3 cells. *Cell Growth Different* 1991; **2**: 209-14.
63. Smith PJ. Topoisomerase inhibitors: new twists to anticancer drug action. *Oncology Today* 1991; **3**: 4-9.
64. Pommier Y. DNA topoisomerase I and II in cancer chemotherapy. *Cancer Chemother Pharmacol* 1993; **32**: 103-8.
65. Glisson B, Gupta R, Smallwood-Kent S, Ross W. Characterisation of acquired epipodophyllotoxins resistance in a Chinese hamster ovary cell line: loss of drug-stimulated DNA cleavage activity. *Cancer Res* 1986; **46**: 1934-8.
66. Davies SM, Robson CN, Davies SL, Hickson ID. Nuclear topoisomerase levels correlate with sensitivity of mammalian cells to intercalating agents and epipodophyllotoxins. *J Biol Chem* 1988; **263**: 17724-72.
67. Deffie AM, Bosman DJ, Goldenberg GJ. Evidence for a mutant allele of the gene for DNA topoisomerase II in adriamycin-resistant P388 murine leukemia cells. *Cancer Res* 1989; **49**: 6879-82.
68. Beck WT, Danks MK, Wolverton JS, Kim R, Chen M. Drug resistance associated with altered DNA topoisomerase II. *Adv Enzyme Regul* 1993; **33**: 113-27.
69. Wang LF, Ting CY, Lo CK, Su JS, Mickley LA, Fojo AT, Whang-Peng J, Hwang J. Identification of mutations at DNA topoisomerase I responsible for camptothecin resistance. *Cancer Res* 1997; **57**: 1516-22.
70. Sklar M. Increased resistance to *cis*-diaminedichloroplatinum(II) in NIH3T3 cells transformed by *ras* oncogenes. *Cancer Res* 1988; **48**: 793-7.
71. Ishonishi S, Hom DK, Thiebaut FB, Mann SC, Andrews PA, Basu A, Laso JS, Eastman A, Howell SB. Expression of the c-Ha-ras oncogene in mouse NIH3T3 cells induces resistance to cisplatin. *Cancer Res* 1991; **51**: 5903-9.
72. Sanchez-Prieto R, Vargas JA, Carnero A, Marchetti E, Romero J, Duran A, Lacal JC, Cajal SR. Modulation of cellular chemoresistance in keratinocytes by activation of different oncogenes. *Int J Cancer* 1995; **60**: 235-43.
73. Peters GJ, Wets M, Keepers YPAM, Oskam R, Van Ark-Otte J, Noordhuis P, Smid K, Pinedo HM. Transformation of mouse fibroblasts with the oncogenes *H-ras* or *trk* is associated with pronounced changes in drug sensitivity and metabolism. *Int J Cancer* 1993; **54**: 450-5.
74. Sklar MD, Prochownik EV. Modulation of cisplatin resistance in Friend erythroleukemia cells by *c-myc*. *Cancer Res* 1991; **51**: 2118-23.



75. Niimi SK, Nakagawa K, Yokota J, Tsunokawa Y, Nishio K, Terashima Y, Shibuya M, Terada M, Saijo N. Resistance to anticancer drugs in NIH3T3 cells transformed with *c-myc* and/or *c-Ha-ras* genes. *Br J Cancer* 1991; **63**: 237-41.
76. Denis NA, Kitzis A, Kruh J, Dautry F, Corcos D. Stimulation of methotrexate resistance and dihydrofolate reductase gene amplification by *c-myc*. *Oncogene* 1991; **6**: 1433-57.
77. Scanlon KJ, Jiao L, Funato T, Wang W, Tone T, Rossi JJ, Kashani-Sabet M. Ribozyme mediated cleavage of *c-fos* mRNA reduces gene expression of DNA synthesis enzymes and metallothioneins. *Proc Natl Acad Sci USA* 1991; **88**: 10591-5.
78. Masumoto N, Nakano S. Cell signaling and CDDP resistance. *Gan To Kagaku Ryoho* 1997; **24**: 424-30.
79. El-Deiry WS. Role of oncogenes in resistance and killing by cancer therapeutic agents. *Curr Opin Oncol* 1997; **9**: 79-87.
80. Burt RK, Garfield S, Johnson K, Thorgerirsson SS. Transformation of rat liver epithelial cells with *v-Ha-ras* or *v-raf* causes expression of MDR-1, glutathione-S-transferase-P and increased resistance to cytotoxic chemicals. *Carcinogenesis* 1988; **9**: 2329-32.
81. Woessner RD, Chung TDY, Hofmann GA, Matern MR, Mirabelli CK, Drake FH, Johnson RK. Differences between normal and *ras*-transformed NIH 3T3 cells in expression of the 170 kD and 180 kD forms of topoisomerase II. *Cancer Res* 1990; **50**: 2901-8.
82. Binetruy B, Smeal T, Karin M. *Ha-ras* augments *c-jun* activity and stimulates phosphorylation of its active domain. *Nature* 1991; **351**: 122-7.
83. Thrall BD, Meadows GG. Induction of glutathione content in murine melanocytes after transformation with *c-Ha-ras* oncogene. *Carcinogenesis* 1991; **12**: 1319-23.
84. Chin KV, Ueda K, Pastan I, Gottesman MM. Modulation of activity of the promoter of the human *mdr1* gene by *ras* and *p53*. *Science* 1992; **255**: 459-62.
85. Spalletticernia D, Dagnano I, Salvatore C, Portella G, Zupi G, Vecchio G, Lancetti P. Transformation by *v-ras* oncogene correlates with an increased drug resistance in an epithelial thyroid cell system. *Int J Oncol* 1995; **6**: 647-54.
86. Toffoli G, Viel A, Tumioto L, Buttazzi P, Biscontin G, Boiocchi M. Sensitivity pattern of normal and *H-ras* transformed NIH3T3 fibroblasts to antineoplastic drugs. *Tumori* 1989; **75**: 423-8.
87. Osmak M, Beketić-Orešković L, Matulić M, Sorić J. Resistance of human larynx carcinoma cells to cisplatin, gamma irradiation and methotrexate do not involve overexpression of *c-myc* or *c-Ki-ras* oncogenes. *Mutat Res* 1993; **303**: 113-20.
88. Osmak M, Kapitanović S, Vrhovec I, Beketić-Orešković L, Jernej B, Eljuga D, Škrk J. Characterization of human breast adenocarcinoma SK-BR-3 cells resistant to doxorubicin. *Neoplasma* 1997; **44**: 157-62.
89. Vaux DL. Toward an understanding of the molecular mechanisms of physiological cell death. *Proc Natl Acad Sci USA* 1993; **90**: 786-9.
90. Smets LA. Programmed cell death (apoptosis) and response to anti-cancer drugs. *Anti-Cancer Drugs* 1994; **5**: 3-9.
91. Osmak M, Abramić M, Brozović A, Hadžija M. Cell response to low repeated doses of ionising radiation: inhibition of apoptosis in cisplatin treated human cells. *Period Biol* 1997; **99**: 329-33.
92. Barry MA, Behnke CA, Eastman A. Activation of programmed cell death (apoptosis) by cisplatin, other anticancer drugs, toxins and hyperthermia. *Biochem Pharmacol* 1990; **40**: 2353-62.
93. Evans DL, Dive C 1993 Effects of cisplatin on the induction of apoptosis in proliferating hepatoma cells and nonproliferating immature thymocytes. *Cancer Res* 1993; **55**: 2133-9.
94. Lane DP. P53, guardian of the genome. *Nature* 1992; **358**: 15-16.
95. Lowe SW, Ruley HE, Jacks T, Houseman DE p53-dependent apoptosis modulates the cytotoxicity of anticancer agents. *Cell* 1993; **74**: 957-67.
96. Anthony DA, McIlwrath AJ, Gallanger WM, Edlin ARM, Brown R. Microsatellite instability, apoptosis and loss of p53 function in drug-resistant tumor cells. *Cancer Res* 1996; **56**: 1374-81.
97. Fujiwara T, Grimm EA, Mukhopadhyay T, Zhang W-W, Owen-Schaub LB, Roth JA. Induction of chemosensitivity in human lung cancer cells in vivo by adenovirus - mediated transfer of the wild-type p53 gene. *Cancer Res* 1994; **54**: 2287-91.
98. Wosikowski K, Regis JT, Robey RW, Alvarez M, Buters JTM, Gudas JM, Bates SE. Normal p53 status and function despite the development of drug resistance in human breast cancer cells. *Cell Growth Different* 1995; **6**: 1395- 403.
99. Hockenbery DM, Nunez G, Millman C, Schreiber RD, Korsmeyer SJ. Bcl-2 is an inner mitochondrial membrane protein that blocks programmed cell death. *Nature* 1990; **348**: 334-6.
100. Reed JC. Bcl-2 and regulation of programmed cell death. *J Cell Biol* 1994; **124**: 1-6.
101. Miyashita T, Reed JC. Bcl-2 oncoprotein blocks chemotherapy induced apoptosis in a human leukemia cell line. *Blood* 1993; **81**: 151-7.
102. Yin X-M, Oltvai ZN, Korsmeyer SJ. BH1 and BH2 domains of Bcl-2 are required for inhibition of apoptosis and heterodimerization with Bax. *Nature* 1994; **369**: 609-19.

103. Zhao R, Rabo YB, Egyhazi S, Anderson A, Edgren MR, Linder S, Hansson J. Apoptosis and c-jun induction by cisplatin in a human melanoma cell line and drug-resistant daughter cell-line. *Anti-Cancer Drugs* 1995; **6**: 657-68.
104. Schuurhuis GJ, Broxterman HJ, de Lange JHM, Pinedo HM, van Heijningen THM, Kuiper CM, Scheffer GL, Scheper RJ, van Kalken CK, Baak JAP, Lankelma J. Early multidrug resistance, defined by changes in intracellular doxorubicin distribution, independent of P-glycoprotein. *Br J Cancer* 1991; **64**: 857-61.
105. Breuninger L, Saptarshi P, Gaughan K, Miki T, Chan A, Aaronson SA, Kruh GD. Expression of multidrug resistance-associated protein in NIH/3T3 cells confers multidrug resistance associated with increased drug efflux and altered intracellular drug distribution. *Cancer Res* 1995; **55**: 5342-27.
106. Borst P. Genetic mechanisms of drug resistance. *Acta Oncol* 1991; **4**: 87-105.
107. Osmak M, Eljuga D. The response of two vincristine resistant human larynx carcinoma cell clones to chemotherapeutic drugs. *Radiol Oncol* 1992; **26**: 140 - 4.
108. Beketić-Orešković L, Osmak M. Human larynx carcinoma cells resistant to cis-diamminedichloroplatinum(II): Cross-resistance pattern. *Neoplasma* 1994; **41**: 171-6.
109. Osmak M, Bizjak L, Jernej B, Kapitanović S. Characterization of carboplatin-resistant sublines derived from human larynx carcinoma cells. *Mutat Res* 1995; **347**: 141-50.
110. Osmak M. Repeated doses of gamma rays induce resistance to N-methyl-N-nitro-N-nitrosoguanidine in Chinese hamster cells. *Radiat Res* 1988; **115**: 609-16.
111. Osmak M, Perović S. Multiple fractions of gamma rays induced resistance to cis-dichlorodiammineplatinum (II) and methotrexate in human HeLa cells. *Int J Radiation Oncology Biol Phys* 1989; **16**: 1537-41.
112. Hill BT Interactions between antitumor agents and radiation and the expression of resistance. *Cancer Treatment Reviews* 1991; **18**: 149-90.
113. Osmak M, Horvat D. Chromosomal analysis of Chinese hamster V79 cells exposed to multiple gamma-ray fractions: induction of adaptive response to mitomycin C. *Mutat Res* 1992; **282**: 259-63.
114. Osmak M, Kapitanović S, Miljanić S. Low doses of gamma rays can induce the expression of *mdr* gene. *Mutat Res* 1994; **324**: 35-41.
115. Mattern J, Effert T, Volm M. Overexpression of P-glycoprotein in human lung carcinoma xenografts after fractionated irradiation in vivo. *Radiat Res* 1991; **127**: 335-8.
116. Osmak M, Užarević B. Mechanisms involved in resistance of preirradiated Chinese hamster V79 cells to cytotoxic drugs are multifactorial. *Res Exp Med* 1991; **191**: 413-21.
117. Dempke WCM, Shellard SA, Hosking LK, Fichtinger-Schepmen AMJ, Hill BT. Mechanisms associated with the expression of cisplatin resistance in a human ovarian tumor cell line following exposure to fractionated X-irradiation. *Carcinogenesis* 1992; **13**: 1209-15.
118. McClean S, Whelm RDT, Hosking LK, Hodges GM, Thompson FH, Meyers MB, Schuurhuis GJ, Hill BT. Characterization of the P-glycoprotein over-expressing drug resistance phenotype exhibited by Chinese hamster ovary cells following their in-vitro exposure to fractionated X-irradiation. *Biochim Biophys Acta* 1993; **1177**: 117-26.
119. Osmak M. Multifactorial molecular mechanisms are involved in resistance of preirradiated human cervix carcinoma cells to cis-dichlorodiammineplatinum (II) and vincristine. *Neoplasma* 1993; **440**: 97-101.
120. Osmak M, Matulić M, Sorić J. Multiple fractions of gamma rays do not induce overexpression of *c-myc* or *c-Ki-ras* oncogenes in human cervical carcinoma cells. *Neoplasma* 1993; **40**: 359-62.



## Genetic polymorphisms of xenobiotic metabolizing enzymes in human colorectal cancer

Vita Dolžan<sup>1</sup>, Metka Ravnik-Glavac<sup>1,2</sup>, Katja Breskvar<sup>1</sup>

<sup>1</sup>Institute of Biochemistry, Medical Faculty, <sup>2</sup>Laboratory of Molecular Pathology, Institute of Pathology, Medical Faculty, Ljubljana, Slovenia

---

*It was proposed that both hereditary and environmental factors contribute to the development of colorectal cancer (CRC). Carcinogenic polycyclic aromatic hydrocarbons (PAHs) from food or tobacco smoke can form DNA adducts and thus initiate carcinogenesis after metabolic activation via cytochrome P4501A1 (CYP1A1). Intermediate metabolites are detoxified by conjugation with glutathione S-transferases. Our aim was to look for inherited metabolic susceptibility to CRC. We used PCR-based genotyping approach to determine the frequencies of polymorphic alleles of two cytochromes P450 (CYP2D6 and CYP1A1) and two glutathione S-transferases (GSTM1 and GSTT1) in DNA samples from 31 sporadic, 25 familial CRC cases and 73 healthy controls. The difference in frequencies of poor metabolisers due to CYP2D6 gene polymorphism was close to the limit of statistical significance between sporadic CRC and healthy control group ( $\chi^2 = 5.52$ ,  $m=2$ ,  $p=0.06$ ) despite the small sample size. The frequencies of either CYP1A1 MspI, GST M1 or GST T1 genotypes were not significantly different in both CRC cases and in controls. Although our study suggests some difference in metabolic susceptibility between sporadic and familial CRC, further studies are needed to investigate the combined effect of polymorphic genes involved in carcinogen metabolism in a larger group of patients with defined exposure to dietary carcinogens and smoking.*

*Key words: colorectal neoplasms-genetics; polymorphism (genetics); cytochrome P-450CYP1A1; cytochrome P-450 CYP2D6; glutathione transferases*

---

### Introduction

It is generally accepted that both hereditary and environmental factors contribute to the development of colorectal cancer (CRC). A genetic model for colorectal tumorigenesis

suggested by Faeron and Vogelstein proposed that colorectal tumors arise due to mutations in oncogenes and tumor suppressor genes.<sup>1</sup> The sequences of adenoma to carcinoma transition are well established.<sup>2</sup> However, the earliest events in human colorectal tumor formation are not well defined. As far as environmental factors are concerned a large proportion of human cancers is known to be caused by chemicals from the environment.<sup>3</sup>

Correspondence to: Dr. Vita Dolžan, MD, Institute of Biochemistry, Medical Faculty, Vrazov trg 2, 1000 Ljubljana, Slovenia. Phone: +386 61 1320 019; Fax: +386 61 1320 016; E-mail: dolzan@ibmi.mf.uni-lj.si

A strong association has been observed between colorectal cancer and consumption of broiled and grilled meat. Exposure of food to pyrolysis can lead to the formation of compounds such as polycyclic aromatic hydrocarbons (PAHs), heterocyclic amines and others.<sup>4</sup> In addition to diet, tobacco smoking was also associated with colorectal cancer.<sup>5</sup> It is possible that PAHs in food exposed to pyrolysis and in tobacco smoke can play a role in some of the genetic alterations leading to colorectal tumor development.<sup>5</sup>

Most environmental chemicals have to be metabolically activated to their ultimate carcinogenic form and individual differences in metabolism of precarcinogenic substances exist due to polymorphisms in many enzymes involved in this process. So, after sufficient exposure to carcinogen individual differences in its metabolism may result in different genetic susceptibility to the development of cancer.<sup>3</sup>

Carcinogens as well as other xenobiotics are usually metabolized in two consecutive steps. Phase I is an activation step and phase II is the detoxification step. Enzymes from the cytochrome P450 families 1, 2 and 3 (CYP1, CYP2 and CYP3 respectively) are the main enzymes involved in the oxidative activation of chemical compounds into reactive electrophilic form.<sup>3</sup> Among others, CYP1A1 is involved in activation of variety of chemical carcinogens to their ultimate carcinogenic forms, particularly PAHs from tobacco smoke and PAHs and aromatic amines from food exposed to pyrolysis. CYP2D6 is involved in metabolism of many drugs and yet undefined carcinogens from tobacco smoke.<sup>6</sup> In the detoxification reaction the activated substance is conjugated with some organic acid or intracellular glutathione to form inactive water-soluble metabolites. This reactions are mainly catalyzed by N-acetyl transferases (NATs) and glutathione S-transferases (GSTs). There are four known mammalian classes of soluble GSTs:  $\alpha$ ,  $\mu$ ,  $\pi$  and  $\tau$ ,

which allow for a broad overlapping substrate specificity. Among them, GST  $\mu$  and  $\tau$  are polymorphic and as such of interest in molecular epidemiological studies. GST  $\mu$  is expressed in the liver, leukocytes, colon and other tissues, but it is absent in approximately half of the population due to a deletion (GSTM1\*null allele). It catalyses conjugation of epoxides with glutathione and may thus protect individuals against chemical mutagens or carcinogens, among others also carcinogens from tobacco smoke. Although the predominant role of GST is in detoxification, certain glutathione conjugation reactions, particularly those involving halogenated alkanes and alkenes can result in the formation of reactive electrophiles that are toxic and carcinogenic.<sup>6</sup>

Initiation of tumorigenesis by a chemical compound *in vivo* requires at least three successive reactions: First, metabolic conversion of chemically inert compounds to a reactive electrophilic form has to occur. This is an obligatory initiation step in chemical carcinogenesis. Next, adducts have to form between these reactive metabolites and DNA, resulting in base changes or DNA rearrangements. Finally, these DNA alterations must be fixed and must lead to oncogene activation. Enhanced activity of phase I enzymes or decreased activity of phase II enzymes result in higher amount of activated carcinogen and increased formation of DNA adducts.<sup>3</sup> This mechanism implies that the presence and activity of relevant xenobiotic metabolizing enzymes contribute to the risk of cancer development.<sup>3</sup> However, genetic susceptibility factor only becomes relevant if sufficient exposure to carcinogen occurs. Risk factors for tumor development include the extent of environmental exposure to a procarcinogen as well as the host susceptibility factor due to the polymorphism of drug metabolizing enzymes involved in the formation of activated carcinogen.

In our study we wished to find out if

genetic polymorphism of xenobiotic metabolism represents a risk factor for CRC. The frequency of polymorphic alleles of two cytochrome P450 dependent monooxygenases (CYP1A1 and CYP2D6) and two glutathione S-transferases (GST M1 and GST T1), supposed to be associated with higher cancer risk, were determined in DNA samples from Slovenian sporadic and familial CRC patients and healthy controls.

### Materials and methods

DNA samples from 31 sporadic and 25 familial CRC patients were analyzed. Seventy-three DNA samples from 107 healthy controls previously analyzed for CYP2D6<sup>7</sup> were included in the study. No clinical data regarding patient characteristics, the localization or stage of tumor or epidemiological data considering exposure were obtained at this stage of the study.

PCR- based genotyping approach was used to determine the frequencies of polymorphic alleles of two cytochrome P450-dependent monooxygenases (CYP2D6 and CYP1A1) and two glutathione S-transferases (GSTM1 and GSTT1).

PCR followed by restriction with BstNI enzyme was used to distinguish between the wild type allele (CYP2D6wt) and deficiency allele CYP2D6B.<sup>8</sup> Allele specific PCR with two pairs of primers was used to distinguish between the wild type allele and deficiency allele CYP2D6A.<sup>9</sup>

The polymorphism in 3' flanking region of CYP1A1 gene was analyzed by PCR and restriction with MspI.<sup>10</sup>

Triplex PCR was used to analyze for GST M1 and T1 null alleles. Conserved beta globin primers were used as internal control.<sup>11</sup>

### Results and discussion

The frequencies of CYP2D6 wt, A and B alleles were 90.9 %, 7.6 % and 1.5 % in sporadic CRC cases and 80.8 %, 19.2 % and 0 % in familial CRC cases. The frequencies of CYP2D6 alleles in the healthy control population studied previously were as follows: CYP2D6A 1 %, CYP2D6B 21 %, and CYP2D6wt 78 % of all alleles.<sup>7</sup> CYP2D6 phenotype frequencies in CRC patients and in controls are presented in Table 1. The phenotype was predicted according to the genotype.<sup>12</sup> Individuals homozygous for two deficiency alleles were considered poor (slow) metabolizers (PM), heterozygotes for one deficiency allele were considered heterozygous extensive metabolizers (HEM) and homozygotes for two wild type alleles were considered extensive metabolizers (EM). As presented in Table 1, no PM of debrisoquine was identified in sporadic CRC cases, while 8 % of familial CRC and 7 % of healthy controls were identified as PM. The difference in PM frequencies between sporadic CRC and healthy control group is close to the limit of statistical significance ( $\chi^2 = 5.52$ ,  $m=2$ ,  $p=0.06$ ) despite the small sample size. There

**Table 1.** CYP2D6 phenotype frequencies in CRC cases and controls

	Cases (number)	CYP2D6 EM	CYP2D6 HEM	CYP2D6 PM
CRC total	56	0.75	0.21	0.04
- sporadic	31	0.84	0.16	0.00
- familial	25	0.64	0.28	0.08
Controls	107	0.63	0.31	0.07

**Table 2.** CYP1A1 MspI genotype frequencies in CRC cases and controls

	Cases (number)	CYP1A1 A	CYP1A1 B	CYP1A1 C
CRC total	56	0.86	0.12	0.02
- sporadic	31	0.84	0.13	0.03
- familial	25	0.88	0.12	0.00
Controls	73	0.81	0.18	0.01

was no statistically significant difference in CYP2D6 phenotype distribution between familial CRC cases and healthy controls.

CYP1A1 MspI genotype frequencies in CRC patients and in controls are presented in Table 2. The predominant genotype in both CRC cases as well as healthy controls is genotype A which indicates homozygotes for two wild type alleles in which the MspI restriction site is absent. Genotype B indicates heterozygotes for one wild type allele and one allele with mutation creating MspI restriction site. Genotype C which indicates homozygotes for two alleles with MspI restriction site present is very rare in both CRC cases and in controls. It was shown that CYP1A1 inducibility and enzymatic activity is increased in individuals with genotype C.<sup>10</sup> Genotype C frequency seemed to be slightly higher in sporadic CRC cases than in familial CRC cases or controls, however, the difference in frequencies of CYP1A1 MspI genotypes was not statistically significant ( $\chi^2 = 1.67$ ,  $m=4$ ,  $p=0.80$ ).

GST M1 and GST T1 genotype frequencies in CRC patients and in controls are presented in Table 3. GST M1 and GST T1 positive genotype indicates individuals homozygous or heterozygous for the presence of GST M1 or GST T1 gene respectively, while the null genotype indicates individuals homozygous for the deletion of GST M1 or GST T1 gene respectively. The frequencies of GST M1 as well as GST T1 genotypes were not significantly different in both CRC cases and controls.

On the basis of our results we can conclude that inherited metabolic susceptibility to carcinogens from the environment seems to be higher in sporadic than in familial CRC. Polymorphic CYP2D6 gene probably has some role in colorectal carcinogenesis in our population. Enhanced metabolic activation of PAHs was observed in CYP1A1 MspI C genotype<sup>10</sup> but its frequency in Slovenian population is probably too low to contribute significantly to colorectal tumor formation. It is interesting that this polymorphism was related to an increased risk for in situ CRC in the Japanese and Hawaiians, but not in the Caucasians.<sup>13</sup> The discrepancy between the above and our study may be due to a low frequency of CYP1A1 susceptibility allele in our as well as in other Caucasian populations, which limits the statistical power of analysis in small groups of patients. Another possible explanation is that PAHs may influence the earliest genetic alterations leading to colorectal tumorigenesis and their role may be masked in advanced disease. Our results also indicate that the polymorphic GST genes probably do not represent a significant risk factor for colorectal carcinogenesis.

However, we must keep in mind that cancer is a polygenic disease and the penetrance of any single gene is not sufficient to produce an observable effect. Colorectal cancer results from multiple mutations and it may be difficult to demonstrate a direct involvement of P450s and GSTs in colorectal cancer, especially in advanced disease. However, genetic differences in metabolism of carcino-

**Table 3.** GST M1 and GST T1 genotype frequencies in CRC cases and controls

	Cases (number)	GST M1 positive	GSTM1 null	GSTT1 positive	GSTT1 null
CRC total	56	0.50	0.50	0.79	0.21
- sporadic	31	0.52	0.48	0.81	0.19
- familial	25	0.48	0.52	0.76	0.24
Controls	73	0.48	0.52	0.78	0.22

gens may influence the earliest genetic alterations leading to colorectal tumorigenesis.

Although our study suggests a difference in metabolic susceptibility in sporadic and familial CRC, further studies are needed to investigate the combined effect of polymorphic genes involved in carcinogen metabolism in a larger group of patients with defined exposure to dietary carcinogens and smoking.

### Acknowledgments

The authors would like to acknowledge dr. Koželj and Prof. Križman from the Univ. Dept. of Gastroenterology for their contribution of blood samples from familial colorectal cancer patients, and Prof. Golouh from the Institute of Oncology for his contribution of normal tissue samples of sporadic colorectal cancer patients. We would also like to acknowledge Prof. Bohinjec and Blanka Vidan – Jeras from the Tissue Typing Center, Blood Transfusion Center of Slovenia, for their contribution of DNA samples from healthy controls. This work was financially supported by the Ministry of Science and Technology of Slovenia.

### References

1. Fearon ER, Vogelstein B. A genetic model for colorectal tumorigenesis. *Cell* 1990; **61**:759-67.
2. Vogelstein B, Kinzler KW. The multistep nature of cancer. *Trends Genet* 1993; **9**: 138-41.
3. Kawajiri K, Fujii-Kuriyama Y. P450s and human cancer. *Jpn J Cancer Res* 1991; **82**: 1325-35.
4. Sugimura T, Sato S. Mutagens – carcinogens in foods. *Cancer Res* 1985; **34**: 2415S-21S.
5. Giovannucci E, Rim EB, Stampfer MJ, Colditz GA, Ascherio A, Kearney J et al. A prospective study of cigarette smoking and risk of colorectal adenoma and colorectal cancer in U.S. men. *J Natl Cancer Inst* 1994; **86**: 183-91.
6. Wolf CR. Metabolic factors in cancer susceptibility. *Cancer Surv* 1990; **9**: 437-74.
7. Dolžan V, Rudolf Z, Breskvar K. Human CYP2D6 gene polymorphism in Slovene cancer patients and healthy controls. *Carcinogenesis* 1995; **16**: 2675-8.
8. Gough AC, Miles JS, Spurr NK, Moss JE, Gaedik A, Eichelbaum M, Wolf CR. Identification of primary gene defect at the cytochrome P450 CYP2D6 locus. *Nature* 1990; **347**: 773-5.
9. Heim M, Meyer UA. Genotyping of poor metabolizers of debrisoquine by allele-specific PCR amplification. *Lancet* 1990; **336**: 529-32.
10. Hayashi S, Watanabe J, Nakachi K, Kawajiri K. Genetic linkage of lung cancer associated MspI polymorphisms with amino acid replacement in the heme binding region of the human cytochrome P450 1A1 gene. *J Biochem* 1991; **110**: 407-11.
11. Chen C-L, Liu Q, Relling MV. Simultaneous characterization of GST M1 and T1 polymorphisms by polymerase chain reaction in American whites and blacks. *Pharmacogenetics* 1996; **6**: 187-91.
12. Wolf CR, Smith CAD, Gough AC. Relationship between the debrisoquine hydroxylase polymorphism and cancer susceptibility. *Carcinogenesis* 1992; **13**: 1035-8.
13. Sivaraman L, Leatham MP, Yee J, Wilkens LR, Lau AF, LeMarechand L. CYP1A1 genetic polymorphisms and in situ colorectal cancer. *Cancer Res* 1994; **54**: 3692-5.





## ***In vitro* generation of cytotoxic T lymphocytes against mutated *ras* peptides**

**Antonio Juretić<sup>1</sup>, Mirko Šamija<sup>1</sup>, Zdenko Krajina<sup>1</sup>, Damir Eljuga<sup>1</sup>,  
Marko Turić<sup>1</sup>, Michael Heberer<sup>2</sup> and Giulio C Spagnoli<sup>2</sup>**

<sup>1</sup> University Hospital for Tumors, Zagreb, Croatia and <sup>2</sup> Departments of Surgery  
and Research-ZLF, University of Basel, Basel, Switzerland

---

*Mutations of the ras proto-oncogenes represent frequent genetic alterations in human cancers. These mutations appear as single-point mutations causing single amino acid substitutions at residues 12, 13 or 61 (activated p21 ras proteins). Therefore, peptides encompassing ras mutations appear to represent an appealing target for active immunotherapy procedures. By using a computer program, selecting appropriate HLA-A2.1 binding motifs from defined protein sequences, ras nonapeptides encompassing mutations in positions 12 and 61 with a putative binding capacity for HLA-A2.1 molecules were identified and synthesized. Generation of primary cytotoxic T cell lymphocyte (CTL) response was attempted by weekly restimulations of peripheral blood lymphocytes from healthy donors in the presence of irradiated autologous Epstein Barr virus transformed lymphoblastoid cells (EBV cell lines) and IL-2 and IL-4. Periodically, cultured cells were tested for their killing capacity using as target cells HLA-A2.1+ EBV cells previously pulsed with different combinations of the peptides under investigation. After eight rounds of restimulation reproducible cytotoxic activity against EBV target cells pulsed with two nonamers encompassing ras 61 Gln→Leu mutation was detectable in one donor. Thus, the results obtained indicate that it is possible to induce from PBM of healthy donors CTL specific for peptides encompassing 61 GLN→LEU ras gene mutation following repeated weekly in vitro restimulations.*

*Key words: oncogene protein p21 (ras); point mutation; T-lymphocytes, cytotoxic*

---

### **Introduction**

Neoplastic transformation is caused by a stepwise accumulation of a series of genetic alterations affecting oncogenes and tumor suppressor genes. The expression of mutated

proteins encoded by these genes is restricted to abnormal cells thus raising the possibility to consider these molecules as tumor specific antigens. On the other hand, the long-standing goal of cancer immunotherapy is to stimulate the immune rejection of tumors. Based on the assumption that T lymphocytes might be able to eradicate cancer cells as effectively as they kill autologous virus-infected cells or allogeneic cells, tumor immunologists have

Correspondence to: Prof. dr. sc. A. Juretić, Department of Radiation Oncology, University Hospital for Tumors, HR-10 000 Zagreb, Ilica 197, Croatia. Fax: +385-1-3775 536.

## Materials and methods

been trying to identify specific target antigens displayed by cancer cells that could make them recognizable to cytolytic T lymphocytes (CTL). The identification and selection of these potential human cancer antigens and specific epitopes as targets for CTL is now in a highly dynamic phase. Specific peptides that bind to human major histocompatibility complex (HLA) molecules have now been identified for melanoma-associated antigens. The identification of other human carcinoma-associated antigens and epitopes that can be recognized by human T cells is also under active investigation. Molecules, such as prostate specific antigen (PSA), *c-erbB/2*, *MUC-1*, point mutated *ras*, point mutated *p53*, and carcinoembryonic antigen (CEA) are possible such candidates.<sup>1,2,3</sup>

We investigated the potential antigenic epitopes encompassing mutations of *ras* proteins using as responders, peripheral blood lymphocytes from healthy donors. Mutations of the *ras* proto-oncogenes represent frequent genetic alterations in human cancers, detectable in 90 % of pancreatic carcinomas, 40-50 % of colorectal tumors, 20-40 % of lung carcinomas and approximately 30 % of acute myelogenous leukemias. These mutations appear as single-point mutations causing single amino acid substitutions at residues 12, 13 or 61 (activated p21 *ras* proteins).<sup>4,6</sup>

Therefore, we explored the possibility to define conditions permitting the use of synthetic peptides encompassing „mutant“ residues of activated *ras* proteins for the induction of specific CTL responses. In the present study we applied a recently described protocol,<sup>7</sup> which is based on stimulation of large numbers of naïve lymphocytes with the antigen (peptides) and on concomitant application of Tetanus toxoid, IL-2 and of IL-4.

### *Cells and media*

The medium used throughout this study was RPMI 1640 supplemented with 2 mM L-glutamine, 1 % non-essential amino acids, 1 % sodium pyruvate, penicillin (100 U/ml), streptomycin (100 mg/ml) (all from Gibco Ltd, Paisley, UK) and with 10 % heat inactivated human AB-serum (Blutspendezentrum, SRK, Basel) (complete medium). Human peripheral blood mononuclear cells (PBMC) were obtained from the heparinized peripheral venous blood from a group of HLA-A2.1 healthy donors. Mononuclear cells were isolated by standard gradient centrifugation over Lymphoprep cushion (800 g for 20 minutes). After two washings cells were resuspended in complete medium. PBMC were also used as a cellular source for the generation of Epstein-Barr virus (EBV) transformed lymphoblastoid cell lines.<sup>8</sup>

### *Synthetic peptides*

Peptides were synthesized by solid-phase method using 9050 Millipore peptide synthesizer (Millipore, Volketswil, Switzerland). Synthesis was performed as suggested by the manufacturer. The peptides were purified to homogeneity and analyzed by HPLC. Their purity as analyzed by HPLC was routinely found to exceed 90 %. Synthesized peptides were designed by using a computer program (a gift of Dr. J. D'Amato, Leiden, Holland;<sup>9</sup>) based on the amino acid motifs found in the known HLA-A2.1 binding peptides. This program represents a useful scanning tool for the identification of potential HLA-A2.1 restricted peptides. We thus synthesized a panel of seven peptide nonamers encompassing *ras* mutations in positions 12 and 61. The sequences of these seven nonamers (single-letter code sequences) together with their arbitrary HLA-A2.1 binding scores are

**Table 1.** Synthetic peptides used *in vitro* either for the generation of *ras* specific CTL or for the pulsing of EBV target cells in cytotoxic assays. An amino acid (a.a.) sequence and HLA-A2.1 binding score of the seven synthesized nonapeptides encompassing *ras* oncogene mutations in positions 12 and 61 is indicated

Peptide	Mutation		Amino acid sequence	HLA-A2.1 binding score <sup>x</sup>
	a.a. position	a.a. change		
pool <sup>x</sup> 1				
<i>ras</i> 1	61	Q to L	-G <sub>60</sub> LEEYSAMR <sub>68</sub> -	96
<i>ras</i> 2	61	Q to L	-L <sub>53</sub> DILDTAGL <sub>61</sub> -	48
<i>ras</i> 3	61	Q to L	-I <sub>55</sub> LDTAGLEE <sub>63</sub> -	48
pool 2				
<i>ras</i> 4	61	Q to K	-T <sub>58</sub> AGKEEYSA <sub>66</sub> -	96
<i>ras</i> 5	61	Q to K	-I <sub>55</sub> LDTAKKEE <sub>63</sub> -	48
pool 3				
<i>ras</i> 6	12	G to V	-V <sub>9</sub> GAVGVGKS <sub>17</sub> -	128
<i>ras</i> 7	12	G to V	-Y <sub>4</sub> KL V V V G A V <sub>12</sub> -	96

<sup>x</sup> Initially, *in vitro* stimulation of PBMC was attempted by using pools of two or three synthesized peptides. Binding score, expressed as arbitrary units, was calculated by taking advantage of a specific computer program (9).

reported in Table 1. A correlation can be expected between high score and binding to HLA-A2.1.<sup>9</sup> The peptides were dissolved in DMSO (Sigma, Buchs, Switzerland) as a stock solution (at 20 mg/ml). For *in vitro* experiments they were further diluted in complete medium (10 mg/ml final concentration).

#### Generation of CTL.

Generation of primary CTL response was attempted by taking advantage of a recently described protocol.<sup>7</sup> The initial *in vitro* stimulations were performed by using „bulk cultures“ containing large numbers of PBMC in the presence of synthetic peptides. During the initial seven days the medium was also supplemented with tetanus toxoid (1 mg/ml) to provide „helper“ function. Briefly, 25-75 × 10<sup>6</sup> PBMC were stimulated with mixtures of *ras*-derived peptides (pool 1, pool 2 or pool 3 peptides, Table 1) in 10 ml of complete medium in the presence of tetanus toxoid (1 mg/ml). Subsequently, Ficoll purified lymphoblasts underwent weekly restimulations

in the presence of irradiated, autologous EBV cells pulsed with combinations of appropriate peptides (pool 1, pool 2 or pool 3 peptides). Exogenous IL-2 and IL-4 were added twice per week at low doses (10 U/ml and 1 U/ml, respectively). Periodically, <sup>51</sup>Cr release tests (killing assays) were performed, by using, as target cells HLA-A2.1<sup>+</sup> EBV cells,

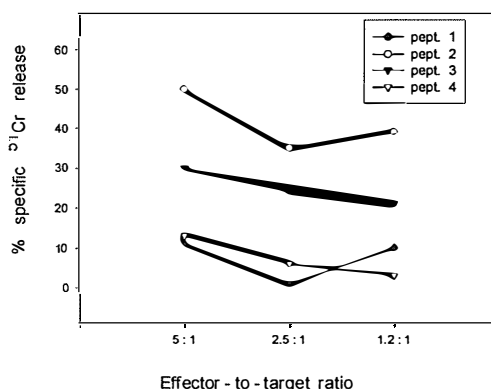


**Figure 1.** Specificity of bulk-cultured CTL undergoing *in vitro* re-stimulations with mutant *ras* peptides 1, 2 and 3 (pool 1 peptides). As target cells, HLA-A2.1<sup>+</sup> EBV-transformed B cells, pulsed with indicated individual peptides, were used.

previously pulsed with the different combinations of peptides under investigation. Briefly, EBV cells were first labelled with a Na<sup>51</sup>Cr solution (Dupont, Regensdorf, Switzerland) as described.<sup>10</sup> Afterwards, they were pulsed for 1 hr at 37°C with defined peptides at 10 mg/ml final concentration. Following extensive washings, target cells were resuspended at 10<sup>5</sup> cells/ml final concentration and added to different numbers of effector cells in U-bottom, 96-well trays. Cultures were incubated for 4 hours at 37°C in a 5% CO<sub>2</sub> humidified atmosphere. Supernatants were then collected and specific <sup>51</sup>Cr release was calculated according to the standard formula as described.<sup>10</sup> Antibody blocking studies were performed by adding monoclonal antibodies in the form of hybridoma supernatants to killing assays, at 1:3 final dilution.

Results and discussion

Using a panel of mutated p21 *ras* peptides a significant specific killing could be detected after about 8 restimulation cycles in one PBMC donor out of five tested. We were able to demonstrate that the CTL recognized a p21 *ras* nonapeptide encompassing a Q→L (Gln→Leu) mutation in position 61. CTL recognized EBV target cells preincubated with either peptide 2 or peptide 3. The results

from one such representative experiment are presented in Figure 1. Preincubation of EBV target cells with wild type peptides did not result in their recognition by CTL and subsequent killing (Table 2). Killing of EBV target cells preincubated with a mutant *ras* nonapeptide could be blocked by anti-HLA-A2.1 monoclonal antibodies, consisted with a specifically restricted recognition (Table 3). When further analyzed, our CTL appeared to be monoclonal in nature, since all CD8<sup>+</sup> T cell clones generated express Vb14 gene product in combination with Jβ2.7 and Cβ2 (data not shown,<sup>11</sup>).

Our data are in agreement with similar results obtained by others, by taking advantage of different culture conditions.<sup>12</sup> The characterization of mechanisms underlying HLA class I restricted antigen presentation and the identification of the peptide motifs allowing binding of antigenic epitopes to defined HLA determinants permit testing the immunogenicity of specific reagents in terms of capacity to induce CTL responses. Considering the role of mutated oncogenes or of tumor suppressor genes in the transformation processes and their specific expression in neoplastic cells, their products could represent the ultimate target for tumor specific active immunotherapies. Accordingly, we report here that we were able to generate *in vitro* a primary peptide specific CTL response

Table 2. Recognition of EBV target cells pulsed by wild type *ras* peptide by CTL generated with the pool 1 of mutated *ras* peptides

Effector to target ratio	% specific <sup>51</sup> Cr release EBV target cells preincubated with	
exp. 1	mutant <i>ras</i> 2 peptide	wild type peptide
2:1	32	0
1:1	28	1
0.5:1	12	0
exp. 2	mutant <i>ras</i> 3 peptide	wild type peptide
5:1	56	13
2.5:1	35	2
1.2:1	22	0

**Table 3.** Effect of anti-HLA-A2.1 monoclonal antibody on the killing of EBV target cells

Effector to target ratio	% specific <sup>51</sup> Cr release	
	EBV target cells preincubated with ras 3 mutant peptide monoclonal antibody	monoclonal antibody
	anti-HLA-A2.1	anti-Mage3
10:1	7	69
5:1	5	72
2.5:1	1	45
1.2:1	3	32

against peptides encompassing mutation at position 61 in *ras* oncogene. The limitations of the experimental system described above are the number of restimulation cycles (8 rounds) and low frequency of responding donors (one out of five). Therefore, research for more practical immunization conditions is currently being pursued. In addition, the capacity to generate specific CTL should be comparatively analyzed in patients and healthy donors.

### Acknowledgement

This work was supported by grants from Swiss Cancer League (grant 466 to A.J.), and by Swiss National Fond (grant 3100-039509 to A.J.).

### References

- Cheever MA, Disis ML, Bernhard H, Gralow JR, Hand SL, Huseby ES, Qin HL, Takahashi M, Chen W. Immunity to oncogenic proteins. *Immunol Rev* 1995; **145**: 33-59.
- Urban JL, Schreiber H. Tumor antigens. *Annu Rev Immunol* 1992; **10**: 617-44.
- Van Pel A, van der Bruggen P, Coulie PG, Brichard VG, Lethe B, Van den Eynde, Uyttenhove C, Renauld, J-C., Boon, T. Genes coding for tumor antigens recognized by cytolytic T lymphocytes. *Immunol Rev* 1995; **145**: 229-50.
- Barbacid M. *ras* genes. *Ann Rev Biochem* 1987; **56**: 779-827.
- Barbacid M. *ras* oncogenes: their role in neoplasia. *Eur J Clin Invest* 1990; **20**: 225-35.
- Bos JL. *ras* oncogenes in human cancer: a review. *Cancer Res* 1989; **49**: 4682-9.
- Cerny A, Fowler P, Brothers MA, Houghton M, Schlicht H, Chisari F. Induction *in vitro* of a primary human antiviral cytotoxic T cell response. *Eur J Immunol* 1995; **25**: 627-30.
- Spagnoli GC, Schaefer C, Willmann TE, Kocher T, Amoroso A, Juretic A, Zuber M, Lüscher U, Harder F, Heberer M. Peptide-specific CTL in tumor-infiltrating lymphocytes from metastatic melanomas expressing *MART-1/Melan-A*, *gp100* and *Tyrosinase* genes : a study in an unselected group of HLA-A2.1-positive patients. *Int. J. Cancer (Pred. Oncol.)* 1995; **64**: 309-15.
- D'Amato J, Houbiers JG, Drijfhout JW, Brandt RM, Schipper R, Bavinck JN, Melief CJM, Kast WM. A computer program for predicting possible cytotoxic T lymphocyte epitopes based on HLA class I peptide-binding motifs. *Hum. Immunol* 1995; **43**:13-8.
- Juretic A, Spagnoli GC, von Bremen K, Horig H, Filgueira L, Lüscher U, Babst R, Harder F, Heberer M. Generation of lymphokine-activated killer activity in rodents but not in humans is nitric oxide dependent. *Cell Immunol* 1994; **157**: 462-77.
- Juretic A, Juergens-Goebel J, Schaefer C, Noppen C, Willman T, Kocher T, Zuber M, Harder F, Heberer M, Spagnoli GC. Cytotoxic T lymphocyte responses against mutated p21 ras peptides: an analysis of specific T cell receptor gene usage. *Int J Cancer* 1996; **68**: 471-8.
- Van Elsas A, Nijman HW, Van der Minne CE, Mourer JS, Kast WM, Melief CJM, Schrier PI. Induction and characterization of cytotoxic T-lymphocytes recognizing a mutated p21ras peptide presented by HLA-A\*0201. *Int J Cancer* 1995; **61**: 389-96.



## Differential expression of Bcl-2 protein in non-irradiated or UVC-irradiated murine myeloid leukaemia (ML) cells

Marijana Popović Hadžija and Marija Poljak Blaži

Department of Molecular Medicine, Ruđer Bošković Institute, Zagreb, Croatia

---

*In this work, we examined the expression of Bcl-2 protein in myeloid leukaemia (ML) cells and the effect of UVC-light on the expression level. The protein of bcl-2 oncogene was detected by immunocytochemical method. In spleen cells of healthy RFM donors was detected 34.3% of Bcl-2 positive cells. When leukaemia came to the non terminal phase (NTP) more than 50% of cells expressed this protein. However, in terminal phase (TP) of leukaemia growth, only 24.4% Bcl-2 positive cells was determined. After UVC irradiation, the expression of Bcl-2 protein was significantly higher in spleen cells of healthy donors. However, UVC light did not change the expression of Bcl-2 in cells of both investigated phases of ML growth. Bcl-2 protein may be involved in the resistance of ML cells to UVC light.*

*Key words: myeloid, leukaemia; UVC light, Bcl-2 protein*

---

### Introduction

The *bcl-2* (B-cell lymphoma/leukaemia 2) gene becomes involved in chromosomal translocations in many humans B-cell lymphoma.<sup>1</sup> Chromosomal translocation t (14;18) frequently occurs in non-Hodgkin's B-cell lymphomas. In that case, the *bcl-2* gene moves from its normal location at 18q21 into *cis*-configuration with strong enhancer elements associated with immunoglobulin heavy-chain locus at 14q32,<sup>2</sup> resulting in deregulated *bcl-2* gene expression primarily through transcriptional mechanisms. The altered levels of Bcl-2 protein found in these

cells is thought to contribute to the pathogenesis of these B-cell neoplasms.<sup>1</sup> Interestingly, translocations involving *bcl-2* gene have not been described in T-cell leukaemias and lymphomas. Reed and co-workers presume two possible explanations; the conditions contributing to the specific chromosomal breaks and recombinations do not exist in T-cell or *bcl-2* translocations occur at the stage of T-cell differentiation when *bcl-2* fails to confer a selective growth advantage.<sup>1</sup> High levels of Bcl-2 protein production have been also reported in a wide variety of human solid tumours and leukaemias even in the absence of translocation or other gross alterations in the structure of *bcl-2* gene, including adenocarcinomas of the prostate and colon, neuroblastomas, acute myelogenous leukaemias and chronic lymphocytic leukaemias.<sup>2,3</sup>

---

Correspondence to: Dr. Marijana Popović Hadžija, Department of molecular medicine, Ruđer Bošković Institute, P. O. Box 1016, Bijenička c. 54, 10000 Zagreb, Croatia. Tel: +385 1 456-064; Fax: +385 1 468 00 84; E-mail: hadzija@olimp.irb.hr



The *bcl-2* proto-oncogene encodes a 26 kDa protein, which is localized in the inner and the outer mitochondrial membrane, the nuclear envelope and the endoplasmic reticulum.<sup>4</sup> This protein is structurally and functionally unique in that it bears little or no significant homology with other known cellular proteins.<sup>5</sup> Bcl-2 protein contributes to malignant cell expansion by blocking the normal physiological turnover of cells death (apoptosis), rather than by increasing the rate of cellular proliferation.<sup>6,7</sup> Recent findings are beginning to reveal details of the mechanisms by which Bcl-2 protein suppress cell death. Namely, evidence from cell transfection studies indicated that Bcl-2 might have a membrane transport function, with reported effects on  $\text{Ca}^{2+}$  flux and protein translocations across some of the intracellular membranes where this protein is localized.<sup>8</sup> The mechanism by which Bcl-2 protein create channels has not been explored in detail.

Apoptosis is a fundamental biologic process which allows the cell to actively participate in its own death. Leukaemia and tumour cells, which expressed *bcl-2* gene, are more resistant to induction of apoptosis by chemotherapeutic drugs, irradiation and other agents. Namely, during the process of apoptosis "megapores" on the mitochondrial membrane were opened and apoptogenic protease activators (cytochrome c and apoptosis-inducing factor, AIF) released from mitochondria (Figure 1). It has repercussions on the generation of oxygen free radicals and the release of mitochondrial proteins into the cytosol in order to activate the caspases, that are the terminal effectors of apoptosis.<sup>9</sup> Overexpression of Bcl-2 protein inhibited mitochondrial permeability, and thus inhibited programmed cell death.<sup>10</sup> Bcl-2, therefore, plays a significant role, not only in the origins of cancer, but also in its treatment.<sup>2</sup>

In previous work, we showed that ML cells could survive irradiation with very high dose of UVC-light ( $1280 \text{ J/m}^2$ ), but normal bone

marrow cells died even after small dose ( $5 \text{ J/m}^2$ ).<sup>11</sup> Also, we have shown previously that UVC light induced apoptosis in high percent of spleen cells of healthy mice, but in spleen of ML bearing mice induction of apoptosis was weaker and was expressed latter.<sup>12</sup> That was the reason, why we looked at expression of Bcl-2 protein in ML cells and the effect of UVC light on the expression level of Bcl-2. During the ML growth we distinguished two phases, non terminal and terminal, because the expression of some oncogenes are different in different stages of disease.<sup>12,13</sup>

### Materials and methods

In experiments RFM/Rij Zgr mice, bred at our Institute were used. ML was induced by sublethal X-irradiation of mice 1965. and since than the leukaemia was transplanted by spleen cells of moribund mice, or cells were kept frozen in liquid nitrogen. Mice injected intravenously with  $10^6$  cells died with high leucocyte number in the blood, enlarged spleens and livers. Spleen cells were tested 9 (non terminal phase of disease NTP) or 12 days (terminal phase TP) after inoculation of  $10^6$  ML cells. Cell suspensions of healthy and leukaemic spleen ( $8.5 \times 10^6$  cells per ml in Hank's solution without phenol red, in thin layer, 0.2 mm) were irradiated with UVC light by four germicidal lamps (Phillips, 15 watts). Doses of UVC light were 50, 100, 1000 and  $50000 \text{ J/m}^2$ . Before exposition to UV light, erythrocytes were lysed in hypotonic salt solution. During exposition the suspension was constantly stirred by a magnetic rod.

Bcl-2 protein was detected by immunocytochemical method described by Kranz and co-workers.<sup>14</sup> Ten  $\mu\text{l}$  of cell suspension ( $6 \times 10^6$  cells/ml) was dropped on slide coated with poly-L-lysine and incubated for 30 min at  $4^\circ\text{C}$ . The slide was washed in phosphate-

buffered saline (PBS), pH 7.4, followed by fixation for 7 min at 20 °C with freshly prepared 0.05% glutaraldehyde (grade 1; Sigma) in PBS. For the differential staining of endogenous peroxidases, 10 µl PBS containing 0.1% 4-chloro-1-naphthol (Sigma) and 0.015% hydrogen peroxide (Merk) was added to each spot and incubated for 15 min at 20 °C, followed by washing the slide in PBS. In order to permeabilized membranes, spots were than incubated for 15 min at 20 °C with PBS containing 0.04% polyoxyethylene 10 cetyl ether (Brij 56; Sigma), followed by spots washing. Non-specific binding of primary antibody was blocked by applying MAG solution (MEM with 0.2% albumin and 0.2% gelatine, Gibco). Monoclonal antibody mouse IgG anti Bcl-2 (Oncogene Science), in optimized dilution (1:40) was applied for 30 min at room temperature. After washing the slides in PBS, secondary antibody goat immunoglobulins to mouse immunoglobulins (Jackson ImmunoResearch), diluted 1:100 in MAG, was added on each spots and incubated 30 min at room temperature. After that, the slides were washed by simply dipping into PBS. The immunoperoxidase reaction was performed for 25 min at 20 °C using a freshly prepared mixture of 94 ml 0.05 M phosphate buffer, pH 6.9, 6 ml dimethyl sulfoxide (DMSO; Merck) containing 0.167% 3-amino-9-ethylcarbazole (Sigma) and 15 µl 30% hydrogen peroxide (Merck). Slides were then stained for 20 sec with Mayer's acid hemalaun, rinsed in tap water, and mounted with phosphate-buffered glycerol. The number of positive or negative cells was evaluated under the light microscope (Reichert,  $\times 502$ ). The nuclei of positive cells were brown, while nuclei of negative cells were blue. Experiments were done three times in triplicate. The positive cells was determined by scoring at least 100 cells on each spot; finally 900 cells were counted for each point showed in results.

Statistical analyses were performed using

Model 1 ANOVA to determine whether differences existed among the group means, followed by a paired Student's *t* distribution to identify the significantly different means ( $p = 0.05$ ).

## Results

Bcl-2 protein was expressed in 34.3% of spleen cells of healthy RFM donors, which were used as control cells (Figure 2). However, spleen cells of leukaemia bearing mice 9 days after inoculation of ML cells (NTP), expressed Bcl-2 protein in significant higher percentage (56.7%) than control cells (Figure 2). Opposite to this, in TP of leukaemia growth the percentage of Bcl-2 positive cells was significantly smaller than in sample of "healthy" spleen cells or spleen cells of NTP of leukaemia (Table 1). In that case, we detected only 24.4% of Bcl-2 positive cells (Figure 2).

Spleen cells suspensions of healthy mice and leukaemia bearing mice of both phases were irradiated with UVC light (doses 50, 100, 1000 and 50000 J/m<sup>2</sup>) and than the presence of Bcl-2 protein was determined. After UVC irradiation with all used doses, the number of "healthy" spleen cells which expressed Bcl-2 protein significantly increased (Table 1). The range of positive cells was from 44% to 58.4% (Figure 2).

Different effect was detected after UVC irradiation of leukaemic cells of NTP. Namely, UVC light did not provoke any significant increase the number of Bcl-2 expressing cells (Table 1). In that case the percentage of Bcl-2 positive cells was from 56.7% in unirradiated sample, to 52% or 64% in irradiated samples (Figure 2).

Nearly the same effect was observed after UVC exposition of leukaemic cells of TP. In TP of ML growth this range of positive cells in irradiated samples was from 24% to 29.6% (Figure 2). The exception was at a dose of 100

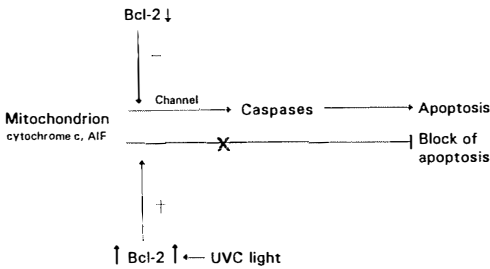


Figure 1. The role of Bcl-2 protein in apoptosis.

J/m<sup>2</sup>, where significant increase was detected in the percentage (32.8%) of Bcl-2 expressing cells (Table 1).

Discussion

Since its discovery over ten years ago as an oncogenic protein involved in many human tumours, *bcl-2* gene and their protein are topic of many investigations because of its anti-apoptotic action. Bcl-2 protein can function as channels for ions, proteins or both, across intracellular membranes like the outer mitochondrial membrane, the endoplasmic reticulum and the nuclear envelope.<sup>10</sup> The mechanism by which Bcl-2 create channels in membranes has not been explored in detail, but preliminary indications are that at least aspects of the process may be similar to the bacterial toxins.<sup>10</sup>

Cells undergo apoptosis when exposed to a variety of cytotoxic agents, like a radiation. However, it is known that some leukaemia cell lines are resistant to apoptosis induced by irradiation.<sup>2</sup> This is in connection with our previously work, where we determined apoptosis in spleen cells of healthy and leukaemia bearing RFM donors, 4 or 24 hours after UVC irradiation.<sup>12</sup> Irradiated "healthy" spleen cells died by apoptosis in significantly higher percentage than unirradiated cells, detected 4 as well 24 hours after irradiation. Opposite to healthy spleen cells, unirradiated ML cells did not enter in apoptosis, and we did not find correlation between doses of UVC light and apoptosis of leukaemic cells of TP, tested 4 and 24 hours after irradiation. For that could be responsible Bcl-2 protein and their anti-apoptotic effect.

It was the reason why we investigated the presence of Bcl-2 protein in spleen cells of healthy and in ML bearing RFM mice. During the ML growth was observed two phases, non terminal and terminal. The spleen of NTP of leukaemia has a few leukaemic cells, while in TP of disease most of cells are leukaemic. We supposed that, the presence of oncogenic proteins (like Bcl-2 protein) was also different at the different stages of disease, as we showed earlier for c-Myc protein.<sup>15</sup> Thus, in the early period of leukaemia growth (NTP) only 14.3% of c-myc positive

Table 1. The number of Bcl-2 positive cells of healthy RFM mice (control) and leukaemia bearing mice of non terminal (NTP) and terminal (TP) phase. Experiments were done in triplicate. For each point showed in Table 1 and Figure 1, 900 cells were counted

Dose (J/m <sup>2</sup> )	Control cells mean ± se (%)	Leukaemic cells of NTP mean ± se (%)	Leukaemic cells of TP mean ± se (%)
0	34.3 ± 4 (34.3)	56.7 ± 1.4 (56.7)	24.4 ± 2.1 (24.4)
50	48.5 ± 2.1 <sup>a</sup> (48.5)	60.0 ± 1.8 (60.0)	28.0 ± 1.4 (28.0)
100	58.4 ± 1.5 <sup>a</sup> (58.4)	52.0 ± 1.9 (52.0)	32.8 ± 1.6 <sup>b</sup> (32.8)
1000	54.4 ± 1.7 <sup>a</sup> (54.4)	64.0 ± 1.9 (64.0)	29.6 ± 1.7 (29.6)
50000	44.0 ± 1.5 <sup>a</sup> (44.0)	60.0 ± 1.4 (60.0)	24.0 ± 1.8 (24.0)

<sup>a</sup> = significant difference relative to non irradiated control sample  
<sup>b</sup> = significant difference relative to non irradiated sample of ML of TP

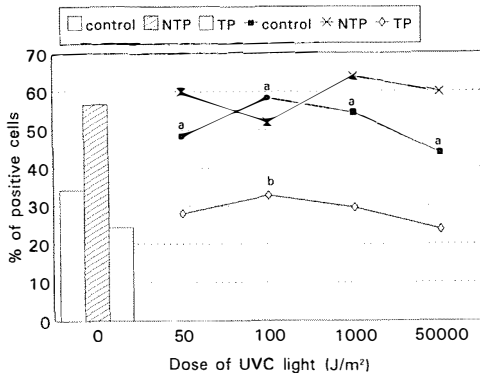


**Figure 2.** The presence of Bcl-2 protein in spleen cells of healthy mice (control) and leukaemic bearing mice of non terminal (NTP) and terminal phase (TP) of disease.

<sup>a</sup> = significant difference relative to value of non irradiated control sample

<sup>b</sup> = significant difference relative to value of non irradiated sample of ML of TP

cells was found, as opposed to the terminal phase of leukaemia (TP) when even 89.7% of c-myc positive cells were detected. From literature is also known, that alterations of gene expression is in connection with disease progression. For example, inactivation of *p53* gene is quite rare in the chronic phase of chronic myeloid leukaemia, while relatively frequent (around 25%) in the acute phase.<sup>13</sup>

In case of Bcl-2 protein, we found the greater expression in NTP of leukaemia, than in "healthy" spleen cells or in cells of TP of leukaemia. We suppose that, like other oncogenes, auto-regulation of Bcl-2 protein synthesis was lost in this malignant cells,<sup>16</sup> and that is reason of different expression of Bcl-2 protein. However, when leukaemia came to the terminal phase, the mice died during a few hours and ML cells were destroyed.

It is well known that different kind of radiation (as well as UVC light) are carcinogens which can activate different classes of oncogenes.<sup>17</sup> The actively transcribed genes which possessed damage in DNA are preferentially repair by mechanism of DNA repair which exist in all mammalian cells. Today, increased

exposure to environmental UVC is a result of depletion of atmospheric ozone. In our experiment we used UVC light doses from 50 to 50000 J/m². So wide range of UVC doses we used in our earlier experiments, where the high resistance of ML cells was detected. Also, we examined the ability of UVC light to activate acellular factor, which is possible to induced the malignant transformation of bone marrow cells.<sup>18</sup> There is no doubt that UVC light activated *bcl-2* gene expression in control spleen cells (in comparison to unirradiated cells). But, UVC light did not change the expression of Bcl-2 protein in myeloid leukaemia cells (of both phases). These results agree with our previous finding and our opinion that ML cells could not die by apoptosis. Therefore, leukaemic cells accumulated in spleen and liver causing splenomegaly and hepatomegaly, typically symptoms of leukaemia disease.

### Acknowledgement

This work was supported by grant from the Ministry of Science and Technology Republic of Croatia.

### References

1. Reed CJ, Cuddy M, Haldara S, Croce C, Peter Nowell, Makover D, et al . Bcl2-mediated tumorigenicity of a human T-lymphoid cell line: Synergy with Myc and inhibition by Bcl2 antisense. *Proc Natl Acad Sci* 1990; 87: 3660-4.
2. Torigoe T, Millan AJ, Takayama S, Taichman R, Miyashita T, Reed CJ. Bcl-2 inhibits T-cell-mediated of a leukaemia cell line. *Cancer Res* 1994; 54: 4851-4.
3. Hanada M, Delia D, Aiello A, Stadtmayer E, Reed J. *bcl-2* gene hypomethylation and high-level expression in B-cell chronic lymphocytic leukaemia. *Blood* 1993; 82: 1820-8.
4. Krajewski S, Tanaka S, Takayama S, Schibler JM, Fenton W, Reed CJ. Investigation of the subcellu-

- lar distribution of the *bcl-2* oncoprotein: Residence in the nuclear envelope, endoplasmic reticulum and outer mitochondrial membranes. *Cancer Res* 1993; **53**: 4701-14.
5. Hockenbery D, Nunez G, Milliman C, Schreiber DR, Korsmeyer JS. Bcl-2 is an inner mitochondrial membrane protein that blocks programmed cell death. *Nature* 1990; **348**: 334-6.
  6. Reed J. Bcl-2 and the regulation of programmed cell death. *J Cell Biol* 1994; **124**: 1-6.
  7. Oltvai NZ, Milliman CL, Korsmeyer JS. Bcl-2 heterodimerizes *in vivo* with a conserved homolog, Bax, that accelerates programmed cell death. *Cell* 1993; **74**: 609-19.
  8. Ryan JJ, Prochownik E, Gottlieb AC, Apel JJ, Marino R, Nunez G, et al. c-myc and bcl-2 modulate p53 function by altering p53 subcellular trafficking during the cell cycle. *Proc Natl Acad Sci USA* 1994; **91**: 5878-82.
  9. Petit PX, Susin SA, Zamzami N, Mignotte B, Kroemer G. Mitochondria and programmed cell death: back on the future. *FEBS Lett* 1996; **396**: 7-13.
  10. Reed CJ. Double identity for proteins of the Bcl-2 family. *Nature* 1997; **387**: 773-6.
  11. Poljak Blaži M, Osmak M, Hadžija M. Resistance of human and mouse myeloid leukaemia cells to UV radiation. *Photochem Photobiol* 1988; **50**: 85-9.
  12. Poljak Blaži M, Popović Hadžija M, Hadžija M. c-Myc, p53 proteins and apoptosis in UV-irradiated or not mouse myeloid leukaemia cell. In press.
  13. Nakai H, Misawa S. Chromosome 17 abnormalities and inactivation of the *p53* gene in chronic myeloid leukaemia and their prognostic significance. *Leukaemia Lymphoma* 1995; **19**: 213-1.
  14. Kranz BR, Thiel E, Thierfelder S. Immunocytochemical identification of meningeal leukaemia and lymphoma: Poly-L-lysine-coated slides permit multimer analysis even with minute cerebrospinal fluid cell specimens. *Blood* 1989; **73**: 1942-8.
  15. Popović Hadžija M, Poljak Blaži M, Pavelić K. Presence of c-Myc protein in murine myeloid leukaemia cells during growth and after irradiation. *Anticancer Res* 1997; **17**: 115-8.
  16. Penn LJZ, Brooks MW, Laufer EM, Land H. Negative autoregulation of *c-myc* transcription. *EMBO J* 1990; **4**: 1113-21.
  17. Garte SJ, Burns FJ. Oncogenes and radiation carcinogenesis. *Environ Health Perspect* 1991; **93**: 45-9.
  18. Poljak Blaži M, Popović M, Osmak M. Malignant transformation of bone marrow cells by nuclei and supernatant of killed murine myeloid leukaemia cells. *Period Biol* 1992; **94**: 201-8.

## Direct delivery of chemotherapeutic agents for the treatment of hepatomas and sarcomas in rat models

S. Pendas<sup>1,2</sup>, M. J. Jaroszeski<sup>1</sup>, R. Gilbert<sup>3</sup>, M. Hyacinthe<sup>1</sup>, V. Dang<sup>1</sup>, J. Hickey<sup>3</sup>, C. Pottinger<sup>1</sup>, P. Illingworth<sup>1</sup> and R. Heller<sup>1</sup>

<sup>1</sup>University of South Florida, College of Medicine, Department of Surgery, <sup>2</sup>Maimonides Medical Center, Department of Surgery Brooklyn, NY, <sup>3</sup>University of South Florida, College of Engineering, Department of Chemical Engineering, USA

---

*The combination of a chemotherapeutic agent and electric pulses has been termed electrochemotherapy (ECT). This procedure is based on the premise that electric pulses can increase the uptake of molecules through the cell membrane due to permeabilization of the membrane through a process called electroporation. This procedure has been successful in increasing the effectiveness of anti-tumor agents (electrochemotherapy; ECT). Response rates of >80% have been obtained in both animal and human trials for several types of skin malignancies using ECT with bleomycin. This study was initiated to determine if ECT could be used to effectively treat internal tumors such as hepatomas in an animal model and human rhabdomyosarcomas in athymic rats. Bleomycin, cisplatin, doxorubicin, 5-fluorouracil, and taxol were used in conjunction with electric pulses. Following an intra tumor injection of a single drug, electric pulses were administered directly to the tumor. For the hepatoma model, ECT worked the best with cisplatin and bleomycin, yielding complete response rates of about 70%. The other drugs used to treat hepatomas were ineffective. Bleomycin combined with electric pulses resulted in a 100% response rate for sarcoma; response rates with cisplatin and doxorubicin were low. These studies indicate that ECT is a technically feasible procedure for visceral tumors and soft tissue sarcomas.*

*Key words: liver neoplasms, experimental; rhabdomyosarcoma; electroporation; bleomycin; cisplatin; doxorubicin; fluorouracil*

---

### Introduction

The delivery of drugs to cancerous tissue is an important modality in the potential treatment of various tumors. Most anti-tumor drugs have an intracellular mode of action.

However, for many of these drugs, the cell membrane is often times a significant barrier which reduces the effectiveness by restricting intracellular access. As a result, it is essential to find a mechanism to deliver the drugs through the cell membrane more efficiently. Therefore, it is possible to increase the therapeutic potential of these drugs by increasing the permeability of the tumor cell membranes.

Correspondence to: Richard Heller, Ph.D., University of South Florida, College of Medicine Department of Surgery, MDC Box 16, 12901 Bruce B. Downs Blvd., Tampa, FL 33612-4799, Tel: 813 974-3065, Fax: 813 974-2669, E-mail: rheller@com1.med.usf.edu

Electric pulses can be used to temporarily and reversibly permeabilize cell membranes.<sup>1-4</sup> The transient alteration of the cell membranes permeability using electric pulses is known as electroporation. Over the past twenty years electric fields have been used successfully as a method of targeting molecules to tissues,<sup>5,6</sup> electrofusing cells to tissues<sup>7-9</sup> and increasing the uptake of certain drugs by cells.<sup>10,11</sup>

Recently, work has been performed demonstrating that electroporation could be used to enhance the effectiveness of chemotherapeutic agents. This combination of electric pulses and anti-tumor agents is known as electrochemotherapy (ECT).<sup>12, 13</sup> The increased effectiveness of these anti-tumor agents is a direct result of electroporation facilitating the uptake of drugs through the cell membrane which has been made transiently more permeable. Electric pulses delivered to the tumor are non-cytotoxic, and cell membrane permeability returns to baseline levels several minutes after the treatment with electric pulses.

Bleomycin has been the drug most often used for ECT for several reasons. Bleomycin is a very potent cytotoxic molecule when introduced inside the cell. The drug works by causing single stranded and double stranded breaks in DNA.<sup>14-17</sup> In addition, only a few hundred molecules are sufficient to be cytotoxic.<sup>10,18</sup> Since bleomycin has an intracellular mechanism of action, the drug must be able to enter the cell to be effective. However, bleomycin is a relatively nonpermeant drug<sup>10</sup> showing minimal intracellular concentration with a systemic dose. Thus, bleomycin cytotoxicity is dependent upon membrane permeability.

Several studies have been performed in both mice and rats and have shown that when bleomycin is administered in combination with electroporation its effectiveness as an anti-tumor agent is greatly enhanced. These studies were done with a variety of

tumor types including, melanoma, hepatocellular carcinoma, lung carcinoma, breast carcinoma, fibrosarcoma, glioma and cervical carcinoma.<sup>12,13,19-32</sup> In addition, the combination of electroporation with other chemotherapeutic agents has also been tested.<sup>23,33</sup> One agent that has shown promise is cisplatin. Although cisplatin is a more permeant drug than bleomycin its effectiveness was augmented by electroporation of cells *in vitro* as well as tumors *in vivo*.<sup>33</sup>

Several clinical studies have shown the potential of electrochemotherapy as an anti-tumor treatment for a variety of cutaneous malignancies.<sup>34-40</sup> Initial trials utilized bleomycin administered intravenously followed by local administration of electric pulses directly to the tumor. Response rates for the treatment of squamous cell carcinoma of the head and neck were 70% with complete responses of 50-60%.<sup>34,35,37</sup> The treatment of melanoma and basal cell carcinoma yielded response rate of 70% with a complete response rate of 33%.<sup>36,39</sup> Subsequent trials for the treatment of melanoma and basal cell carcinoma utilized intratumor administration of bleomycin in conjunction with electric pulses. Response rates in this trial were as high as 99% with a complete response rate of 90%.<sup>39,40</sup>

The results of the animal and human studies have been extremely encouraging. Since electroporation is based on general physical principles and has been shown to work on most mammalian cells, studies have been initiated to examine if ECT could be used to treat other tumor types. The study reported here, examines the use of this antitumor therapy for the treatment of hepatoma and soft tissue sarcoma in rat models. The effects of ECT with bleomycin, cisplatin, taxol, 5-FU and doxorubicin on established hepatomas was investigated first. Sarcomas were then treated with ECT using bleomycin, cisplatin and doxorubicin. Taxol and 5-FU were not used to treat sarcomas because they were

found to be ineffective in the hepatoma model.

## Materials and methods

### *Cell lines and culture methods*

*Visceral tumor study:* N1S1 rat hepatoma cells (ATCC CRL-1604; American Type Culture Collection, Rockville, MD, USA) were grown in Swimms S-77 medium modified to contain, 4mM L-glutamine, 0.01% Pluronic F68, 9% fetal calf serum, and 90µg/ml gentamycin sulfate. Cells were maintained in humidified air that contained 5% CO<sub>2</sub>. In addition, the cells used for this study were greater than 95% viable.

*Soft tissue sarcoma tumor study:* Human A204 rhabdomyosarcoma cells (HTB 82; American Type Culture Collection, Rockville, MD, USA) were used to induce tumors in nude rats. The cell line was grown in McCoy's 5A medium (Mediatech, Washington, DC, USA) supplemented with 10% (v/v) fetal bovine serum (PAA Laboratories, Newport Beach, CA, USA) and 90µg/ml gentamycin sulphate (Gibco, Grand Island, NY, USA). Cells were grown in a humidified atmosphere that contained 5% CO<sub>2</sub>. Confluent cultures were prepared for use by detaching with a nonenzymatic cell dissociation solution (Sigma, St. Louis, MO, USA). The trypan blue exclusion dye method was used to determine the viability of all harvested cell batches. Cell viability was greater than 95% for all batches used in this study.

### *Animals and tumor induction*

Tumors were induced in both male Sprague-Dawley rats using N1S1 rat hepatoma cells and nude rats using human A204 sarcoma cells. General anesthesia was administered using isoflurane. Rats were first placed in an induction chamber that was charged with a

mixture of 5% isoflurane in oxygen for several minutes. These rats were subsequently fitted with a standard rodent mask and kept under general anesthesia using 3% isoflurane.

*Hepatoma study:* the right median lobe of the rat was surgically exposed and injected with 1X10<sup>6</sup> viable N1S1 cells, suspended in 0.5 ml of saline. The animals were closed with surgical staples immediately after injection with tumor cells. The tumors were allowed to grow for 7-10 days. This procedure yielded hepatomas that were approximately 0.75cm in diameter.

*Sarcoma study:* male athymic rats (Harlan Sprague Dawley, Inc., Indianapolis, IN, USA) that were 3-4 weeks old at the time of tumor induction were used for the sarcoma tumor study. Tumors were induced by injecting 8X10<sup>6</sup> cells, contained in 70µl of saline, into the biceps femoris muscle of each rear limb of the athymic rats. Tumors were allowed to grow for 7 to 10 days resulting in sarcomas that were 6 to 8mm in diameter for the case of small sarcomas. Large sarcomas were allowed to grow for greater than 35 days which produced tumors that were 18 to 20 mm in diameter.

### *Tumor treatment*

*Treatment of hepatoma:* After the establishing tumors in the right median lobes, ECT was performed. Bleomycin, cisplatin, taxol, 5-FU, or doxorubicin were injected directly into tumors using different doses in order to determine the effect of each drug separately after the delivery of electric pulses. All doses were administered in a volume of 100 µl. Control animals that did not receive drug therapy received a 100 µl saline injection. Electric pulses were administered ninety seconds after the intratumor injection by inserting a circular array of 6 needle electrodes <sup>41,42</sup> (BTX 878-2a; Genetronics, Inc., San Diego, CA, USA) to a depth of 5 mm around the



peripheral tissue of all tumors so that the entire tumor was contained within the array of needles. The time between drug injection and electric pulse administration was reduced to 90 seconds from the standard of ten minutes, which was used in previous studies,<sup>25</sup> due to the highly vascular nature of hepatoma tumors. Six electric pulses with a field strength of 1000 V/cm were delivered via the inserted needle electrodes in a manner that rotated the applied field around the treatment site.<sup>29,41</sup> A lower field strength was used to treat the hepatoma tumors vs the sarcoma tumors because of the lower impedance of liver tissue compared to skin tissue. These pulses were administered using a DC generator (BTX T820 generator; Genetronics, Inc., San Diego CA, USA), and the pulses were 99 $\mu$ s in duration with a one second interval between the initiation of each pulse.

*Treatment of sarcoma:* After injection of human sarcoma cells in the rear limbs of athymic rats, all animals developed firm palpable tumors. All drugs were administered by intratumor injection in a volume that was equal to 25% of the tumor volume. The chemotherapeutic agents were administered at the following concentrations: bleomycin 5 units/ml, cisplatin 1 mg/ml and doxorubicin 20 mg/ml. Control animals that did not receive a chemotherapeutic agent were given an intratumor injection of saline that was equal to 25% of the tumor volume.

The delivery of electric fields to sarcoma tumors was similar to hepatoma electrical treatment except that the electric pulses were administered ten minutes after injection with the chemotherapeutic agent or saline. In addition, the electrode was placed around the perimeter of each tumor to a maximum depth of 1 cm so that the entire tumor was encompassed within the needle array. The ratio of the applied voltage for each pulse to the electrode spacing was 1300 V/cm.<sup>29,41</sup> A larger field strength was used in the treatment sarcoma tumors due to higher tissue impedance.

Large sarcomas were too big to fit within the volume delineated by the needle array electrode. These tumors were electrically treated by multiple insertions of the electrode until the entire tumor volume received pulses.

Protocols for the treatment of small and large sarcomas were designed for a single ECT treatment and multiple ECT treatments. Electrochemotherapy was administered once for single treatment experiments and a maximum of three times for multiple treatment scenarios. All single treatment animals received ECT on the same day. Similarly, all multiple treatment animals received their first ECT treatment on the same day. For animals that received multiple treatment, ECT was administered again when palpable tumor within the original treatment site was first detected.

#### *Tumor measurements*

*Hepatoma study:* At days 7 and 14 post ECT treatment, all the animals induced with hepatoma tumors were surgically explored, and the tumors were examined for evidence of response to treatment. Tumor volumes were measured prior to and after treatment using the formula  $V = \frac{abc}{6} \pi$ . Measurements were made using a digital Vernier caliper. Objective responses to ECT treatment was determined based on reduction in tumor volume. A complete response was when no visible tumor was evident. Greater than 50% reduction in tumor volume was considered a partial response, and stable disease was less than 50% reduction in tumor volume. Progressive disease was when the tumor volume continued to increase in size. An objective response was defined as the sum of complete and partial responses. For long term studies, the animals were checked every 14-21 days after day 14.

*Sarcoma study:* Another study was conducted to confirm the efficacy of ECT in the treatment of highly aggressive human sarco-

ma tumors induced in the rear limbs of male athymic rats. Response to electrochemotherapy treatment was also based on tumor volume. Tumor volume was determined on 3 mutually orthogonal measurements (a,b,c) of the nodule, and the tumor volume was based on the formula  $V = abc \pi/6$ . Tumors were measured prior to treatment and then at 7 day intervals after treatment. Each tumor was categorized as a complete response, partial response, stable disease, or progressive disease at 28 days post treatment. Animals were considered cured if complete responses were maintained for 100 days.

### Histologic analysis

Tissue specimens were fixed overnight in 10% formalin and then processed for routine histopathological examination. Briefly, specimens were dehydrated through a sequence of 50, 70, 95 and 100% ethanol, cleared in xylene and then embedded in paraffin wax. Sections were cut with a microtome (three sections per specimen) and stained with hematoxylin-eosin. The overall condition of the tissue was examined with respect to cellular integrity.

### Statistical analysis

The Fisher's test for 2 X 2 contingency tables was used to determine the statistical significance of the complete response rates between the treatment and the control groups. For this test, partial response, stable disease and progressive disease were considered incomplete responses.

## Results

A total of 223 established hepatoma tumors were treated in the visceral tumor study and 89 tumors were treated in the sarcoma study. Four different treatment groups were exam-

ined. These groups included those with no treatment (D-E-), electrical treatment (D-E+), drug treatment (D+E-), and combined drug and electric pulses (D+E+).

### ECT for hepatomas

**Treatment with bleomycin:** Objective responses were obtained in 84.5% of the tumors treated with both bleomycin (0.5 unit/tumor) and electric pulses (D+ E+ group). This group also had a 69% complete response rate (Table 1). Tumors that received drug only (D+E-) or only electric pulses (D-E+) or no treatment (D-E-), were found to have 100% progressive disease (Table 1). The response was based on tumor measurements taken 14 days after treatment. The complete response rate for the D+E+ group differed significantly ( $p < 0.01$ ) from the other groups. Incomplete responses were considered to be those animals which had progressive disease, stable disease, and partial responses. The number of complete responses for the D+E+ treatment group was significantly greater ( $P < 0.01$ ) than the number of complete responses in each of the control (D-E-, D-E+, and D+E-) groups. In addition, no adverse effects from the treatment were observed in any of the animals.

**Treatment with other chemotherapeutic agents:** The ability to augment the effectiveness of other chemotherapeutic agents when

**Table 1.** Treatment of rat hepatomas with bleomycin

Treatment	n	% PD <sup>a</sup>	% SD <sup>b</sup>	% PR <sup>c</sup>	% CR <sup>d</sup>
D-E-	9	100	0	0	0
D-E+	9	100	0	0	0
D+E-	10	90	0	0	10
D+E+	13	15.5	0	15.5	69

a: PD = Progressive disease = tumor increasing in size Day 14 compared to Day 0

b: SD = Stable disease = tumor decreasing less than 50% in size Day 14 compared to Day 0

c: PR = Partial response = tumor decreasing in size more than 50% Day 14 compared to Day 0

d: CR = Complete Response = no tumor present on Day 14

combined with electric fields was tested in the N1S1 rat hepatoma model. The treatment was performed as described above using various concentrations of cisplatin, doxorubicin, taxol and 5-FU. Examination of responses at day 14 showed that hepatomas treated with 0.0357 mg of cisplatin and electric fields resulted in a complete response rate of 67% (Table 2) which is similar to the result obtained with bleomycin. The higher tested cisplatin dose (0.357 mg per tumor) resulted in toxicity related deaths in 40% of the animals in the D+E- and D+E+ groups. The delivery of three different doxorubicin doses, two

5-FU doses, and two taxol doses with electric pulses resulted in low or no complete response rates (Table 2). With all drugs tested, except cisplatin, treatment with drug only or pulses only resulted in little or no response (Table 2). In addition, the toxicity related deaths for doxorubicin of 2 and 3 mg per tumor ranged from 78 - 100%.

Treatment with cisplatin using a dose of 0.0357 mg per tumor was repeated to determine the long term effect of the therapy. A 0.0357 mg cisplatin dose was used because it was what resulted in a high complete response in the initial experiments. The com-

Table 2. Treatment of rat hepatomas with other drugs

Treatment	Drug	Dose <sup>a</sup>	n	% PD <sup>b</sup>	% SD <sup>c</sup>	% PR <sup>d</sup>	% CR <sup>e</sup>
D+E-	5 FU <sup>f</sup>	0.5 mg	4	100	0	0	0
D+E+	5 FU	0.5 mg	5	100	0	0	0
D+E-	5 FU	5.0 mg	10	100	0	0	0
D+E+	5 FU	5.0 mg	10	100	0	0	0
D+E-	DOX <sup>g</sup>	1 mg	9	89	11	0	0
D+E+	DOX	1 mg	8	75	12.5	0	12.5
D+E-	DOX	2 mg	9 <sup>h</sup>	11	0	11	0
D+E+	DOX	2 mg	9 <sup>h</sup>	11	0	11	0
D+E-	DOX	3 mg	8 <sup>i</sup>	-	-	-	-
D+E+	DOX	3 mg	8 <sup>i</sup>	-	-	-	-
D+E-	CIS <sup>j</sup>	0.00357 mg	7	100	0	0	0
D+E+	CIS	0.00357 mg	6	100	0	0	0
D+E-	CIS	0.0357 mg	6	83	17	0	0
D+E+	CIS	0.0357 mg	6	33	0	0	67
D+E-	CIS	0.357 mg	10 <sup>k</sup>	0	10	10	40
D+E+	CIS	0.357 mg	9 <sup>k</sup>	11	0	0	44
D+E+	TAX <sup>l</sup>	0.308	5	100	0	0	0
D+E-	TAX	0.308	5	100	0	0	0
D+E+	TAX	0.0038	5 <sup>m</sup>	100	0	0	0
D+E-	TAX	0.0038	5 <sup>m</sup>	100	0	0	0

a: dose of drug per tumor  
b: PD = Progressive disease = tumor increasing in size Day 14 compared to Day 0  
c: SD = Stable disease = tumor decreasing less than 50% in size Day 14 compared to Day 0  
d: PR = Partial response = tumor decreasing in size more than 50% Day 14 compared to Day 0  
e: CR = Complete Response = no tumor present on Day 14  
f: 5 FU = 5 Fluorouracil  
g: DOX = Doxorubicin  
h: 7 animals died due to toxicity prior to day 14  
i: 8 animals died due to toxicity prior to day 14  
j: CIS = Cisplatin  
k: 4 animals died due to toxicity prior to day 14  
l: TAX = Taxol  
m: 2 animals died prior to day 14

plete response rate at 35 days for the D+E+ group was 70% (Table 3) with 60% remaining tumor free for greater than 100 days (cure). These results confirmed the initial experiments. The D+E- group had a 35 day complete response rate and cure rate (100 days) of 30% (Table 3). The other control groups (D-E+ and D-E-) showed no response.

#### ECT for sarcoma

*Treatment with bleomycin:* Examination of the effectiveness of using a single ECT treatment with bleomycin to treat soft tissue sarcoma was performed in an athymic rat model. Tumor response was based on the reduction in tumor volume 28 days after ECT treatment. No objective responses were seen in

the D-E-, D-E+, or D+E- control groups (Table 4). All tumors in the control groups showed progressive disease with the exception of one animal which had a tumor that remained stable after treatment with drug only. In contrast, animals in the D+E+ group had a complete response rate of 100% (Table 4). All animals in this group had no palpable tumors 7 days after treatment. Between days 35 and 100, seven of the tumors recurred. Five of the ECT treated tumors (42%) responded completely for 100 days and were considered cured. The complete response rate of the D+E+ group was significantly different from each of the control groups ( $p < 0.001$ ). To confirm the results of this study, random biopsies of the remaining scar from D + E + tumors as well as tumors from control groups

**Table 3.** Treatment of hepatomas with cisplatin (0.0357 mg/100  $\mu$ l)

Group	n	Volume Initial	Final	% PD <sup>a</sup>	% SD <sup>b</sup>	% PR <sup>c</sup>	% CR <sup>d</sup>	% Cures <sup>e</sup>
D-E-	8	82.8	12032	100	0	0	0	0
D-E+	10	75.4	7926	100	0	0	0	0
D+E-	10	140.0	16037	70	0	0	30	30
D+E+	10	120.0	480.1	30	0	0	70	60

a: PD = Progressive disease = tumor increasing in size Day 35 compared to Day 0

b: SD = Stable disease = tumor decreasing less than 50% in size Day 35 compared to Day 0

c: PR = Partial response = tumor decreasing in size more than 50% Day 35 compared to Day 0

d: CR = Complete Response = no tumor present on Day 35

e: Cure = No evidence of tumor 100 days after treatment

**Table 4.** Treatment of rat sarcomas with bleomycin (5 U/ml); injection volume is 25% tumor volume (single treatment)

Group	n	Volume Initial	Day 28	% PD <sup>a</sup>	% SD <sup>b</sup>	% PR <sup>c</sup>	% CR <sup>d</sup>	% Cure <sup>e</sup>
D-E-	12	220.2	3005.9	100	0	0	0	0
D-E+	12	281.2	2998.4	100	0	0	0	0
D+E-	12	140.0	2414.5	91.7	8.3	0	0	0
D+E+	12	278.7	0	0	0	0	100	42
D+E+ <sup>f</sup>	8	4621.9	2035.0	12.5	0	37.5	50	12.5

a: PD = Progressive disease = tumor increasing in size Day 28 compared to Day 0

b: SD = Stable disease = tumor decreasing less than 50% in size Day 28 compared to Day 0

c: PR = Partial response = tumor decreasing in size more than 50% Day 28 compared to Day 0

d: CR = Complete Response = no tumor present on Day 28

e: Cure = No evidence of tumor 100 days after treatment

f: Retreatment of D+E- tumors after >35 days (treatment of large tumors)

were taken at day 28. All tumors in the control group showed evidence of malignant sarcoma cells with a high mitotic rate and minimal necrosis of the tumor. However, tumors in the D + E + group showed a few anucleated tumor cell associated with abundant necrotic tissue suggestive of no residual viable tumor.

To examine if the therapy would work on large tumors, tumors of the D+E- group, showing no response 35 days after treatment were treated with ECT. The treatment of these large tumors resulted in a 50% complete response rate and a 37.5% partial response rate (Table 4). In addition, treatment of these large tumors only had a cure rate of 12.5%.

The low cure rate obtained with both small and large tumors was surprising due to the high complete response rate. It is possible that the single treatment was not sufficient to eliminate all tumor cells. Previous work in mouse models with subcutaneous tumors had demonstrated an increased cure rate when multiple treatments were performed.<sup>31</sup> Therefore, an additional experiment was performed to determine if multiple ECT treatments with bleomycin would be beneficial. Small tumors that received multiple ECT treatments showed a cure rate of 83.3% (Table 5) compared to the 42% cure rate obtained with single treatment (Table 4). Treatment of large tumors with multiple treatments resulted in a cure rate of 100% (Table 5).

*Treatment with other chemotherapeutic agents:*The effectiveness of treating sarcoma with cisplatin or doxorubicin in combination with electric pulses was studied. Cisplatin was administered at a dose of 1 mg/ml via intratumor injection. The injection volume was equivalent to 50% of the tumor volume. Two treatment groups were used, drug alone (D+E-) or drug with electric pulses (D+E+). The D+E+ group had a 33% complete response at 28 days and a 33% cure rate (Table 6). The D+E- group had a 17% complete response rate and 17% cure rate (Table 6). Doxorubicin was administered at a dose of 20 mg/ml via intratumor injection. The injection volume was equivalent to 100% of the tumor volume. The D+E+ group had a 17% complete response at 28 days and a 0% cure rate (Table 6). The D+E- group had a 0% complete response rate and 0% cure rate (Table 6). Doxorubicin treatment had a high toxicity as 5 of 6 animals died in each group. All deaths occurred prior to day 14. However, tumor volumes were obtained on day 7 and at time of death.

Discussion

Primary hepatocellular carcinoma is associated with chronic hepatitis B infection and liver cirrhosis. Approximately 80% of patients who develop hepatomas are positive for hepatitis B surface antigen.<sup>43</sup> These patients have

Table 5. Multiple treatment of sarcomas with bleomycin (5 U/ml); injection volume is 25% tumor volume

Group	n	Volume		% PD <sup>a</sup>	% SD <sup>b</sup>	% PR <sup>c</sup>	% CR <sup>d</sup>	% Cure <sup>e</sup>
		Initial	Final					
D+E-	5	213.2	1538.3	80	0	0	20	20
D+E+	6	183.0	25.9	0	16.7	0	83.3	83.3
D+E+	6	3158.2	0	0	0	0	100	100

a: PD = Progressive disease = tumor increasing in size Day 28 compared to Day 0  
b: SD = Stable disease = tumor decreasing less than 50% in size Day 28 compared to Day 0  
c: PR = Partial response = tumor decreasing in size more than 50% Day 28 compared to Day 0  
d: CR = Complete Response = no tumor present on Day 28  
e: Cure = No evidence of tumor 100 days after treatment

**Table 6.** Treatment of rat sarcomas (single treatment)

Treatment	Drug	Dose <sup>a</sup>	n	% PD <sup>b</sup>	% SD <sup>c</sup>	% PR <sup>d</sup>	% CR <sup>e</sup>	% Cure <sup>f</sup>
D+E-	CIS <sup>g</sup>	1.0 mg	6	66	17	0	17	17
D+E+	CIS	1.0 mg	6	50	17	0	33	33
D+E-	DOX <sup>h</sup>	20 mg	6	100	0	0	0	0
D+E+	DOX	20 mg	6	83	0	0	17	0

a: dose of drug per ml

b: PD = Progressive disease = tumor increasing in size Day 28 compared to Day 0

c: SD = Stable disease = tumor decreasing less than 50% in size Day 28 compared to Day 0

d: PR = Partial response = tumor decreasing in size more than 50% Day 28 compared to Day 0

e: CR = Complete Response = no tumor present on Day 28

f: Cure = No evidence of tumor 100 days after treatment response determined 35 days after treatment

g: CIS = Cisplatin

h: DOX = Doxorubicin

chronic subclinical hepatitis infection for many years, and most of them go on to develop advanced liver disease including hepatic cirrhosis. Currently, the treatment of primary hepatocellular carcinoma remains a significant problem not only in the United States, but in third world countries which have a higher incidence of chronic hepatitis B infection.<sup>44</sup> In addition, the diagnosis of hepatocellular carcinoma is made late in the disease process and the chance for curative therapy is relatively low. Since most patients diagnosed with hepatomas have liver cirrhosis and a limited hepatic reserve, they do not tolerate major hepatic resections. Therefore, new and less invasive treatment modalities with higher cure rates are clearly needed to effectively eliminate these tumors.

Hepatic resection of primary hepatocellular carcinoma carries a low 5 year survival rate of 18 to 36%.<sup>44</sup> Furthermore, patients with hepatomas and advanced liver cirrhosis are not candidates for major liver resections. Survival after hepatic resection is dependent on the patients hepatic reserve and whether the liver is able to undergo adequate regeneration after a major resection. A large study of 444 consecutive hepatic resections at John Cochran Veterans Affairs Medical Center demonstrated that hepatic resections in patients with hepatomas is a dangerous procedure with a 21% operative mortality, com-

pared to a 4% operative mortality for major liver resections done for colorectal metastases.<sup>45</sup> Since modalities such as standard chemotherapy, major liver resections, and liver transplantation have been used with very limited success, ECT using cisplatin or bleomycin is an attractive alternative for liver tumors which have been deemed surgically nonresectable due to hepatic failure and advanced liver cirrhosis. ECT can also benefit patients with multiple unresectable tumors and tumors which can not be removed due to their location near vital structures. In addition, animal and human studies demonstrate that ECT is a less invasive and a more effective cytoreductive procedure, which carries a lower morbidity and mortality.

To confirm the effectiveness of ECT, several experiments were conducted using electric pulses and direct intratumor injection of bleomycin to treat measurable liver tumors induced in rats. Hepatomas treated with ECT using bleomycin showed statistically significant responses. These responses are consistent with prior studies and they are readily reproducible. Objective responses were obtained in 84.5% of the tumors treated with both electric pulses and bleomycin. This group also had a 69% complete response rate. Of interest, tumors that received electric pulses only (D-E+), or no treatment (D-E-) were found to have 100% progressive disease.

A minimal 10% response rate resulted in tumors treated with bleomycin alone (D+E-).

Several other drugs were also examined for use with ETC. The only drug that showed any effectiveness was cisplatin. The best response using cisplatin was obtained with a dose of 0.0357mg in combination with electric pulses. A 67% complete response rate was obtained. No responses were observed in tumors treated using cisplatin without electric pulses. The study was extended to determine long term responses with cisplatin at this dose. ECT with cisplatin (0.0357 mg) resulted in a 60% cure rate (no evidence of disease for 100 days). Treatment with cisplatin alone resulted in a 30% cure rate. The results presented in this study demonstrate that electric pulses combined with either bleomycin or cisplatin is a safe and effective treatment. ECT can be used to treat liver lesions that are locally extensive, centrally located, or near vital structures. In addition, ECT is a safe alternative in patients with liver cirrhosis and in patients with multiple non resectable lesions.

The soft tissue sarcoma studies also demonstrate the applicability of ECT in the treatment of aggressive human sarcoma tumors. A study was performed using a combination of ECT and intratumor injection of bleomycin to treat human soft tissue sarcomas in athymic rats. No objective responses were seen in the D-E-, D- E+, or D+ E-control groups. All tumors in these control groups showed progressive disease with the exception of one animal which remained stable after treatment with drug only. In contrast, animals in the D+E+ group had a complete response rate of 100%. However, the cure rate of small sarcoma tumors which received a single treatment of ECT was only 42%, and the cure rate of the large tumors was even less (12.5%). Therefore, a trial of multiple ECT treatments was performed to improve the overall cure rates. As a result, small tumors (approximately 250 mm<sup>3</sup>) that

received multiple ECT treatments showed a cure rate of 83.3% compared to the 42% cure rate obtained with a single treatment. The multiple treatment protocol increased the cure rate of large tumors (4000 mm<sup>3</sup>) from 12.5% to 100%. Of interest, the delivery of cisplatin and doxorubicin with electric pulses resulted in minimal antitumor effects.

The current treatment of soft tissue sarcomas have met with limited success, and the survival rates for adults with these tumors remains very poor. In addition, the complete elimination and the successful long term cure rate of highly aggressive sarcoma tumors remains a significant problem today. The use of adjuvant radiation therapy and chemotherapy is of some value in adult patients, but the most effective treatment of aggressive sarcoma tumors is extensive local resection. However, surgical treatment may not be a technically feasible option in tumors which are too extensive for adequate surgical resection or for tumors that are located near vital structures. In contrast, the electrically mediated delivery of bleomycin is a technically feasible and highly effective treatment alternative for sarcoma patients who would otherwise require an amputation because their tumors are located close to joints, bones, and nerves or other vital structures. Since ECT treatment preserves limb function, it can be used in patients as a limb sparing procedure. In conclusion, ECT is a safe procedure with minimal morbidity and functional disability, which may be used in the treatment of aggressive sarcomas that are not amenable to limb sparing surgery.

### Acknowledgements

This work was supported by research grants from Genetronics, Inc. San Diego, CA; American Cancer Society (DHP-84436) and the University of South Florida Departments of Chemical Engineering and Surgery.

## References

1. Chang DC, Chassy BM, Saunders JA, Sowers AE, editors. *Guide to electroporation and electrofusion*. San Diego, Academic Press, 1992.
2. Neumann E, Schaefer-Ridder M, Wang Y, Hof-schneider PH. Gene transfer into mouse lyoma cells by electroporation in high electric fields. *EMBO J* 1982; **1**: 841-5.
3. Potter H. Electroporation in biology: methods, applications and instrumentation. *Anal Biochem* 1988; **174**: 361-73.
4. Weaver JC. Electroporation: a general phenomenon for manipulating cells and tissues. *J Cell Biochem* 1993; **51**: 426-35.
5. Powell KT, Morgenthaler AW, Weaver JC. Tissue electroporation: observation of reversible electrical breakdown in viable frog skin. *Biophys J* 1989; **56**: 1163-71.
6. Prausnitz MR, Bose VG, Langer R, Weaver JC. Electroporation of mammalian skin: a mechanism to enhance transdermal drug delivery. *PNAS* 1993; **90**:10504-8.
7. Grasso RJ, Heller R, Cooley JC, Heller EM. Electrofusion of individual animal cells directly to intact corneal epithelial tissue. *Biochim Biophys Acta* 1989; **980**: 9-14.
8. Heller R and Grasso RJ. Transfer of human membrane surface components by incorporating individual human cells into intact animal tissue by cell-tissue electrofusion *in vivo*. *Biochim Biophys Acta* 1990; **1024**: 185-8.
9. Heller R, Gilbert R. Biological applications of cell-tissue electrofusion. In: Chang DC, Chassy BM, Saunders JA and Sowers AE, eds. *Guide to electroporation and electrofusion*. San Diego: Academic Press, 1992: 393-410.
10. Mir LM, Banoun H, Paoletti C. Introduction of definite amounts of nonpermeant molecules into living cells after electroporabilization: direct access to the cytosol. *Exp Cell Res* 1988; **175**: 15-25.
11. Orlowski S, Belehradek JJr, Paoletti C, Mir LM. Transient electroporabilization of cells in culture. *Biochem Pharmacol* 1988; **37**: 4727-33.
12. Mir LM, Orlowski S, Belehradek JJr, Paoletti C. Electrochemotherapy: potentiation of antitumor effect of bleomycin by local electric pulses. *Eur J Cancer* 1991; **27**: 68-72.
13. Belehradek JJr, Orlowski S, Poddevin B, Paoletti C, Mir LM. Electrochemotherapy of spontaneous mammary tumors in mice. *Eur J Cancer* 1991; **27**: 73-6.
14. Pron G, Belehradek JJr, Mir LM. Identification of a plasma membrane protein that specifically binds bleomycin. *Biochem Biophys Res Commun* 1993; **194**: 333-7.
15. Muraoka Y, Takita T. Bleomycins. *Cancer Chemotherapy and Biological Response Modifiers Annual* 1990; **11**: 58-66.
16. Mir LM, Tounekti O, Orlowski S. Bleomycin: Revival of an old drug. *Gen Pharmacol* 1996; **27**: 745-8.
17. Povirk LF, Hogan M, Dattagupta C. Binding of bleomycin to DNA: Intercalation of the bithiazole rings. *Biochemistry* 1979; **18**: 96-101.
18. Poddevin B, Orlowski S, Belehradek JJr, Mir LM. Very high cytotoxicity of bleomycin introduced into the cytosol of cells in culture. *Biochem Pharmacol* 1991; **42(S)**:67-75.
19. Okino M, Marumoto M, Kanesada H, Kuga K, Mohri H. Electrical impulse chemotherapy for rat solid tumors. *Proc Jpn Cancer Congress* 1987; **46**: 420.
20. Okino M, Esato K. The effects of a single high voltage electrical stimulation with anticancer drug on *in vivo* growing malignant tumors. *Jpn J Surg* 1990; **20**: 197-204.
21. Okino M, Tomie H, Kanesada H, Marumoto M, Morita N, Esato K, Suzuki H. Induction of tumor specific selective toxicity in electrical impulse chemotherapy-analysis of dose response curve. *Oncologia* 1991; **24**: 71-9.
22. Okino M, Tomie H, Kanesada H, Marumoto M, Esato K, Suzuki H. Optimal electric condition in electrical impulse chemotherapy. *Jpn J Cancer Res* 1992; **83**: 1095-101.
23. Kanesada H. Anticancer effect of high voltage pulses combined with concentration dependent anticancer drugs on Lewis lung carcinoma. *J Jpn Soc Cancer Ther* 1990; **25**: 2640-48.
24. Salford LG, Persson BRR, Brun A, Ceberg CP, Kongstad PCh, Mir LM. A new brain tumor therapy combining bleomycin with *in vivo* electroporabilization. *Biochem Biophys Res Commun* 1993; **194**: 938-43.
25. Heller R, Jaroszeski M, Leo-Messina J, Perrott R, Van Voorhis N, Reintgen D, Gilbert R. Treatment of B16 melanoma with the combination of electroporation and chemotherapy. *Bioelectrochem Bioener* 1995; **36**: 83-7.



26. Sersa G, Cemazar M, Miklavcic D, Mir LM. Electrochemotherapy: variable anti-tumor effect on different tumor models. *Bioelectrochem Bioener* 1994; **35**: 23-7.
27. Yamaguchi O, Irisawa C, Baba K, Oghihara M, Yokota T, Shiraiwa Y. Potentiation of antitumor effect of bleomycin by local electric pulses in mouse bladder tumor. *Tohoku J Exp Med* 1994; **172**: 291-3.
28. Dev SB, Hofmann GA. Electrochemotherapy-a novel method of cancer treatment. *Cancer Treatment Rev* 1994; **20**: 105-15.
29. Jaroszeski M. J, Gilbert R, Heller R. Successful treatment of hepatomas with electrochemotherapy in a rat model. *Biochim Biophys Acta* 1997; **1334**: 15-8.
30. Heller R, Jaroszeski M, Perrott R, Messina J, Gilbert R. Effective treatment of B16 melanoma by direct delivery of bleomycin using electrochemotherapy. *Melanoma Res* 1997; **7**: 10-8.
31. Jaroszeski M, Gilbert R, Perrott R, Heller R. Effectiveness of treating B16 melanoma with multiple treatment electrochemotherapy. *Melanoma Res* 1996; **6**: 427-33.
32. Yabushita H, Yoshikawa K, Hirata F, Hojyoh T, Fukatsu H, Noguchi M, Nakanishi M. Effects of electrochemotherapy on CaSki cells derived from a cervical squamous cell carcinoma. *Gynecol Oncol* 1997; **65**: 297-303.
33. Sersa G, Cemazar M, Miklavcic D. Antitumor effectiveness of electrochemotherapy with cis-dichlorodiammineplatinum(II) in mice. *Cancer Res* 1995; **55**: 3450-55.
34. Mir LM, Belehradek M, Domenge C, Orlowski S, Poddevin JJr, Schwab G, Luboinnski B, Paoletti C. Electrochemotherapy, a novel antitumor treatment: first clinical trial. *CR Acad Sci Paris* 1991; **313**: 613-8.
35. Belehradek M, Domenge C, Luboinnski B, Orlowski S, Belehradek J, Mir LM. Electrochemotherapy, a new antitumor treatment: first clinical phase I-II trial. *Cancer* 1993; **72**: 3694-700.
36. Heller R. Treatment of cutaneous nodules using electrochemotherapy. *J Florida Med Assoc* 1995; **82**: 147-50.
37. Rudolf Z, Stabuc B, Cemazar M, Miklavcic D, Vodovnik L, Sersa G. Electrochemotherapy with bleomycin. The first clinical experience in malignant melanoma patients. *Radiol Oncol* 1995; **29**: 229-35.
38. Domenge C, Orlowski S, Luboinnski B, De Baere T, Schwaab G, Belehradek Jr, Mir LM. Antitumor electrochemotherapy: new advances in the clinical protocol. *Cancer* 1996; **77**: 956-63.
39. Heller R, Jaroszeski MJ, Glass LF, Messina JL, Rapaport DP, DeConti RC, Fenske NA, Gilbert RA, Mir LM, Reintgen DS. Phase I/II trial for the treatment of cutaneous and subcutaneous tumors using electrochemotherapy. *Cancer* 1996; **77**: 964-71.
40. Reintgen DS, Jaroszeski MJ, Heller R. Electrochemotherapy, a novel approach to cancer. *Journal of the Skin Cancer Foundation XIV* 1996; **83**: 17-9.
41. Gilbert R, Jaroszeski MJ, Heller R. Novel electrode designs for electrochemotherapy. *Biochem Biophys Acta* 1997; **1334**: 9-14.
42. Hofmann GA, Dev SB, Nanda GS. Electrochemotherapy: transition from laboratory to the clinic. *IEEE Eng Med Biol* 1996; **15**: 124-32.
43. Arthur MJ, Hall AJ, Wright R. Hepatitis B, hepatocellular carcinoma, and strategies for prevention. *Lancet* 1984; **1**: 607.
44. Millis JM and Tompkins RK. Malignant liver tumors. In: Cameron JC, ed. *Current surgical therapy*. St. Louis, Mosbey. 1995: 277-80.
45. Nadig DE, Wade TP, Fairchild RB, Virgo KS, Johnson FE. Major hepatic resection. Indications and results in a national hospital system from 1988 to 1992. *Arch Surg* 1997; **132**: 115-9.

## Longitudinal study of malignancy associated changes in progressive cervical dysplasia

Margareta Fležar<sup>1</sup>, Jaka Lavrenčak<sup>1</sup>, Mario Žganec<sup>2</sup>, and Marija Us – Krašovec<sup>1</sup>

<sup>1</sup>Institute of Oncology, <sup>2</sup>Faculty of Electrical Engineering, Ljubljana, Slovenia

---

*Eight of 29 patients with progressive CIN were followed for 2 to 10 years. Their consecutive Pap smears were destained and stained according to Feulgen thionin method. Cyto-Savant™ high resolution image cytometer (Oncometrics Technol. Corp., Vancouver, Canada) was used for image acquisition and analysis. Average values of nuclear texture features and their probability distributions for consecutive Pap smears from each patient were calculated. Three out of 5 discriminant MAC, highDNAamount, highDNAcomp and highDNAarea, were found to increase as a function of time in 5 out of 8 patients. A preliminary analysis which was performed on non-standardized archival material demonstrated a monotonous increase of discrete texture features as a function of time in patients with progressive CIN.*

*Key words: cervix dysplasia; image cytometry; cell nucleus*

---

### Introduction

The goal of an efficient screening of uterine cervical smears is the eradication of invasive cancer of the cervical squamous epithelium. This could be achieved by an early detection and subsequent treatment of precancerous lesions. However, the debatable issue remains the treatment of moderate dysplasias (CIN 2). The follow up of the patients with moderate dysplasias that were not treated showed that some of these lesions regressed to mild dysplastic lesions or even regressed back to normal squameous epithelium, while some progressed to severe dysplasia, carcino-

ma in situ and invasive carcinoma. At the time of diagnosis of moderate dysplasia one cannot predict whether the lesion will progress and whether the treatment of the lesion should be administered. Additional diagnostic tools would therefore be helpful to establish the biological potential of moderate dysplasias.

Some authors claim that the analysis of cells and – or nuclei by means of image cytometers can yield data about the progression or regression of the lesions.<sup>1,2,3</sup> Their hypothesis is based on measurements of chromatin structure and organization (nuclear texture features). Moderate dysplastic lesions that will progress to cancer differ from the ones that will regress mainly in nuclear texture features. The combination of nuclear texture features discriminating

Correspondence to: Margareta Fležar, MD, MSc, Institute of Oncology, Dept. Cytopathology, Zaloška 2, 1105 Ljubljana. Tel: +386 61 323 063 ext. 4946; Fax: +386 61 1314 180; E-mail: miflezar@onko-i.si

between the two lesions that have a different biological potential is described as MAC (malignancy associated changes) or in some other studies as kariometric factors.<sup>1,2,4</sup>

In our previous study we found significant differences between progressive and regressive moderate dysplasias (CIN 2) by image cytometric analysis in five nuclear texture features which could be explained as MAC.<sup>5</sup> In the present study our aim was to determine the time of onset of MAC which would be characteristic for progressive moderate dysplasias. The occurrence of MAC was studied on normal intermediate cells present in the cervical smears obtained by the routine screening program.

**Materials and methods**

From the files of 3 different laboratories, 29 patients with progressive and 21 patients with regressive moderate dysplasias (CIN 2) were found. However, only 8 patients (ages 22 to 42 years) were followed up with at least three consecutive cervical smears before the diagnosis of progression to CIN 3 (severe dysplasia or carcinoma in situ) was established (Table 1). Their follow-up ranged from 2 to 10 years.

The cervical smears that were originally Papanicolaou stained were destained in acid alcohol and nuclear DNA was stained stechiometrically according to modified Feulgen

method by thionin. Image cytometric analysis was performed by an automated high resolution image cytometer Cyto-Savant™ (Oncometrics Technol. Corp., Vancouver, Canada).<sup>6</sup>

From the several hundred nuclei acquired automatically, we selected an average of 76 ranging from 15 to 177, well preserved nuclei of normal (non-diagnostic) intermediate squamous cells per cervical smear. Over 100 nuclear features and most importantly nuclear texture features were calculated for each nucleus scanned, detailed description and formulas of nuclear features are described elsewhere.<sup>7</sup> Probability distributions were calculated for each nuclear texture feature, however, longitudinal observation of MAC appearance was performed only for the nuclear texture features found to have discriminative power between progressive and regressive moderate dysplasias in our previous study (Table 2). These features belong to the group of discrete nuclear texture features and reflect subtle differences in condensation between the neighbouring chromatin particles.

**Results**

The longitudinal observation of discriminating nuclear texture features showed a monotonous increase of values of 3 out of 5 nuclear texture features as a function of time in progressive moderate dysplasias in 5 patients.

The values of "highDNAcomp" increased through the time, that is from the first smear, diagnosed as moderate dysplasia, to the last one diagnosed as severe dysplasia or carcinoma (Figure 1). In five patients (patients 2, 5, 6, 7, 8) we observed a slight decrease, no increase, or slight increase of value between the first and the second smear. However, a substantial increase was found between their second and the third (last) smear. In two patients (patients 3, 4) the values of "highD-

**Table 1.** Patient's diagnosis, age at the time of diagnosis and the length of follow-up in years

Patient	Diagnosis	Age at diagnosis (years)	Follow-up (years)
1	CIN 3	23	2
2	CIN 3	33	6
3	CIN 3	29	9
4	CIN 3	29	7
5	CIN 3	23	6
6	CIN 3	42	10
7	CIN 3	25	6
8	CIN 3	22	3

**Table 2.** Nuclear texture features, which discriminated between progressive and regressive dysplasias

Discriminative nuclear texture features	
HighDNAarea:	Fraction of the total nuclear area occupied by high condensed chromatin
HighDNAamount:	Ratio of IOD* of high condensed chromatin ( $IOD^*_{high}$ ) to IOD*
HighDNAcomp**:	Shape of high condensed chromatin

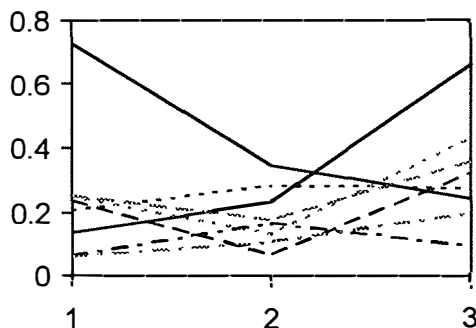
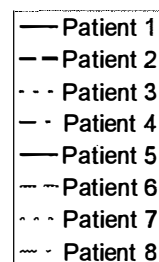
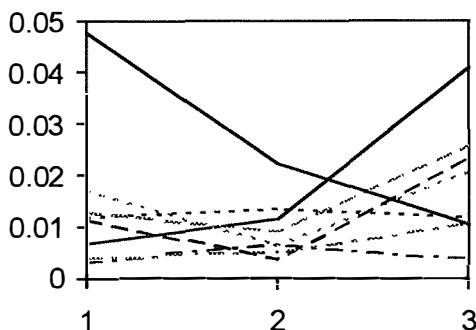
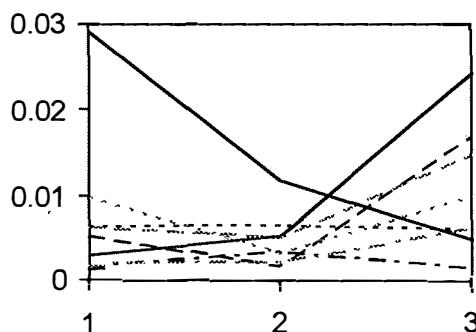
\* Integrated Optical Density    \*\* highDNAcompactness

NAcomp" remained basically unchanged throughout the whole period, even though there was a slight increase between their first and the second smear. One patient (patient 1) showed exactly a reverse pattern of nuclear feature changes, that is an overall decrease in the value of this feature throughout the period.

A very similar pattern in changes of values was found for "highDNAamount" (Figure 2). Again, five patients (patients 2, 5, 6, 7, 8) showed slight or no increase or even some decrease between the first and the second smear, and significant increase between their second and the last smear. The same two patients (patients 3, 4) presented with relatively unchanged values of this feature throughout the period. One patient (patient 1), the same as above, showed significant decrease in "hiDNAamount" values from her first to the last smear.

In addition, the longitudinal observation of "highDNAarea" showed a similar pattern of changes to the other two features in the same five patients (patients 2, 5, 6, 7, 8) (Figure 3). For this feature the values for five patients were practically unchanged between the first and the second smear. Afterwards, the values increased substantially. Two patients (patients 3, 4) had the constant values of this feature through the time, and, again, in one patient (patient 1) the values decreased from her first to the last smear.

Other features that were discriminative in the previous study did not show a convincing pattern of increase in the majority of patients.

**Figure 1.** The dynamics of "highDNAcomp" in consecutive smears of patients with progressive dysplasias.**Figure 2.** The dynamics of "highDNAamount" in consecutive smears of patients with progressive dysplasias.**Figure 3.** The dynamics of "highDNAarea" in consecutive smears of patients with progressive dysplasias.

## Discussion

Population screening of cervical smears for an early detection of preneoplastic lesions of uterine cervix is becoming an important issue in health care programs in different countries all over the world. Some countries have already established efficient screening programs that cover high percentage of women, while others are still in the process of introducing a widespread screening. A successful screening program detects more women with early preneoplastic changes, such as mild and moderate dysplasias of cervical epithelium.<sup>8</sup> By light microscopy it is not possible to assess the biologic behaviour of cervical dysplasias. To avoid the overtreatment of women harbouring dysplasias with nonprogressive course, they should possibly be defined as such by an additional diagnostic analysis.

Image cytometry was used to measure the chromatin structure and organization in cervical neoplastic lesions objectively. Initially, the nuclei of diagnostic cells in dysplastic lesions were analyzed and cytometric differences between the nuclei of different grades of dysplasias were reported.<sup>9,10</sup> These studies were mostly performed as a part of projects that would introduce automated image cytometric screening of cervical smears, and nuclear texture features were used to correct classification of the cells into normal and dysplastic ones.

Besides, the subvisual chromatin changes were also studied in normal intermediate cells, which were also present in the cervical smears together with dysplastic cells.<sup>11, 12, 13, 14, 15</sup> Subtle chromatin changes were first detected by means of light microscopy examination in normal cells of patients with a malignant disease and were described as malignancy associated changes (MAC).<sup>16</sup> With the development of high resolution image cytometers the MACs were objectively measured and they were found not only in

connection with different malignant tumors, but also in normal cells of dysplastic lesions, hence also in dysplasias of cervical epithelium.<sup>1,2,11,12,13,14,15</sup>

Subsequently, the idea of MAC was introduced in the studies of progression or regression of cervical dysplastic lesions. Some authors claim that chromatin structure of progressive dysplastic lesion differs from the structure of regressive lesions.<sup>1,2,3</sup> In our previous study we were also able to discriminate between the two types of lesions by using certain nuclear texture features.<sup>5</sup> However, the dynamics of subvisual chromatin structure changes as a function of time has not been studied yet. In our small group of patients, followed-up for 2 to 10 years, the increase of discriminative nuclear texture features in subsequent smears was found in some patients in normal intermediate cells. Since the discriminative texture features from the previous study reflect the condensed portion of chromatin particles in the nucleus, the results of this study suggest a condensation of chromatin with the progression of the lesion. A larger data set with more patients involved in the study should be made to confirm our observations. Also, a larger and more consistent increase of the feature values could be expected, if there were no variations in the initial preparation (the effect of fixation and original staining), which were found to cause differences in nuclear texture features.<sup>17</sup> Besides, nuclear texture features are also influenced by the age of the patients, vaginal inflammations and hormonal status.<sup>13,18</sup>

We expect that more extensive image cytometric studies on different grades of cervical dysplasias will define which patients would progress to more severe lesions and which lesions will regress. If several subsequent smears of the same patient were obtained through a more efficient screening program, we could retrospectively learn more precisely, when the exact progression begins. Accord-

ingly, most appropriate treatment would be planned and most of all the aggressive overtreatment of patients, still in childbearing age, would be avoided.

### Acknowledgment

This work was partly supported by the Slovenian Ministry of Science and Technology, grant No. J3-7956.

### References

1. Palcic B, MacAulay C. Malignancy associated changes. Can they be employed clinically? In: Weid GL, Bartels PH, Rosenthal D, Schenk U, ed. *Compendium on the computerized cytology and histology laboratory*. Chicago; Tutorials of cytology, 1994; 157-65.
2. Palcic B. Nuclear texture: Can it be used as a surrogate endpoint marker? *J Cell Biochem* 1994; **Suppl 19**: 40-6.
3. Hanselaar A, MacAulay C, Palcic B, Garner D, LeRiche J. Discrimination between progressive and regressive cervical intraepithelial neoplasia (CIN) by DNA-cytometry. *Analyt Cell Pathol* 1992; **4**: 165, Abstract 134.
4. Bibbo M, Montag AG, Lerma-Puertas E, Dytch HE, Leelakusolvong S, Bartels PH. Karyometric marker features adjacent to invasive carcinoma. *Analyt Quant Cytol Histol* 1989; **11**: 281-2.
5. Kodrič T, But-Cigler N, Vrh- Jermančič J, Lavrenčak J, Žganec M, Us - Krašovec M. Nuclear texture features of normal intermediate cells in progressive and regressive/persistent cervical intraepithelial lesions. *Acta Cytol* 1997; **41**: 1210, Abstract.
6. Jaggi B, Poon S, Ponitfex B, Fengler J, Marquis J, Palcic B. A quantitative microscope for image cytometry. *Proc SPIE* 1991; **1448**: 89-97.
7. Doudkine A, MacAulay C, Poulin N, Palcic B. Nuclear texture measurements in image cytometry. *Pathologica* 1995; **87**: 286-99.
8. Koss L. The Papanicolaou test for cervical cancer detection. A triumph and a tragedy. *JAMA* 1989; **261**: 737-43.
9. Wied GL, Bartels PH, Dytch HE, Pishotta FT, Yamauchi K, Bibbo M. Diagnostic marker features in dysplastic cells from the uterine cervix. *Acta Cytol* 1982; **26**: 475-83.
10. Hanselaar A. DNA cytometry of cervical intraepithelial neoplasia. PhD Thesis, Katholieke Universiteit Nijmegen, October 1990.
11. Bibbo M, Bartels PH, Sychra JJ, Wied GL. Chromatin appearance in intermediate cells from patients from uterine cancer. *Acta Cytol* 1981; **25**: 23-8.
12. Bartels PH, Bibbo M, Dytch HE, Pishotta FT, Yamauchi K, Wied GL. Diagnostic marker displays for intermediate cells from uterine cervix. *Acta Cytol* 1982; **26**: 29-34.
13. Haroske G, Bergander St, König R. Frequency and diagnostic reliability of subvisual morphologic markers for malignancy in the cervical epithelium. *Arch Geschwulstforsch* 1988; **58**: 159-68.
14. Haroske G, Kunze KD, Dimmer V, Meyer W. Some remarks on preinvasive cervical neoplasia - an image analysis study. *Arch Geschwulstforsch* 1985; **55**: 245-52.
15. Haroske G, Bergander St, König R, Meyer W. Application of malignancy-associated changes of cervical epithelium in a hierarchic classification concept. *Anal Cell Pathol* 1990; **2**: 189-98.
16. Nieburgs HE, Goldberg AF, Bertini B, Silagi J, Pacheco B, Reisman H. Malignancy associated changes (MAC) in blood and bone marrow cells of patients with malignant tumors. *Acta Cytol* 1967; **11**: 415-23.
17. Fležar M, Us - Krašovec M. Differences in nuclear texture features caused by different initial fixation and duration of hydrolysis. *Anal Cell Pathol* 1997; **13**: 60, Abstract 16.
18. Kwikkel HJ, Boon ME, van Rijswijk MMM. Masking effect of hormonal contraceptives on discriminative features of visually normal intermediate cells in positive and negative cervical smears. *Anal Quant Cytol Histol* 1986; **8**: 227-32.



## Image cytometry analysis of normal buccal mucosa smears: influence of smoking and sex-related differences

Jaka Lavrenčak<sup>1</sup>, Margareta Fležar<sup>1</sup>, Mario Žganec<sup>2</sup>, Marija Us – Krašovec<sup>1</sup>

<sup>1</sup>Institute of Oncology, Department of Cytopathology, <sup>2</sup>Faculty of Electrical Engineering, Ljubljana, Slovenia

---

*To get more information about the influence of smoking on chromatin pattern of normal buccal mucosa cells and to assess sex-related differences in nuclear features, quantitative analysis of normal buccal mucosa smears was performed. In this study, buccal smears were collected from 78 healthy subjects. Image cytometry analysis was performed on Feulgen-thionin stained smears. Probability distributions of 78 nuclear features were calculated for both, cell-by-cell and slide-by-slide classifications. Seven nuclear features showed discriminative ability between smokers and non-smokers; most of them were nuclear texture features. Statistical analysis of nuclear features in groups of females and males showed that only two nuclear features were different. It is concluded that smoking should be considered in image cytometry analysis of lesions in oral cavity.*

*Key words: mouth mucosa; image cytometry; smoking; cell nucleus; sex factors*

---

### Introduction

During the last decades, semi-automated and, lately, fully automated high-resolution image cytometry has been used in research work.<sup>1,2</sup> Using image cytometer, different morphometric, densitometric and texture features of cell nuclei can be measured and analysed. In a number of studies on tissue sections and cell samples from different pre-cancerous and cancerous lesions, the diagnostic value and prognostic ability of quanti-

tative methods have been already tested.<sup>1-7,10,13</sup> It seems that malignancy associated changes (MAC), the term that was introduced by Nieburgs *et al.*<sup>14</sup> and denotes subtle changes in chromatin organisation in the nuclei of normal-appearing cells in patients with malignant diseases, can be objectively assessed by image cytometry.<sup>2,3,7,8</sup> However, in the field of quantitative cytometry there are still several, yet unsolved methodological problems. It is supposed that, besides pathological processes themselves,<sup>6,9,10,12</sup> many factors from the environment may affect nuclear features. Hence, the buccal mucosa cells may be affected by age, sex, smoking, consumption of alcohol and infection.<sup>3,4,16,17</sup>

In the present study, we used high resolu-

---

Correspondence to: Jaka Lavrenčak, M.Sc., Institute of Oncology, Department of Cytopathology, Zaloška 2, SI-1105 Ljubljana, Slovenia. Tel.: +386 61 323 063 ext. 49-46; Fax.: +386 61 131 41 80; E-mail: jlavrencak@onko-i.si



tion image cytometry to analyse the influence of smoking on nuclear features of normal squamous cells of the buccal mucosa as well as potential sex-dependent differences in nuclear features.

### Materials and methods

The cell samples were taken from 78 healthy subjects. The study group consisted of 52 females and 26 males without any clinical evidence of cancer. Among them, there were 22 smokers and 56 non-smokers. Buccal mucosa cells were collected with a wooden spatula. Liquid transport medium was used to resuspend and transport cell samples. Membrane filtration method and filter imprint technique were used for smear preparation. Two smears were prepared parallelly, one for light-microscopy examination and another for image cytometry analysis. The slides for light-microscopy examination were Papanicolaou stained. All buccal mucosa smears were cytopathologically diagnosed as normal. The smears for image cytometry analysis were fixed in Delaunay fixative and air-dried. After fixation, the slides were postfixed in Böhm-Sprenger fixative and stoichiometrically stained for DNA by modified Feulgen-thionin method.

Image acquisition and analysis were performed by Cyto-Savant™ high resolution image cytometer (Oncometrics Technol. Corp., Vancouver, Canada).<sup>15</sup> The image analysis system consists of a MicroImager 1400 digital camera with a light transducer and a charge-coupled device (CCD), which is made up of 1320 × 1035 individual sensor elements. The size of each sensor element is 6,8 µm × 6,8 µm. The digital camera is mounted on a Nikon light microscope with 20 × PlanApo objective lens with numerical aperture 0,75. This assures an effective pixel size, a square of 0,34 µm × 0,34 µm (~ 0,1 m<sup>2</sup>). The photometric resolution is 256 gray levels.

The slides were scanned automatically with Acquire program. Only intermediate cell nuclei of the buccal mucosa were selected for further analysis. The nuclei that were either overlapped or degenerated or out of focus, were manually separated and were not included in the statistical analysis. For each nuclear image, 78 nuclear features were calculated by the image analysis system. The statistical analysis was performed separately for smokers/non-smokers group and for females/males group. The probability distribution for each nuclear feature was calculated for 22 smokers (n=11665 cells) and for 56 non-smokers (n=24505 cells). Like for the smokers/non-smokers group, the probability distributions for each nuclear feature were also calculated for 52 females (n=25387 cells) and 26 males (n=10783 cells).

### Results

Out of 78 analysed nuclear features, one morphometric and 6 nuclear texture features were discriminative between smokers and non-smokers: area, lowDNAarea, medDNAarea, low\_av\_dst, lowDNAamount, lowDNAcomp and range-extreme (for description of nuclear features see Appendix 1). In cell-by-cell analysis, discriminative ability of those nuclear features ranged from 56,8 % to 58,6 %, whereas in slide-by-slide analysis, discriminative ability was between 55,8 % and 67,1 %. Nuclear features with best discriminative ability between smokers and non-smokers on the basis of cell-by-cell and slide-by-slide classifications are listed in Table 1.

The results of statistical analysis for sex-dependent groups (females and males) showed that only two nuclear features were different: range\_extreme and fractal1\_area (Appendix 1). In cell-by-cell analysis, discriminative ability ranged from 55 % to 56,8 % whereas in slide-by-slide analysis, it was between 60 % and 64,3 %. Nuclear features

**Table 1.** Nuclear features with best discriminative ability between smokers and non-smokers on the basis of cell-by-cell and slide-by-slide classifications

	Cell-by-cell classification (%)	Slide-by-slide classification (%)
Area	57,8	67,1
LowDNAarea	58,4	65,7
MedDNAarea	58,6	64,3
Low_av_dst	58,2	67,1
LowDNAamount	58,3	65,7
LowDNAcomp	58,3	65,7
Range_extreme	56,8	55,7

with best discriminative ability between females and males on the basis of cell-by-cell and slide-by-slide classifications and are presented in Table 2.

## Discussion

In previous light microscopy and image cytometry studies about the effect of age and smoking on normal cells in head and neck region as well as the sex-related differences, discrepant results were obtained. In 1973, Pappelis *et al.*<sup>17</sup> reported that a diversified nuclear area might be an indicator of the maturation status of buccal mucosa epithelium rather than age dependent changes. On the other hand, Cowpe *et al.*<sup>4</sup> believed that size variation of buccal mucosa nuclei is significantly age dependent.

Burger *et al.*<sup>3</sup> and Reith *et al.*<sup>13</sup> studied the

effect of smoking on buccal and nasal mucosa cells by image cytometer. In Burger's study, 17 smokers (n=1297 cells) and 46 non-smokers (n=3822 cells) were included. The linear discriminative analysis of nuclear features showed a 57,5 % correct cell classification, but differences between the specimens were not significant. Reith *et al.*<sup>13</sup> studied the effect of smoking on normal nasal mucosa cells of nickel workers. In this study, 9 smokers without dysplasia (n=608 cells) and 6 non-smokers (n=536 cells) were included. Although the number of analysed cells was small, they found significant differences in nuclear features between smokers and non-smokers. The results showed that 73,2 % of the cells of smokers and non-smokers could be correctly classified. In terms of specimen classification only one of non-smokers was incorrectly classified.

The results of our study, in which much larger number of cells was analysed than in previous studies, indicate that smoking can cause subtle changes of chromatin pattern. Our study group consisted of 22 smokers (n=11665 cells) and 56 non-smokers (n=24505 cells). Nuclear features showed discriminative ability between smokers and non-smokers in both, cell-by-cell and slide-by-slide analyses. In none of these studies, smoking habits, such as smoking period and number of cigarettes per day, were considered as factors which could also have an affect on nuclear chromatin pattern.

In addition, we investigated the sex-related differences in nuclear features of normal buccal mucosa cells. Two nuclear texture features showed 60 % and 64,3 % discriminative ability in slide classification. The statistical analysis was performed on the group of 52 females (n=25387 cells) and 26 males (n=10783 cells). Burger *et al.*<sup>3</sup> found four nuclear texture features that showed significant discriminative ability between sexes. According to them, sex dependent differences might be due to hormonal status or

**Table 2.** Nuclear features with best discriminative ability between females and males on the basis of cell-by-cell and slide-by-slide classifications

	Cell-by-cell classification (%)	Slide-by-slide classification (%)
Range_extreme	56,8	60
Fractal1_area	55	64,3

might be caused by an expression of X-chromosome (Barr body). Their study was performed on the group of 38 females (n=3338 cells) and 25 males (n=1781 cells). The overall correct cell classification was 62,8 % with significant specimen classification of 71,4 %. In contrast to the studies above, Cowpe *et al.*<sup>4</sup> studied nuclear area of buccal smears of 55 females and 50 males and did not find any differences. The relationship between nuclear and cell size of buccal mucosa smears and the stage of the menstrual cycle was not detected. In this study the smears were stained by Papanicolaou method. In our investigation, we analysed smears that were stoichiometrically stained for DNA by Feulgen-thionin method. Therefore, the discrepancy in results could be due to different staining procedures.

In conclusion, our pilot study suggests that smoking should be considered in image cytometry analysis of lesions in oral cavity. However, to get more reliable information about the influence of smoking on buccal cells as well as the sex-related differences, larger number of buccal mucosa smears should be analysed. Furthermore, for more reliable assessment of chromatin changes, also smoking habits, consumption of alcohol, medical history of healthy subjects and maturation of buccal mucosa epithelium should be considered.

## Appendix 1

Nuclear feature named *area* is a morphological nuclear feature that represents the nuclear area. Nuclear features *lowDNAarea*, *medDNAarea*, *low\_av\_dst*, *lowDNAamount* and *lowDNAcomp* are discrete nuclear texture features that are based on segmentation of nuclei into discrete regions of high, medium and low chromatin condensation. Nuclear feature *range\_extreme* is a local extreme nuclear texture feature that is calculated as

the difference between the highest local maximum and the lowest local minimum of smoothed image. Nuclear feature *fractal1\_area* is a fractal nuclear texture feature that represents measurements of the area of a three-dimensional surface, created by the nuclear optical density function.<sup>11</sup>

## Acknowledgement

This work was partly supported by the Slovenian Ministry of Science and Technology, grant No. J3-7956.

## References

1. Böcking A, Striepecke E, Auer H, Füzesi L. Static DNA Cytometry: Biological Background, Technique and Diagnostic Interpretation. In: Wied GL, Bartels PH, Rosenthal DL, Schenck U. *Compendium on the Computerized Cytology and Histology Laboratory*. Tutorials of Cytology, Chicago, Illinois, USA 1994: 107-28.
2. Palcic B, MacAulay C. Malignancy associated changes: can they be employed clinically? In: Wied GL, Bartels PH, Rosenthal DL, Schenck U. *Compendium on the Computerized Cytology and Histology Laboratory*. Tutorials of Cytology, Chicago, Illinois, USA 1994: 157-65.
3. Burger G et. al. Malignancy associated changes in squamous epithelium of the head and neck region. *Anal Cell Pathol* 1994; 7: 181- 93.
4. Cowpe JG, Longmore RB, Green MW. Quantitative exfoliative cytology of normal oral squames: an age, site and sex-related survey. *J Roy Soc Med* 1985; 78: 995-1004.
5. Cowpe JG, Longmore RB. Nuclear area and Feulgen DNA content of normal buccal mucosal smears. *J Oral Pathol* 1981; 10: 81-6.
6. Cowpe JG. Quantitative exfoliative cytology of normal and abnormal oral mucosal squames: preliminary communication. *J Roy Soc Med* 1984; 77: 928-31.
7. Klawe H, Rowinski J. Malignancy associated changes (MAC) in cells of buccal smears detected by means of objective image cytometry. *Acta Cytol* 1974; 18: 30-3.
8. Ogden GR, Cowpe JG, Green MW. The effect of distant malignancy upon quantitative cytologic

- assessment of normal oral mucosa. *Cancer* 1990; **65**: 477-80.
9. Schulte EKW, Joos U, Kasper M, Eckert HM. Cytological detection of epithelial dysplasia in the oral mucosa using Feulgen-DNA-image cytometry. *Diag Cytopathol* 1991; **7**: 436-41.
  10. Tucker JH, Cowpe JG, Ogden GR. Nuclear DNA content and morphometric characteristics of normal, premalignant and malignant oral smears. *Anal Cell Pathol* 1994; **6**: 117-28.
  11. Doudkine A, MacAulay C, Poulin N, Palcic B. Nuclear texture measurements in image cytometry. *Pathologica* 1995; **87**: 286-99.
  12. Longmore RB, Cowpe J. Nuclear area and Feulgen DNA content of normal and abnormal oral squames. *Anal Quant Pathol Histol* 1982; **4**: 33-8.
  13. Reith AK, Reichborn-Kjennerud S, Aubele M, Jütting U, Burger G. Biological monitoring of chemical exposure in nickel workers by imaging cytometry (ICM) of nasal smears. *Anal Cell Pathol* 1994; **6**: 9-21.
  14. Nieburgs HE, Herman BE, Reisman H. Buccal mucosa changes in patients with malignant tumors. *Lab Invest* 1962; **11**: 180-8.
  15. Jaggi B, Poon S, Pontifex B, Fengler J, Palcic B. A quantitative microscope for image cytometry. *J SPIE* 1991; **1448**: 89-97.
  16. Brown AM, Young A. The effects of age and smoking on the maturation of the oral mucosa. *Acta Cytol* 1970; **14**: 566-9.
  17. Pappelis GA, Pappelis AJ, Courtis WS. Nuclear dry mass and area variations in human buccal mucosa cells. *Acta Cytol* 1973; **17**: 37-41.



# The number of mitoses in simple and complex type carcinomas of the mammary gland in dogs

Polona Juntos

*Institute of Pathology, Forensic and Administrative Veterinary Medicine, Veterinary Faculty,  
University of Ljubljana, Ljubljana, Slovenia*

---

*According to the WHO classification mammary gland tumours in dogs are classified into simple and complex type. General opinion is that the complex type carcinomas have better prognosis than the simple type carcinomas. The aim of this research was to quantify and compare the mitotic activity in both types of carcinomas. Sixty-five simple type and 99 complex type carcinomas were included in the study and two methods for counting of mitoses were compared: mitotic activity index (MAI) and number of mitoses per square millimetre ( $M/mm^2$ ). Both methods showed significant ( $P=0.0001$  for MAI; and  $P=0.0089$  for  $M/mm^2$ ) differences between simple and complex type carcinomas with respect to the number of mitoses. The number of mitoses in individual tumours varied from 0 to 95 per ten high power fields in simple type carcinomas and from 0 to 57 in complex type carcinomas. The average number of mitoses was higher when only one tumour was present and lower when there were multiple tumours. Our results confirm the lower mitotic potential of the epithelial parts of complex type mammary gland carcinomas in comparison with simple type carcinomas. This fact certainly contributes to better prognosis of the disease, especially if myoepithelial cells are a predominant component of the tumour.*

*Key words: mammary neoplasms; dogs; mitotic index*

---

## Introduction

Mammary gland tumours are the most common neoplasias in dogs. They represent 25% to 50% of all tumours encountered in this species. WHO classification of animal tumours divides mammary gland tumours (benign and malignant) into simple and com-

plex type. The simple type tumours consist of epithelial or myoepithelial cells only, whereas the complex type tumours consist of both types of cells in different proportions. Most authors agree that the complex type carcinomas have better prognosis and that the epithelial component of tumour is a fraction generally responsible for the metastatic spreading of tumour cells to regional and distant lymph nodes and other target locations.<sup>1,2</sup>

High mitotic activity is a feature characteristic for highly aggressive tumours. The num-

Correspondence to: Polona Juntos, Institute of Pathology, Forensic and Administrative Veterinary Medicine, Veterinary Faculty, University of Ljubljana, Gerbičeva 60, 1000 Ljubljana, Slovenia. Tel: +386 61 17 79 153; Fax: +386 61 334 091; E-mail: juntospo@mail.vf.uni-lj.si

ber of mitoses has been established as an important prognostic factor in breast cancer in women. It serves as one of the indicators of the tumour proliferation rate, although the techniques used for counting of mitoses are rather inconsistent.<sup>3-7</sup> In dogs, a relationship between the number of mitoses and the prognosis of mammary gland tumours is not clearly defined. The aim of this study was to evaluate the number of mitoses in two types of mammary gland tumours in dogs:

- a) the simple type carcinomas consisting of epithelial cells only, and
- b) the epithelial parts of the complex type carcinomas.

### Materials and methods

Mitoses were counted in routinely prepared, paraffin embedded and haematoxylin eosin stained 4mm thick tissue sections, using a light microscope (high power field – 450mm field diameter, NA 0.70, magnification 400x) and image analysis system Prodit 5.2 (Buro Medische Automatisering – BMA, The Netherlands). Mitoses in 10 high power fields were counted according to the rules recommended by van Diest and coworkers which were followed as much as possible.<sup>8</sup> Some minor modifications were made due to the differences in architecture of human and animal mammary gland tumours. Necrotic, inflamed or haemorrhagic parts of tumours were avoided and so were the cartilaginous and bony parts. In the complex type carcinomas, only the tissue with epithelial cells was analysed for mitotic activity, whereas the parts consisting entirely of myoepithelial cells were excluded from the analysis. Only the cells with clear signs of mitosis were counted, others were ignored. The number of mitoses assessed as mitotic activity index (MAI) was correlated to the number of mitoses calculated per square millimetre ( $M/mm^2$ ). The mitosis mean value, standard

error ( $\pm SE$ ), maximum number and mediana were calculated for each group of tumours examined by the two methods. Differences between the methods and tumour groups were evaluated statistically by the analysis of variance, Student's t-test, Pearson's correlation coefficients and Mann-Whitney (Wilcoxon) test, using statistics package Statgraphics.<sup>9</sup>

Sixty-five simple type and 99 complex type mammary gland carcinomas were analysed. As mammary gland tumours in dogs may appear as single (solitary) tumours, invading only one mammary gland or as multiple tumours invading two or more mammary glands, we divided both main groups of carcinomas (simple and complex type) into subgroups according to the number of primary tumours diagnosed. Using this classification, 29 simple type carcinomas were categorised as single and 36 as multiple. Among the complex type carcinomas, 51 were single and 48 multiple. Depending on the quantity of myoepithelial cells, the complex type carcinomas were further divided into two subgroups: a) tumours consisting predominantly of epithelial cells (74 tumours) and b) tumours consisting predominantly of myoepithelial cells (27 tumours). In this last group, 10 tumours were solitary and 17 were multiple.

### Results

Results are summarized in Tables 1 and 2. Distribution plot of mitoses in individual groups is presented in Figure 1.

Simple type carcinomas and epithelial parts of the complex type carcinomas differed significantly in the number of mitoses ( $P=0.0001$ , for the MAI method;  $P=0.0089$ , for the  $M/mm^2$  method). Values obtained by the two methods were highly correlated ( $r=1.000$ ,  $P=0.0001$ ). The number of mitoses was considerably higher in solid tumours, classified as simple type carcinomas or complex type

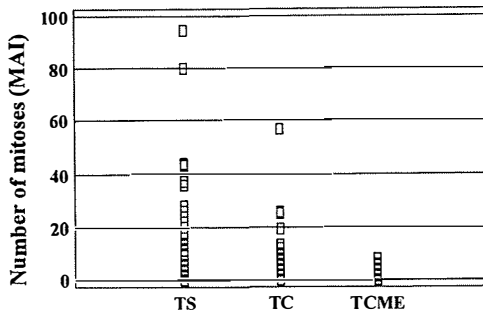


**Figure 1.** Scatterplot of the number of mitoses calculated as mitotic activity index (MAI) in simple (TS) and complex type (TC) mammary gland carcinoma and in complex type carcinoma with the prevalence of myoepithelial cells (TCME).

**Table 1.** The mean number of mitoses (SE  $\pm$ ) in simple and complex type carcinomas and complex type carcinoma with the prevalence of myoepithelial cells (ME), calculated per ten high power fields (MAI) and as the mean number per square millimetre (M/mm<sup>2</sup>)

Tumour type	MAI	M/mm <sup>2</sup>
simple	12.02	7.69
n = 65	SE $\pm$ 1.79	SE $\pm$ 1.40
complex	4.13	0.86
n = 99	SE $\pm$ 0.72	SE $\pm$ 0.57
complex - ME	2.03	1.33
n = 27	SE $\pm$ 0.23	SE $\pm$ 0.14

**Table 2.** The mean, standard error (SE  $\pm$ ), maximum number and mediana for the number of mitoses assessed as MAI in solitary and multiple tumours of simple and complex type and in complex type tumours with the prevalence of myoepithelial cells (ME)

Tumour type	MAI	SE $\pm$	Maximal	Mediana
Simple				
solitary	16.83	2.29	95	6.0
multiple	8.14	1.19	44	3.0
Complex				
solitary	4.75	0.88	57	2.0
multiple	3.48	0.49	26	2.0
Complex-ME				
solitary - ME	1.90	0.20	5	1.5
multiple - ME	2.29	0.24	8	2.0

carcinomas with solid parts. MAI varied from 0 to 95 per ten high power field in simple type carcinomas, from 0 to 57 in complex type carcinomas and from 0 to 8 in predominantly myoepithelial complex type carcinomas. Significant difference was also found between the subgroups of solitary and multiple tumours in simple type carcinomas ( $P=0.0361$ ).

## Discussion

A limited number of published papers examine and discuss the importance of counting of mitoses in the mammary gland tumours in dogs. In most of those papers, mitoses are mentioned only briefly and their significance is not fully analysed and evaluated with respect to the prognosis of the disease.<sup>10</sup> The reason that counting of mitoses in mammary gland tumours in dogs has not been widely accepted as a prognostic tool may be associated with morphological specificities of the mammary gland tumours in this species. Mammary gland tumours in dogs often contain a large number of myoepithelial cells, which are seldom found in breast tumours in



women. In dogs, this type of cells is present in about 50% of tumours, but is less common in malignant tumours.<sup>1,11</sup> Hampe and Misdorp<sup>1</sup> describe simple type carcinomas in bitches as highly infiltrative tumours that readily produce metastases to regional and distant lymph nodes and lungs. Survival period after diagnosis and surgery of this type of carcinomas is usually short. On the other hand, the complex type carcinomas grow in a more expansive way and metastases are not so common. Malignant part of the complex type carcinomas that expresses its metastatic potential is usually the epithelial component of the tumour. Survival period of animals with the complex type carcinomas is relatively long. Expansive, nodular and lobulated growth is common in complex type carcinomas, whereas growth along the lymph vessels is rare. Histological distinction between highly differentiated carcinomas of this type and complex adenomas can be very difficult. Numerous mitoses, high cellularity and relatively large amount of necrosis are usual indicators of malignancy. These criteria, however, are rather subjective, therefore, the number of mitoses could serve as a decisive criterion in dubious cases.

Lack of standardisation of methods used for counting the mitoses in mammary gland tumours is not the only problem encountered in diagnosis and prognosis of animal tumours. In dogs, nearly half of the diagnosed mammary gland tumours are multicentric or multiple.<sup>12</sup> They are not necessarily all malignant and often they are of different cellular origin. Malignant neoplasms may occur together with benign tumours or another malignant tumour of completely different type.<sup>13,14</sup> A pathologist often gets only one tumour or just a part of it for histopathological examination and that may not necessarily be the part responsible for metastases or recurrence of the tumour.

The objectives of our research were to quantify and compare the mitotic activity in

simple and complex type carcinomas (including complex type carcinomas with the prevalence of myoepithelial cells) in order to evaluate the importance of counting the mitoses for the prognosis of mammary gland tumours in dogs. Furthermore, we wanted to contribute to the efforts to standardise the methods used for counting the mitoses in mammary gland tumours. We also evaluated the number of mitoses in solitary and multiple tumours, expecting that these two groups would not differ significantly.

Both methods (MAI and  $M/mm^2$ ) indicate that the simple type carcinomas and the epithelial parts of the complex type carcinomas differ significantly in the number of mitoses ( $P=0.0001$  for MAI, and  $P=0.0089$  for and  $M/mm^2$ ). As we expected, the number of mitoses was higher in solid carcinomas, regardless whether they were classified as simple type carcinomas or complex type carcinomas with solid parts. The number of mitoses in epithelial parts of the complex type mammary gland carcinomas was significantly lower than in the epithelial simple type carcinomas. These results disagree with some previously published observations. Misdorp and Hart<sup>13</sup> found no differences between the complex and simple type carcinomas with respect to the number of mitoses. They concluded that neither mitoses nor other constituents of histological grade (differentiation, anaplasia) could be used for the prognosis of disease. However, they assumed that the complex type carcinomas have better prognosis than simple type carcinomas, due to the lower grade of anaplasia. In contrast to some other opinions,<sup>15,16</sup> Bostock<sup>17</sup> suggested that histological characteristics, including mitoses, are less important for the prognosis of canine and feline mammary gland tumours than the mode of growth at the edge of the tumour mass.

We found no significant differences in the number of mitoses between the carcinomas of complex type belonging to the subgroups

of solitary and multiple tumours, regardless the quantity of myoepithelial cells. However, in simple type carcinomas, differences in mitotic activity between the subgroups of solitary and multiple tumours were found. This findings were somewhat unexpected. They may be associated with different mode of development of solitary and multiple tumours. In case of multiple tumours, initial hormonal imbalances that affect several mammary glands, may lead to the development of preneoplastic lesions, which may gradually transform into the lower grade neoplastic lesions with lower number of mitoses and slower rate of growth. On the contrary, solitary tumours often exhibit faster mode of development and growth that is reflected also in higher number of mitoses.

### Conclusions

The number of mitoses could be an important prognostic factor in the mammary gland tumours in dogs; a better prognosis can be predicted for the complex type carcinomas than for the simple type; more mitoses and more rapid growth can be expected in solitary tumours than in multiple tumours. The worst prognosis may be expected in solid solitary carcinomas and the best one when tumours are multiple and of the complex type, especially in tumours with the prevalence of myoepithelial cells. The number of mitoses could be a decisive criterion in cases where the distinction between the benign and malignant tumours is not clear and morphological evaluation alone is not conclusive. For the final evaluation of the number of mitoses as a prognostic factor in mammary gland tumours in dogs, further studies, employing a larger number of samples and a long-term follow up of the patients, are necessary.

### References

1. Hampe JF, Misdorp W. Tumours and dysplasias of the mammary gland. *Bull WHO* 1974; **50**: 111-37.
2. Bostock DE. The prognosis following the surgical excision of canine mammary neoplasms. *Eur J Cancer* 1975; **11**: 389-96.
3. Simpson JF, Dutt PL, Page DL. Expression of mitoses per thousand cells and cells density in breast carcinomas. *Hum Pathol* 1992; **23**: 608-11.
4. Haapasalo H, Pesonen E, Collan Y. Volume corrected mitotic index (M/V-INDEX). The standard of mitotic activity in neoplasms. *Path Res Pract* 1989; **185**: 551-4.
5. Diest PJ van, Baak JPA. The morphometric prognostic index is the strongest prognosticator in premenopausal lymph node negative and lymph node-positive breast cancer patients. *Hum Pathol* 1991; **22**: 326-30.
6. Kate TK Ten, Belien JAM, Smeulders AWM, Baak JPA. Method for counting mitoses by image processing in Feulgen stained breast cancer sections. *Cytometry* 1993; **14**: 241-50.
7. Cross SS, Start RD, Smith JHF. Does delay in fixation affect the number of mitotic figures in processed tissue? *J Clin Pathol* 1990; **43**: 597-9.
8. van Diest PJ, Baak JPA, Matze-Cok P et al. Reproducibility of mitosis counting in 2.469 breast cancer specimens: Results from multicenter morphometric mammary carcinoma project. *Hum Pathol* 1992; **23**: 603-7.
9. Statgraphics® Plus. User manual. Version 2. Manugistics, Inc. Rockville 1995.
10. Lagadic M, Estrada M, Camadro JP, Durand P, Goebel J. Tumeurs mammaires de la Chienne: criteres du pronostic histologique et intérêt d'un grading. *Rec Med Vet* 1990; **166**: 1035-41.
11. Fowler EH, Wilson GP, Koestner A. Biologic behavior of canine mammary neoplasms based on a histogenetic classification. *Vet Pathol* 1974; **11**: 212-29.
12. Juntas P. Assessment of proliferative activity of the mammary gland tumours in the dog by morphometrical analysis of AgNORs, mitotic activity and tumour marker PCNA. University of Ljubljana, Veterinary faculty. Ljubljana 1997. 161 pp. Thesis.
13. Brodey RS, Goldschmidt MH, Roszel JR. Canine mammary gland neoplasms. *J Am Anim Hosp Assoc* 1983; **19**: 61-90.

14. Fowler EH, Wilson GP, Koestner A. Biologic behavior of canine mammary neoplasms based on a histogenetic classification. *Vet Pathol* 1974; **11**: 212-29.
15. Misdorp W, Hart AAM. Prognostic factors in canine mammary cancer. *J Natl Cancer Inst* 1976; **56**: 779-86.
16. Gilbertson SR, Kurzman ID, Zachrau RE, Hurvitz AI, Black MM. Canine mammary epithelial neoplasms: Biologic implications of morphologic characteristics assessed in 232 dogs. *Vet Pathol* 1983; **20**: 127-42.
17. Sarli G, Benazzi C, Preziosi R, Marcato PS. Assessment of proliferative activity by anti-PCNA monoclonal antibodies in formalin-fixed, paraffin embedded samples and correlation with mitotic index. *Vet Pathol* 1995; **32**: 93-6.
18. Bostock DE. Canine and feline mammary neoplasms. *Br Vet J* 1986; **142**: 506-15.

## Influence of UV-B radiation on Norway spruce seedlings (*Picea abies* (L.) Karst.)

Jože Bavcon<sup>1</sup>, Nada Gogala<sup>1</sup>, Alenka Gabersčik<sup>2</sup>

<sup>1</sup>Biotechnical Faculty, Department of Biology, <sup>2</sup>National Institute of Biology, Ljubljana, Slovenia

---

On the basis of the hypothesis that the ultraviolet radiation is one of the main causes for damage at higher altitudes, we have monitored the effect of UV radiation on Norway spruce for two and a half years. The influence of UV-B radiation on *Picea abies* (L.) Karst. seedlings cultured in pots in open greenhouses was examined by measuring photochemical efficiency of photosystem II, changes in chlorophyll a, b, and changes in anthocyanins. The seedlings were grown in a mixture of peat and vermiculite (4:1). We used Osram ultravitaluks bulbs as a source of UV-B radiation. In the experiment plants were treated with  $21.24 \pm 3.5$  kJ/m<sup>2</sup> and  $31.9 \pm 2.5$  kJ/m<sup>2</sup>. The control plants were grown under ambient conditions in the greenhouse without artificial source of UV-B radiation. The mean yearly values were as high as  $11.5 \pm 5.2$  kJ/m<sup>2</sup>. The photochemical efficiency of photosystem II (PS II) in experimental plants did not vary during the experiment. It showed obvious decrease in the winter period, due to low temperatures and physical draught. The decrease in chlorophyll a and b, was already detected after one year of treatment with simultaneous changes in a/b ratio. An increase of anthocyanins amount was detected as well.

**Key words:** trees-radiation effects; ultraviolet rays; seeds growth and development; chlorophyll; anthocyanins

---

### Introduction

UV-B radiation is a short wave length, non ionizing radiation (less than 400 nm) which represents about 7% of total solar radiation. It consists of UV-A (320-400 nm), UV-B (280-320 nm) and UV-C (below 280 nm). UV-C radiation is very harmful to organisms, but it is filtered in the ozonosphere.<sup>1</sup> UV-B radiation represents only 0.3% of the radiation

reaching the earth surface, but it is still on the increase.<sup>2</sup> The effect is harmful, because UV-B radiation is absorbed by macromolecules, as are also proteins and nucleic acids.<sup>3</sup>

Numerous researches showed that the effect of UV-B radiation under experimental or natural conditions was species specific<sup>1,3</sup> and that it exerted different changes. In *Phaseolus vulgaris* the changes in chlorophyll were observed.<sup>4</sup> In one year seedlings of *Pinus taeda* L., the decrease of photosynthesis was established at the beginning, but later on it reached the normal level. Simultaneously, the formation of total UV-B absorbing sub-

---

Correspondence to: Jože Bavcon Ph.D., Biotechnical Faculty, Department of Biology, Večna pot 111, 1000 Ljubljana, Slovenia. Tel: +386 61 1271 280; Fax: +386 61 273 390; E-mail: joze.bavcon@quest.arnes.si

stances were detected.<sup>5</sup> The increase of UV-B radiation in *P. taeda* caused a significant decrease in photochemical efficiency of PS II.<sup>6</sup>

*Pinus banksiana* Lamb., *Picea mariana* Mill. B.S.P. and *Picea glauca* Moench showed higher production of total UV-B absorbing substances when treated with an increased level of UV-B radiation.<sup>7</sup> *Pinus pinea* L. and *Pinus halepensis* Mill. exhibited slight changes in variable and maximal fluorescence ratio ( $F_v/F_m$ ) in one-year treatment under experimental conditions.<sup>8</sup>

The aim of our research was to estimate the effect of UV-B radiation on photochemical efficiency of PS II, chlorophyll *a* and *b* and anthocyanins contents in the seedlings of *Picea abies* (L.) Karst.

### Materials and methods

Seeds of Norway spruce were sown in clay pots in a peat-vermiculite mixture (4:1). The greenhouses were opened at both sides to assure air circulation. The seedlings were irradiated for 8 hours a day with different quantities of UV-B radiation. The source of UV-B radiation was 300W Osram Ultra-Vitalux bulbs with a spectrum similar to sunlight in mountainous areas (Technical documentation, OSRAM). The level of radiation was measured by means of UV-B sensor (peak sensitivity  $313 \pm 2$  nm, bandwidth - full width at half maximum  $26 \pm 1$  nm, Delta T Devices). Over 8-hour period the measured values were as follows:  $11,7 \pm 5,2$  kJm<sup>-2</sup> (control),  $21,24 \pm$  kJm<sup>-2</sup> (experimental level I) and  $31,9 \pm 2,5$  kJm<sup>-2</sup> (experimental level II). The environmental conditions in the greenhouses were similar to those outside. We have monitored the effect of UV radiation on Norway Spruce for two and a half years.

*In vivo* chlorophyll fluorescence was measured with a PSM fluorometer (Plant Stress Meter, Biomonitor, Sweden). Before the mea-

surements, plants were kept in the dark for 30 min. Measurements were performed once or twice a month from December 1992 to October 1994. Fast (5 seconds) kinetics was measured.

The photochemical efficiency of photosystem II can be estimated by the  $F_v/F_m$  ratio, where  $F_m$  stands for peak or maximum fluorescence and  $F_v$  is variable fluorescence (peak level minus initial level,  $F_m - F_o$ ).<sup>9</sup> Excitation energy harvested by the photosystem II antennae is transferred and utilised by photosystem II reaction centres for photochemistry of photosystem II.

Every two months chlorophyll contents were determined in one-year old needles. The chlorophyll was extracted from fresh material with 100% acetone.<sup>10</sup> The chlorophyll content was expressed in mg per unit of dry weight of needles.

Relative contents of the anthocyanins were extracted in one-year old needles using 1% HCl in methanol.<sup>11</sup> The samples were being shaken for two days in the shaker at a temperature of 2-5 °C in the dark.

The significant differences between control and treated plants were tested with Student's t-test.

### Results

Measurements of fluorescence kinetics showed no differences among the groups after two and a half years of treatment (Figure 1). The decrease of photochemical activity due to physical draught in the winter period which had already been observed in the first year of measurements was detected the following year as well.

Figures 2 and 3 present the results of chlorophyll content analyses in the monitored period. The differences among the three groups of plants indicated an obvious influence of UV-B radiation. In the first year the amount of chlorophyll *a+b* decreased in

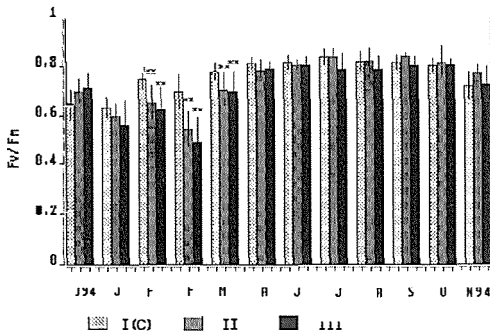


Figure 1. Variable versus maximal fluorescence (relative units) determined in spruce seedlings in the course of time. Values are the average of measurements on ten samples; vertical bars represent standard error; \*  $P \leq 0.05$ , \*\*  $P \leq 0.01$ , without asterisk - not significant).

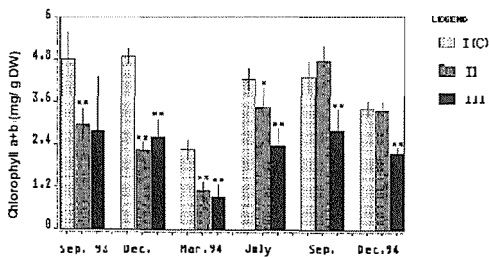


Figure 2. The amount of chlorophyll a+b ( $\text{mg g}^{-1}\text{DW}$ ) in the needles of spruce seedlings. Values are the average of 5 samples (SE means standard error; \*  $P \leq 0.05$ , \*\*  $P \leq 0.01$ , without asterisk - not significant).

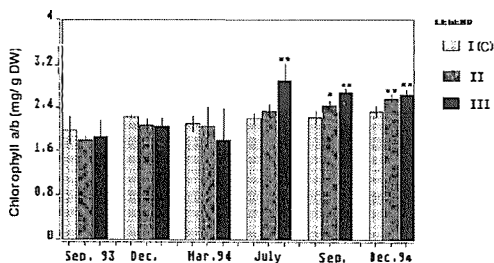


Figure 3. The chlorophyll a/b ratio in the needles of spruce seedlings. Values are the average of 5 samples (SE means standard error; \*  $P \leq 0.05$ , \*\*  $P \leq 0.01$ , without asterisk - not significant).

treated plants in comparison to the control ones, but on the other hand we observed an increase in chlorophyll a/b ratio. In the second year the differences were even more evi-

dent and they showed similar trend during the whole period.

Relative anthocyanins contents in the needles (Figure 4) measured at the end of the experiment increased only in the plants treated with the highest UV-B radiation treatment. The other two groups showed negative values. This is not the indication that the anthocyanins are not present in the other two groups, but that the product of the chlorophyll decay prevailed in comparison with the anthocyanins.

## Discussion

Our measurements of fluorescence kinetics are not in agreement with previous researches of Shawna<sup>6</sup> who observed a decrease of  $F_v/F_m$  ratio in *Pinus taeda*. In the same investigation no effect on photosynthesis were observed, what was also the conclusion of the investigations of Sullivan<sup>5</sup> and our previous researches.<sup>12</sup> In the case of additional stress exerted by drought the significant changes of  $F_v/F_m$  in *Pinus pinea* and *Pinus halepensis* were detected.<sup>8</sup> The same pattern was observed during our winter measurements, when  $F_v/F_m$  showed the decrease in control and in treated plants as well. This decrease seems to be the consequence of the

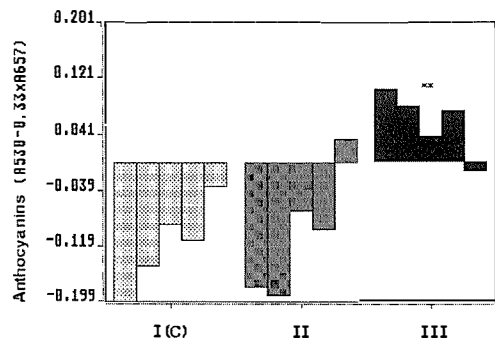


Figure 4. The variability of anthocyanins among five spruce seedlings for each treatment. (\*  $P \leq 0.05$ , \*\*  $P \leq 0.01$ , without asterisk - not significant).

physical draught due to freezing of the substrate in the pots.

The increase of chlorophyll a/b ratio in the second year corresponds to the results of an earlier research<sup>4</sup> which investigated the influence of UV-B radiation on beans. In the same plant the decrease of total chlorophyll content was observed.<sup>13</sup> Significantly lower chlorophyll a+b were obtained in our experiment already in the first year<sup>12</sup> and, the following year, these differences were even more obvious. This is surprising since several authors who investigated other conifer species reported no influence on chlorophyll content.<sup>5,8</sup>

The reason for the lack of differences in photochemical efficiency of PS II between treated and control plants could be due to higher contents of anthocyanins, which offer the protection against enhanced UV-B radiation.<sup>1,5</sup> Different researchers measured higher amounts of UV-B absorbing substances in treated plants<sup>14,5,7</sup> what was also the case in our experiment. In *Pinus taeda* seedlings these substances were formed after six weeks of treatment, what could be the reason for an unchanged level of photosynthesis.<sup>5</sup> Higher level of UV-B absorbing substances were detected in *Abies lasiocarpa* and *Picea engelmannii* under UV-B treatment.<sup>15</sup> Low sensitivity to UV-B radiation is in close relation with the penetration of this part of light spectrum into the leaf. This is more expressed in conifers which are better protected with UV-B absorbing substances in comparison to herbal plants,<sup>16,17</sup> what could also be the reason for differences in photosynthesis. Only a small quantity of UV-B radiation was proved to penetrate in the mesophyll tissue of newly expanding leaves of two subalpine conifer species.<sup>18</sup> All the measurements on conifers including ours, showed great plasticity in response to UV-B radiation.<sup>12,15,18</sup>

## References

1. Stapleton AE. Ultraviolet radiation and plants: Burning questions. *Plant Cell* 1992; 4: 1353-8.
2. Blumthaler M, Ambach W. Indication of increasing solar ultraviolet-B radiation flux in alpine regions. *Science* 1990; 248: 206-8.
3. Diffey BL. Possible errors involved in the dosimetry of solar UV-B radiation. In: Worrest RC & Caldwell MM (Ed) NATO ASI Series G8. Stratospheric ozone reduction, solar ultraviolet radiation and plant life. Springer-Verlag Berlin Heidelberg 1986: 75-87.
4. Deckmyn G, Martens C, Impens I. The importance of the ratio UV-B/photosynthetic active radiation (Par) during leaf development as determining factor of plant sensitivity to increased UV-B irradiance: effects on growth, gas exchange and pigmentation of bean plants (*Phaseolus vulgaris* cv. Label). *Plant Cell Environment* 1994; 17: 295-301.
5. Sullivan JH, Teramura AH. The effects of ultraviolet -B radiation on loblolly pine. I. Growth photosynthesis and pigment production in greenhouse-grown seedlings. *Physiologia Plantarum* 1989; 77: 202-7.
6. Schawna LN, Sullivan JH, Teramura AH, Delucia EH. The effects of ultraviolet-B radiation on photosynthesis of different aged needles in field - grown loblolly pine. *Tree Physiology* 1993; 12: 151.
7. Yakimchuk R, Hoddinot J. The influence of ultraviolet-B light and carbon dioxide enrichment on the growth and physiology of seedlings of three conifer species. *Can J For Res* 1994; 24: 1-8.
8. Petropoulou Y, Kyprisiss A, Nikolopoulos D, Manetas Y. Enhanced UV-B radiation alleviates the adverse effects of summer draught in two mediterranean pines under field conditions. *Physiologia Plantarum* 1995; 94: 37-44.
9. Öquist G, Wass R. A portable, microprocessor operated instruments for measuring chlorophyll fluorescence kinetics in stress physiology. *Physiologia Plantarum* 1988; 73: 211-7.
10. Lichtenthaler KH, Rindler U. Chlorophyll fluorescence signatures as vitality indicator in forest decline research. In: K. Lichtenthaler (ed). *Applications of Chlorophyll Fluorescence* 1988; 143-9.
11. Mancinelli AL, Huang Yang CP, Lindquist P, Anderson OR, Rabino I. Photocontrol of anthocyanin synthesis. *Plant Physiol* 1975; 55: 251-7.
12. Bavcon J, Gaberščik A, Batič F. Influence of UV-B

- radiation on photosynthetic activity and chlorophyll fluorescence kinetics in Norway spruce (*Picea abies* (L.) Karst.) seedlings. *Trees* 1996; **10**: 172-6.
13. Strid A, Porra RJ. Alterations in pigment content in leaves of *Pisum sativum* after exposure to supplementary UV-B. *Plant Cell Physiology* 1992; **33**:1015-23.
  14. Strack D, Heilemann J, Wray V, Dirks H. Structure and accumulation patterns of soluble and insoluble phenolics from Norway spruce needles. *Phytochemistry* 1989; **28**: 2071-8.
  15. DeLucia EH, Day TA, Vogelmann TC. Ultraviolet-B and visible light penetration into needles of two species of subalpine conifers during foliar development. *Plant Cell Environment* 1992; **15**: 921-9.
  16. Day TA, Martin G, Vogelmann TC. Penetration of UV-B radiation in foliage: evidence that the epidermis behaves as a non-uniform filter. *Plant Cell Environment* 1993; **16**: 735-41.
  17. Day TA. Relating UV-B radiation screening effectiveness of foliage to absorbing-compound concentration and anatomical characteristics in a diverse group of plants. *Oecologia* 1993; **95**: 542-50.
  18. Tevini M. UV-B effects on terrestrial plants and aquatic organisms. *Progress in Botany* 1994; **55**: 174-90.





# Monitoring drug release and polymer erosion from therapeutically used biodegradable drug carriers by EPR and MRI *in vitro* and *in vivo*

Karsten Mäder

Department Pharmaceutics and Biopharmacy, Phillips-University Marburg, Marburg, Germany

---

*The in vivo performance of anticancer drugs is very often limited by their poor bioavailability, serious side effects and short half lives. During the last years, biodegradable drug carriers have been developed to overcome these problems. Despite the clinical use of these delivery systems, there is a rather poor understanding of the detailed mechanisms of drug release and polymer erosion, particularly in vivo. The paper demonstrates how noninvasive magnetic resonance techniques ESR and MRI may contribute to increase our understanding of the in vivo fate of biodegradable drug delivery systems.*

*Key words: antineoplastic agents; infusion pumps, implantable; drug carriers; biodegradation; magnetic resonance imaging; electron spin resonance spectroscopy*

---

## Introduction

The therapeutical use of drugs is often limited by their poor bioavailability, short half lives and serious side effects. To overcome these problems, biodegradable drug delivery systems (BDDS) have been developed which provide a local release at a desired rate (from days to months). Several biodegradable drug carriers containing GnRH agonists are now commercial products for the treatment of prostate cancer. Examples include biodegradable implants (PROFACT-DEPOT<sup>®</sup>, ZOLADEX<sup>®</sup>) and microparticles (DECAPEPTYL-

DEPOT<sup>®</sup>, ENANTONE-DEPOT<sup>®</sup>). They are implanted or injected subcutaneously and provide a controlled drug delivery from 1 to 3 months. The matrix of these systems is made from poly( $\alpha$ -hydroxy-esters) and degrades *in vivo* into lactic and glycolic acid. Another example of the clinical use of BDDS is the treatment of glioma with the GLIADEL<sup>TM</sup>-implant. In this case, BCNU is released locally over 2-3 weeks from polyanhydride wafers implanted in brain. Compared to intravenous injection, this approach results in higher local, but lower systemic drug concentrations, thereby enhancing the therapeutic effect and reducing serious side effects of the drug.

The *in vivo* performance of the BDDS results from the complex interaction between the drug, the polymer and the biological sys-

---

Correspondence to: Dr. Karsten Mäder, Department Pharmaceutics and Biopharmacy, Phillips-University Marburg, Ketzerbach 63, D-35037 Marburg, Germany. Tel: +49 6421 28 5831; Fax: +49 6421 7016; E-mail: maeder@mail.uni-marburg.de

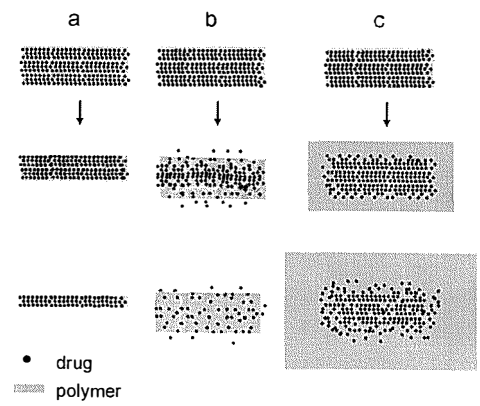


**Figure 1.** Principle schemes of erosion- (a), diffusion- (b) and swelling- (c) controlled drug release.

tem. Despite the clinical use and the encouraging results which have been obtained, there is still a rather poor understanding of the detailed mechanisms of drug release and polymer degradation. For example, the causes for different results observed *in vitro* and *in vivo* remained speculative.<sup>1</sup>

In general, the incorporated drug may be released by three different mechanisms (Figure 1). The mechanism that actually determines the overall release kinetics results from the ratio of the kinetics of water penetration, drug solubilization and diffusion,

polymer swelling and polymer erosion. For example, in the case of erosion controlled release, the rate of polymer erosion is faster compared to the rate of drug diffusion and polymer swelling. As long as a constant surface area exist, a constant drug release can be realized by erosion controlled systems (Figure 1 and Table 1). In the case of diffusion and swelling controlled drug release, the release rate decreases with time due to the increase in the distance to the polymer surface. It is important to realize that the exposure of the solubilized drug to the polymer microenvironment prior to the release may cause drug hydrolysis and drug inactivation. These processes are more likely to occur in diffusion and swelling controlled drug release.

An appropriate characterization *in vivo* is a prerequisite to achieve progress in the improvement of the existing systems and the development of new BDDS with optimized profiles of drug release and polymer clearance. The desired characteristics of the analytical techniques include sensitivity for key processes of drug release and polymer erosion (water penetration, solubilization of the drug, polymer degradation and erosion) and

**Table 1.** Characteristics of different drug release mechanisms

	Drug release mechanism		
	Erosion controlled	Diffusion controlled (case I)	Swelling controlled
Release kinetics for tablet shape (diameter >> thickness)	Constant release (zero order)	release rate decreases with time ( $\sim \sqrt{t}$ )	release rate decreases with time ( $> \sqrt{t}$ )
Polymer erosion (mass loss)	simultaneous with drug release	after drug release	after drug release
Size of the polymer matrix	decreases simultaneously with drug release	remains constant during time of drug release	increases during time of drug release
Time of drug solubilization inside the matrix prior to release	zero or very short	long	long
Danger of drug decomposition prior to release	low	high	high

noninvasiveness. The drawbacks of the analytical methods currently employed (size exclusion chromatography, differential scanning calorimetry, electron microscopy) necessitate sample separation from the biological surrounding which is difficult for micro- and nanoparticulate systems and may lead to artifacts. Isotopic labelling does not permit the characterization of key processes of drug delivery, such as water penetration and polymer degradation. Magnetic resonance based techniques are promising candidates to follow BDDS *in vivo* due to their noninvasiveness and their sensitivity to water concentration and water mobility. The development of low frequency EPR spectrometers makes it now feasible to conduct noninvasive measurements on living mammals.<sup>2</sup> The sensitivity is high enough to detect free radicals derived from xenobiotics<sup>3</sup> or drugs<sup>4</sup> and reactive intermediates of metal ions.<sup>5,6</sup> Spin trapping techniques can be used to detect and image radicals with short half lives.<sup>7,8,9</sup> The following examples illustrate how electron paramagnetic resonance spectroscopy (EPR) and nuclear magnetic resonance imaging (MRI) give unique information about the processes of drug delivery and polymer degradation *in vitro* and *in vivo*.

## Results and discussion

Gamma irradiation is widely used to sterilize BDDS. Some drug or polymer derived radicals which are formed during irradiation are very stable at room temperature under dry conditions. However, they will decay immediately after water induced solubility of the surrounding matrix. Therefore, these endogenous signals may be used to compare the velocity of water penetration between *in vitro* and *in vivo*. The realization of this concept has been demonstrated on gentamicin loaded polyanhydrides, which were subcutaneously implanted in mice.<sup>10</sup>

The application of EPR can be expanded to diamagnetic BDDS by the introduction of nitroxyl radicals. Low molecular weight nitroxides may serve as model drugs. Another possibility is to use spin labelled drugs (for example spin labeled peptides) or spin labelled polymers. A large variety of nitroxides permits the choice of the compound with the most appropriate characteristics (mol. weight, hydrophilicity, acidity etc.). The EPR spectra give information about:

1. nitroxide concentration (by double integration of the EPR spectra)
2. micropolarity (by the hyperfine coupling constants)
3. microviscosity (by the shape of the EPR spectra)

which can be used to elucidate the release mechanism. Figure 2 demonstrates how the percentage of water solubilized and nonsolubilized nitroxides can be estimated by spectral simulation. The percentage of undissolved nitroxides is easily underestimated in the EPR spectrum due to the large line width which leads to small signal amplitudes. Therefore, the integration of spectra is desirable. It is possible to indicate on the mechanism of drug release directly from the information of the EPR spectra. Results of previous studies demonstrate that diffusion controlled processes contribute to the release mechanism of clinically used polymers.<sup>11,12,13</sup> Erosion controlled release was observed only in the case of the polyanhydride bis-carboxyphenoxypropane, a polymer which is used clinically to deliver BCNU against glioma.<sup>13</sup> The EPR method is also able to follow complex release mechanisms: Drug release from poly(fatty acid dimer-sebacic acid) polymers involves water penetration, polymer degradation with precipitation of the monomers and incorporated drug molecules, resolubility and diffusion.<sup>12</sup> Further information on the release processes can be

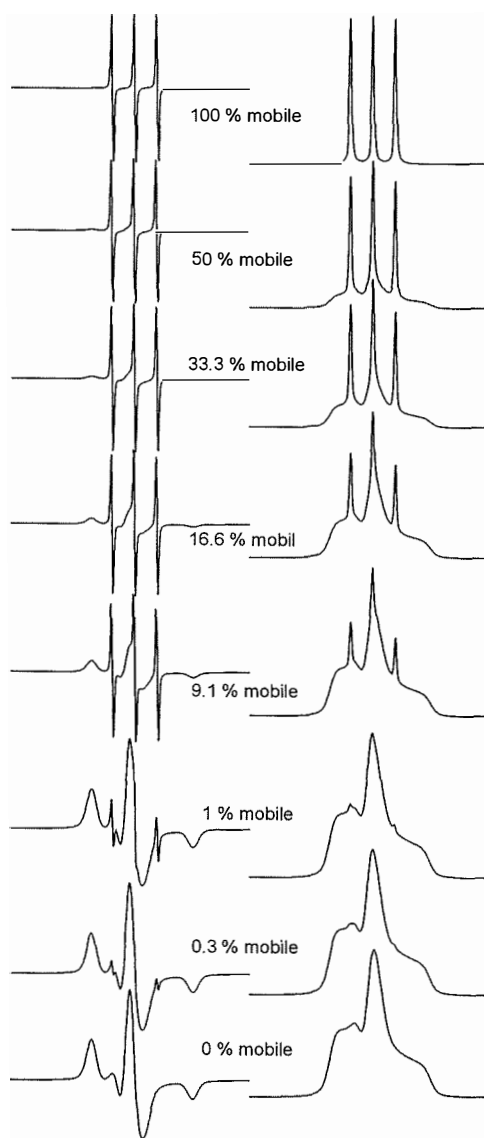


**Figure 2.** Spectral simulation of the EPR spectra (1. derivative of microwave absorption, left) and their integrated form (right) of the superposition of water solubilized, mobile nitroxides and non solubilized nitroxide molecules. Note that the signal amplitude of the water solubilized nitroxides is much higher than the signal amplitudes of the nonsolubilized form due to the narrow line width.

achieved by simultaneous monitoring of distinct polymer layers which can be realized *in vitro* by spectral-spatial EPR-imaging.<sup>14</sup> The spatial resolution of the current *in vivo* EPR imaging machines is in the range of few millimeters<sup>15</sup> and not sufficient to resolve heterogeneity within a millimeter sized implant. However, a distinct regions of the implant can be separated by means of different nitroxide isotopes.<sup>13</sup>

An important parameter is the pH inside the degrading polymer matrix. The acidity influences the polymer degradation rate, solubility of the incorporated drug and drug stability. An acidic pH may result from the polymer degradation, because the polymers which are clinically used degrade into  $\alpha$ -hydroxyacids (polyesters) or dicarboxylic

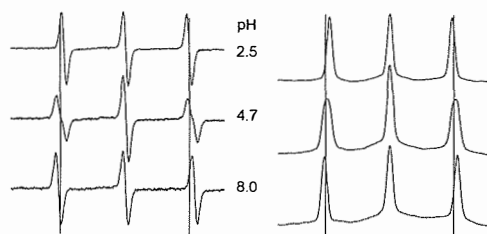
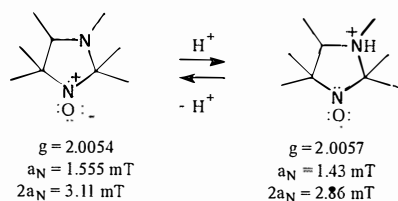


**Figure 3.** Top: Basic principle of the pH-measurement by imidazolidine nitroxides. Protonation of the nitrogen in position 3 decreases the spin density of the nitrogen atom of the radical moiety, which results in a decreased hyperfine splitting constant and an increased g-value. Bottom: Influence on the pH on the experimental 1.1 GHz EPR-spectra (left) and their integrated form of the pH-sensitive nitroxide 2,2,3,4,5,5-Hexamthyl-imidazolidine-1-oxid. The EPR spectrum at pH = pKa = 4.7 results from a superposition of the protonated and the nonprotonated form of the radical.

acids (polyanhydrides). However, the acidity inside the matrix is difficult to predict due to an uncertain monomer concentration and possible influences of incorporated drugs or penetrating ions. There was no information available about the acidity of the microenvironment inside BDDS *in vivo* due to the lack of suitable techniques. The development of pH-sensitive nitroxides<sup>16</sup> made it possible to study the pH inside degrading polymers non-invasively and continuously *in vivo* (Figure 3). A pH drop from 5 to 2 was observed in biodegradable polyester implants in mice.<sup>11</sup> Clearly, such an acidic microenvironment may lead to drug decomposition prior to drug release.

Complementary information can be obtained by the combination of the EPR studies with nuclear magnetic resonance imaging.<sup>12,13</sup> MRI provides information concerning the implant shape and size, edema and encapsulation. The cause of incomplete nitroxide release was found by the MRI detection of the encapsulation of the implant.<sup>12</sup> Care must be taken to conclude from low MRI contrast to the absence of water inside the implant, because small pore sizes may lead to very short relaxation times. Therefore, drug release may be completed, although no increase in MRI signal intensity was observed.<sup>12,13</sup> This water can be detected indirectly by EPR using spin probes.

In summary, drug release from BDDS is a promising approach in the field of cancer treatment. Magnetic resonance techniques EPR and MRI can provide unique and additional information needed to understand the mechanisms of drug release and polymer degradation. They permit also the *in vivo* characterization of submicron sized delivery systems,<sup>17</sup> which are otherwise only detected by radiolabeling. Ongoing developments in the field of EPR-imaging will result in new opportunities to monitor the localization and physical state of the delivery system (hydration, microviscosity, micro-pH).

## Acknowledgment

The author acknowledges the cooperation with the laboratory of Prof. HM Swartz (Dartmouth Medical School, NH, USA) and Prof. A. Domb (Hebrew University Jerusalem, Israel). This work was supported by grants from the German Academic Exchange Service (DAAD) and the German Research Foundation (DFG MA 1648/1-1).

## References

1. Wu MP, Tamada JA, Brem H, Langer R. In vivo versus in vitro degradation of controlled release polymers for intracranial surgery. *J Biomed Mat Res* 1994; 28: 387-95.
2. Eaton GR, Eaton SS, Ohno K. EPR-Imaging and in vivo EPR. Boca Raton: CRC press, 1991.
3. Fuji H, Zhao B, Koscielniak J, Berliner J. In vivo EPR studies of the metabolic fate of nitrosobenzene. *Magn Res Med* 1994; 31: 77-80.
4. Mäder K, Bacic G, Swartz HM. In vivo detection of anthralin derived free radicals in the skin of hairless mice by low frequency electron paramagnetic resonance spectroscopy. *J Invest Dermatol* 1995; 104: 514-7.
5. Liu K, Jiang J, Swartz HM, Shi X. Low frequency detection of chromium-(V) formation by chromium-(VI) reduction in whole mice. *Arch Biochem Biophys* 1994; 313: 248-52.
6. Liu KJ, Mäder K, Shi X, Swartz HM. Reduction of carcinogenic Cr(VI) on the skin of living rat. *Magn Res Med* 1997; 38: 524-6.
7. Halpern HJ, Yu C, Barth E, Peric M, Rosen GM. In situ detection, by spin trapping, of hydroxyl radical markers produced from ionizing radiation in tumor of a living mice. *Proc Nat Acad Sci* 1995; 92: 796-800.
8. Jiang JJ, Liu KJ, Jordan SJ, Swartz HM, Mason RP. Detection of free radical metabolite formation using in vivo EPR spectroscopy - evidence for rat hemoglobin thiol radical formation following administration of phenylhydrazine. *Arch Biochem Biophys* 1996; 330: 266-70.
9. Yoshimura T, Yokoyama H, Fujii S, Takayama F, Oikawa K, Kamada H. In-vivo EPR detection and imaging of endogenous nitric-oxide in lipopolysaccharide-treated mice. *Nature Biotechnol* 1996; 14: 992-4.

10. Mäder K, Domb A, Swartz HM. Gamma sterilization induced radicals in biodegradable drug delivery systems. *Appl Rad Isot* 1996; **47**: 1669-74.
11. Mäder K, Gallez B, Liu KJ, Swartz HM. Noninvasive in vivo characterization of release processes in biodegradable polymers by low frequency Electron Paramagnetic Resonance Spectroscopy. *Biomaterials* 1996; **17**: 459-63.
12. Mäder K, Cremmilleux Y, Domb A, Dunn JF, Swartz HM: In vitro / in vivo comparison of drug release and polymer erosion from biodegradable P(FAD-SA) polyanhydrides - a noninvasive approach by the combined use of Electron Paramagnetic Resonance Spectroscopy and Nuclear Magnetic Resonance Imaging. *Pharmaceut Res* 1997; **14**: 820-6.
13. Mäder K, Bacic G, Domb A, Elmalak O, Langer R, Swartz HM. Noninvasive in vivo monitoring of drug release and polymer erosion from biodegradable polymers by EPR spectroscopy and NMR imaging. *J Pharm Sci* 1997; **86**: 126-34.
14. Mäder K, Nitschke S, Stösser R, Borchert HH, Domb A. Nondestructive and localised assesment of acidic microenvironments inside biodegradable polyanhydrides by spectral spatial Electron Paramagnetic Resonance Imaging (EPRI). *Polymer* 1997; **38**: 4785-94.
15. Alecci M, Ferrari M, Quaresima V, Sotgiu A, Ursini CL. Simultaneous 280 MHz EPR imaging of rat organs during nitroxide radical clearance. *Biophys J* 1994; **67**: 1274-9.
16. Khramtsov VV, Weiner LM: Proton exchange in stable nitroxyl radicals: pH sensitive spin probes, In: Volodarsky LB (ed.) Imidazoline nitroxides. Boca Raton: CRC press 1988: Vol. 2, 37-80.
17. Yamaguchi T, Itai S, Hayashi H, Soda S, Hamada A, Utsumi H. In vivo ESR studies on pharmacokinetics and metabolism of parenteral lipid emulsion in living mice. *Pharmaceut Res* 1996; **13**: 729-33.

## Bone marrow toxicity and antitumor action of adriamycin in relation to the antioxidant effects of melatonin

Valentina Rapozzi<sup>1</sup>, Laura Perissin<sup>1</sup>, Sonia Zorzet<sup>2</sup>, Marina Comelli<sup>1</sup>, Irene Mavelli<sup>1</sup>, Marjeta Šentjurc<sup>3</sup>, Alja Pregelj<sup>3</sup>, Milan Schara<sup>3</sup> and Tullio Giraldi<sup>1</sup>

<sup>1</sup>Department of Biomedical Sciences and Technologies, University of Udine, <sup>2</sup>Department of Biomedical Sciences, University of Trieste, Italy, <sup>3</sup>Jozef Stefan Institute, Ljubljana, Slovenia

---

Melatonin has been reported to possess numerous properties, including antioxidant effects. Some antitumor drugs, such as anthracyclines, display a pro-oxidant activity which is held responsible for their toxicity to normal tissues of the host. The aim of this work was, therefore, to preliminarily examine the effects of melatonin on the bone marrow toxicity caused by the treatment with adriamycin in CBA mice bearing TLX5 lymphoma. After a single treatment with adriamycin (28–40 mg/kg i.v.), the administration of a single pharmacological dose of melatonin (10 mg/kg s.c.) reduced the acute mortality of the hosts from 9/16 to 2/16. The antitumor action of adriamycin, consisting in the increase in survival time of animals which were not affected by the acute toxicity of the drug, was not reduced by melatonin. Melatonin also attenuated the reduction in the number of bone marrow GM-CFU caused by adriamycin, and significantly restored the reduced and total glutathione levels. Moreover, the use of Fenton reaction and free radical determination via spin trapping, show that melatonin acts as a direct free radical scavenger. The data reported indicate that melatonin attenuates the bone marrow toxicity of adriamycin with a mechanism consistent with its antioxidant properties.

**Key words:** lymphoma; doxorubicin-adverse effects; bone marrow; melatonin; mice

---

### Introduction

The pineal gland and its indole hormone, melatonin, have been shown in numerous experimental studies to be involved in cancer progression. In the 30's, Engel suggested a link between the pineal gland and cancer.<sup>1,2</sup> Cancer treatment with pineal extracts has

been performed later in the clinic, resulting in a reported retardation in the progression of the disease and in an improvement of the quality of life of the patients.<sup>3</sup>

The role of pineal gland and of melatonin for cancer growth has been investigated rather extensively in laboratory animals. Surgical pinealectomy resulted in the increased growth *in vivo* of different types of experimental tumors.<sup>4–8</sup> Tumor growth was correspondingly attenuated in pinealectomized animals by the administration of exogenous

---

Correspondence to: Prof. Tullio Giraldi, Department of Biomedical Sciences, University of Trieste, Via L. Giorgieri 7, 34100 Trieste, Italy. Tel: +39-40-6763539; Fax: +39-40-577435; E-mail: giraldi@univ.trieste.it



melatonin.<sup>9-11</sup> Tumor growth inhibition *in vivo* and *in vitro* following treatment with melatonin in non pinealectomized animals has been described in some instances,<sup>12-16</sup> although contrasting reports showing a stimulation of tumor growth are also available in the literature.<sup>17,18</sup>

In Lewis lung carcinoma bearing mice melatonin has been shown to increase the therapeutic index of the antitumor drugs cyclophosphamide and etoposide, since it protects the bone marrow stem cells from the apoptosis induced by these drugs while it does not reduce their antitumor action. This effect of melatonin was suggested to occur via interaction with its receptors on T-helper lymphocytes in the bone marrow,<sup>19</sup> leading to the stimulation of the production of a Th cell factor constituted of two cytokines named MIO (melatonin induced opioids). In turn, this factor would act on bone marrow stromal cells inducing the release of hematopoietic growth factors.<sup>20</sup>

On the other hand, melatonin has been shown to cause potent direct antioxidant effects, rapidly scavenging hydroxyl<sup>21,22</sup> and peroxyl radicals.<sup>23</sup> Additionally, melatonin can also upregulate endogenous antioxidant defenses, as shown for glutathione peroxidase activity.<sup>24,25</sup> The antioxidant action of melatonin is also supported by experiments indicating that it decreases the DNA damage caused by ionizing radiation in cultured cells,<sup>26</sup> the *in vivo* cataract formation induced by BSO in rats,<sup>27,28</sup> the DNA damage caused by chemical carcinogen safrol,<sup>29</sup> as well as the kainate excitotoxicity in cerebellar granular neurons.<sup>30</sup>

The anthracycline antitumor drug, adriamycin, is being widely used in the clinic. The most serious adverse effects limiting the applicable dose intensity are myelosuppression, gastrointestinal toxicity and acute cardiac toxicity eventually leading to cumulative late cardiomyopathy.<sup>31</sup> Numerous studies investigated the underlying mechanisms and

oxidative damage to membrane lipids and to other cellular components, which are believed to be a major factor in the cardiac toxicity of adriamycin and other anthracyclines.<sup>32-36</sup>

The aim of this work was, therefore, to examine the effects of the administration of adriamycin, of exogenous melatonin, or of their combination, in terms of toxicity for the host and antitumor activity in mice implanted with TLX5 lymphoma. The acute toxicity for the host has been evaluated in terms of lethality, as well as of the effects on bone marrow stem cells. The possible relevance of oxidative damage caused by adriamycin, and its prevention by melatonin, has been determined measuring glutathione levels in bone marrow cells. The direct free radical scavenger activity of melatonin was evaluated in a model system, using Fenton reaction and free radicals determination via spin trapping and EPR at different concentrations of melatonin. The results obtained are reported hereafter.

## Materials and methods

### Reagents

Melatonin was a kind gift of Prof. Fraschini, University of Milano, Italy. Adriamycin was obtained from Pharmacia S.p.A. Milano, Italy, and the other reagents used were purchased from Sigma Chemical Co, Sigma Chimica Divisione della Sigma-Aldrich S.r.l., Milano, Italy.

### Animals and tumor transplantation

The animals used were male CBA/LAC mice weighting 22-25 g, belonging to a conventional local breeding colony. The animals were provided food and water *ad libitum*, and were kept constantly at a 12/12 light/dark cycle (lights on from 8 a.m. to 8 p.m.). TLX5 lymphoma was originally provided by the

Chester Beatty Research Institute, London, England. Tumor implantation was performed by injecting each mouse i.p. with 0.1 ml of a suspension containing  $10^5$  viable tumor cells. The tumor cells, obtained from donors inoculated 8 days before, were washed by centrifugation at 500xg and resuspended in PBS after counting for trypan blue exclusion.

#### *Drug treatment*

Melatonin was dissolved in 0.9 % NaCl saline containing 4 % ethanol, and was administered s.c. in a volume of 0.05 ml/10 g of body weight. Adriamycin was dissolved in 0.9 % NaCl solution, and was administered i.v. in 0.05 ml/10 g of body weight or i.p. in 0.1 ml/10 g of body weight, as indicated. The treatment with melatonin was performed at 8 p.m. (light off), whereas the treatment with adriamycin was applied at 9 p.m..

#### *GM-CFU assay*

The number of granulocyte/macrophage-colony forming units (GM-CFU) was determined after *in vivo* treatment with the drugs tested. Following sacrifice,  $10^5$  viable bone marrow cells were incubated in 0.3 % semisolid agar in RPMI 1640 medium containing 10 % fetal calf serum and 10 % lung conditioned medium (LCM) as a source of stimulating factors. LCM was prepared by mincing the lungs from 2 mice into small pieces and incubating the pieces at 37°C with 5 % CO<sub>2</sub> for 3 days in RPMI 1640 medium containing 10 % fetal calf serum. The cultures were kept for 7 days at 37°C in humidified air and then examined by phase contrast microscopy; colonies containing more than 50 cells were counted as GM-CFU.

#### *Glutathione assays*

The reduced (GSH) and oxidized (GSSG) glutathione levels were measured in bone mar-

row by a high-performance liquid chromatography (HPLC) technique. Bone marrow samples were processed following the method of Reed *et al.*<sup>37</sup> Briefly, 1 ml of bone marrow cell suspension in 0.9 % NaCl ( $10^6$  cells) was added to 0.05 ml of 70 % perchloric acid. After protein precipitation, 0.5 ml of the supernatant was treated immediately with 50 ml of 0.08M fresh aqueous solution of iodoacetic acid and then neutralized with an excess of NaHCO<sub>3</sub>. After 60 min in the dark at room temperature, 0.5 ml of an alcoholic solution of 1-fluoro-2,4-dinitrobenzene (1.5 ml/ 98.5 ml absolute ethanol) was added, and the reaction was left to proceed for 4 hours in the dark. The samples were then chromatographed using a reverse-phase ion exchange column microbondapak NH<sub>2</sub> 3.9 x 300 mm (Waters). Glutathione levels were related to protein content in the samples, which was determined by the method of Lowry *et al.*<sup>38</sup>

#### *Spin trapping experiment*

Free radical scavenging activity of melatonin was measured in phosphate buffered saline containing 0.1 mM EDTA (pH 7, 320 mosmol). The buffer was supplemented with spin trap 5,5-dimethyl-1-pyrroline N-oxide (DMPO, 1 mM), 0.02 mM FeSO<sub>4</sub>·7H<sub>2</sub>O and 0.01 % (w/v) of H<sub>2</sub>O<sub>2</sub> (final concentrations). The intensity of the EPR spectra of DMPO-OH adduct was measured in presence and absence of different concentrations of melatonin in the course of the reaction.<sup>39</sup>

#### *Statistical analysis*

Tabled values are group means  $\pm$  SD. Data were subjected to Kruskal-Wallis analysis of variance, as well as Kaplan Meier, logrank and Cox proportional hazard analysis as appropriate. All analyses were performed using standard procedures implemented in the Systat package (SYSTAT Inc., Evanston, IL).

Results

*Antitumor activity and toxicity of melatonin and adriamycin*

In TLX5 lymphoma bearing mice, adriamycin displays a significant antitumor action when administered i.v. as a single dose of 28 mg/kg, the survival time of the treated mice being significantly increased in comparison with drug untreated controls, as determined by Kaplan-Meier analysis. The stratification of the data and log-rank analysis indicated a significant effect for adriamycin (chi-square = 17.2, DF = 2,  $P < 0.0001$ ), and the absence of significant effects for melatonin 10 mg/kg s.c. (chi-square = 1.18, DF = 1,  $P = 0.278$ ). Bivariate Cox proportional hazard analysis further indicated that adriamycin constituted a significant negative risk factor (HR = 0.192, 95 % CL 1.486 – 0.025), whereas the effects of melatonin were insignificant (HR = 1.253, 95 % CL 9.66 – 0.163).

On the contrary, the toxicity of adriamycin, as indicated by the number of toxic deaths occurring before day 9, was significantly reduced by melatonin. Indeed, the total number of such toxic deaths in the dose

range of 28-40 mg/kg adriamycin was 9/16; when the treatment with adriamycin was combined with melatonin, the number of toxic deaths was significantly reduced to 2/16, Yates corrected chi-square = 4.987, DF = 1,  $P = 0.026$  (Table 1).

*Effects of melatonin and adriamycin on bone marrow granulocyte / macrophage – colony forming units*

The treatment with melatonin (20 mg/kg s.c.), which was devoid of effects by itself, significantly reverted the reduction in the number of GM-CFU which was caused by the administration of a single i.v. dose of 28 mg/kg adriamycin (Kruskall-Wallis analysis of variance, chi-square=3.87, DF=1,  $P=0.049$ ) (Table 2).

*Effects of melatonin and adriamycin on glutathione levels*

The treatment with 10 mg/kg melatonin s.c. significantly restored the reduction in reduced, oxidized and total glutathione levels, which was caused by the administration of 3 weekly doses of 5 mg/kg adriamycin i.p (Kruskall-Wallis analysis of variance, chi-square=3.87, DF=1,  $P=0.049$ ) (Table 3).

**Table 1.** Toxicity-related deaths and increase in the survival of CBA mice implanted with TLX5 lymphoma and treated with adriamycin and melatonin

Adriamycin mg/kg	Melatonin	Toxicity-related deaths	Mean survival time
–	–	0/9	10.1
40	–	7/8	9
40	+	2/8	14.8
28	–	2/8	18.5
28	+	0/8	17.3

Groups of 8 CBA male mice were implanted on day 0 with  $10^5$  TLX5 lymphoma cells. On day 1 they were treated at 8 p.m. with melatonin (10mg/kg s.c.) and at 9 p.m. with adriamycin (i.v.) as indicated. Acute toxic deaths were those occurring before day 9. Mean survival time was determined using Kaplan Meier statistics (for the results of statistical analysis see the Results section).

*Free radical scavenging activity of melatonin*

Free radical scavenging activity of melatonin was detected in spin trapping experiments using Fenton reaction as a model for production of hydroxyl radicals. DMPO-OH adducts were detected by EPR. Only a very slow decrease of this adduct with time was observed. When Fenton reaction was initiated in the presence of melatonin, the intensity of EPR spectra was decreased, indicating the scavenging activity of melatonin, which prevents binding of OH radical to DMPO. The intensity of EPR spectra decreased with increasing concentration of melatonin. A sig-

**Table 2.** Granulocyte/macrophage colony forming units in the bone marrow of normal CBA mice treated with adriamycin and melatonin

Adriamycin	Melatonin	GM-CFU
–	–	67.2 ± 24.1
–	+	42.3 ± 10.3 <sup>a</sup>
+	–	15.0 ± 2.2 <sup>ab</sup>
+	+	41.3 ± 8.1 <sup>b</sup>

Each value is the mean ± S.D. obtained in groups of 6 tumor-free Cba male mice. The animals were treated on day 1 with melatonin (20 mg/kg s.c.) at 8 p.m. and with adrimycin (28 mg/kg i.v.) at 9 p.m. as indicated. The animals were sacrificed on day 5, and the number of granulocyte/macrophage colony forming units (GM-CFU) in 10<sup>5</sup> bone marrow cells was determined. The data were subjected to ANOVA analysis; the results are presented in the Results section. Means marked with the same letters are significantly different, Tukey test,  $P < 0.5$ .

nificant decrease by about 30 % of the initial value was observed with 50 mM melatonin (Figure 1). The results are in good agreement with recently published data on the same system.<sup>40</sup>

## Discussion

The data reported show that the administration of 10 mg/kg melatonin in the evening in TLX5 lymphoma bearing mice significantly reduces the host toxicity of adriamycin at the

doses of 28 and 40 mg/kg administered 1 hour later, as indicated by the reduction in the occurrence of acute early toxic deaths. At the same time, adriamycin administered at a dose of 28 mg/kg significantly increases the survival time of the TLX5 lymphoma bearing mice which were not affected by acute treatment-related toxicity. The concurrent administration of melatonin does not reduce the magnitude of the antitumor effects of adriamycin. The reduction in the proportion of acute toxic deaths caused by adriamycin is accompanied by a significant reduction in the number of bone marrow GM-CFU in the treated animals, and this reduction is significantly attenuated by melatonin which is devoid of significant effects by itself. The doses of melatonin used are devoid of evident toxic effects on the host; they are also devoid of any antitumor action in TLX5 lymphoma bearing mice, as indicated by the lack of a significant prolongation in the life span of the treated animals (unreported results).

The presently observed attenuation of bone marrow toxicity of adriamycin by melatonin is similar to that observed by Maestroni *et al.* examining the effects of melatonin on the toxicity and antitumor action of cyclophosphamide and etoposide. In mice bearing Lewis lung carcinoma, the antitumor action of both drugs was retained after melatonin treatment, whereas their hematological

**Table 3.** Glutathione levels in the bone marrow cells of normal CBA mice treated with adriamycin and melatonin

Adriamycin	Melatonin	GSH	GSSG	GSH/GSSG	tGSH
–	–	5.3 ± 0.61	0.20 ± 0.04	21.5 ± 1.95	5.5 ± 0.65
+	–	3.4 ± 0.23	0.14 ± 0.01	24.6 ± 0.82	3.6 ± 0.25
+	+	6.6 ± 1.15	0.27 ± 0.07	23.9 ± 1.71	6.9 ± 1.59

Each value is the mean ± S.D. obtained in groups of 4 tumor-free CBA mice. The animals were treated once a week for 3 weeks with melatonin (10 mg/kg s.c.) at 8 p.m. and with adriamycin (5 mg/kg i.p.) at 9 p.m. as indicated. Glutathione levels were determined in the bone marrow cells of animals sacrificed 3 days after the last treatment. The values of reduced glutathione (GSH), oxidized glutathione (GSSG) and total glutathione (tGSH) are expressed as nmol/mg protein. The experiment was performed in duplicate, and the data were subjected to Kruskal-Wallis analysis of variance; the results are presented in the Results section.

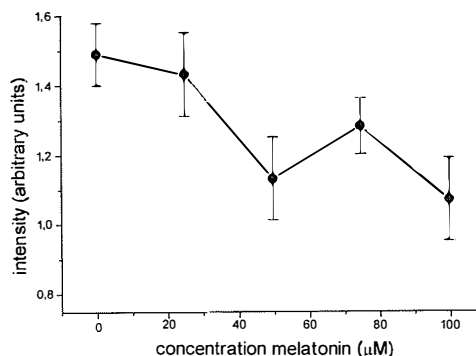


**Figure 1.** EPR spectra intensity decrease of spin adduct DMPO-OH with increasing concentration of melatonin. Final concentrations: 1mM DMPO, 0.02 mM Fe<sup>2+</sup>, 0.01% H<sub>2</sub>O<sub>2</sub> in PBS (pH 7) with 0.1 mM EDTA. Each point is a mean value of 5 measurements, the bars indicate standard deviations.

toxicity was significantly reduced.<sup>41,42</sup> The mechanism by which melatonin attenuates the hematological toxicity of cyclophosphamide and etoposide has been studied in detail by the same authors.<sup>19,20,43</sup> Their results indicate that melatonin binds to helper T-lymphocytes, inducing the release of a Th cell factor constituted of two cytokines named MIO (melatonin induced opioids). In turn, this factor acts on bone marrow stromal cells inducing the release of hematopoietic growth factors, such as GM-CSF.<sup>44</sup>

The reduction of bone marrow toxicity of adriamycin by melatonin might be caused by a mechanism alternative to that involving MIO, consisting of the antioxidant action of melatonin exerted against the pro-oxidant effects of adriamycin. In fact, the results obtained by Fenton reaction and EPR show that melatonin possesses a direct and concentration-dependent free radical scavenger activity within the concentration range 20-100 mM. Moreover, melatonin significantly restores to control values the levels of reduced, oxidized and total glutathione which have been lowered by adriamycin in bone marrow cells. These results indicate

that melatonin may attenuate the oxidative damage caused by adriamycin in bone marrow stem cells. Assuming a distribution of administered melatonin occurring in total body water, its peak concentration should fall in a concentration range between 10 and 100 mM, which is consistent with the possibility of a direct interaction with adriamycin oxygen reactive species. This direct free radical scavenging action is accompanied by an indirect mechanism consisting in the restoration of the levels of reduced glutathione which have been lowered by adriamycin. The data presented here do not allow to assess the relative importance of the mechanisms presently proposed, and do not permit evaluation of their relevance in relation to that involving MIO forwarded by Maestroni and co-workers.<sup>44</sup>

In conclusion, the results presented show that the administration of a pharmacological dose of melatonin to TLX5 lymphoma bearing CBA mice does not decrease the antitumor action of adriamycin, while the acute host toxicity of this drug is significantly reduced, thus suggesting that an enhancement in the dose intensity of adriamycin can be achieved by its combination with exogenously administered melatonin. Bone marrow toxicity of adriamycin is attenuated by melatonin through a mechanism consistent with a direct and indirect antioxidant action of melatonin which is effective against the pro-oxidant action of adriamycin. These data appear to encourage the study of the effect of endogenous melatonin and of the administration of melatonin at pharmacological doses on other organ directed toxicity of anthracyclines. Early and late cardiac toxicity of anthracyclines deserve particular attention, since they are of crucial importance as factors limiting the dose intensity tolerated clinically, and since they have been attributed to an oxidative mechanism.<sup>45-48</sup> Moreover, the data reported also appear to encourage the study of endogenous melatonin concentra-

tion and its rhythmic variations in relation to the chronotoxicological data obtained for anthracyclines in laboratory animals<sup>49</sup> and in clinical antitumor chemotherapy.<sup>50</sup>

### Acknowledgments

This work was supported by the Italian National research Council (CNR) Special Project "ACRO" contract no. 96.00574.PF39, and by MURST 40 % to Prof. T. Giraldi, U.S.U. 1995.

### References

- Engel P. Über den einfluss von hypophysenvorderlappenhormonen und epihormonen auf das wachstum von impftumoren. *Z Krebsforsch* 1934; 4: 281-91.
- Engel P. Wachstumbeeinflussende hormone und tumorwachstum. *Z Krebsforsch* 1935; 41: 488-96.
- Hofstatter R. Beitrag zur therapeutischen verwendung von zirbelextrakten. *Wien Klin Wschr* 1950; 62: 338-9.
- Rodin AE. The growth and spread of Walker 256 carcinoma in pinealectomized rats. *Cancer Res* 1963; 23: 1545-50.
- Barone RM, Das Gupta TK. Role of pinealectomy and melatonin on Walker 256 carcinoma in rats. *J Surg Oncol* 1970; 2: 313-22.
- Das Gupta TK, Terz J. Influence of pineal gland on the growth and spread of melanoma in the hamster. *Cancer Res* 1967; 27: 1306-11.
- Lapin V. Influence of simultaneous pinealectomy and thymectomy on the growth and formation of metastases of the Yoshida sarcoma in rats. *Exp Pathol* 1974; 9: 108-12.
- Wrba H, Lapin V, Dostal V. The influence of pinealectomy and of pinealectomy combined with thymectomy on the oncogenesis caused by polyoma virus in rats. *Osterreichische Z Onkol* 1975; 2: 37-9.
- El-Domeiri AA, Das Gupta TK. Reversal by melatonin of the effect of pinealectomy on tumor growth. *Cancer Res* 1973; 33: 2830-3.
- El-Domeiri AA, Das Gupta TK. The influence of pineal ablation and administration of melatonin on growth and spread of hamster melanoma. *J Surg Oncol* 1976; 8: 197-205.
- Aubert C, Janiaud P, Lecalvez J. Effect of pinealectomy and melatonin on mammary tumor growth in Sprague-Dawley rats under different conditions of lighting. *J Neural Transm* 1980; 47: 121-30.
- Narita T, Kudo H. Effect of melatonin on B16 melanoma growth in athymic mice. *Cancer Res* 1988; 45: 4175-7.
- Regelson W, Pierpaoli W. Melatonin: a rediscovered antitumor hormone? Its relation to surface receptors, sex steroid metabolism, immunologic response and chronobiologic factors in tumor growth and therapy. *Cancer Invest* 1987; 5: 379-85.
- Blask DE. Melatonin in oncology. In: Yu HS, Reiter RJ, eds. *Melatonin: Biosynthesis, physiological effects, and chemical applications*. Boca Raton: CRC Press, 1993: 447-77.
- Hill SM, Blask DE. Effects of the pineal hormone melatonin on the proliferation and morphological characteristics of human breast cancer cells (MCF-7) in culture. *Cancer Res* 1988; 48: 6121-6.
- Cos S, Fernandez F, Sanchez-Barcelo EJ. Melatonin inhibits DNA synthesis in MCF-7 human breast cancer cells in vitro. *Life Sci* 1996; 58: 2447-53.
- Hamilton T. Influence of environmental light and melatonin upon mammary tumor induction. *Br J Surg* 1969; 56: 764-6.
- Stanberry LR, Das Gupta TK, Beattile CW. Photoperiodic control of melanoma growth in hamsters: influence in pinealectomy and melatonin. *Endocrinology* 1983; 113: 469-75.
- Maestroni GJM, Flamigni L, Hertens E, Conti A. Biochemical and functional characterization of melatonin-induced opioid in spleen and bone marrow T-helper cells. *Neuroendocrinol Lett* 1995; 17: 145-52.
- Maestroni GJM, Conti A. Melatonin and the immune-hematopoietic system therapeutic and adverse pharmacological correlates. *Neuroimmunomodulation* 1996; 3: 325-32.
- Tan DX, Chen LD, Poeggeler B, Manchester L C, Reiter R J. Melatonin: a potent, endogenous hydroxyl radical scavenger. *Endocrine J* 1993; 1: 57-60.
- Sewerynek E, Poeggeler B, Melchiorri D, Reiter RJ. H<sub>2</sub>O<sub>2</sub>-induced lipid peroxidation in rat brain homogenates is greatly reduced by melatonin. *Neurosci Lett* 1995; 195: 203-5.
- Pieri C, Marra M, Moroni F, Recchioni ., Marcheselli F. Melatonin: A peroxyl radical scavenger more effective than vitamin E. *Life Sci* 1994; 15: PL271-PL6.
- Barlow-Walden LR, Reiter RJ, Abe M, Pablos M, Menendez-Pelaez A, Chen LD, Poeggeler B. Mela-

- tonin stimulates brain glutathione peroxidase activity. *Neurochem Int* 1995; **26**: 497-502.
25. Sewerynek E, Abe M, Reiter RJ, Barlow-Walden LR., Chen LD, McCabe JJ, Roman LY, Diaz-Lopez B. Melatonin administration prevents lipopolysaccharide-induced oxidative damage in phenobarbital-treated animals. *J Cell Biochem* 1995; **58**: 436-44.
  26. Vijayalaxmi, Reiter RJ Meltz ML. Melatonin protects human blood lymphocytes from radiation-induced chromosome damage. *Mutat Res* 1995; **346**: 23-31.
  27. Abe M. Reiter RJ, Orhii PB, Hara M, Poeggeler B. Inhibitory effect of melatonin on cataract formation in newborn rats: Evidence for an antioxidant role of melatonin. *J Pineal Res* 1994; **17**: 94-100.
  28. Li ZR, Reiter RJ, Fujimori O, Oh CS, Duan YP. Cataractogenesis and lipid peroxidation in newborn rats treated with buthionine sulfoximine: Preventive actions of melatonin. *J Pineal Res* 1997; **22**: 117-23.
  29. Tan DX, Reiter RJ, Chen LD, Poeggeler B, Manchester LC, Barlow-Walden LR. Both physiological and pharmacological levels of melatonin reduce DNA adduct formation induced by the carcinogen safrole. *Carcinogenesis* 1994; **15**: 215-8.
  30. Giusti P, Franceschini D, Petrone M, Manev H, Floreani M. In vitro and in vivo protection against kainate-induced excitotoxicity by melatonin. *J Pineal Res* 1996; **20**: 226-31.
  31. Billingham ME, Mason JW, Bristow MR, Daniels JR: Anthracycline cardiomyopathy monitored by morphological changes. *Cancer Treat Rep* 1978; **62**: 865-72.
  32. Singal RK, Deally MR, Weinberg LE. Subcellular effects of adriamycin in the heart: A concise review. *J Mol Cell Cardiol* 1987; **19**: 817-28.
  33. Sinha BK, Politi PM: Anthracyclines. *Cancer Chemother Biol Resp Modifiers Annu* 1990; **11**: 45-57.
  34. Olson RD, Mushlin PS: Doxorubicin cardiotoxicity analysis of prevailing hypothesis. *FASEB J* 1990; **4**: 3076-86.
  35. Myers C. Anthracyclines. *Cancer Chemother Biol Resp Modifiers Annu* 1988; **10**: 33-9.
  36. Ito H, Miller SC, Billingham ME, Akimoto H, Torti SV, Wade R, Gahlmann R, Lyons G, Kedes L, Torti FM: Doxorubicin selectively inhibits muscle gene expression in cardiac muscle cells in vivo and in vitro. *Proc Natl Acad Sci USA* 1990; **87**: 4275-9.
  37. Reed DJ, Babson JR, Beatty PW, Brodie AE, Ellis W, Potter DW: High-Performance-Liquid-Chromatography analysis of nanomole levels of glutathione, glutathione disulfide, and related thiols and disulfides. *Anal Biochem* 1980; **106**: 55-62.
  38. Lowry OH, Rosebrough NS, Fan AL, Randall RJ. Protein measurement with the Folin phenol reagent. *J Biol Chem* 1951; **193**: 265-75.
  39. Buettner GR, Mason RP. Spin-trapping methods for detecting superoxide and hydroxyl free radicals in vitro and in vivo. *Methods Enzymol* 1990; **186**: 127-33.
  40. Matuszak Z, Reszka KJ, Chignell CF. Reaction of melatonin and related indoles with hydroxyl radicals: EPR and spin trapping investigations. *Free Rad Biol Med* 1997; **23**: 367-72.
  41. Maestroni GJM, Covacci V, Conti A. Hematopoietic rescue via T-cell-dependent, endogenous granulocyte-macrophage colony-stimulating factor induced by the pineal neurohormone melatonin in tumor-bearing mice. *Cancer Res* 1994; **54**: 2429-32.
  42. Maestroni GJM, Conti A, Lissoni P: Colony-stimulating activity and hematopoietic rescue from cancer chemotherapy compounds are induced by melatonin via endogenous interleukin 4. *Cancer Res* 1994; **54**: 4740-3.
  43. Maestroni GJM. T-helper -2 lymphocytes as a peripheral target of melatonin. *J Pineal Res* 1995; **18**: 84-9.
  44. Maestroni GJM, Hertens E, Galli P, Conti A, Pedrinis E. Melatonin-induced T-helper cell hematopoietic cytokines resembling both interleukin-4 and dinorphin. *J Pineal Res* 1996; **21**: 131-9.
  45. Bacher NR, Groden SL, Gee MV. Anthracycline antibiotic augmentation of microsomal electron transport and radical formation. *Mol Pharmacol* 1977; **13**: 901-10.
  46. Olson RD, Boerth RC, Gerber JG, Nies AS. Mechanism of adriamycin cardiotoxicity: Evidence for oxidative stress. *Life Sci* 1981; **29**: 1393-401.
  47. Mimnaugh EG, Truth MA, Bhatnagar M, Gram TE. Enhancement of reactive oxygen-dependent mitochondrial membrane lipid peroxidation by the anticancer drug adriamycin. *Biochem Pharmacol* 1985; **34**: 847-56.
  48. Nowak D, Drzewoski J. Anthracycline -induced oxidative stress- its role in the development of cardiac damage. *Cancer J* 1996; **9**: 296-303.
  49. Sadzuka Y, Takino Y. Effect of seasonal variation on lipid peroxide level and glutathione peroxidase activity in the mouse before and after adriamycin administration. *Toxicology Letters* 1992; **61**: 49-56.
  50. Hrushesky WJM, Bjarnason GS. The Application of circadian chronobiology to cancer chemotherapy. In: De Vita VT, Helmann S, Rosenberg SA, eds. *Cancer-Principles & Practice in Oncology*. Lippincott, 1993: 2666-86.

# Diffusion-weighted magnetic resonance imaging in the early detection of tumour response to therapy

Nick J.F. Dodd<sup>1</sup>, S. Zhao<sup>2</sup> and J.V. Moore<sup>1</sup>

<sup>1</sup>Paterson Institute for Cancer Research and <sup>2</sup>North West Medical Physics,  
Christie Hospital (NHS) Trust, Manchester, United Kingdom

---

*Early detection of the effects of therapy offers distinct clinical advantages for the management of the patient, since the response of a tumour to a particular therapy may vary considerably from patient to patient. A pre-clinical tumour model was used to study the effects of two novel therapies, photodynamic therapy and electrotherapy, in addition to a well established modality, radiotherapy. In each case, diffusion-weighted magnetic resonance imaging was found to be of value in determining the therapeutic response, within two days of treatment. Following photodynamic therapy, the apparent diffusion coefficient (ADC) of water in those regions of the tumour that became necrotic showed a marked increase within one day of treatment, while no significant increase was detectable in those regions that remained viable. A similar increase in ADC was observed following electrotherapy, whether anodic or cathodic, the increase being detected within minutes of treatment in the regions of primary damage and within about one day in the regions of secondary ischaemic necrosis. The changes produced by radiotherapy were less marked than those produced by the other therapies, but, following doses that produce a high proportion of killing, there was a statistically significant increase in ADC within one or two days of treatment.*

*Key words: neoplasms, experimental-therapy; photodynamic therapy; electric stimulation therapy; radiotherapy; magnetic resonance imaging*

---

## Introduction

The ability to monitor non-invasively and at early times, the cytotoxic effects of cancer treatment in an individual subject is potentially of great clinical value. This is particularly true of new forms of therapy, where the

response of a specific tumour type to a standard treatment regime may not have been extensively studied. Photodynamic therapy (PDT) involves injection of a non-toxic photosensitizing drug, followed by exposure to visible light at non-thermal levels. The extent of tumour destruction produced by a given dose of photosensitizer and incident light is strongly influenced by the biodistribution of the drug and absorption of light within the tumour and in surrounding tissue.<sup>1</sup> In the case of electrotherapy, our preliminary stud-

---

Correspondence to: Dr. N.J.F. Dodd, Paterson Institute for Cancer Research, Christie Hospital (NHS) Trust, Manchester M20 9BX, UK. Tel: +44-161-446 3151; Fax: +44-161-446 3109; E-mail: ndodd@picr.man.ac.uk



ies<sup>2-4</sup> suggest that the efficacy of the treatment may be strongly influenced by precise placement of the electrodes and the vascular architecture of the tumour. Consequently considerable inter-patient variability in tumour response to therapy may occur. This is observed even in a well established treatment such as radiotherapy, where the outcome is influenced by intrinsic radiosensitivity of the tumour cells and the hypoxic fraction.

Proton MRI offers a potential method for non-invasive monitoring of the efficacy of cancer treatment. Our previous studies<sup>1,5</sup> using an experimental mammary (T50/80) tumour have shown that, within 24 h of PDT, regions of high signal intensity in a  $T_2$ -weighted image correlated well with histological necrosis. Moreover, using MRI to assess the proportion by volume of the tumour tissue destroyed by treatment, this correlated with the subsequent delay in tumour regrowth. Further studies,<sup>6</sup> using the AT6/22 prostate tumour, showed that  $T_2$ -weighted images taken 24 h after PDT similarly demonstrated the presence of treatment-induced necrosis as areas of hyperintensity. However, the contrast between viable and necrotic regions was less marked than previously observed in the mammary tumour model. In both tumour models, differences between  $T_2$  (and  $T_1$ ) of viable tumour tissue and treatment-induced necrosis were of the same order as variations between individual tumours and could not be used as a reliable marker of tissue state. We show here that MR measurement of the apparent diffusion coefficient (ADC) of tumour water provides a quantitative marker of PDT-induced necrosis both for the mammary tumour<sup>7</sup> and also for the prostate tumour<sup>6</sup> although the untreated tumours show markedly different absolute values of ADC.

The effects of electrotherapy on the mouse mammary tumour<sup>4</sup> and on normal rat liver<sup>3</sup> have been detected by  $T_2$ -weighted MR images, but the effects of radiotherapy are

reported to produce little or no significant changes in the  $T_1$ - or  $T_2$ -weighted images of animal tumours<sup>8-10</sup> or human brain tumours.<sup>11</sup> The effects of radiotherapy are normally only detected by MRI at a late stage, when changes in tumour volume can be readily observed. We have now applied the diffusion method to monitoring the early effects of PDT, electrotherapy and radiotherapy in our experimental systems.

## Materials and methods

The tumours were a T50/80 mouse mammary tumour<sup>12</sup> and a Dunning rat AT6/22 prostate tumour, both implanted subcutaneously in nude, immune-suppressed mice. The tumours were treated with photodynamic therapy, electrotherapy or radiotherapy when they reached a volume  $>600 \text{ mm}^3$ . PDT involved i.p. injection of  $40 \text{ mg kg}^{-1}$  of haematoporphyrin esters in saline, followed 24 h later by illumination with 630 nm light at  $100 \text{ mW cm}^{-2}$  from a laser, to a dose of  $80\text{--}150 \text{ J cm}^{-2}$ . Electrotherapy involved insertion of a gold needle electrode into the tumour while the animal lay on a copper plate counter-electrode, covered with a conducting gel (Dracard, Maidstone, UK) and a current of 5 mA was passed for 15–30 min. For radiotherapy, tumours were exposed to 300 kV X-rays at a dose rate of  $4 \text{ Gy min}^{-1}$ , to a dose of 30 Gy, while the bulk of the animal was protected by a lead shield.

Magnetic resonance imaging was performed with a 4.7 T Biospec system. Proton images were acquired with a 2.5 cm diameter surface coil. For diffusion measurements, a pair of gradients of maximum amplitude  $20 \text{ mT m}^{-1}$  and duration 20 ms, separated by 12 ms were used. This gave a maximum gradient factor,  $b$ , of  $0.68 \times 10^9 \text{ s m}^{-2}$ . The apparent diffusion coefficient of the tumour water in each region ( $D_i$ ) was calculated by the method of Le Bihan *et al.*<sup>13</sup>, using the formula:

$$D_i = \ln[S_0/S_1]/[b_1 - b_0]$$

where  $S_0$  and  $S_1$  are the signal intensities measured with gradient factors  $b_0$  and  $b_1$  respectively.

## Results

### Photodynamic therapy

The ADC of water in the untreated mammary tumour was approximately half that in the prostate tumour (T50/80:  $D = 0.23 \pm 0.02 \times 10^{-9} \text{ m}^2\text{s}^{-1}$ ; AT6/22:  $D = 0.61 \pm 0.03 \times 10^{-9} \text{ m}^2\text{s}^{-1}$ ). However, following PDT of either tumour type, the ADC in those regions of the tumour that became necrotic showed a marked increase ( $p < 0.0001$ ), within 1 day of treatment (T50/80:  $D = 1.04 \pm 0.03 \times 10^{-9} \text{ m}^2\text{s}^{-1}$ ; AT6/22:  $D = 1.23 \pm 0.06 \times 10^{-9} \text{ m}^2\text{s}^{-1}$ ), while showing no significant increase in those regions that remained viable (Figure 1). Subsequent histological examination of the tumours confirmed the assignments based on ADC increase.

### Electrotherapy

The magnitude of the changes in ADC observed following electrotherapy, either anodic or cathodic (Table 1), were found to be similar to those induced by PDT. In contrast, the timescale of development of damage was different. Primary damage, occurring symmetrically around the implanted electrode, was detectable by MRI or by histology within minutes of treatment. In some tumours treated by electrotherapy, secondary ischaemic damage appeared approximately 1 day after treatment (Figure 2). This latter type of damage was similar in nature to the PDT-induced damage. Both types of electrotherapy-induced damage were clearly delineated by the increased ADC and were distinguished from one another by their different rates of development.

### Radiotherapy

The changes produced by radiotherapy were less marked than those produced by PDT or electrotherapy, but, following doses that produce a high proportion of cell killing (e.g. 30

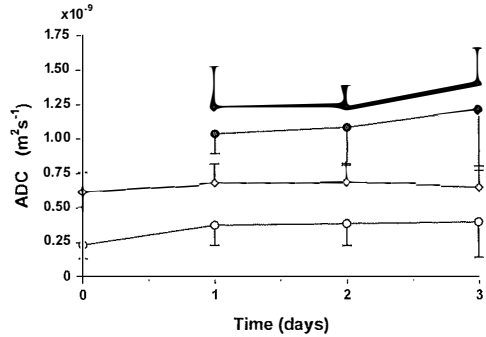


**Figure 1.** Changes in tumour water ADC with time after photodynamic therapy, in T50/80 mammary tumours (○, ●) ( $n=16$ ) and AT6/22 prostate tumours (◇, ◆) ( $n=22$ ), showing mean and standard error. The open symbols denote viable tumour tissue and the closed symbols denote necrotic tissue.

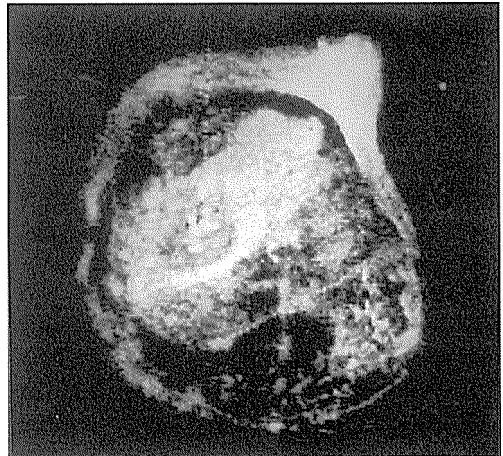


**Figure 2.** Proton magnetic resonance image of a T50/80 tumour, one day after electrotherapy with a gold needle anode in the tumour and a current of 5 mA passed for 30 minutes. The image shows a hyperintense ring of dermal oedema around the tumour (particularly thickened at the upper right hand edge), a diffuse circular area within the tumour (slightly left of centre) representing the primary necrotic damage and an approximately oval hyperintense region of secondary ischaemic necrosis (from the left hand edge to top right) that was not observable immediately after electrotherapy.

**Table 1.** ADC of tumour water in different regions of T50/80 mammary and AT6/22 prostate tumours after electrotherapy

Tumour	Viable tissue D x 10 <sup>9</sup> (m <sup>2</sup> s <sup>-1</sup> )	1° damage D x 10 <sup>9</sup> (m <sup>2</sup> s <sup>-1</sup> )	2° damage D x 10 <sup>9</sup> (m <sup>2</sup> s <sup>-1</sup> )
T50/80	0.33±0.02 (n=30)	1.00±0.06 (n=13)	1.25±0.06 (n=4)
AT6/22	0.58±0.04 (n=9)	1.04±0.10 (n=6)	

Gy), there was a small, but statistically significant, increase in ADC within 1 or 2 days of treatment. Comparing the two tumour types (Figure 3), it can be seen that the ADC of the irradiated mammary tumour increased to approximately the value observed in the unirradiated prostate tumour. Experiments currently in progress suggest that the increase in ADC may be proportional to the extent of cell killing, as measured by tumour growth delay.

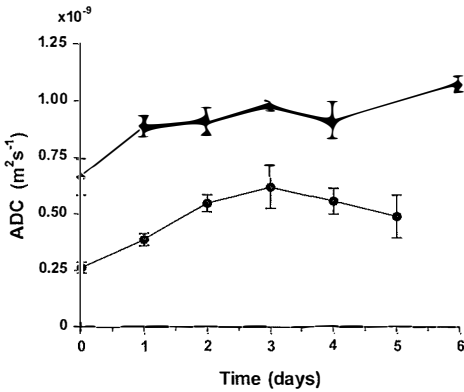


**Figure 3.** Changes in tumour water ADC with time after radiotherapy (30 Gy) in T50/80 (●) (n=12) and AT6/22 tumours (◆) (n=10), showing mean and standard error.

**Discussion**

It has previously been reported<sup>14,15</sup> that when cells are degraded, as in the necrotic regions of a tumour, this region shows a greater ADC than the viable tissue. *In vivo*, the principal mode of action of PDT is believed to be acute injury to the vasculature, with vascular collapse leading to prompt and massive secondary ischaemic necrosis, detectable histologically at about 24 h after treatment. Con-

sistent with this effect, we have observed an increase in tumour water ADC in the regions of PDT-induced necrosis, within about 24 h of treatment, irrespective of the initial value of the ADC in the untreated tumour. We have previously shown<sup>3</sup> that secondary ischaemic necrosis is also induced by electrotherapy in normal rat liver and have now shown that it also occurs in some of our experimental tumours. However, the irregular nature of the tumour vasculature and the possibility of collateral blood flow results in less predictable secondary damage than in highly organized liver tissue. The primary necrosis induced by electrotherapy is detectable immediately after treatment and, like the secondary necrosis, causes a significant increase in ADC. Consequently, diffusion-weighted MRI and measurement of ADC provide qualitative and quantitative delineation of the extent of necrosis induced by PDT or by electrotherapy. This non-invasive technique may be invaluable in the management of patients by these new forms of therapy and assist in their clinical acceptance. Towards this aim, we have demonstrated that PDT-induced necrosis can be detected in our experimental tumour models using a mid-field whole-body clinical MR scanner<sup>16</sup>.

The effects of ionizing radiation are more diffuse than those of PDT and electrotherapy. Consequently they are more difficult to detect. Although radiotherapy is a well established and widely used mode of therapy, the earliest indication that a tumour has responded to treatment is normally a reduction in volume or slowing of the growth rate. This can be detected by conventional imaging techniques. However, diffusion-weighted

MRI may provide a much earlier indication of treatment efficacy, thereby allowing the radiation dose to be optimized at an early stage during a course of treatment. Although the results presented above are for a single high dose of radiation, we have demonstrated similar changes in ADC during more clinically relevant fractionated doses,<sup>17</sup> to these experimental tumours. Experiments are currently in progress to seek a correlation between change in ADC and biological endpoint, e.g. tumour growth delay.

Increases in ADC have recently been reported in experimental tumours treated with gene therapy<sup>18</sup> and also with cyclophosphamide,<sup>19</sup> 5-fluorouracil<sup>20,21</sup> or 1,3-bis(2-chloroethyl)-1-nitrosourea,<sup>22</sup> in which cases the maximum relative increase in tumour water ADC appeared to be related to therapeutic response. Diffusion-weighted magnetic resonance imaging appears highly promising in the early detection of tumour response to a wide range of treatment modalities.

### Acknowledgement

The expert technical assistance of Mr. D. Broadbent is gratefully acknowledged. Financial support was provided by the Cancer Research Campaign and, in part, by the North Western Regional Health Authority.

### References

1. Moore JV, Dodd NJF, Wood B. Proton nuclear magnetic resonance imaging as a predictor of the effects of photodynamic therapy. *Br J Radiol* 1989; **62**: 869–70.
2. Griffin DT, Dodd NJF, Moore JV, Pullan BR, Taylor TV. The effects of low-level direct current therapy on a preclinical mammary carcinoma: tumour regression and systemic biochemical sequelae. *Br J Cancer* 1994; **69**: 875–8.
3. Griffin DT, Dodd NJF, Zhao S, Pullan BR, Moore JV. Low-level direct electrical current therapy for hepatic metastases. I. Preclinical studies on normal liver. *Br J Cancer* 1995; **72**: 31–4.
4. Dodd NJF, Moore JV, Taylor TV, Zhao S. Preliminary evaluation of low-level direct current therapy using magnetic resonance imaging and spectroscopy. *Phys Medica* 1993; **9**: 285–9.
5. Dodd NJF, Moore JV, Poppitt DG, Wood B. *In vivo* magnetic resonance imaging of the effects of photodynamic therapy. *Br J Cancer* 1989; **60**: 164–7.
6. Dodd NJF, Lee LK, Moore JV, Zhao S. MRI monitoring of the effects of photodynamic therapy on prostate tumours. *Proceedings 3rd Annual Meeting Soc Magn Reson Med* 1995, 1368.
7. Zhao S, Dodd NJF, Moore JV. Magnetization transfer and diffusion in mouse mammary tumours following photodynamic therapy. *Proceedings 2nd Annual Meeting Soc Magn Reson Med* 1994, 1043.
8. Bakker CJG, Vriend J. Proton spin-lattice relaxation studies of tissue response to radiotherapy in mice. *Phys Med Biol* 1983; **28**: 331–40.
9. Kroeker RM, Stewart CA, Bronskill MJ, Henkelman RM. Continuous distributions of NMR relaxation times applied to tumours before and after therapy with x-rays and cyclophosphamide. *Magn Reson Med* 1988; **6**: 24–36.
10. Le Moyec L, Pellen P, Merdrignac-Le Noan G, Le Lan J, Chenal C, de Certaines JD. Proton NMR relaxation times of experimental Lewis lung carcinoma after irradiation. *Radiother Oncol* 1988; **13**: 1–8.
11. Houdek PV, Landy HJ, Quencer RM, Sattin W, Poole CA, Green BA, Harmon CA, Pisciotto V, Schwade JG. MR characterization of brain and brain tumour response to radiotherapy. *Int J Radiat Oncol Biol Phys* 1988; **15**: 213–8.
12. Moore JV. The dynamics of tumour cords in an irradiated mouse mammary carcinoma with a large hypoxic cell component. *Jpn J Cancer Res* 1988; **79**: 236–43.
13. Le Bihan D, Breton E, Lallemand D, Grenier P, Cabanis E, Laval-Jeantet M. MR imaging of intravoxel incoherent motions: application to diffusion and perfusion in neurological disorders. *Radiology* 1986; **161**: 401–7.
14. Henkelman RM. Diffusion-weighted MR imaging: a useful adjunct to clinical diagnosis or a scientific curiosity? *Am J Roent* 1990; **155**: 1066–8.
15. Maier CF, Paran Y, Bendel P, Rutt BK, Degani H. Quantitative diffusion imaging in implanted human breast tumours. *Magn Reson Med* 1997; **37**: 576–81.
16. Dodd NJF, Zhu XP, Dobson MJ, Watson Y, Hawnaur JM, Adams JE. Application of high resolution diffusion imaging in the early detection of tumour response to photodynamic therapy using a 0.5 Tesla conventional whole body MR scanner.

- 5th. Meeting ISMRM, Vancouver. Proceedings 1997, 1073.
17. Dodd NJF, Zhao S. Early detection of tumour response to radiotherapy using MRI. *Phys Medica* 1997; 13 (Suppl. 1): 56–60.
18. Poptani H, Ollikainen A, Gröhn O, Kainulainen R, Ylä-Herttuala S, Kauppinen R. 5th. Meeting ISMRM, Vancouver. Proceedings 1997, Monitoring the efficacy of gene therapy in experimental rat glioma: serial  $T_2$  and diffusion weighted MRI study. 1071.
19. Zhao M, Pipe JG, Bonnett J, Evelhoch JL. Early detection of treatment response by diffusion-weighted  $^1\text{H}$ -NMR spectroscopy in a murine tumour in vivo. *Br J Cancer* 1996; 73: 61–4.
20. Zhao M, Evelhoch. Relationship between 5-fluorouracil- or cyclophosphamide-induced changes in tumor apparent diffusion coefficient and therapeutic response in three murine tumours. 5th. Meeting ISMRM, Vancouver. Proceedings 1997, 1074.
21. Lemaire L, Howe LA, Rodrigues L, Griffiths JR. In vivo assessment of primary mammary rat tumours response to chemotherapy using diffusion-weighted  $^1\text{H}$ -NMR spectroscopy. 5th. Meeting ISMRM, Vancouver. Proceedings 1997, 1070.
22. Ross BD, Zhao J, Ercolani M, Ben-Joseph O, Stegman LD, Chenevert TL. Noninvasive quantitation of chemotherapeutic cell kill in experimental intracranial brain tumours using MRI: correlation with changes in diffusion MRI. 5th. Meeting ISMRM, Vancouver. Proceedings 1997, 1072.

# Plasma membrane fluidity alterations in cancerous tissues

Marjeta Šentjunc<sup>1</sup>, Miha Sok<sup>2</sup> and Gregor Serša<sup>3</sup>

<sup>1</sup>Jožef Stefan Institute, <sup>2</sup>University Medical Center, <sup>3</sup>Institute of Oncology,  
Ljubljana, Slovenia

---

*Plasma membrane is a heterogeneous structure with several coexisting domains having different fluidity characteristics. It plays an important role in the control of cell growth, differentiation and transformation. Fluidity of the whole plasma membrane reflects the ordering and dynamics of phospholipid acyl chains in specific membrane domains, as well as the fraction of each domain in the membrane. Changes in the membrane fluidity affect processes on the membrane such as transport, enzyme activities and expression of the receptors.*

*In this paper we present results of our recent electron paramagnetic resonance (EPR) studies of plasma membrane fluidity characteristics, which take into account heterogeneous nature of the plasma membrane. By the computer simulation of the EPR spectra line-shapes, the number of coexisting domains in the plasma membrane, their relative portion in the membrane as well as the ordering and dynamics of each domain can be determined. Therefore, we could distinguish the contribution of the relative portion of each domain from the contribution of fluidity alterations in the domain to the entire fluidity changes in the membrane.*

*Two examples will be discussed: membrane fluidity characteristics of excised lung tumor tissues and influence of microtubule depolymerizing agent vinblastine on membrane fluidity of vinblastine sensitive and resistant HeLa cells.*

*Key words: membrane, fluidity, electron paramagnetic (spin) resonance, cancer*

---

## Introduction

### *Plasma membrane fluidity*

Plasma membrane is a heterogeneous structure, composed of lipids and proteins (enzymes, receptors, transport proteins) with

or without the attached oligosaccharides. It regulates the transport of ions and chemicals and plays an important role in the control of cell growth, differentiation and transformation.<sup>1</sup> Lipids are arranged in lipid bilayer, and can be treated as an anisotropic two-dimensional liquid in which constituent molecules undergo translational and rotational motion at a rate characteristic for viscous oil. It is characterised by membrane fluidity, which is in opposite relation to membrane microvis-

Correspondence to: Dr. Marjeta Šentjunc, Jožef Stefan Institute, Jamova 39, 1000 Ljubljana, Slovenia. Phone: +386 61 1773 689; Fax: +386 61 1235 400; E-mail: marjeta.sentjunc@ijs.si

cosity.<sup>2</sup> In the membrane, where the structure is heterogeneous, fluidity in different regions is different. In such a case the term fluidity is used to describe the motional freedom of lipid-soluble molecular probe within the bilayer. It is described by order parameter ( $S$ ), time-averaged deviation of the acyl chains from the normal to the bilayer plane, and rotational correlation time ( $\tau_c$ ), time required for the molecules to forget what were their previous spatial orientations.<sup>3</sup> Membrane fluidity regulates the dynamics of conformational changes and the lateral mobility of membrane proteins. Changes in membrane fluidity influence membrane processes such as transport, enzyme activities and receptor expression. Fluidity of plasma membrane seems to be biologically very important since bacteria, yeast and other organisms whose temperature fluctuates with that of the environment, change the fatty acid composition of the membrane in order to maintain a relatively constant fluidity.<sup>1</sup>

Main factors which influence the fluidity are: composition of lipids and distribution of integral and peripheral proteins within the bilayer. Main lipid components of plasma membrane are phospholipids. Membranes are fluid if lipids are in liquid crystalline phase and rigid if lipids are in gel phase. Phospholipids with short acyl chains or non-saturated bonds in the chain make bilayer more fluid. Phospholipids of the same type tend to aggregate and as a consequence a phase separation in the bilayer can occur, therefore domains with different fluidity characteristics are formed. Another important lipid constituent of the plasma membrane is cholesterol, which composes 30 to 50 mol % of all lipids in eucaryotes. In this cholesterol concentration region a new type of phase is obtained in which the acyl chains are more highly orientationally ordered than in the fluid phase of pure phospholipid system (liquid-ordered phase). In this way cholesterol tends to regulate or completely elimi-

nates the possible phase transitions of phospholipids from solid to fluid phase. Besides, it decreases permeability for water molecules and enhances mechanical stability of bilayer.<sup>2</sup> Highly non-saturated acyl chains (20:4 and 20:6) are unlikely to associate with cholesterol, while highly saturated phospholipids, such as sphingomyelin preferentially interacts with cholesterol, creating highly saturated and non-saturated lipid domains.<sup>1</sup>

Another factor which contributes to membrane heterogeneity is specific interactions between lipids and proteins.<sup>4</sup> Lipid-protein interactions influence the distribution of lipids around proteins which cause the formation of domains with different fluidity characteristics. The important parameters for the interaction are polar heads (charge, size) and matching of acyl chains with the hydrophobic span of proteins (length and fluidity of acyl chains). Influence of polar heads is stronger as that of the chains. It is also influenced by pH, temperature and ionic strength.

#### *Fluidity in malignant cells*

There are some typical cellular alterations observed after neoplastic transformation which are in close relation to plasma membrane fluidity. Transport of ions and chemicals is altered as well as membrane permeability, phagocytosis or endocytosis, etc. Typically is increased lectin agglutinability, which is generally correlated with enhanced ability of lectin binding sites on transformed cells to move laterally through the plasma membrane. This enhanced mobility may be a consequence of the increased plasma membrane fluidity.<sup>5</sup>

However, plasma membrane fluidity measurements in malignant cells are controversial.<sup>5</sup> According to the literature most tumor cells *in vitro* exhibit higher membrane fluidity than their normal progenitors. For example, such differences were observed in Mal-

oney sarcoma-virus transformed murine tumor cells,<sup>6</sup> in leukemic T lymphocytes,<sup>7</sup> in human CLL lymphocytes,<sup>8</sup> in mouse malignant lymphoma cells,<sup>9</sup> in rat colon tumor cells,<sup>10</sup> in mouse Morris 7288C hepatoma cells,<sup>11</sup> in human ovarian carcinoma cells.<sup>12</sup> However, in KiMSV transformed rat kidney cells,<sup>13</sup> in virally, chemically or tumorigenically transformed 3T3 cells,<sup>14</sup> in hepatoma cells<sup>15</sup> and in T lymphocytes from untreated patients with Hodgkin's disease<sup>16</sup> decreased membrane fluidity was found, in comparison to corresponding controls. In freshly excised tumors only a few studies have been performed. In excised local and metastatic LM cell tumor tissues<sup>17,18</sup> and in malignant brain tumors<sup>19</sup> more fluid plasma membranes were observed as in the corresponding non-malignant samples.

One possible reason for the measured differences in plasma membrane fluidity is the technique of measurements. Most investigations were performed with EPR or fluorescence polarisation method. In both methods a probe, which measures the properties of its surrounding, has to be introduced into the membrane. It should be stressed, that in the measurements reported, heterogeneous membrane structure composed of several coexisting domains with different fluidity was not taken into account. Only an average order parameter and correlation time were measured, which include the contribution of different domains and could be biased in favour of more fluid domains. Besides, the parameters could be biased by preferential distribution of the probe in certain type of domains.

Having this in mind the model for computer simulation of the EPR spectra line shape was developed,<sup>20</sup> which takes into account heterogeneity of the plasma membrane. It will be described in more details in the next section. We present two examples where this method has been applied. One is *in vitro* model where fluidity of two types of

HeLa cells was compared: wild type and the type resistant to the chemotherapeutic drug vinblastine. In the other example the study was performed on excised human lung tumor tissue and fluidity characteristics for different types of tumors were determined.

### EPR method

In our electron paramagnetic resonance (EPR) studies lipophilic spin probe methylester of 5-doxyl palmitate (MeFASL (10,3)) was used, which is sparsely dissolved in water solutions but very well dissolved in lipids. It is incorporated preferentially into the membrane bilayer of cells and/or tissues. Since it is reduced very fast in hypoxic conditions by oxy redox systems in cells and tissues, which are primarily located at the site of ubiquinone in mitochondria<sup>21</sup> we believe that the main EPR signal observed corresponds to the EPR spectrum in the plasma membranes.

For rough estimation of relative changes in plasma membrane fluidity a maximal hyperfine splitting  $2A_{\parallel}$ , which is related to the average order parameter ( $S_{ef}$ ), and/or empirical correlation time  $\tau_{ep}$  can be determined from the EPR spectra.<sup>22</sup>

$$S_{ef} = k(A_{\parallel} - A_{\perp}) / (A_{zz} - A_{xx}) \quad (2)$$

$k$  = correction due to the polarity of spin probe environment

$A_{\parallel}$  and  $A_{\perp}$  = measured maximal and minimal hyperfine splitting (Figure 2. A).

$A_{zz}$  and  $A_{xx}$  = hyperfine coupling constants of MeFASL(10,3).

Empirical correlation time  $\tau_{ep}$  is given by the expression:

$$\tau_{ep} = k\Delta H_0 (h_0/h_{-1} - 1)^{1/2} \quad (3)$$

where  $\Delta H_0$ ,  $h_0$ , and  $h_{-1}$  are parameters which can be measured from the EPR spectra.  $\Delta H_0$  is the line-width of the middle line of the EPR spectra, while  $h_0$ , and  $h_{-1}$  are amplitudes of



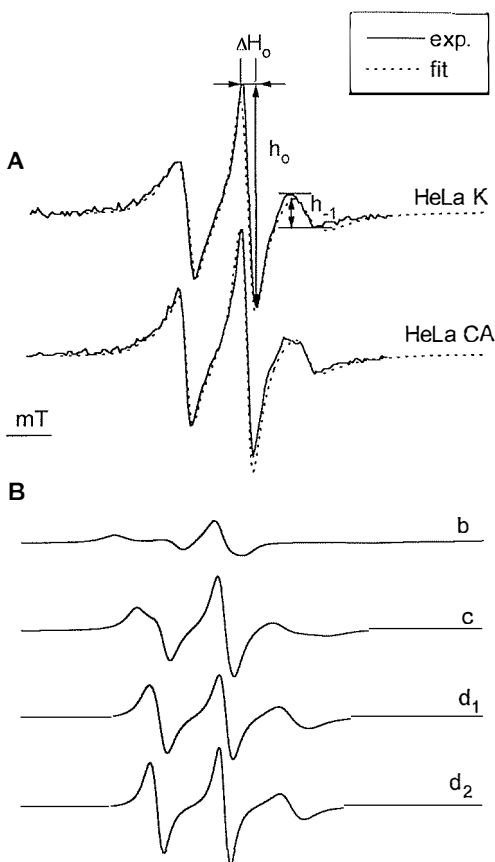


**Figure 1.** Typical EPR spectra of MeFASL(10,3) in the membrane of HeLa K<sub>0</sub> and HeLa CA cells.

**A.** Full line: experimental spectra, dotted line: the best fit to the experimental spectra, taking into account that the experimental spectra are superimposition of the spectra of three coexisting domains (b,c,d), which are presented in B together with the corresponding fluidity parameters  $S$  and  $\tau_c$ .

**B.** Computer simulation of the EPR spectra of three coexisting domains in HeLa K and HeLa CA cells: domain b (spectrum b), domain c (spectrum c). Spectrum b and c are the same for HeLa K and HeLa CA ( $S = 0.7$  and  $0.32$ , respectively and  $\tau_c = 4.0$  ns and  $2.0$  ns, respectively) and domain d (spectrum d1 for HeLa K,  $S = 0.15$ ,  $\tau_c = 1.5$  ns and spectrum d2 for HeLa CA with  $S = 0.10$  and  $\tau_c = 1.0$  ns).

middle- and low-field line (Figure 1.A.),  $k$  is constant typical of the spin probe used. The relation is valid only for fast isotropic motion of spin probes and can be used as a rough

approximation to estimate relative membrane alterations under different influences.<sup>22</sup>

However, to obtain more precise information about the heterogeneous structure of bilayer with several coexisting domains with different order parameter ( $S$ ) and correlation time ( $\tau_c$ ) the line shape of the experimental EPR spectra should be compared with the spectra calculated by the model which takes into account heterogeneous bilayer structure with several coexisting domains. In the model an isotropic motion of spin probe molecules around the long molecular axis and the restricted motion in the direction parallel to the long molecular axis of lipids is used. In the calculation the number of domains and the relative portion of each domain ( $W$ ), which is related to the area occupied with the particular domain, is varied as well as the fluidity parameters  $S$  and  $\tau_c$  of each domain. Beside the ordering parameter and correlation time the line width of the middle line is also included as a variable which describes the anisotropy of the two parameters, as well as the ratios  $g/g_i$  and  $a/a_i$ , which include the difference in the polarity of the spin probe surroundings.<sup>20</sup> From the best fit with experimental spectra relative portion of each domain in the membrane as well as their ordering and dynamics could be determined. Therefore, we could distinguish the contribution of the relative portion of each domain from the contribution of fluidity alterations within the domain, to the entire fluidity changes in the membrane.

### Membrane fluidity of vinblastine sensitive and resistant HeLa cells

Depolymerization of microtubules by microtubule depolymerizing drugs, such as vinblastine (VLB), colchicine and vincristine, the antimitotic alkaloids commonly used as chemotherapeutic drugs that arrests many mammalian cells in the metaphase of mitosis

by its action on microtubules, were shown to be responsible for changes in the plasma membrane fluidity.<sup>23,24</sup> On the other hand, several studies indicate that pre-treatment of tumors with a low VLB dose can facilitate uptake of other chemotherapeutic drugs. With respect to these observations we suppose that, among the other factors, facilitated uptake of drugs after VLB treatment could be associated with increased fluidity of the plasma membrane of VLB sensitive cells. On the basis of these findings it would be interesting to compare the fluidity characteristics of cells which are sensitive to VLB with those which are resistant to VLB.

Membrane fluidity of human uterine carcinoma cells (HeLa K cells) was compared with the fluidity of a subclone HeLa CA cells, which was proved to be resistant against vinblastine (VLB)(our results, sent for publication). The cells were grown in Eagle minimal essential medium (EMEM) supplemented with 10 % FCS. In some experiments the cells were incubated for 1 hour with VLB (1 ng/ml). For EPR measurements the cells were trypsinized 48 hours after removal of VLB and spin labelled with MeFASL(10,3) as described elsewhere.<sup>23</sup> The EPR spectra were recorder on Bruker ESP 300 X-band EPR spectrometer.

EPR spectra of HeLa K and HeLa CA cells are presented in Figure 1. For a rough estimation of membrane fluidity changes, empirical correlation time  $\tau_{ep}$  was calculated from the EPR spectra in Figure 1 using the expression (3). Empirical correlation time in HeLa CA cells ( $\tau_{ep} = 2.08$  ns) was significantly lower than in HeLa K cells ( $\tau_{ep} = 2.43$  ns,  $p < 0.001$ ). A significant decrease in  $\tau_{ep}$  was also observed after treatment of HeLa K cells with VLB ( $\tau_{ep} = 2.16$  ns). However, treatment of HeLa CA cells with VLB did not significantly affect  $\tau_{ep}$ , compared to the untreated HeLa CA cells. Similar results were already obtained previously for Chinese hamster ovary cell lines<sup>24</sup> where a decrease of order

parameter of resistant mutant was observed in comparison to the wild type CHO cells with 5-doxyl stearic acid as a spin probe. Treatment with microtubule depolymerizing agents have the same influence as on HeLa cells. Also in our previous work on spindle cell sarcoma similar results were obtained.<sup>23</sup> In these studies only an average fluidity characteristics were measured, (an average order parameter  $S$  or average correlation time  $\tau_{ep}$ .<sup>23,24</sup>). In the present experiment heterogeneity of plasma membrane was taken into account and by computer simulation of the EPR spectra line-shape, the information about the domain structure alteration in the plasma membrane was obtained, additionally to the average  $\tau_{ep}$  alterations.

In Figure 1 (dotted lines) the best fits to the experimental spectra are presented. The calculated spectra which fitted the best to the experimental spectra of HeLa CA and HeLa K cells (Figure 1, full line) were superimposition of three spectra (Figure 1.B). These spectra correspond to the spin probe molecules in three different types of domains (b, c, d) with different order parameter ( $S$ ) and correlation time ( $\tau_c$ ). The spectrum of VLB resistant HeLa CA cells could not be fitted adequately if only altered ratio between the domains was taken into account. For good fit it was necessary to decrease the order parameter  $S$ , of the most fluid domain (d) (spectrum d2 in Figure 1.B.). The portion of this domain in HeLa CA was slightly smaller ( $W = 25\%$ ) than in HeLa K cells ( $W = 30\%$ ). On the other hand, treatment of HeLa K cells with VLB did not change fluidity characteristics ( $S$  and  $\tau_c$ ) of membrane domains; only the portion of different domains was changed. In HeLa K portion of domain b and d was 30 % and in HeLa K treated with VLB portion of domain b was 20 % and of domain d it was 40 %. The portion of the middle domain c remained unchanged (40 %).

From the results obtained it could be concluded that the reason for the average fluidity

decrease, observed from  $\tau_{ep}$  measurements for HeLa CA cells and VLB treated HeLa K cells is not of the same origin. The altered ordering and dynamics of the most fluid domain (d) in HeLa CA cells indicates that the composition of domain d is altered in comparison to HeLa K cells, while after treatment of HeLa K cells with VLB the composition of domains remain the same, but the portion of domains in the membrane change. An increased content of non-saturated acyl chains, and/or decreased cholesterol content may be the reason for the increased fluidity of the most fluid domain (d) in HeLa CA in comparison to HeLa K cells. On the other hand it seems that the treatment of HeLa K cells with VLB, which causes depolymerization of microtubules, triggers some rearrangement of membrane constituents in a way which favours the less ordered regions in the membrane.

### Membrane fluidity characteristics of excised lung tumor tissues

In this study we used EPR with spin probes to investigate membrane fluidity in human lung cancer tissues specimen, cut at the time of resection. By computer simulation of the EPR spectral line-shape we wanted to distinguish the contribution to the EPR spectra of the membrane fluidity alterations within domains, from the alteration in the portion of each domain in the membrane.

Fiftyone lung cancer samples from patients with predominantly non small lung cancer, who were operated at Department of Thoracic Surgery, University Medical Centre in Ljubljana from June 1988 to June 1990 were analysed by EPR. From lung resectat the samples of cancer and histologically normal tissue were cut for EPR analysis, which was performed not more then two hours after operation. The samples were cut to cca 0.5 mm thick slices, weighting from 10 to 20 mg.

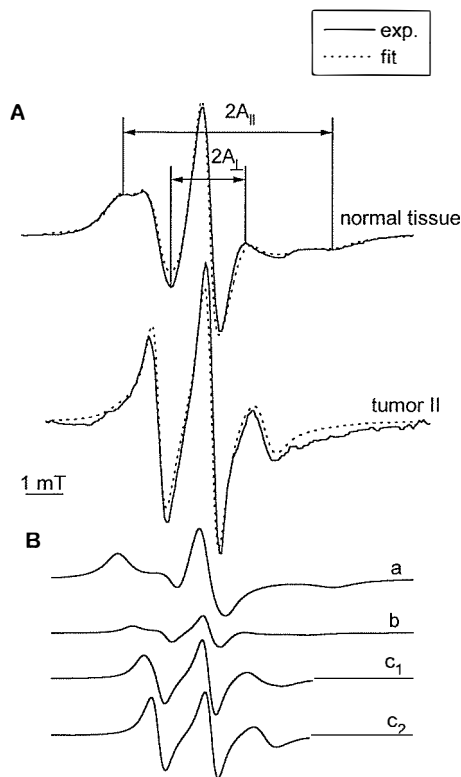


**Figure 2.** Typical EPR spectra of MeFASL(10,3) in the membrane of normal lung tissue, and in lung cancer tissues (Cancer II). Full line: experimental spectra, dotted line: calculated spectra, taking into account that the experimental spectra are superimposition of EPR spectra of three coexisting domains (a, b, c), with fluidity parameters ( $S$  and  $\tau_c$ ) presented in Table 1. Computer simulation of the EPR spectra of MeFASL(10,3) in three coexisting domains in normal lung tissue and in lung cancer (cancer II), calculated with the parameters presented in Table 1. Spectra a and b, which correspond to the domain a and b are the same for both tissues, while spectra c<sub>1</sub> and c<sub>2</sub> correspond to the most fluid domain in normal lung tissue and in malignant tissue, respectively.

They were immersed for 30 min into 0.1 mmol/l solution of MeFASL(10,3) in phosphate buffered saline (PBS) (0.01 ml of 10 mmol/l MeFASL(10,3) in ethanol solution was added to 1 ml of PBS).

Typical EPR spectra of normal lung tissue and of lung cancer are shown in Figure 2A. The calculated line shapes of such heterogeneous EPR spectra, which fitted the best the experimental spectra are superimposition of three spectra (Figure 2.B), which correspond to the spin probe molecules in three different types of domain with different order parameters ( $S$ ). The parameters, by which the best fits of the calculated spectra to the experimental spectra were obtained, are presented in Table 1 for normal tissue and for two different lung cancer samples (cancer I and cancer II).

Our results demonstrate that plasma membranes in lung cancer samples are more fluid than the membranes in normal lung tissue. The alterations observed are connected with an enlargement of the most fluid and less ordered domains as well as with an increased fluidity of these domains in malignant tissues. This is reflected in a decrease of order parameter  $S$  from 0.25 in normal tissue to 0.05 in malignant tissues. This indicates that the lipid composition of the most fluid domains is altered, and could be most probably ascribed to a decreased cholesterol content in plasma membrane of tumor tissue. This is in accordance with other studies which showed that the membranes of tumor cells were more fluid than the membranes of normal cells.<sup>7,8,9</sup> According to Vitols<sup>25</sup> there

are two possible explanations for enhanced plasma membrane fluidity of tumor cells: rapid cholesterol turnover and plasma membrane shedding in tumor cells. Adequate cholesterol/phospholipid molar ratio in plasma membrane is maintained by cell's own cholesterol biosynthesis and intense receptor mediated endocytosis of serum cholesterol.<sup>25,26</sup> The consequence could be a decreased serum cholesterol level in tumor bearing subjects, which was found in tumor bearing mice<sup>26</sup> and in cancer patients with tumor of different origin described in many epidemiological and clinical studies.<sup>27,28,29</sup> On the other hand, cholesterol is lost from plasma membrane by continuous exfoliation or shedding of membrane vesicles, which are reach in antigens and cholesterol.<sup>30,31,32</sup>

From Table 1 it is also evident that two cancer types differ only in the ratio of domains with different fluidity, while the ordering and dynamics of these domains does not change significantly. Enlargement of the most fluid domain and a decrease of the area with the most ordered domain could be attributed to the protein and/or antigen redistribution in the membrane. This could be connected with bulbs formation in tumor cells, which could be the first step in plasma membrane shedding.

**Table 1.** EPR fluidity parameters  $S$ , and  $\tau_c$  and the portion of each domain in the membrane  $W$  used in the calculation of the EPR spectra of MeFASL(10,3) in the membrane of lung tissues presented in Figure 1, which gave the best fit to the experimental spectra

	Normal* tissue			Cancer I			Cancer II		
Domain	a	b	c	a	b	c	a	b	c
$S$	0.8	0.5	0.25	0.8	0.5	0.05	0.8	0.5	0.05
$\tau_c$ (ns)	2.0	2.0	2.0	2.0	2.0	2.0	2.0	2.0	2.0
$W$ (%)	0.72	0.10	0.18	0.43	0.27	0.3	0.3	0.15	0.55

\* normal tissue was taken from the periphery of resected lung far away from tumor

## Conclusions

In this review article we showed two examples of EPR investigation: on cultured malignant cells and on non-treated human tissues taking into account heterogeneity of plasma membrane. With this approach the fluidity changes within certain membrane domain were distinguished from the alteration in the portion of domains in the membrane. In this way we could obtain additional information about the modification of lipid and/or protein composition in the domain and about the redistribution of membrane components within the membrane.

The general observation was that in tumor tissues the fluidity of the most fluid domain is increased, what could correspond to the decreased cholesterol concentration in plasma membrane. In different tumors only the area of domains is altered, while the fluidity of domain is basically unchanged. Similar observations were also obtained for two HeLa cell lines. They differ in the fluidity characteristics of certain domains, while the treatment of VLB sensitive cells with VLB, only altered the area of domains.

In further membrane fluidity investigations it should be also taken into account that different probes could preferentially be dissolved in different domains, more or less reach with cholesterol or proteins. Therefore different probes should be applied.

## References

1. Alberts B, Bray D, Lewis J, Raff M, Roberts K, Watson JD. *Molecular Biology of the Cell*. London: Garland Publishing, Inc, 1989: 275-341.
2. Bloom M. The physics of soft, natural materials. *Physics in Canada* 1992; **48**: 7-16.
3. Alvarado Cader A, Butterfield DA, Watkins BA, Hong Chung B, Hennig B. Electron spin resonance studies of fatty acid-induced alterations in membrane fluidity in cultured endothelial cells. *Int J Biochem Cell Biol* 1995; **27**: 665-73.
4. Marsh D. Lipid-protein interactions and heterogeneous lipid distribution in membranes. *Mol Membr Biol* 1995; **12**: 59-64.
5. Ruddon RW. *Cancer biology*. Oxford: Oxford University Press, 1995: 103-7.
6. Tarabozetti G, Perin L, Bottazzi B, Mantovani A, Giavazzi R, Salmona M. Membrane fluidity affects tumor cell motility, invasion and lung colonizing potential. *Int J Cancer* 1989; **RR44**: 707-13.
7. Yang YZ, Hao TL, Qian M, Dai WX, Huangfu YM, Zhang ZH. Normal and leukemic lymphocyte membrane fluidity and response to stimulation with ConA and PHA. *J Tongji Med Univ* 1989; **9**: 143-7.
8. Deliconstantinos G. Physiological aspects of membrane lipid fluidity in malignancy. *Anticancer Res* 1987; **7**: 1011-21.
9. Inbar M. Fluidity of membrane lipids: A single cell analysis of mouse normal lymphocytes and malignant lymphoma cells. *FEBS Lett* 1976; **67**: 180-5.
10. Dudeja PK, Dahiya R, Brasitus TA. The role of sphingomyelin synthetase and sphingomyelinase in 1,2-dimethylhydrazine induced lipid alterations of rat colonic plasma membranes. *Biochim Biophys Acta* 1986; **863**: 309-12.
11. Benko C, Hilkmann H, Vigh L, van Blitterswijk WJ. Catalytic hydrogenation of fatty acyl chains in plasma membranes; effect on membrane lipid fluidity and expression of cell surface antigens. *Biochim Biophys Acta* 1987; **896**: 129-35.
12. Mann SC, Andrews PA, Howell SB. Comparison of lipid content, surface membrane fluidity, and temperature dependence of cis-diamminedichloroplatinum(II) accumulation in sensitive and resistant human ovarian carcinoma cells. *Anticancer Res* 1988; **8**: 1211-5.
13. Schara M, Šentjurs M, Cotič L, Pečar S, Palčič B, Monti-Bragadin C. Spin label study of normal and Ki-MSV transformed rat kidney cell membranes. *Stud Biophys* 1977; **62**: 141-RR50.
14. Parola AH. Membrane dynamic alteration associated with cell transformation and malignancy. In: Galeotti T, Cittadini A, Neri G, Papa S, eds. *Membranes in tumor growth*. Amsterdam: Elsevier biomedical press, 1982: 69-81.
15. Mahler SM, Wilce PA, Shanley BC. Studies on regenerating liver and hepatoma plasma membranes. Membrane fluidity and enzyme activity. *Int J Biochem* 1988; **20**: 613-9.
16. Aleksijevic A, Cremel G, Mutet C, Giron C, Hubert P, Waksman A, Falkenrodt A, Oberling F, Mayer S, Lang JM. Decreased membrane "fluidity" of T lymphocytes from untreated patients with Hodgkin's disease. *Leuk Res* 1986; **10**: 1477-84.
17. Kier AB, Parker MT, Schroeder F. Local and metastatic tumor growth and membrane proper-

- ties of LM fibroblast in athymic (nude) mice. *Biochim Biophys Acta* 1988; **938**: 434-46.
18. Kier AB. Membrane properties of metastatic and non-metastatic cells cultured from C3H mice injected with LM fibroblast. *Biochim Biophys Acta* 1990; **1022**: 365-72.
19. Šentjerc M, Schara M, Auersperg M, Jezernik M and Kveder M. Characterization of malignant tissue by EPR. *Studia Biophys* 1990; **136**: 201-8.
20. Žel J, Svetek J, Črne H and Schara M. Effects of aluminum on membrane fluidity of the mycorrhizal fungus *Amanita muscaria*. *Physiologia Plantarum* 1993; **89**: 172-6.
21. Swartz HM, Šentjerc M, Kocherginsky N. Metabolism of nitroxides and their products in cells. In: Kocherginsky N and Swartz HM Eds. *Nitroxide spin labels: Reactions in Biology and Chemistry*. Boca Raton: CRC press, 1995: 113-47.
22. Marsh D. Electron spin resonance: spin labels. In: Grell E, ed. *Membrane spectroscopy*. Berlin: Springer Verlag, 1981: 52-141.
23. Serša G, Čemažar M, Šentjerc M, Us-Krašovec M, Kalebić S, Drašlar K, Auersperg M. Effect of vinblastine on cell membrane fluidity and the growth of SA-1 tumor in mice. *Cancer Letters* 1994; **79**: 53-60.
24. Aszalos A, Yang GC and Gottesman MM. Depolymerization of microtubules increases the motional freedom of molecular probes in cellular plasma membranes. *J Cell Biol* 1985; **100**: 1357-62.
25. Vitols S, Peterson C, Larsson O, Holm P, Aberg B. Elevated uptake of low density lipoproteins by human lung cancer tissue in vivo. *Cancer Res* 1992; **52**: 6244-7.
26. Van Blitterswijk WJ, Damen J, Hilkmann H, de Widt J. Alterations in biosynthesis and homeostasis of cholesterol and in lipoprotein patterns in mice bearing a transplanted lymphoid tumor. *Biochim Biophys Acta* 1985; **816**: 46-56.
27. Alexopoulos CG, Blatsios B, Avgerinos A. Serum lipids and lipoprotein disorders in cancer patients. *Cancer* 1987; **60**: 3065-70.
28. Winawer SJ, Flehinger BJ, Buchalter J, Herbert E, Shike M. Declining serum cholesterol levels prior to diagnosis of colon cancer. A time-trend, case-control study. *JAMA* 1990; **263**: 2083-5.
29. Faintuch J, Cobraitz R, Martin Nieto AR, Yagi OK, Zilberstein B, Cecconello I, Pinotti HW, Wesdorp RI. The prognosis value of cholesterol level in malnourished patients with esophageal carcinoma. *Nutricion Hospitalaria* 1993; **8**: 352-7.
30. Black PH. Shedding from the cell surface of normal and cancer cells. *Adv Cancer Res* 1980; **32**: 75-199.
31. Petitou M, Tuy F, Rosenfeld C, Mishal Z, Paintrand M, Jasnin C, Mathe G, Inbar M. Decreased microviscosity of membrane lipids in leukemic cells: Two possible mechanisms. *Proc Natl Acad Sci USA* 1978; **75**: 2306-10.
32. Van Blitterswijk WJ, de Veer G, Krol JH, Emmelot P. Comparative lipid analysis of purified plasma membranes and shed extracellular membrane vesicles from normal murine thymocytes and leukemic GRS1 cells. *Biochim Biophys Acta* 1982; **688**: 495-504.



## On mechanisms of cell plasma membrane vesiculation

Veronika Kralj-Iglič<sup>1</sup>, Urška Batista<sup>1</sup>, Henry Hägerstrand<sup>2</sup>, Aleš Iglič<sup>1,3</sup>,  
Janja Majhenc<sup>1</sup>, Miha Sok<sup>4</sup>

<sup>1</sup>Institute of Biophysics, Medical Faculty, Ljubljana, Slovenia, <sup>2</sup>Department of Biology, Åbo Akademy University, Åbo/Turku, Finland, <sup>3</sup>Faculty of Electrical Engineering, Ljubljana, Slovenia, <sup>4</sup>Department of Thoracal Surgery, Clinical Center, Ljubljana, Slovenia

---

*Vesiculation of the cell membrane is studied. It is proposed that the shape of the membrane segment free of the cytoskeleton is driven towards the shape of its maximal possible difference between the two membrane layer areas by the rearrangement of the laterally mobile membrane constituents. It is shown that the shapes corresponding to the extrema of the area difference can be spherical, planar and cylindrical, depending on the enforced constraints. Correspondingly, the spherical vesicles and the cylindrical protrusions observed in vesiculating MCF7 cancer (human breast adenocarcinoma) cells are shown. The proposed mechanism of vesiculation also provides an explanation for different relative content of some substances in the membrane of the released vesicles than in the membrane of the residual cells.*

*Key words: budding; membrane bilayer; vesiculation*

---

### Introduction

Membranes of some cells can form during the budding process small protrusions which are eventually released from the membrane as vesicles. The amount of the involved membrane varies from relatively large portions with or without enclosed elements of the cytoplasmic material to very small fragments filled only with the cytosol. It is a common feature that the disruption of the cytoskeleton or its detachment from the membrane bilayer occurs prior to vesiculation. It was

also observed that the membrane of the released vesicles differs from the membrane of the residual cell in the relative content of some membrane constituents, indicating that the rearrangement of the membrane constituents occurs during the budding. The vesiculation is therefore a mechanism through which the cell membrane loses some substances. In cancer cells the budding and vesiculation process occurs spontaneously thereby causing a continuous loss of some important substances from the cell membrane and leading to the alteration of the cell function.<sup>1,2,3</sup>

A system that is due to its simplicity convenient to study the general features of the membrane budding and vesiculation is the

---

Correspondence to: dr. Veronika Kralj-Iglič, Institute of Biophysics, Medical Faculty, Lipičeva 2, SI-1000 Ljubljana, Slovenia; Tel.: +386-61-314-127; Fax.: +386-61-131-51-27; E-mail: vera.kralj-iglic@biofiz.mf.uni-lj.si.



mammalian erythrocyte. In erythrocytes, it was found that a wide variety of treatments and conditions such as incubation with dimyristoyl phosphatidyl choline vesicles,<sup>4,5</sup> incubation with various amphiphiles,<sup>6,7</sup> ATP depletion<sup>8</sup> and extreme pH in the suspension<sup>9,10</sup> may influence the vesiculation process. As the features observed in vesiculation of the erythrocytes are relevant also in general<sup>11</sup>, there is a possibility to manipulate the cancer cells in such a way as to stabilize the membrane and prevent the loss of the important membrane constituents from the membrane. It is therefore of interest to understand the mechanisms taking place in membrane budding and vesiculation. In this work we focus on the features involving the membrane segments that are already detached from the cytoskeleton.

## Material and methods

### *The proposed mechanism of budding and vesiculation*

The proposed mechanism is schematically represented in Figure 1.

In the description of the membrane segment the membrane is taken to be a two dimensional liquid composed of phospholipid molecules, in which various other molecules such as the membrane proteins are embedded. The embedded molecules are more or less free to move laterally over the membrane surface. The connections of the membrane with the intracellular and the extracellular matrix are of importance, since they may impose limits and obstacles for the lateral motion of the membrane constituents. The disruption or detachment of the cytoskeleton from the membrane thus increases the pool of the laterally mobile molecules.

It is proposed that following the detachment of the cytoskeleton, the development of

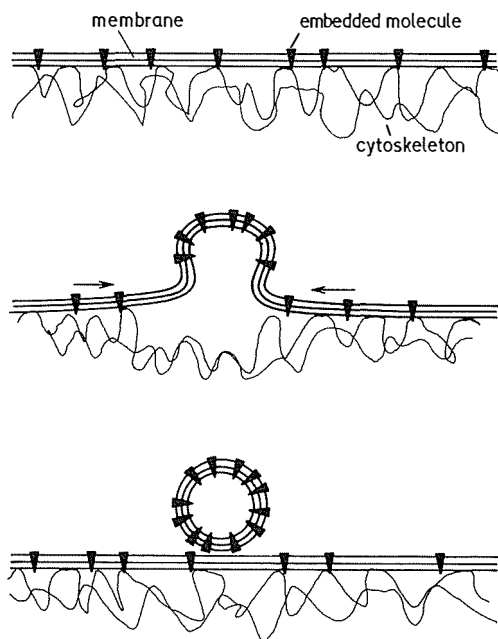


**Figure 1.** A scheme of the proposed mechanism of the budding process. The membrane with embedded molecules that favour large membrane curvature is shown. First, the membrane becomes locally detached from the cytoskeleton thereby increasing the pool of laterally mobile embedded molecules. The membrane segment free of the cytoskeleton then forms a protrusion as this is energetically favourable. The laterally mobile membrane embedded molecules accumulate in the region of favourable curvature so that the area density of the number of the embedded molecules is higher in the membrane of the vesicles than in the membrane of the residual cell.

the bud can be described as a local event involving the cytoskeleton free membrane segment. Further, it is proposed that the exchange of the laterally mobile membrane constituents between the membrane segment and the membrane of the residual cell provides the driving mechanism for the bud development, ending with the formation of the vesicle.

As the cytoskeleton free membrane segment is very small comparing to the membrane of the residual cell, the membrane of the residual cell can be treated as a reservoir for the laterally mobile membrane con-

stituents. The energy of the embedded molecule at a given site in the membrane depends on the local membrane curvature,<sup>12</sup> so that the laterally mobile molecules tend to accumulate in the regions at which the membrane curvature is energetically more favourable while the membrane segment attains the shape with larger regions of the favourable curvature.<sup>12</sup> As a result, a protrusion of the membrane exhibiting higher curvature than the residual cell is formed and the laterally mobile membrane constituents that favour large curvature accumulate in the protrusion.

In turn, the molecule that favours large curvature may be expected to occupy larger portion of the outer membrane layer than the inner one. A presence of such a molecule in the membrane segment increases the area of the outer layer of the segment with respect to the area of the inner one. If the cytoskeleton free membrane segment forms a bud, the laterally mobile molecules that favour large membrane curvature flow to the bud from the membrane of the residual cell and cause the area of the outer layer of the segment to increase relative to the inner one. The process may proceed up to a limit imposed by the geometrical constraints where the shape of the maximal possible area difference is reached.

### Theory

In order to obtain the shapes of the bilayer segment of an extreme area difference  $\Delta A$  at a given area of the bilayer neutral surface  $A$  a variational problem is stated by constructing a functional

$$G = \Delta A - \lambda_A (\int dA - A), \quad (1)$$

where for thin bilayers

$$\Delta A = h \int (C_1 + C_2) dA, \quad (2)$$

$\lambda_A$  is the Lagrange multiplier,  $C_1$  and  $C_2$  are

the principal membrane curvatures,  $\Delta A$  is the area element and  $h$  is the distance between the neutral surfaces of the two bilayer monolayers in the direction perpendicular to the membrane surface. The analysis is restricted to axisymmetric shapes. It is chosen that the symmetry axis of the body coincides with the  $x$  axis, so that the shape is given by the rotation of the function  $y(x)$  around the  $x$  axis. In this case the principal curvatures are expressed by  $y(x)$  and its derivatives with respect to  $x$ ;  $y' = \partial y / \partial x$  and  $y'' = \partial^2 y / \partial x^2$ , as  $C_1 = 1/y(1+y'^2)^{1/2}$  and  $C_2 = -y''/(1+y'^2)^{3/2}$  while the area element is  $\Delta A = 2\pi (1+y'^2)^{1/2} y dx$ . The sign of the principal curvatures is taken to be positive for a sphere. Inserting the above expressions for  $C_1$ ,  $C_2$  and  $\Delta A$  into (1) and rearranging, the functional normalized with respect to  $2\pi h$  becomes

$$G = \int g(x, y, y', y'') dx \quad (3)$$

where

$$g(x, y, y', y'') = 1 - yy''/(1+y'^2) - \lambda_A y (1+y'^2)^{1/2}, \quad (4)$$

$\lambda_A = A_A/h$ . The variation  $\delta G = 0$  is performed by solving the Poisson – Euler equation

$$\frac{\partial g}{\partial y} - \frac{d}{dx} \left( \frac{\partial g}{\partial y'} \right) + \frac{d^2}{dx^2} \left( \frac{\partial g}{\partial y''} \right) = 0. \quad (5)$$

Obtaining the necessary differentiations of (4), the Poisson – Euler equation is expressed as

$$2y''/(1+y'^2)^2 + \lambda_A ((1+y'^2)^{-1/2} - yy'''(1+y'^2)^{-3/2}) = 0. \quad (6)$$

If the area of the segment is fixed ( $\lambda_A \neq 0$ ), there is an analytical solution of (6), given by a circle of the radius  $r_{cir}$ :  $y = (r_{cir}^2 - x^2)^{1/2}$ . This solution represents spheres of a radius  $1/r_{cir} = \lambda_A$ , and a segment of a plane  $1/r_{cir} = 0$ . If the area  $A$  is not fixed i.e if  $\lambda_A = 0$  the possi-

ble analytical solution of the equation (6) is a constant  $y = \text{const}$ , representing a cylinder.

### Experiment

**Cells:** The cells MCF7 (human breast adenocarcinoma) were grown in Eagle MEM, supplemented with 1 percent nonessential amino acids, 10 percent fetal calf serum (FCS), penicillin (100 U/ml) and streptomycin (100  $\mu\text{g/ml}$ ) at 37°C in a CO<sub>2</sub> incubator.

**Induction of membrane vesiculation:** Exponentially growing MCF7 cells were detached by 0.25 percent trypsin solution. The cells were resuspended in Eagle MEM without FCS and put on ice (4°C). After one hour the cell suspension was placed on 37°C for two hours.<sup>13</sup> The cells were then observed by the phase contrast microscope (Obj. Ph 3, 100X, NA 1.2).

### Results and discussion

It was shown above that the shapes of the bilayer segment corresponding to the extreme difference between the two monolayer areas are spherical, planar and cylindrical. The spherical shape and a planar circular segment are characterized by one parameter, respectively. The respective parameter can be determined from the constraint requiring a fixed area. Therefore the sphere and the planar segment can be established as the shapes of the extreme area difference.<sup>14</sup> If the sphere is involved, the extremum is a maximum, as calculated by the minimization of the membrane bending energy for a sequence of shapes describing the formation of a spherical vesicle.<sup>15</sup> In order to establish a cylindrical shape as a shape of the extreme area difference, a boundary condition should be stated, such as a requirement for a fixed radius of the cylinder. It can be concluded that the spherical and the planar shapes of the maximal area difference are connected to the fixed

area of the membrane segment while the cylindrical shape is unconstrained, but confined at its radius.

The theoretical predictions are compared to the phenomena observed in the experiment. In a vesiculating cancer cell, spherical vesicles as well as cylindrical protrusions can be observed (Figs. 2A and 2B, respectively). The vesiculation was promoted as described in the Material and methods ensuring that the integrity of the cytoskeleton was destroyed.<sup>13</sup> The observed shapes of the vesicles and protrusions correspond well to the theoretically predicted ones.

It was indicated by experiments that the properties of the membrane constituents strongly influence the nature of the protrusions and vesicles. In erythrocyte suspension, incubated with the exogenously added amphiphiles the budding and vesiculation of the erythrocyte membrane was observed.<sup>6,7</sup>

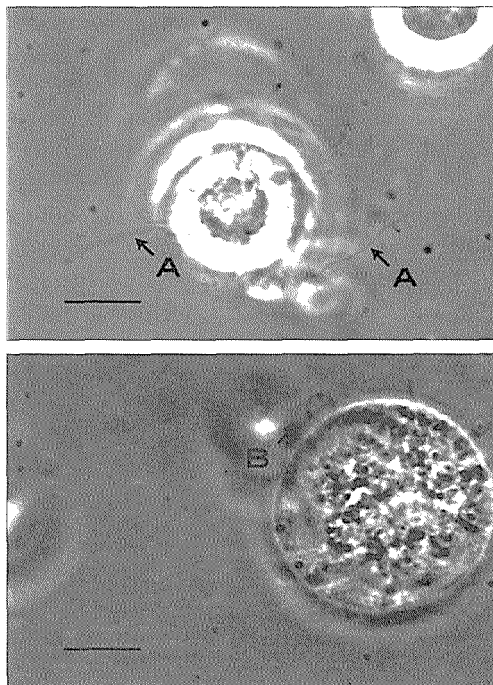


**Figure 2.** A vesiculating MCF7 cancer cell exhibiting a cylindrical protrusion (A) and a spherical vesicle (B), (bar=10 $\mu\text{m}$ ).

The released vesicles were spherical and cylindrical, depending on the species of the added amphiphiles. Besides the properties of the membrane constituents, the manner of the disruption or the detachment of the skeleton may also influence the character of the vesicles by determining the amount of the membrane segment available to the bud, and also by determining the amount of the laterally mobile membrane embedded molecules. In deciding whether the protrusion will lead to a spherical vesicle or to a cylindrical protrusion, it should therefore be established which of the two processes is possible. If both of them are possible it should be distinguished, which of them would be energetically more favourable. In this case, the free energy of the segment under consideration should be minimized, taking into account the local composition of the segment. This is however beyond the scope of this work.

The laterally mobile molecules that favour large membrane curvature are accumulated in the buds which develop into vesicles and are released from the membrane. Thereby the relative content of these molecules in the residual cell membrane is diminished which may be unfavourable regarding the cell function. In this context, adding to the cell membrane the substances that decrease the area difference  $\Delta A$  would tend to inhibit the budding and vesiculation. Indeed, chlorpromazine which was proved to intercalate into the inner membrane layer of erythrocytes<sup>16,17</sup> was also shown to have therapeutic effects in cancer treatment.<sup>18</sup> These promising results encourage further studies of the mechanisms taking place in the membrane during budding and vesiculation.

## References

1. Dolo V, Adobati E, Canevari S, Picone MA, Vittorelli ML. Membrane vesicles shed into the extracellular medium by human breast carcinoma cells carry tumor-associated surface antigens. *Clin Exp Metastasis* 1995; **13**: 277-86.
2. Hakomori S. Tumor malignancy defined by aberrant glycosylation and sphingo(glyco)lipid metabolism. *Cancer Res* 1996; **56**: 5309-18.
3. Black RA, Rausch CT, Kozlosky CJ, Peschon JJ, Slack JL, Wolfson MF *et al.* A metalloproteinase disintegrin that releases tumour-necrosis factor- $\alpha$  from cells. *Nature* 1997; **385**: 729-33.
4. Ott P, Hope MJ, Verkleij AJ, Roelofsens B, Brodbeck U, Van Deenen LLM. Effects of dimyristoylphosphatidylcholine on intact erythrocytes. Release of spectrin - free vesicles without ATP depletion. *Biochim Biophys Acta* 1981; **641**: 79-87.
5. Yamaguchi T, Yamada S, Kimoto E. Effects of cross-linking of membrane proteins on vesiculation induced by dimyristoyl phosphatidylcholine in human erythrocytes. *J Biochem* 1994; **115**: 659-63.
6. Hägerstrand H, Isomaa B. Vesiculation induced by amphiphiles in erythrocytes. *Biochim Biophys Acta* 1989; **982**: 179-86.
7. Hägerstrand H, Isomaa B. Morphological characterization of exovesicles and endovesicles released from human erythrocytes following treatment with amphiphiles. *Biochim Biophys Acta* 1992; **1190**: 409-15.
8. Lutz HU, Liu SC, Palek J. Release of spectrin-free vesicles from human erythrocyte during ATP depletion. *J Cell Biol* 1977; **73**: 548-60.
9. Bobrowska-Hägerstrand M, Iglič A, Hägerstrand H. Erythrocytes vesiculate at high pH. *Cell Mol Biol Lett* 1997; **2**: 9-13.
10. Gros M, Vrhovec S, Brumen M, Svetina S, Žekš B. Low pH induced shape changes and vesiculation of human erythrocytes. *Gen Physiol Biophys* 1996; **15**: 145-63.
11. Wagner GM, Chiu DTY, Yee MC, Lubin BH. Red cell vesiculation - a common membrane physiological event. *J Lab Clin Invest* 1986; **108**: 315-24.
12. Kralj-Iglič V, Svetina S, Žekš B. Shapes of bilayer vesicles with membrane embedded molecules. *Eur Biophys J* 1996; **24**: 311-21.
13. Liepins A, Hillman AJ. Shedding of tumor cell surface membranes. *Cell Biol Inter Rep* 1981; **5**: 15-26.
14. Elsgolc LE. *Calculus of variations* (1963) Pergamon Press, Oxford, pp. 79.

15. Žekš B, Iglič A, Svetina S. Bilayer membrane models and a theoretical analysis of the vesiculation process. *Suppl Minerva Biotechnologica* 1990; **2**: 47.
16. Deuticke B. Transformation and restoration of the biconcave shape of human erythrocytes induced by agents and change of ionic environment. *Biochim Biophys Acta* 1968; **163**: 494 – 500.
17. Sheetz MP, Singer SJ. Biological membranes as bilayer couples. A molecular mechanism of drug-erythrocyte interactions. *Proc Natl Acad Sci* 1974; **71**: 4457 – 61.
18. Levij IS, Polliack A. Inhibition of chemical carcinogenesis in the hamster cheek pouch by topical chlorpromazine. *Nature* 1970; **223**: 1096.

## Tertiary collimator system for stereotactic radiosurgery with linear accelerator

Božidar Casar

Department of Radiophysics, Institute of Oncology, Ljubljana, Slovenia

---

*In the last decade, stereotactic radiosurgery (SRS) with linear accelerator (linac) has become an important irradiation technique for a variety of malignant and benign intracranial lesions. Although there exist some other radiosurgery techniques, linac based SRS meets the requirements needed for SRS with low cost modifications. One of the most important additional parts of the equipment is tertiary collimator system which can be attached onto the linac head. We designed and built such system that can be easily fixed onto linac PHILIPS SL – 75/5 with 5 MV photon energy. In our department, we already use this linac for conventional radiation therapy. Our tertiary collimator system meets all the requirements important for this special modality of radiation therapy. It allows fine centering of the system and has ten various collimators with divergent circular openings having a nominal field diameter ranging from 1.0 cm to 4.0 cm at the isocenter. The accuracy of the system was checked by exposing x – ray films at various gantry positions, and recording misalignment of the beams. The width of penumbra was determined using two different dosimetry techniques (film dosimetry and diode measurements).*

*Key words: radiosurgery – instrumentation; brain disease – surgery; particle accelerators*

---

### Introduction

Stereotactic radiosurgery (SRS) is a focal brain irradiation technique which delivers a high dose of ionizing radiation to stereotactically localized small intracranial lesions in a single session. SRS is a nonstandard radiation therapy technique which was introduced in 1951 by Leksell<sup>1</sup> and is currently performed with three basic modalities: with protons, <sup>60</sup>Co Gamma knife and with megavolt-

age x – ray beams from linear accelerators. As the first two modalities are extremely expensive and are dedicated for SRS alone, in 1980s many centers have introduced linac based SRS.<sup>2-7</sup>

One of the most important modifications, among many others, is to design and build tertiary collimator system for delivering highly collimated linac beams to the target. Many different approaches were taken in the past.<sup>8,9</sup>

Conventional collimators which are part of the head of linac, are inadequate for SRS because they can be set up only for rectangular fields and are too far from the isocenter

---

Correspondence to: Božidar Casar, BSc, Institute of Oncology, Department of Radiophysics, Zaloška 2, SI-1105 Ljubljana, Slovenia. Tel./Fax: +386 61 131 91 08; E - mail: bcasar@onko-i.si

which produces unacceptably large penumbra.

The aim of our project was to design and build a rigid, low cost, yet very precise tertiary collimator system, which can be simply and quickly attached onto the head of our 5 MV PHILIPS – 75/5 linac, presently used in our department for conventional radiation therapy.

### Materials and methods

While designing and assembling our tertiary collimator system (the system was constructed at the Institute for Electronics and Vacuum Technique, Ljubljana, Slovenia), we had to follow many important requirements such as: stability of the system during rotation of the gantry, short distance from tertiary collimators to the isocenter, easy and reproducible attachment of the system onto the head of linac, possibility of precise positioning (centering) of the system, various field diameters at the isocenter and high attenuation of the primary x-ray beam in the collimator walls.

We followed these requirements in designing and assembling of our tertiary collimator system which is constructed of an aluminium plate with a precise mechanical system in its center and a steel holder for various collimator inserts (Figure 1,2). The position of the collimator holder, which moves perpendicularly to the beam axis in two directions, is set by two micrometer regulators. These regulators enable precise and continuous movement of the holder which can be reproduced with precision of 0.1 mm. After reaching a desired position, we can fix both axes, defining the plane, orthogonal to the beam axis, with two large steel regulators to prevent any movement of the collimator holder relative to the rest of the system. The system itself is attached onto the linac head as tight as possible in order to prevent any undesired move-

ment of the whole system during gantry rotation.

Additionally, we made ten different collimators – inserts with circular openings which can be inserted into the steel collimator holder (Figure 3). Collimators are made of lead and openings are continuously tapered to match the beam divergence to minimize the penumbra. The distance from the end of the collimator to the isocenter is 28.3 cm which further minimizes the width of penumbra. Each collimator is cylindrically shaped, having outer diameter of 6 cm and length of 12 cm. Nominal field diameters defined at the isocenter are: 1.0 cm, 1.25 cm, 1.5 cm, 1.75 cm, 2.0 cm, 2.25 cm, 2.5 cm, 3.0 cm, 3.5 cm and 4.0 cm. A diameter of 6 cm is sufficient to fix adjustable collimator jaws (primary and secondary) to a field size

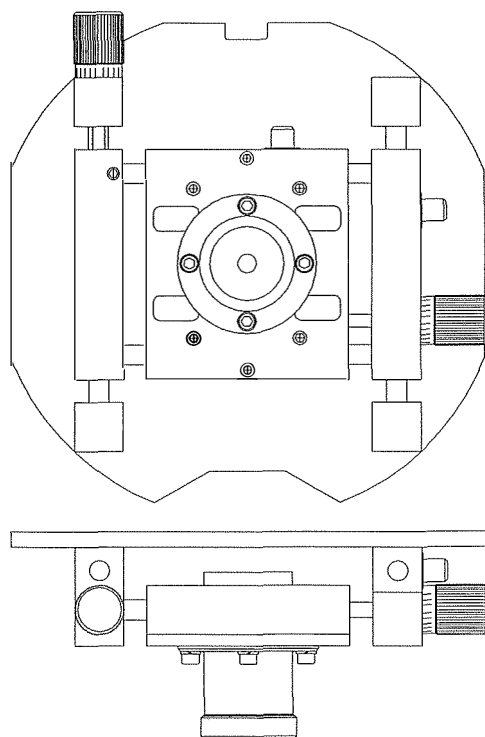


**Figure 1.** Schematic drawings of tertiary collimator system: a) beam axis view and b) side view, perpendicular to the beam axis.

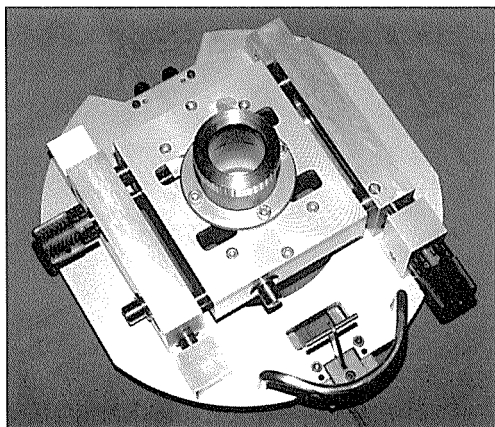


Figure 2. Tertiary collimator system.

5 x 5 cm<sup>2</sup> at the isocenter during irradiation. On the other hand, the length of 12 cm in the direction of beam axis is large enough to attenuate primary x-ray beam to about 1% compared to the output of an unblocked 5 MV beam.

Beam penumbra was measured by scanning beam profiles for each collimator using a) Multidata film densitometer, Kodak X-Omat V radiographic films and a phantom made of white polystyren and b) Scanditronix p-type silicon diodes and Multidata two dimensional water phantom.

## Results

After having centered precisely the collimator system, the alignment of the collimator was checked with lasers fixed to the ceiling and side-walls and optical field center and using radiographic film (Kodak X-Omat V).

First, we placed the film horizontally at the isocenter and exposed it to two parallel opposed beams with gantry angle at 0° and 180° (Figure 4.a); then we placed second film vertically through the isocenter and again exposed it to two parallel opposed beams with gantry angle at 90° and 270° (Figure 4.b). Similar procedure is used in Montreal General Hospital, Canada (McGill University) and

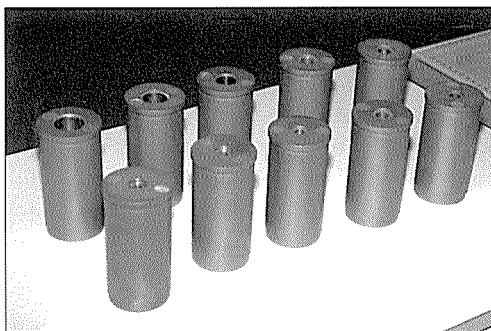


Figure 3. Ten collimators with nominal field diameters at the isocenter: 1.0 cm, 1.25 cm, 1.5 cm, 1.75 cm, 2.0 cm, 2.25 cm, 2.5 cm, 3.0 cm, 3.5 cm and 4.0 cm. Collimators have outer diameter of 6 cm and a length of 12 cm.

in some other centers.<sup>8,10,11</sup>

Conformity of each pair of film exposures is a measure for collimator alignment. In our case, we estimate the shift of one exposure pattern with respect to the other to be less than 0.5 mm (in both cases) and that is well within our tolerance level (1.0 mm).

The width of penumbra (i.e. distance between 20% and 80% isodose line) measurements also yielded very good results.<sup>12</sup> In the first case (film scanning) the width of penumbra ranged from 2.5 mm for 1.0 cm collimator to 3.1 mm for 4.0 cm collimator, while in the case of diode measurements the width of penumbra ranged from 2.6 mm for 1.0 cm collimator to 3.2 mm for 4.0 cm collimator.

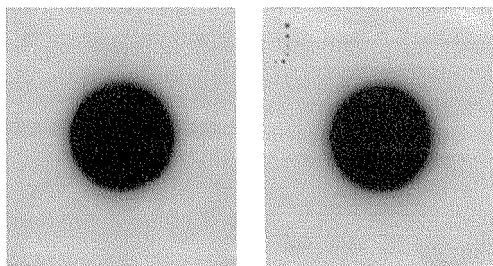


Figure 4. Verification films illustrating collimator alignment. Collimator diameter is 2.5 cm, film is placed at the isocenter, perpendicularly to the beam. Figure a) shows the image for two parallel - opposed beams (gantry angles: 0° and 180°) and Figure b) shows the image for two parallel - opposed beams (gantry angles: 90° and 270°).



## Conclusions

The tertiary collimator system which we designed and built for stereotactic radiosurgery with linear accelerator has very good mechanical and dosimetric properties and can be used for this special radiation therapy technique. Easy handling and relative low cost of production furthermore confirm that our work was successful.

## Acknowledgements

The project was supported by the Ministry of Science and Technology of the Republic of Slovenia. Special thanks go to Prof. Ervin B. Podgoršak from McGill University in Montreal, Canada, for his help and suggestions.

## References

1. Leksell L. The stereotaxis method and radiosurgery of the brain. *Int Chir Scan* 1951; **102**: 316 – 9.
2. Betti OO, Derechinsky VE. Hyperselective encephalic irradiation with linear accelerator. *Acta Neurochir Suppl (Wien)* 1985; **33**: 385 – 90.
3. Colombo F, Benedetti A, Pozza F. External stereotactic irradiation by linear accelerator. *Neurosurgery* 1985; **16**: 154 – 60.
4. Hartmann GH, Schlegel W, Sturm V, et al: Cerebral radiation surgery using moving field irradiation at a linear accelerator facility. *Int J Radiat Oncol Biol Phys* 1985; **11**: 1185– 92.
5. Houdek PV, Fayos JV, Van Buren JM, et al: Stereotaxic radiotherapy technique for small intracranial lesions. *Med Phys* 1985; **12**: 469 – 72.
6. Podgorsak EB, Olivier A, Pla M, et al: Dynamic stereotactic radiosurgery. *Int J Radiat Oncol Biol Phys* 1988; **14**: 115 – 25.
7. Podgorsak EB, Pike GB, Pla M, et al: Radiosurgery with high energy photon beams: A comparison among techniques. *Int J Radiat Oncol Biol Phys* 1989; **16**: 857 – 65.
8. AAPM Report No. 54, Stereotactic radiosurgery. *Report of Task Group 42 Radiation Therapy Committee*. American Institute of Physics 1995.
9. Lutz W, Winston KR, Maleki N. *A system for stereotactic radiosurgery with a linear accelerator*. *Int J Radiat Oncol Biol Phys* 1988; **14**: 373 – 81.
10. Hartmann GH. Quality assurance program on stereotactic radiosurgery: report from a quality assurance task group. Contributing authors: Lutz W, Arndt J, Ermakov I, Podgorsak EB, Schad L, Serago C, Vatnitsky SM. Springer 1995.
11. Podgorsak EB. Medical Physics Unit, McGill University, Montreal, Canada. Private communication 1996.
12. Casar B, Pregelj A. *Tertiary collimator system for stereotactic radiosurgery with linear accelerator and physical parameters of narrow photon beams*. International Conference Life Sciences '97, Book of abstracts & programme. 1997.

## Molekularne spremembe v celicah rezistentnih na citostatike

Osmak M

Največjo oviro za popoln uspeh pri zdravljenju raka predstavljajo tumorske celice in njihova sposobnost razvijanja odpornosti proti citostatikom. Pri razvijanju te sposobnosti sodeljuje več molekularnih mehanizmov: (a) zmanjšano kopičenje zdravila v celici (povečana dejavnost membranskih transporterjev, kot sta P-glikoprotein ali protein, ki je odporen proti več vrstam citostatikov), (b) spremembe v sistemu za detoksifikacijo v celici (višje koncentracije glutationov, metalotioninov ali močnejša dejavnost ustreznih encimov), (c) spremembe v jedrnih encimih (pospešeno popravljanje DNK in/ali višja toleranca poškodb DNK, šibkejša dejavnost topoizomeraz), (d) spremenjena ekspresija onkogenov (ki zvišujejo nivo protektivnih molekul v celici ali zavirajo apoptozo). Odpornost proti zdravilom je večplasten pojav. Kompleksnost molekularnih sprememb v celicah, odpornih proti citostatikom, je velik problem pri zdravljenju raka, ki ga bo tudi v prihodnje težko obvladati.

## Genetski polimorfizem encimov, ki presnavljajo ksenobiotike pri kolorektalnem raku

Dolžan V, Ravnik-Glavač M, Breskvar K

Na nastanek kolorektalnega raka lahko vplivajo dednost in dejavniki iz okolja. Kancerogene snovi, zlasti policiklični aromatski ogljikovodiki iz hrane in tobačnega dima po aktivaciji s citokromi P450 povzročajo tvorbo adduktov na DNA. Detoksifikacijo aktiviranih kancerogenov katalizirajo med drugim tudi glutationske S-transferaze. Želeli smo ugotoviti, ali so genetsko pogojene razlike v metabolizmu ksenobiotikov povezane z večjo dovzetnostjo za nastanek kolorektalnega raka. S postopkom genotipizacije smo določili pogostnost polimorfnih alelov dveh citokromov P450 (CYP2D6 in CYP1A1) in dveh glutationskih S-transferaz (GST M1 in GST T1), vključenih v metabolizem ksenobiotikov. Analizo smo izvedli na vzorcih DNA 31 bolnikov s sporadičnim, 25 bolnikov z družinskim kolorektalnim rakom in 73 zdravih oseb. Pri bolnikih s sporadičnim kolorektalnim rakom je pogostnost oseb, ki zaradi polimorfizma gena CYP2D6 slabo presnavljajo ksenobiotike, manjša kot pri zdravih kontrolah. Ta razlika je kljub majhnemu številu vzorcev blizu meje statistične signifikance ( $\chi^2=5,52$ ,  $m=2$ ,  $p = 0,06$ ). Med obema skupinama bolnikov s kolorektalnim rakom in zdravimi kontrolami pa ni signifikantnih razlik v pogostnosti posameznih genotipov CYP1A1 MspI, GST M1 ali GST T1. Naši rezultati nakazujejo, da je dovzetnost za nastanek kolorektalnega raka, pogojena s presnovo ksenobiotikov, pri sporadični obliki večja kot pri družinski obliki tega raka. Da bi ugotovili, kakšen je skupni vpliv polimorfnih genov, vključenih v presnovo ksenobiotikov na dovzetnost za nastanek kolorektalnega raka, pa so potrebne študije na večji skupini bolnikov z opredeljeno izpostavljenostjo kancerogenom v hrani in tobačnem dimu.

## **Nastajanje citotoksičnih limfocitov T *in vitro* v primerjavi z mutiranimi peptidi ras**

**Juretić A, Šamija M, Krajina Z, Eljuga D, Turić M, Heberer M, Spagnoli GC**

Mutacije proto-onkogenov ras se pogosto odražajo v genskih spremembah rakavih obolenj pri človeku. Te genske spremembe nastajajo kot točkaste mutacije, saj dopuščajo eno samo zamenjavo aminokisline na pozicijah 12, 13 ali 61 (aktivirani proteini p21 ras). Zato so peptidi, ki nastanejo po mutaciji ras, zelo privlačna tarča za aktivne imunoterapevtske postopke. Z računalniškim programom in z izborom ustreznega zaporedja HLA-A2.1 smo odkrili in nadalje sintetizirali nonapeptide ras, ki jih določajo mutacije na pozicijah 12 in 61, z domnevno vezivno sposobnostjo za HLA-A2.1. Odzivnost citotoksičnih limfocitov T (CTL) smo preizkušali enkrat tedensko s ponavljanjem stimulacij limfocitov iz periferne krvi zdravih osebkov ob prisotnosti limfoblastoidnih celic (EBV celične linije), transformiranih z obsevanim avtolognim virusom Epstein-Barr ter IL-2 in IL-4. V več časovnih presledkih smo testirali ubijalsko moč kultiviranih celic in pri tem uporabili celice HLA-A2.1 + EBV kot ciljne celice, ki smo jih pred tem pripravili v različnih kombinacijah proučevanih peptidov. Po osmih ponovljenih stimulacijah je bilo v enem darovalcu mogoče zaslediti obnavljajočo citotoksično aktivnost proti ciljnim celicam EBV, pripravljenim z dvema nonameroma na poziciji 61 Gln'Leu ras. Na osnovi rezultatov raziskave lahko zaključimo, da je iz PBMC zdravih osebkov mogoče z rednimi, enkrat na teden ponovljenimi stimulacijami *in vitro* inducirati citotoksične limfocitne celice CTL, ki so značilne za peptide, nastale z gensko točkasto mutacijo 61 Gln'Leu ras.

## **Razlika v ekspresiji proteina Bcl-2 v mieloidno levkemičnih celicah pri obsevanih miših z ultravijoličnimi žarki in pri neobsevanih miših**

**Popović Hadžija M, Poljak Blaži M**

V članku smo proučevali izraženost proteina onkogen Bcl-2 v mieloidno levkemičnih celicah in ugotavljali učinek ultravijoličnih žarkov nanjo. Protein onkogen Bcl-2 smo določali z imunocitotoksično metodo. V vranici miši RFM je 34,3% celic bilo Bcl-2 pozitivnih. Pri levkemiji v predterminalni fazi smo pri več kot 50% celic zasledili izraženost proteina onkogen Bcl-2, v terminalni fazi pa je bilo le 24,4% Bcl-2 pozitivnih celic. Po obsevanju z ultravijoličnimi žarki je izraženost proteina onkogen Bcl-2 v celicah vranice zdravih donorjev močno narasla, medtem ko ultravijolična svetloba v obeh raziskovanih fazah mieloidne levkemije ni bistveno učinkovala na ekspresijo Bcl-2. Sklepamo, da protein onkogen Bcl-2 vpliva na odpornost mieloidnih levkemičnih celic na ultravijolično svetlobo.

## **Neposredni vnos kemoterapevtov v celice kot način zdravljenja hepatomov in sarkomov na podganah**

**Pendas S, Jaroszeski MJ, Gilbert R, Hyacinthe M, Dang V, Hickey J, Pottinger C, Illingworth P in Heller R**

Kombinirano zdravljenje kemoterapevtikov z električnimi pulzi imenujemo elektrokemoterapija (ECT). S to metodo z električnimi pulzi povzročimo elektropermeabilizacijo celične membrane, to pa povzroči povečen vnos kemoterapevtikov v celico. Ta postopek je bil posebno uspešen pri nekaterih kemoterapevtikih, kot sta bleomicin in cisplatin. Objektivni odgovor je bil dosežen v več kot 80% tako v študijah na poskusnih živalih, kot tudi na bolnikih pri različnih vrstah raka, obakrat pri elektrokemoterapiji z bleomicinom. Namen te študije je ugotoviti ali je elektrokemoterapija z bleomicinom uspešna pri zdravljenju hepatomov in sarkomov, ki rastejo v notranjih organih. Uporabili smo kemoterapevtike bleomicin, cisplatin, doxorubicin, 5-fluorouracil in taksol v kombinaciji z električnimi pulzi. Kemoterapevtike smo injicirali intratumoralno, prav tako električne pulze. Pri zdravljenju hepatomov sta bila najučinkovitejša cisplatin in bleomicin, s 70% popolnim odgovorom na zdravljenje. Ostali kemoterapevtiki so bili neučinkoviti. Pri zdravljenju sarkomov je bil najučinkovitejši bleomicin s 100% odgovorom na zdravljenje. Cisplatin in doxorubicin sta bila manj učinkovita. Na osnovi rezultatov študije lahko zaključimo, da je elektrokemoterapija učinkovita pri zdravljenju tumorjev v visceralnih organih in pri zdravljenju sarkomov.

## **Sledenje MAC (malignancy-associated changes) pri bolnicah s progresivnimi displazijami materničnega vratu**

**Fležar M, Lavrenčak J, Žganec M, Us-Krašovec M**

Osmim od 29 bolnic s progresivnimi displazijami smo sledili 2 do 10 let. Preparate z njihovimi zaporednimi brisi smo razbarvali in ponovno obarvali po Feulgnu s tioninom. Slikovno analizo smo izvedli na citometru Cyto-Savant™ (Oncometrics Technol. Corp., Vancouver, Kanada). Izračunali smo povprečne vrednosti jedrnih značilnosti in njihove verjetnostne porazdelitve za zaporedno odvzete brise pri vsaki bolnici. Tri od 5 MAC, ki so ločile progresivne od regresivnih displazij (highDNAamount, high DNA comp, highDNAarea) v prejšnji raziskavi, so naraščale s časom pri petih od osmih bolnic. Raziskava, za katero smo uporabili arhivske vzorce, ki niso bili enotno pripravljene, je pokazala porast diskretnih jedrnih značilnosti s časom pri bolnicah s progresivnimi displazijami materničnega vratu.

## **Analiza celičnih jeder bukalne sluznice s slikovnim citometrom: vpliv kajenja in spola**

**Lavrenčak J, Flešar M, Žganec M, Us-Krašovec M**

V naši raziskavi smo na celičnih jedrih bukalne sluznice opravili kvantitativno analizo s slikovnim citometrom, da bi ugotovili, kako vplivata kajenje in spol na kromatinsko organizacijo. Analizirali smo brise bukalne sluznice 78 zdravih ljudi. Za analizo s slikovnim citometrom smo celične preparate obarvali po metodi Feulgen-tionin. Izračunali smo verjetnostne porazdelitve za 78 jedrnih značilk ter opravili preizkus razvrščanja celic in razvrščanja preparatov za skupini kadilci/nekadilci in skupini moški/ženske. Rezultati raziskave so pokazali, da se celična jedra kadilcev in nekadilcev razlikujejo v sedmih jedrnih značilkah, večina med njimi sodi med strukturne. Pri primerjavi moških in žensk pa smo ugotovili, da se jedra razlikujejo samo v dveh jedrnih značilkah. Ugotavljamo, da je pri analizi s slikovnim citometrom, v okviru raziskovanja sprememb v ustni votlini potrebno upoštevati vpliv kajenja.

## **Število mitoz v karcinomih mlečne žleze enostavnega in kompleksnega tipa pri psicah**

**Juntos P**

Po klasifikaciji WHO delimo tumorje mlečne žleze pri psicah v enostavni in kompleksni tip. Splošno mnenje je, da imajo karcinomi kompleksnega tipa boljšo prognozo kot karcinomi enostavnega tipa. Cilj naše raziskave je bil kvantitativno oceniti in primerjati mitotično aktivnost pri obeh vrstah karcinomov. Ocenili smo število mitoz v 65 vzorcih karcinomov enostavnega tipa in 99 vzorcih karcinomov kompleksnega tipa. Za oceno smo primerjalno uporabili dve metodi štetja: indeks mitotične aktivnosti (MAI) in število mitoz na kvadratni milimeter ( $M/mm^2$ ). Z obema metodama smo ugotovili značilne razlike v številu mitoz ( $P=0.0001$  za MAI; in  $P=0.0089$  za  $M/mm^2$ ) med karcinomi enostavnega in kompleksnega tipa. Število mitoz v posameznih karcinomih enostavnega tipa je variiralo od 0 do 95 na deset vidnih polj velike povečave in od 0 do 57 pri karcinomih kompleksnega tipa. Povprečno število mitoz je bilo višje v primerih, ko je bil tumor en sam, in nižje kadar je bilo tumorjev pri isti živali več. Naši rezultati potrjujejo manjši mitotični potencial epitelijskih celic karcinomov mlečne žleze kompleksnega tipa v primerjavi s karcinomi enostavnega tipa. To dejstvo gotovo prispeva k boljši prognozi bolezni, še posebno v tistih primerih, kjer je mioepitelijska komponenta prevladujoči del tumorja.

## Vpliv UV-B sevanja na sejanke smreke (*Picea abies* (L.)Karst.)

Bavcon J, Gogala N, Gabersčik A

Na osnovi hipoteze, da je povečano ultravijolično sevanje eden izmed primarnih dejavnikov poškodb v višjih legah, smo dve leti in pol spremljali vpliv UV-B sevanja na sejanke smreke (*Picea abies* (L.)Karst.). V lončnem poizkusu smo v odprtih plastenjakih ugotavljali vpliv UV-B sevanja na fotokemično učinkovitost fotosistema II, spremembo vsebnosti klorofila a, b in antocianov. V plastenjaku z umetnim virom sevanja je bila dnevno izmerjena doza  $21.24 \pm 3,5$  kJ/m<sup>2</sup>, v drugem z nekoliko močnejšim sevanjem pa  $31.9 \pm 2,5$  kJ/m<sup>2</sup>. Za vir sevanja smo uporabili Osram ultravitaluks glivaste žarnice. Kontrolni sejanci so bili v plastenjaku ob normalnih pogojih in ob naravnem viru sevanja  $11,5 \pm 5,2$  kJ/m<sup>2</sup>. Meritve kinetike fluorescence klorofila so pokazale spremembe le v času nizkih zimskih temperatur, medtem ko v ostalem delu leta ni bilo opaziti sprememb v primerjavi s kontrolo. Pri obsevanih rastlinah je prišlo pod vplivom UV-B sevanja po enem letu do spremembe klorofila a in b in do spremembe njunega razmerja. Poleg tega smo zaznali tudi povečanje količine antocianov pri obsevanih rastlinah.

## Ugotavljanje sproščanja zdravil in erozije polimerov s tehnikami EPR in MRI iz biološko razgradljivih prenašalcev zdravil

Mäder K

Delovanje zdravil proti raku in vivo je pogosto močno omejeno zaradi njihove slabe biološke obstojnosti, zelo resnih stranskih učinkov in kratke razpolovne dobe. Takšne težave je mogoče obvladati s prenašalci zdravil, ki so jih znanstveniki razvili v zadnjih nekaj letih. Čeprav te sisteme že uporabljajo v klinične namene, še vedno ne poznamo vseh podrobnosti o mehanizmih sproščanja in eroziji polimerov, še zlasti ne v okolju in vivo. Članek opisuje, da si z magnetno-rezonančnimi tehnikami ESR in MRI lahko pomagamo razložiti podrobnosti delovanja biološko razgradljivih sistemov prenašalcev zdravil in vivo.

## **Antioksidativni efekt melatonina in njegov vpliv na mielotoksičnost in protitumorsko delovanje adriamicina**

**Rapozzi V, Perissin L, Zorzet S, Comelli M, Mavelli I, Šentjerc M, Pregelj A, Schara M, Giraldi T**

Do sedaj objavljena poročila med številnimi lastnostmi melatonina navajajo tudi njegovo antioksidantno delovanje. Nekateri protitumorski kemoterapevtiki, kot npr. antraciklini, kažejo prooksidantno aktivnost, zaradi katere so toksični za normalna tkiva gostitelja. Namen tega dela je bil preliminarно proučiti učinek melatonina na mielotoksičnost, ki jo povzroča terapija z adriamicinom pri CBA miših – nosilcih TLX5 limfoma. Po enkratni terapiji z adriamicinom (20–40 mg/kg i.v.) je aplikacija ene same farmakološke doze melatonina (10 mg/kg s.c.) zmanjšala delež akutne smrtnosti gostitelja od 9/16 na 2/16. Antitumorski učinek adriamicina, ki se kaže v podaljšanju preživetja živali, ki jih ni prizadela akutna toksičnost kemoterapevtika, se zaradi melatonina ni zmanjšal. Melatonin je hkrati tudi zmanjšal po adriamicinu povzročeno redukcijo števila GM-CFU v kostnem mozgu, predhodno znižane in celokupne vrednosti glutaciona pa so se značilno povrnila v izhodiščne meje. Poleg tega je bilo s fentonsko reakcijo in določanjem prostih radikalov s pomočjo spin trapping metode dokazano, da melatonin deluje kot neposreden reagent v kombinaciji s prostimi radikali. Navedeni podatki kažejo, da melatonin zmanjšuje mielotoksičnost adriamicina na način, ki je v skladu z njegovimi antioksidantnimi lastnostmi.

## **Difuzijsko poudarjeno slikanje z magnetno resonanco pri ugotavljanju odzivnosti tumorja na zdravljenje**

**Dodd NJF, Zhao S, Moore JV**

Zgodnje ugotavljanje terapevtskih učinkov je izredno pomembno za nadaljnje zdravljenje bolnikov, saj se odzivnaje tumorja na določen način zdravljenja od bolnika do bolnika precej razlikuje. Za proučevanje učinkov novejših načinov zdravljenja, kot sta fotodinamična terapija in elektroterapija, ki ste se pridružili že močno uveljavljeni radioterapiji, smo uporabili predklinični model tumorja. V vseh primerih se je izkazalo, da z difuzijsko poudarjenim slikanjem z magnetno resonanco lahko zaznamo odziv na zdravljenje že v dveh dneh po pričetku terapije. Pri fotodinamični terapiji se je že po prvem dnevu zdravljenja učinkovit difuzijski koeficient (ADC apparent diffusion coefficient) močno povečal v tistih predelih tumorja, kjer se je pojavila nekroza, medtem ko v neprizadetih predelih tumorja takšnega povečanja nismo opazili. Podobno povečanje učinkovitega difuzijskega koeficienta smo opazili tudi po elektroterapiji, neodvisno od vrste (anodna ali katodna); povečanje smo v primarno poškodovanih predelih tumorja opazili že po nekaj minutah zdravljenja, v predelih s sekundarno ishemično nekrozo pa smo povečanje opazili po enem dnevu zdravljenja. Pri radioterapiji so bile spremembe manjše kot pri drugih načinih zdravljenja, toda pri dozah, ki imajo močan citotoksičen učinek, smo po dveh dnevih zdravljenja opazili statistično pomembno povečanje učinkovitega difuzijskega koeficienta.

## Spremembe v pretočnosti plazemske membrane rakavih tkiv

Šentjurs M, Sok M, Serša G

Plazemska membrana je heterogena struktura, sestavljena je iz več polj z različno stopnjo fluidnosti. Ima pomembno vlogo v nadzoru celične rasti, diferenciacije in transformacije. Fluidnost celotne plazemske membrane se odraža v ureditvi in dinamičnosti fosfolipidnih acilnih verig v specifičnih poljih membrane kot tudi v frakcijah posameznih polj v membrani. Spremembe v fluidnosti membrane vplivajo na procese v njej, kot so transport, dejavnost encimov in izražnost.

V članku predstavljamo rezultate najnovejših raziskav lastnosti fluidnosti plazemske membrane z elektronsko paramagnetno resonanco (EPR), kjer upoštevamo heterogenost plazemske membrane. Z računalniško simulacijo EPR meritev lahko določimo število polj v plazemski membrani, njihov relativni delež v membrani in ureditev ter dinamičnost vsakega polja. Tako je bilo mogoče ugotoviti, kolikšna je razlika med doprinosom relativnega deleža vsakega polja in doprinosom sprememb fluidnosti polja k spremembam fluidnosti celotne plazemske membrane.

V članku obravnavamo dva primera: fluidnost plazemske membrane tumorskega tkiva, izreznega iz pljuč, in vpliv vinblastina na fluidnost plazemske membrane celic HeLa, tako tistih, ki so občutljive na vinblastin, kot tistih, ki so nanj odporne.

## O mehanizmih vesikulizacije plazemske membrane celice

Kralj-Iglič V, Batista U, Hägerstrand H, Iglič A, Majhenc J, Sok M

V študiji obravnavamo vesikulacijo celične membrane. Predpostavljali smo, da oblika segmenta membrane, ki je prost citoskeleta, prehaja proti obliki z največjo možno razliko površin zunanje in notranje plasti membrane zaradi preporazdelitve lateralno gibljivih membranskih sestavin. Pokazali smo, da so oblike, ki ustrezajo maksimumu razlike površin krogelne, ravne in valjaste, odvisno od vezi. Temu ustrezajo okrogli mehurčki in valjasti izrastki, ki smo jih prikazali na MCF celicah (adenokarcinom dojke). Predlagali smo mehanizem vesikulacije, ki vesbuje tudi razlago za različno relativno vsebnost nekaterih snovi v membrani mehurčkov kot v membrani matične celice.



## **Terciarni kolimatorski sistem za stereotaktično radiokirurgijo z linearnim pospeševalnikom**

**Casar B**

V zadnjem desetletju je stereotaktična radiokirurgija postala pomembna radioterapevtska tehnika za različne vrste malignih in benignih možganskih obolenj. Čeprav poznamo še druge radiokirurške tehnike, je radiokirurgija z linearnim pospeševalnikom med najbolj primernimi, saj modifikacija lineranega pospeševalnika ne zahteva visokih stroškov, kljub temu pa zagotavlja visoko natančnost. Med najbolj pomembnimi deli dodatne opreme je terciarni kolimatorski sistem, ki ga lahko pritrdimo na glavo lineranega pospeševalnika. Sistem smo zasnovali in sestavili tako, da ga lahko enostavno pritrdimo na glavo linearnega pospeševalnika PHILIPS SL – 75/5 s fotonsko energijo 5 MV. Ta pospeševalnik že uporabljamo na našem oddelku za konvencionalno radioterapijo. Naš terciarni kolimatorski sistem izpolnjuje vse zahteve te posebne radioterapevtske tehnike. Sistem omogoča natančno centriranje 10 kolimatorjev z divergentnimi krožnimi odprtini z nominalnim premerom polja v izocentru od 1,0 cm do 4,0 cm. Natančnost sistema smo preverili z rentgenskimi filmi pri različnih nastavitvah kota linearnega pospeševalnika in zabeležili ujemanje ali neujemanje pri posameznih žarkih. Posamezna fotonska polja smo izmerili s pomočjo polprevodniških diod in z uporabo filmske dozimetrije.

## Notices

*Notices submitted for publication should contain a mailing address, phone and/or fax number and/or e-mail of a contact person or department.*

### Lung cancer and head and neck cancer

*April, 1998.*

The ESO training course on Lung cancer including head and neck cancer will be offered in Hofburg Conference Center, Vienna, Austria.

Contact European School of Oncology, Office for Central and Eastern Europe, c/o Ärztekammer fuer Wien, Mrs. Dagmar Just, Fortbildungsreferat, Weihburggasse 10-12, 1010 Vienna, Austria; or call +43 1 51 501 293; or fax +43 1 51 501 480.

---

### Radiotherapy

*April, 1998.*

The ESTRO teaching course "Modern Brachytherapy Techniques" will take place in Berlin Germany.

Contact the ESTRO office, Av. E. Mounierlaan, 83/4, B-1200 Brussels, Belgium; or call +32 2 775 9340; or fax +32 16 7795 5494.

---

### Breast cancer

*April, 1997.*

The ESO multidisciplinary educational course on breast cancer will take place in Beirut, Lebanon.

Contact ESO Balkans and Middle East Office, Egnatia Epirus Foundation, 7A Tzavella St., 453 33 Ioannina, Greece; or call +30 651 72315/76992; or fax +30 651 36695.

---

### Oncology

*April, 1998.*

The teaching course "Methodology of Clinical Research" will be organized by ESTRO.

Contact the ESTRO office, Av. E. Mounierlaan, 83/4, B-1200 Brussels, Belgium; or call +32 2 775 9340; or fax +32 16 7795 5494.

*As a service to our readers, notices of meetings or courses will be inserted free of charge.*

*Please sent information to the Editorial office, Radiology and Oncology, Vrazov trg 4, 1105 Ljubljana, Slovenia.*

### Bone tumours

*April or September, 1998.*

The ESO training course on Surgical treatment of malignant bone tumours will take place in Hofburg Conference Center, Vienna, Austria.

Contact European School of Oncology, Office for Central and Eastern Europe, c/o Ärztekammer fuer Wien, Mrs. Dagmar Just, Fortbildungsreferat, Weihburggasse 10-12, 1010 Vienna, Austria; or call +43 1 51 501 293; or fax +43 1 51 501 480.

---

### Molecular Biology

*April 5-8, 1998.*

The ESO advanced course "Molecular Biology for Clinicians" will be offered in Cambridge, United Kingdom.

Contact European School of Oncology, Via Ripamonti 66, 20141 Milan, Italy; or call +39 2 57 305 416; or fax +39 2 57 307 143.

---

### Chemotherapy

*April 18-19, 1998.*

The "4th International symposium on high-dose in Chemotherapy and stem cell transplantation in solid tumors will take place in Berlin, Germany.

Contact Prof. Dr. Wolfgang Siegert, Virchow Klinikum, Abt. Haematologie und Onkologie, Augustenburger Platz 1, 13353 Berlin, Germany.

---

### Radiology

*April 23-25, 1998.*

The 2<sup>nd</sup> Congress of the Croatian Society of Radiology will take place in Osijek, Croatia.

Contact Croatian Congress of Radiology, Osijek Clinical Hospital, Radiology Department, Huttlerova 4, 31000 Osijek, Croatia; or call +385 31 511 511, ext 1541, + 385 31 511 541; or fax +385 31 512 222. E-mail: kbos-rentgen/kb-osijek.tel.hr. <http://www.kbosijek.tel.hr>

### Brachytherapy

*May 10, 1998.*

The endovascular brachytherapy workshop will take place in Napoly, Italy.

Contact Petra van de Bovenkamp, Nucletron M.V., P.O. Box 930, 3900 AX Veenedall, The Netherlands; or call +31 318 557 230, or fax +318 557 190.

---

### Brachytherapy

*May 11-13, 1998.*

The annual brachytherapy meeting GEC-ESTRO will take place in Naples, Italy.

Contact ESTRO Office, Av. E. Mounierlaan, 83/4, B-1200 Brussels, Belgium; or call +32 2 775 9340; or fax +32 2 779 5494. E-mail: martine.dansercoer@estro.be

---

### Radiotherapy

*May 13-17, 1998.*

The "5th International meeting on Progress in Radio-Oncology ICRO/OGRO 6" will take place in Salzburg, Austria.

Contact Prof. Kogelnik, Institute of Radiotherapy, Muellner Hauptstr. 48, A-5020 Salzburg, Austria.

---

### Surgical oncology

*May 14-16, 1998.*

The ESO advanced course "Breast Reconstructive and Cancer Surgery I" will be held in Duesseldorf, Germany.

Contact European School of Oncology, Via Ripamonti 66, 20141 Milan, Italy; or call +39 2 57 305 416; or fax +39 2 57 307 143.

---

### Lung cancer

*May 14-20, 1997.*

The ESO training course "Lung Pathology -Oncology" will be offered in Ioannina, Greece.

Contact ESO Balkans and Middle East Office, Egnatia Epirus Foundation, 7A Tzavella St., 453 33 Ioannina, Greece; or call +30 651 72315/76992; or fax +30 651 36695.

---

### Oncology

*May 16-19, 1998.*

The "ASCO Spring Meeting" will be offered in Los Angeles, CA, USA.

Contact ASCO Headquarters, 435 North Michigan

Av., Suite 1717, Chicago, USA; or call +1 312 644 0828; or fax +1 312 644 8557.

---

### Bladder cancer

*May 22, 1998.*

The ESO refresher day on bladder cancer will take place in University of Vienna, Vienna, Austria.

Contact European School of Oncology, Office for Central and Eastern Europe, c/o Arztekammer fuer Wien, Mrs. Dagmar Just, Fortbildungsreferat, Weihburggasse 10-12, 1010 Vienna, Austria; or call +43 1 51 501 293; or fax +43 1 51 501 480.

---

### Oncology

*May 28-30, 1998.*

The 3rd ESO education convention will take place in Turin, Italy.

Contact European School of Oncology, Viale Beatrice d'Este 37, 20122 Milan, Italy; or call +39 2 5831 7850; or fax +39 2 5832 1266. E-mail: comprevtum/bbs.infosquare.it

---

### Clinical trials

*June, 1998.*

The EORTC course "Clinical Trials Statistics for non Statisticians" will be offered in Brussels, Belgium.

Contact EORTC Education office, Av. E. Mounier 83/11, 1200 Brussels, Belgium; or call +32 2 772 4621; or fax +32 2 772 6233. Internet: <http://www.eortc.be>

---

### Oncology

*June, 1997.*

The ESO training course "From the Molecular to the Bedside Oncology" will be offered in Thessaloniki, Greece.

Contact ESO Balkans and Middle East Office, Egnatia Epirus Foundation, 7A Tzavella St., 453 33 Ioannina, Greece; or call +30 651 72315/76992; or fax +30 651 36695.

---

### Radiotherapy

*June, 1998.*

The ESTRO teaching course "Molecular Oncology for Radiotherapy" will take place in Dublin, Ireland.

Contact the ESTRO office, Av. E. Mounierlaan, 83/4, B-1200 Brussels, Belgium; or call +32 2 775 9344; or fax +32 2 779 5470. E-mail: [germaine.heeren@estro.be](mailto:germaine.heeren@estro.be)

### Hepatology

*June 20-24, 1998.*

The 6<sup>th</sup> international postgraduate course in hepatology and hepatobiliary surgery will be held in Ljubljana, Slovenia.

Contact Valentin Sojar, M.D., Dept. of Abdominal Surgery, University Medical Center Ljubljana, Zaloška 7, 1000 Ljubljana, Slovenia; or call +386 61 322 282, +386 61 132 62 31; or fax +386 61 316 096. E-mail: stevanec/mf.uni-lj.si

### Thoracic Surgery

*October 22-24, 1998.*

The "6<sup>th</sup> European Conference on General Thoracic Surgery" will be held in Portorož, Slovenia.

Contact Organizing Secretariat, Department of

Thoracic Surgery. University Medical Center Ljubljana, Zaloška 7, 1525 Ljubljana, Slovenia; or call +386 61 317 582; or fax +386 61 13 16 006. E-mail: joze.jerman/mf.uni-lj.si

### Radiation protection

*November 11-13, 1998.*

The "4<sup>th</sup> Symposium of the Croatian Radiation Protection Association will be offered in Zagreb, Croatia.

Contact "Ruđer Bošković" Institute, Bijenička c. 54, Zagreb, Croatia; or call +385 1 4561 053; or fax +385 1 4680 098. You can contact also Chairman of the Organizing Committee, Vladimir Lokner Ph.D., APO-Hazardous Waste Management Agency, Savska 41/IV, 10000 Zagreb, Croatia; or call +385 1 6176 736, or fax +385 1 6176 734. Internet: <http://mimi.imi.hr/crpa>

THE **2<sup>nd</sup>** CONGRESS OF THE CROATIAN  
SOCIETY OF RADIOLOGY  

---

OSIJEK, CROATIA  
APRIL 23-25, 1998.

CONTACT:

Croatian Congress of Radiology  
Osijek Clinical Hospital  
Radiology Department  
Huttlerova 4

31000 Osijek, Croatia;

Phone: +385 31 511 511, ext 1541, + 385 31 511 541; Fax: +385 31 512 222

E-mail: kbos-rentgen@kb-osijek.tel.hr.; <http://www.kbosijek.tel.hr>

THE **6<sup>th</sup>** EUROPEAN CONFERENCE  
ON GENERAL THORACIC SURGERY  

---

PORTOROŽ, SLOVENIA  
OCTOBER 22-24, 1998.

CONTACT:

Organizing Secretariat of  
The "6<sup>th</sup> European Conference on Thoracic Surgery"  
Department of Thoracic Surgery  
University Medical Center Ljubljana  
Zaloška 7

1525 Ljubljana, Slovenia

Phone: +386 61 317 582, Fax: +386 61 13 16 006

E-mail: joze.jerman@mf.uni-lj.si

# HEPATOBIILIARY SCHOOL



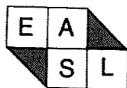
## 6<sup>th</sup> POSTGRADUATE COURSE IN HEPATOLOGY

---

## POSTGRADUATE COURSE IN HPB SURGERY

University of Ljubljana, Faculty of Medicine  
University Medical Center, Ljubljana  
Institute of Oncology, Ljubljana  
HPBA, Slovenija  
Open Society Institute, Slovenia

UNDRE THE AUSPICES OF:  
European Association for the Study of Liver  
International Hepato Pancreato Biliary Association  
Ministry of Science and Technology, Slovenia  
Ministry of Health, Slovenia

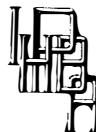


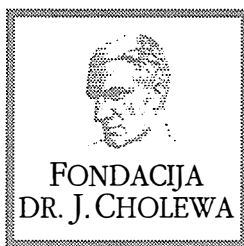
MAILING ADDRESS:  
Valentin Sojar, MD  
University Medical Center Ljubljana  
Dep. of Abdominal Surgery  
Zaloška 7

1000 Ljubljana, Slovenia

Phone: +386 61 322 282, 132 62 31, Fax: +386 61 316 096

E-mail: [stevanec@mf.uni-lj.si](mailto:stevanec@mf.uni-lj.si)

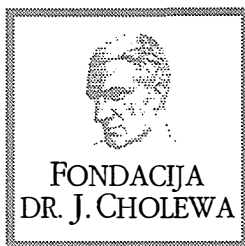




FONDACIJA "DOCENT DR. J. CHOLEWA"  
JE NEPROFITNO, NEINSTITUCIONALNO IN NESTRANKARSKO  
ZDRUŽENJE POSAMEZNIKOV, USTANOV IN ORGANIZACIJ, KI ŽELIJO  
MATERIALNO SPODBUJATI IN POGLABLJATI RAZISKOVALNO  
DEJAVNOST V ONKOLOGIJI.

MESESNELOVA 9  
61000 LJUBLJANA  
TEL 061 15 91 277  
FAKS 061 21 81 13

ŽR: 50100-620-133-05-1033115-214779



## **Activity of "Dr. J. Cholewa" foundation for cancer research and education – report for the first quarter of 1998**

In the year 1997 the "Dr. J. Cholewa" foundation for cancer research and education continued to provide research and educational grants to a number of applicants interested in the problems of oncology in Republic of Slovenia that fulfilled its outlined criteria. Collaboration with the European School of Oncology from Milan in general proceeded as planned, and several steps were taken to ensure better coordination with other similar institutions in Slovenia, notably with Slovenska Znanstvena Fundacija (Slovenian Scientific Foundation) and "Mali Vitez" Foundation.

The Foundation continues to support regular publication of "Radiology and Oncology" international scientific journal, and the regular publication of the "ESO Challenge", the newsletter of the European school of Oncology, both being published and edited in Ljubljana, Slovenia. As was reported at the Assembly of the Foundation meetings in November 1997 and January 1998, it supported the participation of 27 physicians from this country at various national and international oncological scientific meetings in Slovenia and abroad. Research grants were awarded to two of the applicants. It also supported the organisation of two continuous education "Oncological weekend" meetings, that were intended to all in the medical profession interested in problems connected with oncology, the organisation of Surgical Oncology Workshop dealing with problems in the cancer of colon and rectum, the already established and traditional Hepatobiliary School in Ljubljana, European Congress of Cytology and the Scientific Symposium on Epithelial hyperplastic lesions of the Larynx, and Plečnik memorial meeting, all held in Ljubljana, and the Life Sciences meeting in Gozd Martuljek.

For the 1998 it is thus planned to continue to provide grants for the various European School of Oncology courses, research and educational grants for the study in Slovenia and abroad, to provide support for educational and scientific meetings and symposia, and to support publishing and editorial activity from the various fields of oncology in Slovenia.

On January 29th, 1998, a "Dr. J. Cholewa" Honorary Award was presented to Mr. Slavko Fatur for his continuing dedication, hard work and outstanding achievements that have been attained during the course of his presidency of the Foundation.

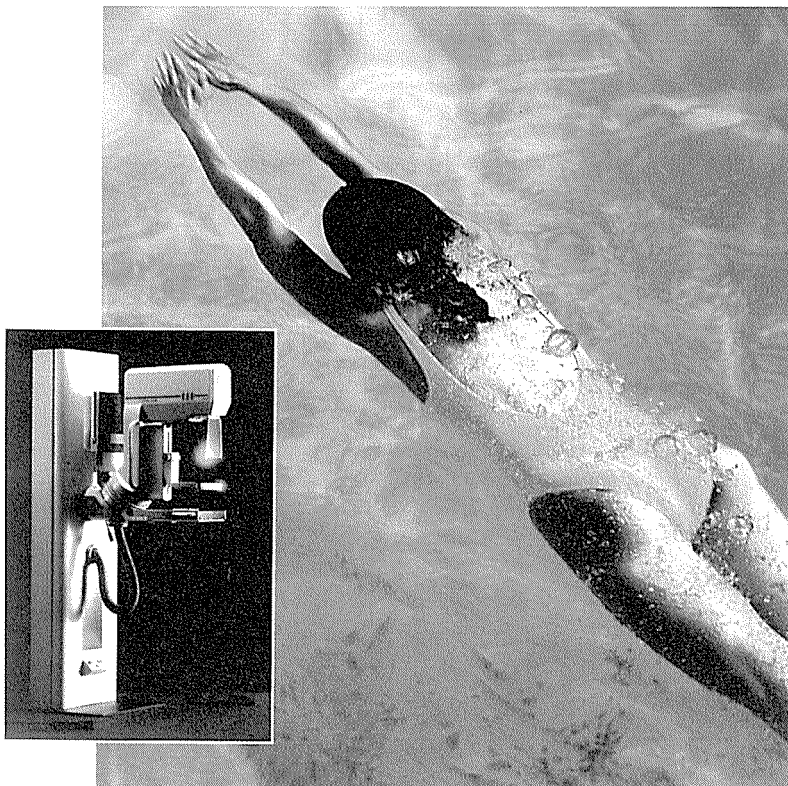
Dr. Jurij Lindtner, professor of surgical oncology, and Dr. Eldar M. Gadžijev, professor of abdominal surgery, were unanimously elected as new members of the Board of directors of the "Dr. J. Cholewa" Foundation for cancer research and education at the Assembly meetings of the Foundation that were held in Ljubljana in October 1997 and January 1998.

Andrej Plesničar, MD  
Tomaž Benulič, MD  
Borut Štabuc, MD, PhD



# SIEMENS

## Rešitve po meri



M a m m o m a t 3 0 0 0 m o d u l a r

## Mammomat 3000 modular

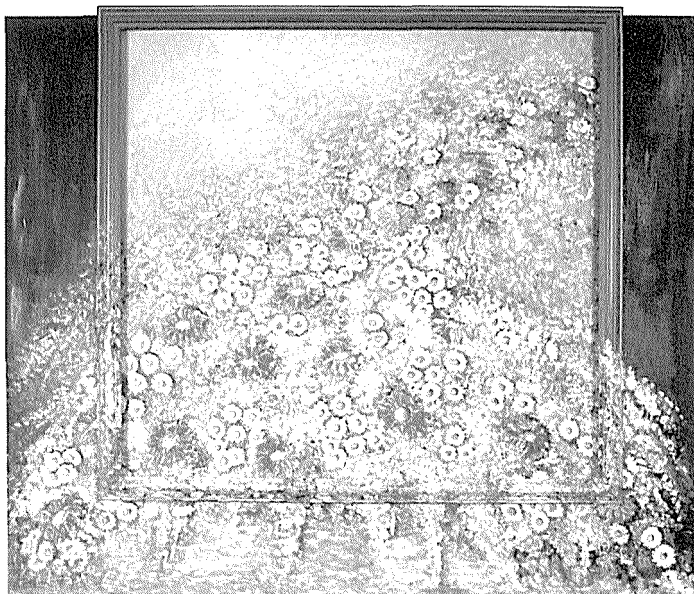
- univerzalni sistem za vse vrste mamografije
- optimizacija doze in kompresije z OPDOSE in OPCOMP sistema
- modularna zgradba zagotavlja posodabljanje sistema
- servis v Sloveniji z zagotovljenimi rezervnimi deli in garancijo
- izobraževanje za uporabnike

SIEMENS d.o.o.  
Dunajska 22  
1511 Ljubljana  
Telefon 061/1746 100  
Telefaks 061/1746 135

# TADOL<sup>®</sup>

*injekcije, kapsule, kapljice, svečke* *tramadol*

## Povrne mik življenja



- centralno delujoči analgetik za lajšanje zmernih in hudih bolečin
- učinkovit ob sorazmerno malo stranskih učinkih
- tramadol je registriran tudi pri ameriški zvezni upravi za hrano in zdravila (FDA)

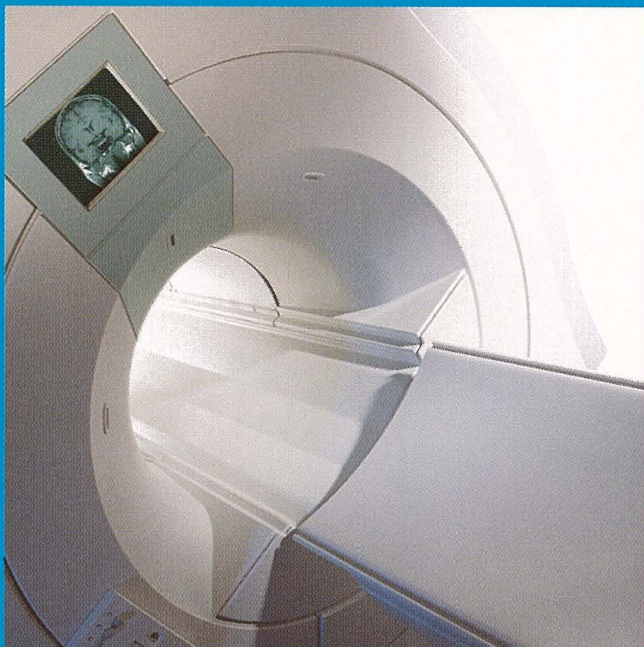
**Kontraindikacije:** Otroci do 1 leta starosti, akutna zastrupitev z alkoholom, uspavali, analgetiki in drugimi zdravili, ki vplivajo na CŽS, zdravljenje z inhibitorji MAO. **Interakcije:** Pri sočasni uporabi zdravil, ki delujejo na osrednje živčevje, je možno sinergistično delovanje v obliki sedacije pa tudi močnejšega analgetičnega delovanja. **Opozorila:** Pri predoziranju lahko pride do depresije dihanja. Previdnost je potrebna pri bolnikih, ki so preobčutljivi za opiate, in pri starejših osebah. Pri okvari jeter in ledvic je potrebno odmerek zmanjšati. Bolniki med zdravljenjem ne smejo upravljati strojev in motornih vozil. Med nosečnostjo in dojenjem predpišemo tramadol le pri nujni indikaciji. Bolnike s krči centralnega izvora skrbno nadzorujemo. **Doziranje:** Odrasli in otroci, starejši od 14 let: 50 do 100 mg 3- do 4-krat na dan. **Otrokom od 1 leta do 14 let** dajemo v odmerku 1 do 2 mg na kilogram telesne mase 3- do 4-krat na dan. **Stranski učinki:** Znojenje, vrtoglavica, slabost, bruhanje, suha usta in utrujenost.

Redko lahko pride do palpitacij, ortostatične hipotenzije ali kardiovaskularnega kolapsa. Izjemoma se lahko pojavijo konvulzije. **Oprema in način izdajanja:** 5 ampul po 1 ml (50 mg/ml), 5 ampul po 2 ml (100 mg/2 ml), uporaba je dovoljena samo v javnih zdravstvenih zavodih ter pravnim in fizičnim osebam, ki opravljajo zdravstveno dejavnost. 20 kapsul po 50 mg, 10 ml raztopine (100 mg/ml), 5 svečk po 100 mg, na zdravniški recept. 11/97. *Podrobnejše informacije so na voljo pri proizvajalcu.*

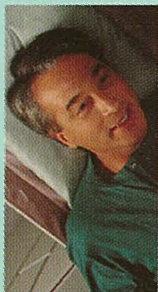


Krka, d. d., Novo mesto  
Šmarješka cesta 6  
8501 Novo mesto

Critics applaud our product design.



Patients just yawn.



It's nice to win design awards, but even more gratifying to know our equipment puts people at ease. Take MR systems. Most have long, narrow tunnels that make a 20 minute exam feel like 20 hours. Ours is short and wide – the most open in the industry. Patients can see out, so they don't get anxious or claustrophobic. Children can be held and comforted, rather than sedated. We're pleased when people get excited about our equipment. But even more pleased when they don't.

*Let's make things better.*



**PHILIPS**



# Safety in Diagnostic Imaging Worldwide

*Nycomed Imaging is proud  
of its role in providing  
for the early, accurate  
diagnosis of disease,  
thus improving patients'  
quality of life and  
prospects for effective  
treatment. The company is  
committed to the continuous  
development of innovative  
imaging products to enhance  
diagnostic procedures.*

**ZASTOPA**  
**HIGIEA d.o.o., Trzin**  
Blatnica 12, 1236 Trzin  
tel.: (061) 1621 101  
fax: (061) 1621 043



Nycomed Imaging AS,  
P.O.Box 4220 Torshov,  
N-0401 Oslo, Norway

## **DISTRIBUCIJA** **SALUS d.d.**

Mašera Spasiča ul. 10  
1000 Ljubljana  
tel.: (061) 1681 144  
fax: (061) 1681 420

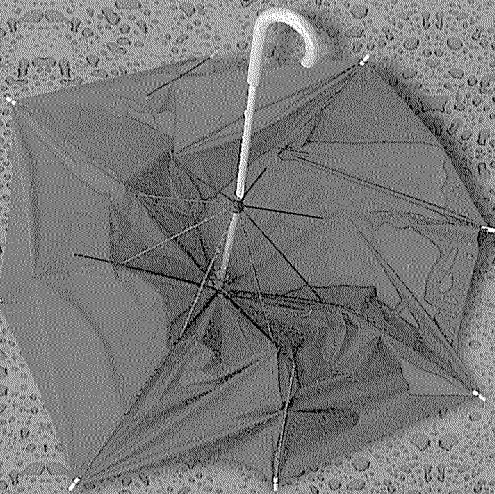


HOFFMANN-LA ROCHE  
Diagnostic Systems

Clinical Chemistry  
Hematology  
Immunology  
Polymerase Chain Reaction (PCR)

Official distributor:  
ADRIA MED d.o.o., Luize Pesjakove 8a  
1000 Ljubljana, Slovenia  
tel.: -- 386 61 1379200, tel./fax: -- 386 61 1376450

Ali dobivajo vaši bolniki z okužbami ustrezno zdravilo?



**Ciprobay®**

ciprofloksacin - originalna Bayerjeva kakovost

- fluorirani kinolon, ki je najuspešnejši v svoji skupini
- Ciprobay® ima med vsemi antibiotiki najpopolnejšo klinično dokumentacijo.
- Ciprobay® ima širok spekter delovanja proti številnim zanj občutljivim mikroorganizmom.

**Ciprobay:** ciprofloksacin: 10 tablet po 250 mg/500 mg in 5 infuzijskih steklenič (50 ml, 100 ml, 200 ml) po 100/200/400 mg. **Doziranje:** je odvisno od indikacije; posamezni odmerek Ciprobaya je 250-750 mg peroralno in 100-400 mg parenteralno. Za bolnike, ki tablet ne morejo zaužiti, predlagamo i.v. uporabo Ciprobaya. Pri očistku kreatinina < 20 ml/min priporočamo polovični odmerek. **Kontraindikacije:** preobčutljivost za ciprofloksacin ali druge kinolone, otroci in mladina v obdobju rasti, nosečnost in dojenje, dokler nimamo dovolj izkušenj o uporabi in dokler ne bo na podlagi ugotovitev pri poskusih na živalih izključena možnost poškodb sklepnega hrustanca med rastjo. Previdnost je potrebna pri starejših bolnikih, epileptikih, in bolnikih s poškodbami osrednjega živčevja. **Oprema:** Ciprobay 250: 10 lakiranih tablet po 250 mg; Ciprobay 500: 10 lakiranih tablet po 500 mg; Ciprobay 100: 5 infuzijskih steklenič po 100 mg; Ciprobay 200: 5 infuzijskih steklenič po 200 mg; Ciprobay 400: 5 infuzijskih steklenič po 400 mg.

**Bayer**



Bayer Pharma d.o.o.

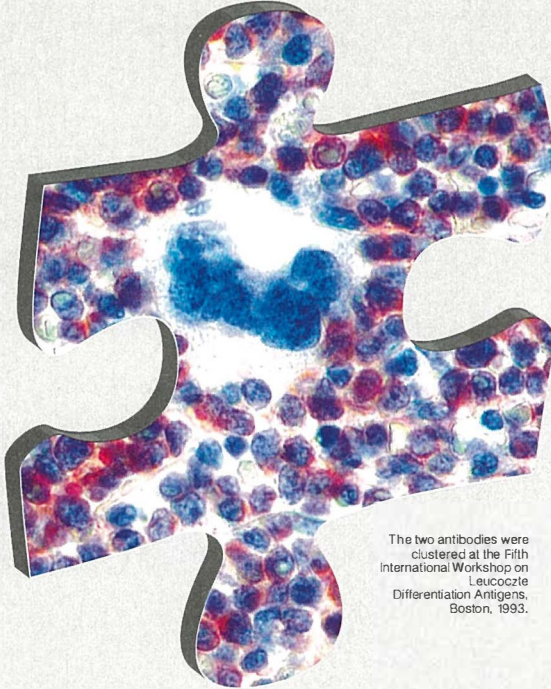




# DAKO

## CD79 $\alpha$ , B Cell Marker

Monoclonal Mouse Anti-Human B Cell



The two antibodies were clustered at the Fifth International Workshop on Leucocyte Differentiation Antigens, Boston, 1993.

### Antibodies available:

Monoclonal Mouse Anti-Human B Cell, CD79a, clone JCB117

Monoclonal Mouse Anti-Human B Cell, CD79a, clone HM57

- Highly specific for B cells at all stages of maturation
- Well documented antibodies
- Important new addition to the range of DAKO B and T Cell Markers
- Unique products, only from DAKO
- Available as two products from the clones JCB117 and HM57
- Applicable on DAKO TechMate™ immunostainers
- Work well on formalin-fixed, paraffin-embedded material

**DAKO - Your Reference in Immunohistochemistry**

**LABORMED**  
*laboratory & medical equipment*

LABORMED d.o.o.  
SLO - 1215 Medvode • Zg. Pirnice 96/c  
Telefon 061/621 098 • Telefax 061/621 415

# GEMZAR®

*gemcitabin hidroklorid*



## Nova *luč* v onkologiji

### INDIKACIJE

- nemikrocelični pljučni karcinom (NSCLC)
- karcinom pankreasa
- karcinom sečnega mehurja

Drugi terapevtski učinki opaženi pri karcinomih dojke, ovarijev, prostate in pri mikroceličnem pljučnem karcinomu (SCLC).

### Oblika in pakiranje

- injekcijska steklenička z 200 mg gemcitabina
- injekcijska steklenička z 1 g gemcitabina

### Sestavine

aktivna učinkovina (gemcitabin hidroklorid), manitol,  
natrijev acetat, natrijev hidroklorid

Dodatne informacije o zdravilu so na voljo v strokovnih publikacijah, ki jih dobite na našem naslovu.



**Eli Lilly** (Suisse) S. A., Podružnica v Ljubljani,  
Ljubljana, Vošnjakova 2, tel.: (061) 319-648, faks: (061) 319-767

**KNOWLEDGE IS POWERFUL MEDICINE**



# **SANOLABOR**



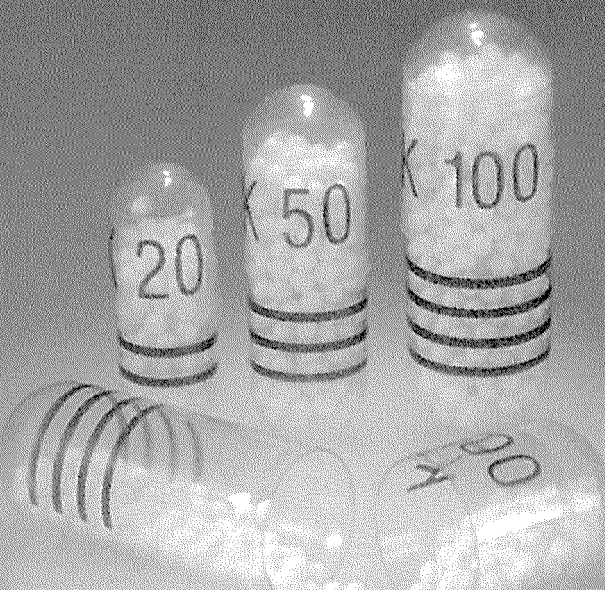
## **Pri nas dobite vse za rentgen!**


- KODAK • SIEMENS • GENERAL ELECTRIC •
- PHILIPS • BENNETT • HITACHI • POLAROID •
- XENOLITE • MAVIG • CAWO •

- rentgenski filmi in kemikalije
- kontrastna sredstva
- rentgenska zaščitna sredstva
- rentgenski aparati, aparati za ultrazvočno diagnostiko, stroji za avtomatsko razvijanje, negatoskopi in druga oprema za rentgen

**SANOLABOR**, Leskoškova 4, 1103 Ljubljana  
Tel.: 061 185 42 11 Fax: 061 140 13 04

# Moč, ki premaga bolečino dan in noč



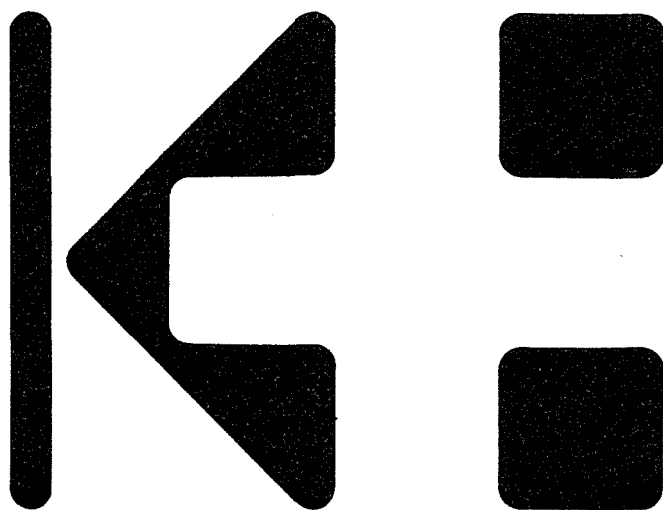
 **Kapanol**<sup>®</sup>  
MORFINIJEV SULFAT

## Prednosti uporabe Kapanola

lažšanje zmerne do močne kronične bolečine • enkrat ali dvakrat dnevno odmerjanje  
izpopolnjena formula s polimeriziranimi peletami, ki omogočajo enakomerno sproščanje morfina 24 ur  
široka izbira v odmerjanju in načinu jemanja

**GlaxoWellcome**

Glaxo Wellcome Export Ltd., Podružnica Ljubljana



# KEMOFARMACIJA

Lekarne, bolnišnice, zdravstveni domovi in  
veterinarske ustanove večino svojih  
nakupov opravijo pri nas.

Uspeh našega poslovanja temelji na  
kakovostni ponudbi, ki pokriva vsa  
področja humane medicine in veterine, pa  
tudi na hitrem in natančnem odzivu na  
zahteve naših kupcev.

KEMOFARMACIJA – VAŠ ZANESLJIVI DOBAVITELJ!



KEMOFARMACIJA

Veletrgovina za oskrbo zdravstva, d.d. / 1001 Ljubljana, Cesta na Brdo 100  
Telefon: 061 12-32-145 / Telex: 39705 KEMFAR SI / Telefax: 271-588, 271-362

## Instructions for authors

**Editorial policy** of the journal *Radiology and Oncology* is to publish original scientific papers, professional papers, review articles, case reports and varia (editorials, reviews, short communications, professional information, book reviews, letters, etc.) pertinent to diagnostic and interventional radiology, computerized tomography, magnetic resonance, ultrasound, nuclear medicine, radiotherapy, clinical and experimental oncology, radiobiology, radiophysics and radiation protection. The Editorial Board requires that the paper has not been published or submitted for publication elsewhere: the authors are responsible for all statements in their papers. Accepted articles become the property of the journal and therefore cannot be published elsewhere without written permission from the editorial board. Papers concerning the work on humans, must comply with the principles of the declaration of Helsinki (1964). The approval of the ethical committee must then be stated on the manuscript. Papers with questionable justification will be rejected.

**Manuscript** written in English should be submitted to the Editorial Office in triplicate (the original and two copies), including the illustrations: *Radiology and Oncology*, Institute of Oncology, Vrazov trg 4, SI-1000 Ljubljana, Slovenia; (Phone: +386 61 132 00 68, Tel./Fax: +386 61 133 74 10, E-mail: gsera@onko-i.si). Authors are also asked to submit their manuscripts on a 3.5" 1.44 Mb formatted diskette. The type of computer and word-processing package should be specified (Word for Windows is preferred).

All articles are subjected to editorial review and review by independent referee selected by the editorial board. Manuscripts which do not comply with the technical requirements stated

herein will be returned to the authors for correction before peer-review. Rejected manuscripts are generally returned to authors, however, the journal cannot be held responsible for their loss. The editorial board reserves the right to ask authors to make appropriate changes in the contents as well as grammatical and stylistic corrections when necessary. The expenses of additional editorial work and requests for reprints will be charged to the authors.

**General instructions** • Radiology and Oncology will consider manuscripts prepared according to the Vancouver Agreement (*N Engl J Med* 1991; **324**: 424-8, *BMJ* 1991; **302**: 6772; *JAMA* 1997; **277**: 927-34.). Type the manuscript double spaced on one side with a 4 cm margin at the top and left hand side of the sheet. Write the paper in grammatically and stylistically correct language. Avoid abbreviations unless previously explained. The technical data should conform to the SI system. The manuscript, including the references may not exceed 15 typewritten pages, and the number of figures and tables is limited to 4. If appropriate, organize the text so that it includes: Introduction, Material and Methods, Results and Discussion. Exceptionally, the results and discussion can be combined in a single section. Start each section on a new page, and number each page consecutively with Arabic numerals.

**Title page** should include a concise and informative title, followed by the full name(s) of the author(s); the institutional affiliation of each author; the name and address of the corresponding author (including telephone, fax and e-mail), and an abbreviated title. This should be followed by the *abstract page*, summarising in less than 200 words the reasons

for the study, experimental approach, the major findings (with specific data if possible), and the principal conclusions, and providing 3-6 key words for indexing purposes. The text of the report should then proceed as follows:

*Introduction* should state the purpose of the article and summarize the rationale for the study or observation, citing only the essential references and stating the aim of the study.

*Material and methods* should provide enough information to enable experiments to be repeated. New methods should be described in detail. Reports on human and animal subjects should include a statement that ethical approval of the study was obtained.

*Results* should be presented clearly and concisely without repeating the data in the tables and figures. Emphasis should be on clear and precise presentation of results and their significance in relation to the aim of the investigation.

*Discussion* should explain the results rather than simply repeating them and interpret their significance and draw conclusions. It should review the results of the study in the light of previously published work.

**Illustrations and tables** must be numbered and referred to in the text, with appropriate location indicated in the text margin. Illustrations must be labelled on the back with the author's name, figure number and orientation, and should be accompanied by a descriptive legend on a separate page. Line drawings should be supplied in a form suitable for high-quality reproduction. Photographs should be glossy prints of high quality with as much contrast as the subject allows. They should be cropped as close as possible to the area of interest. In photographs mask the identities of the patients. Tables should be typed double spaced, with descriptive title and, if appropriate, units of numerical measurements included in column heading.

**References** must be numbered in the order in which they appear in the text and

their corresponding numbers quoted in the text. Authors are responsible for the accuracy of their references. References to the Abstracts and Letters to the Editor must be identified as such. Citation of papers in preparation, or submitted for publication, unpublished observations, and personal communications should not be included in the reference list. If essential, such material may be incorporated in the appropriate place in the text. References follow the style of Index Medicus. All authors should be listed when their number does not exceed six; when there are seven or more authors, the first six listed are followed by "et al.". The following are some examples of references from articles, books and book chapters:

Dent RAG, Cole P. *In vitro* maturation of monocytes in squamous carcinoma of the lung. *Br J Cancer* 1981; **43**: 486-95.

Chapman S, Nakielny R. *A guide to radiological procedures*. London: Bailliere Tindall; 1986.

Evans R, Alexander P. Mechanisms of extracellular killing of nucleated mammalian cells by macrophages. In: Nelson DS, editor. *Immunobiology of macrophage*. New York: Academic Press; 1976. p. 45-74.

**Page proofs** will be faxed to the corresponding author whenever possible. It is their responsibility to check the proofs carefully and fax a list of essential corrections to the editorial office within 48 hours of receipt. If corrections are not received by the stated deadline, proof-reading will be carried out by the editors.

---

*For reprint information in North America Contact: International Reprint Corporation 968 Admiral Callaghan Lane, # 268 P.O. Box 12004, Vallejo; CA 94590, Tel: (707) 553 92 30, Fax: (707) 552 95 24.*

# Za mirno potovanje skozi kemoterapijo

**Navoban**  
tropisetron

- preprečevanje slabosti in bruhanja pri emetogeni kemoterapiji
- učinkovito zdravilo, ki ga odrasli in otroci dobro prenašajo
- vedno 1-krat na dan
- vedno 5 mg

**Skrajšano navodilo za uporabo:** Navoban® kapsule, Navoban® raztopina za injiciranje 2 mg in 5 mg. Serotoninski antagonist. **Oblika in sestava:** 1 trda kapsula vsebuje 5 mg tropisetronovega hidroklorida. 1 ampula po 2 ml vsebuje 2 mg tropisetronovega hidroklorida. 1 ampula po 5 ml vsebuje 5 mg tropisetronovega hidroklorida. **Indikacije:** Preprečevanje slabosti in bruhanja, ki sta posledici zdravljenja s citostatiki. Zdravljenje pooperativne slabosti in bruhanja. Preprečevanje pooperativne slabosti in bruhanja pri bolnicah, pri katerih je načrtovana ginekološka operacija v trebušni votlini. **Odmerjanje in uporaba:** Preprečevanje slabosti in bruhanja, ki sta posledici zdravljenja s citostatiki. **Odmerjanje pri otrocih:** Otroci starejši od 2 let 0,2 mg/kg telesne mase na dan. Največji dnevni odmerek ne sme preseči 5 mg. Prvi dan kot intravenska infuzija ali kot počasna intravenska injekcija. Od 2. do 6. dne naj otrok jemlje zdravilo oralno (raztopino v ampuli razredčimo s pomarančnim sokom ali koka kolo). **Odmerjanje pri odraslih:** 6-dnevna kura po 5 mg na dan. Prvi dan kot intravenska infuzija ali počasna intravenska injekcija. Od 2. do 6. dne 1 kapsula na dan. **Zdravljenje in preprečevanje pooperativne slabosti in bruhanja:** **Odmerjanje pri odraslih:** 2 mg Navobana z intravensko infuzijo ali kot počasna injekcija. Glej celotno navodilo! **Kontraindikacije:** Preobčutljivost za tropisetron, druge antagoniste receptorjev 5-HT<sub>3</sub> ali katerokoli sestavino zdravila. Navobana ne smemo dajati nosečnicam; izjema je preprečevanje pooperativne slabosti in bruhanja pri kirurških posegih, katerih del je tudi terapevtska prekinitve nosečnosti. **Previdnostni ukrepi:** Bolniki z nenadzorovano hipertenzijo; bolniki s prevodnimi ali drugimi motnjami srčnega ritma; ženske, ki dojijo; bolniki, ki upravljajo s stroji ali vozili. **Medsebojno delovanje zdravil:** Rifampicin ali druga zdravila, ki inducirajo jetrne encime. Glej celotno navodilo! **Stranski učinki:** Glavobol, zaprtje, redkeje omotica, utrujenost in prebavne motnje (bolečine v trebuhu in driska), preobčutljivostne reakcije. Zelo redko kolaps, sinkopa ali zastoj srca, vendar vzročna zveza z Navobanom ni bila dokazana. **Način izdajanja:** Kapsule: uporaba samo v bolnišnicah, izjemoma se izdaja na zdravniški recept pri nadaljevanju zdravljenja na domu ob odpustu iz bolnišnice in nadaljnjem zdravljenju. Ampule: uporaba samo v bolnišnicah. **Oprema in odločba:** Zloženska z 5 kapsulami po 5 mg; številka odločbe 512/B-773/97 z dne 10. 11. 1997. Zloženska z 1 ampulo po 2 ml (2 mg/2 ml); številka odločbe 512/B-772/97 z dne 10. 11. 1997. Zloženska z 10 ampulami po 5 ml (5 mg/5 ml); številka odločbe 512/B-771/97 z dne 10. 11. 1997. **Izdavalci:** NOVARTIS PHARMA AG, Basel, Švica. **Imetnik dovoljenja za promet z zdravilom:** NOVARTIS PHARMA SERVICES INC., Podružnica v Sloveniji, Dunajska 22, 1511 Ljubljana, kjer so na voljo informacije in literatura. Preden predpišete Navoban, prosimo preberite celotno navodilo.



